Form and Process

Norwegian studies in the interaction between overland flow and soil surface

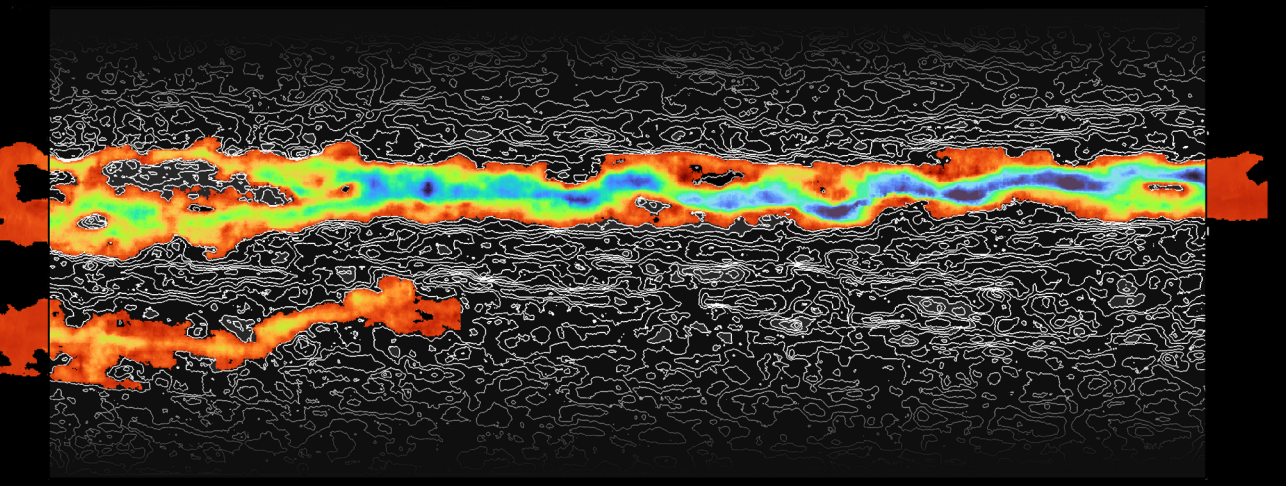

Robert Jan Barneveld

Propositions

1. Digital Elevation Models derived from Terrestrial Laser Scanning are the most reliable reference models for the study of the microtopography of agricultural soil surfaces.
(this thesis)

2. Combating ephemeral gully erosion is the pivotal element in an efficient and effective soil conservation strategy in Norway.
(this thesis)

3. Successful research starts with the mapping of an observed reality into a conceptual model.

4. Displaying certainty is a sign of being underinformed.

5. Predicting has replaced understanding as the overall imperative for scientific research.

6. Carbon markets will reinfoce existing global economic inequality.

7. Canonisation of environmental alarmism obstructs wider societal acceptance of mitigation policies.

Propositions belonging to the thesis, entitled:

Form and Process; Norwegian studies in the interaction between overland flow and soil surface

Robert Jan Barneveld

Wageningen, 8 November 2022

Form and Process; Norwegian studies in the interaction between overland flow and soil surface

Robert Jan Barneveld

Thesis committee

Promotors

Prof. Dr S.E.A.T.M. van der Zee †
Personal chair, Soil Physics and Land Management Group
Wageningen University & Research

Prof. Dr C.J. Ritsema
Professor of Soil Physics and Land Management
Wageningen University & Research

Co-promotor

Dr J. Stolte
Head of Research, Soil and Land Use Section
Norwegian Institute of Bioeconomy Research (NIBIO), Ås, Norway

Other members

Dr A. Eltner, Technical University of Dresden, Germany
Prof. Dr A.J.F. Hoitink, Wageningen University & Research
Prof. Dr J. Mulder, Norwegian University of Life Sciences, Ås, Norway
Dr L.H. Cammeraat, University of Amsterdam

This research was conducted under the auspices of the Graduate School for Socio-Economic and Natural Sciences of the Environment (SENSE).

Form and Process; Norwegian studies in the interaction between overland flow and soil surface

Robert Jan Barneveld

Thesis
submitted in fulfillment of the requirement for the degree of doctor
at Wageningen University
by the authority of the Rector Magnificus,
Prof. Dr A.P.J. Mol
in the presence of the
Thesis Committee appointed by the Academic Board
to be defended in public
on Tuesday 8 November 2022
at 11 a.m. in the Omnia Auditorium.

Robert Jan Barneveld

Form and Process; Norwegian studies in the interaction between overland flow and soil surface

184 pages

PhD thesis, Wageningen University, Wageningen, NL (2022)
with references, with summary in English, Dutch and Norwegian

ISBN 978-94-6447-420-6

DOI 10.18174/577859

ἀγεωμὲτρητος
μηδεὶς
εἰσίτω

Let none but geometers enter here, inscription written over the entrance to the Temple of the Muses in Plato's Academy.

Summary

Soil erosion is a natural process that is accelerated by human activity. Soil loss from agricultural land in Nordic countries is an environmental problem because of its effect on freshwater quality. Agricultural land users in Norway are expected to implement measures to reduce risk of erosion and sediment transport. In order for these measures to be effective, the processes of particle detachment, transport and deposition need to be known. Erosion is driven by four categories of factors: soil, climate, agronomy and topography. In this thesis, some of the relations between topography, or terrain form, and the erosion process are investigated. The effect of erosion on soil surface microtopography is investigated by analysing changes between the digital elevation model (DEM) measured prior to a winter and after the snow melt. The elevation data for the DEM were acquired by a terrestrial laser scanner (TLS), surveying technology that can produce highly accurate point clouds that represent irregularly shaped surfaces and volumes. Unmanned aerial vehicles (UAV) were used to quantify changes to the soil surface at a higher order of magnitude. Ephemeral gullies were surveyed exhaustively in a small headwater catchment for three consecutive years and their volumes calculated. The results of this study show that this form of gully erosion is a significant process for the total sediment losses at the level of a small headwater catchment. A catchment scale analysis was carried out to highlight the areas where erosion control measures can be expected to have the highest efficiency. To this purpose, a terrain index that represents sediment connectivity was combined with erosion risk mapping. The result of this study showed that the differences in connectivity in a headwater catchment of smaller size (< 5 km^2) are too limited to be significant. The effect of topography on erosion and deposition was also investigated by means of the topographic factor (LS) of the Universal Soil Loss Equation (USLE). Several methods to calculate LS have been developed since the inception of the USLE in the 1960s. It was found that the overall performance of these methods was poor, when applied to a real, complex landscape. Common to most methods was the fact that their performance was best for short slope lengths (less than 50 m).

Samenvatting

Bodemerosie is een natuurlijk proces dat wordt versneld door menselijke ingrepen in de natuurlijke omgeving. Bodemverlies vanuit akkerbouwgebieden is een probleem in Skandinavië vanwege het negatieve effect op de kwaliteit van het oppervlaktewater. Er wordt in Noorwegen van boeren verwacht dat ze maatregelen nemen die het risiko op bodemverlies verminderen. Deze maatregelen kunnen alleen efficiënt ontworpen worden, als het proces van erosie, sedimenttransport en depositie goed begrepen wordt. Het erosieproces wordt door een viertal hoofdfactoren gedreven: bodem, klimaat, agronomie en topografie. In dit proefschrift wordt een poging gedaan om enkele van de relaties tussen topografie, of terreinvorm, en het erosieproces beter te begrijpen. Het effect van erosie op de vorm van het bodemoppervlak, of microtopografie, wordt onderzocht aan de hand van geobserveerde veranderingen tussen een digitaal hoogtemodel (DEM) gemeten voor de winter, en een DEM van hetzelfde oppervlak na het smelten van de sneeuw. De hoogtemetingen die aan de DEMs ten grondslag liggen, zijn gedaan met een terrestrische laserscanner (TLS). Deze technologie is ontwikkeld voor de landmeetkunde, en is in staat om grote hoeveelheden puntmetingen te doen om onregelmatige oppervlakken gedetaileerd in kaart te brengen. Drones zijn gebruikt om veranderingen in het bodemoppervlak te kwantificeren die enkele ordes van grootte meer aanzienlijk zijn dan metingen met de TLS. Geul- of vlakslooterosie [1] is in drie opeenvolgende jaren nauwkeurig in kaart gebracht in een klein, door akkerbouw gedomineerd, stroomgebied. De studie laat zien dat deze vorm van erosie een significant deel uitmaakt van de jaarlijkse sedimentbalans. Een volgende studie, ook op het niveau van het kleine stroomgebied, richtte zich op het idenficeren van zones in het stroomgebied die een combinatie van hoge erosiegevoeligheid en een hoge connectiviteit lieten zien. In deze zones kan worden aangenomen dat erosiemaatregelen het meest effectief zijn. Hiervoor is een topografische indexwaarde gebruikt die de hydrologische connectiviteit binnen het stroomgebied kwantificeert. Het resultaat van deze studie was dat de ruimtelijke verschillen in een relatief klein stroomgebied (minder dan 5 km^2) niet voldoende zijn om de effectiviteit van erosiemaatregelen te kunnen differentiëren naar locatie. Het effect van topografie op erosie en depositie is ook onderzocht aan de hand van een andere topografische index: de topopgrafische factor van de USLE (Universal Soil Loss Equation). Er zijn, sinds het ontstaan van de USLE in de jaren 60, verschillende methodes ontwikkeld om deze hellingsfactor te berekenen. De studie laat zien dat de hellingsfactor in het algemeen, ongeacht berekeningsmethode, niet in staat is om de ruimtelijke verdeling van erosie en depositie te representeren in een daadwerkelijk, complex landschap. Het geldigheidsdomein van alle berekeningsmethoden is begrensd tot hellingslengtes van maximaal 50 m.

[1] Het Zuid-Afrikaanse woord dat door W.F. Hermans wordt voorgesteld in zijn collegedictaat over erosie.

Sammendrag

Erosjon er en naturlig prosess som fremskyndes av menneskelige ingrep i naturen. Jordtap fra jordbruksjord i nordiske land er en miljøtrussel på grunn av dens negative påvirkning på overflatevannkvalitet. Jordbrukere i Norge er oppfordret til å gjennomføre tiltak for å begrense risiko for erosjon og for å minske partikkeltransport. Kunnskap om prosessene bak erosjon, sedimenttransport, og deposisjon kreves for å foreslå effektive erosjonstiltak. Erosjon drives av fire ulike typer faktorer: jordsmonn, klima, agronomi og topografi. Denne avhandlingen inneholder fem studier som utforsker forholdet mellom topografi, eller terrengform, og erosjonprosessen. Påvirkningen av erosjon på morfologien til jordas overflate, eller mikrotopografi, ble analysert med hjelp digitale høydemodeller fra før vinteren og etter snøsmeltingen. Terrenghøyde ble målt med en terrestrisk laserscanner; landmålingsutstyr som lager pålitelige og detaljerte modeller av uregelmessige overflater og volumer. Droner (fjernstyrte, ubemannete luftfartøy) ble brukt for å kvantifisere endringer i jordens overflate som resultat av drågerosjon. Spor av graving i dråg og søkk i terrenget ble målt opp i et mindre, jordbruksdominert nedbørsfelt i tre påfølgende år. Studien viser at jordtap som følge av drågerosjon er en signifikant kilde av partikkeltapp på nedbørsfeltnivå. En annen studie anvender en terrengindeks for å identifisere kritiske zoner innen et mindre nedbørfelt hvor tiltak vil være mest effektive. En konnektivitetsindeks ble brukt i kombinasjon med en modelmessig tilnærming til (lokalt) erosjonsrisiko. Studien viser at forskjellene i konnektivitet på nivået til et lite nedbørsfelt (mindre enn 5 km^2) er for små for å gi signifikant avvik. Topografiens effekt på erosjon og deposisjon ble også undersøkt med hjelp av den Universale Jordtapsligningens (USLE) topografiske faktor (LS). Mange ulike metoder til beregning av LS er blitt utviklet siden USLE sin utviklingsfase i 1960-tallene. Studien viser at ingen av metodene er i stand til å representere forholdet mellom erosjon og deposisjon i kompleks, faktisk eksisterende, terreng. Analysen viser at ingen av metodene fungerte bra, når de ble sammelignet med en prosessbasert modell. Mesteparten av metodene viste å ha en gyldighetsdomene som var begrenset til hellingslengder av maksimal 50 m.

Acknowledgements

When I read between the lines of this thesis, I see a group of people who have determined the choice for the subject matter of the presented research and the methods developed and applied. Another group of people have helped me starting and finalising the work behind the thesis.
I first would like to thank those in the union of these categories, first and foremost my supervisors Sjoerd van der Zee, Jannes Stolte and Coen Ritsema. The news about Sjoerd's passing came during the last stages of writing. He has not only given me the opportunity to start the trajectory, but has maintained a level of confidence in a successful conclusion throughout many years of delay and, at times, stagnation. Sjoerd's criticism has sharpened my writing by patiently pointing out unjustified shortcuts in definitions and descriptions. In the course of the years, this has also shaped my ability to think about research. I see this as a gift that I will cherish throughout my career. Jannes has also shown me patience and confidence. To him I owe the opportunity to be part of a group of people with a drive to study erosion in Norway. Without Jannes' continuous effort to keep me on the straight and narrow, my tendency to get involved in other projects would have made completion of this thesis utterly impossible. I thank Prof. Coen Ritsema for his encouragement and guidance, especially during the phase leading up to the final manuscript and the public defense. I want to thank Prof. Leo Stroosnijder who, after an absence of many years, called me back to Wageningen and recommended my candidature to Sjoerd. Dr. Geert Sterk passed away in 2022, much too early. He was my MSc. supervisor in 2001 and to him I owe thanks because of the confidence he showed in my suitability for a PhD. trajectory. I thank Dr. Manuel Seeger for the support and inspiration during the period in which he was my co-supervisor in Wageningen.
The realisation of being a pupil is an experience that is as humbling as it is uplifting, and I want to mention two teachers. To Meester Hoekstra, my fifth grade primary school teacher, I owe the fascination for soil-water-plant interactions. I see this dissertation as the completion of an education that started in the school vegetable garden. To Dr. Hans Schiere, I owe the joy of looking at a problem from a different angle and the realisation that individual choices are not quite so independent from the larger scheme of things.
My parents, Jan en Nelly Barneveld, have continuously shown me confidence while making the Big Choices in life. This means especially much because my choices lead on a path that was sometimes difficult to explain (I could have tried a bit harder at times). Pa en ma; dank jullie voor alles (en dat is een hoop).
Clarieke, Otto, Ivar, Johan en Aage have always come in the first place. But my inability to strike a balance has, at times, resulted in me being physically present, but not mentally. I thank the five of you for keeping up with this, and even more so for tolerating the Long Explanations that I made you, and will continue to make you, suffer about subjects that are as alien to you as Minecraft is to me.
The list of colleagues that have contributed implicitly or explicitly is too long

to include here, but I call out to (in alphabetical order) Atilla, Csilla, Dominika, Hannah, Johannes, Hans Olav, Lillian, Marianne, Sigrun, Simon and Torsten. The inspiration that I got from our conversations, short or long / in the office or on a snowy field cannot be overestimated.
Lastly, I want to mention my friends in the Netherlands. All of them are extremely good at at least one thing, and their abilities have always stimulated me to improve myself. I mention Schalk-Jan (hydrological modeling), Johan (using a computer, instead of the other way around), Ruben (reflection); thanks for being good friends.

Contents

Chapter 1

Introduction

1.1 Soil erosion as a relevant topic

Soil erosion is one of the world's many environmental problems and has been so since the dawn of arable production in the Fertile Crescent. Erosion is a problem for two broad reasons. On-site problems concern soil loss, as nutrient rich top soil is most prone to detachment and transport. This may in time lead to a decline in organic matter content and eventually poorer soil structure. The removal of fertile topsoil will have a negative impact on productivity. Concentrated overland flow may damage the soil surface in the form of gullies that could inhibit farm operations. Off-site problems occur downstream as the result of an influx of soil particles. While sediment is a natural part of the environment, too much of it in surface waters has a detrimental effect on aquatic life. High sediment concentrations hinder the penetration of sunlight, bury spawning grounds and can do physiological damage to aquatic vertebrates. It leads to reductions in the retention potential of dams that serve communities by providing hydropower, irrigation water and flood protection. Sediments may also result in damage to other forms of infrastructure (roads, bridges) and property (houses, arable land). The loss of particle bound phosphorus is closely linked to soil erosion. Temporarily high concentrations of phosphorus can lead to concentrations that are toxic for aquatic life or, in the longer term, eutrophication.

Erosion has long been recognised as an environmental problem. This realisation might be as old as agriculture itself. Leick (2007), for example, mentions measures against water and wind erosion in ancient Mesopotamia and Van Andel and Thirgood (1982) characterise forest management in Ancient Greece as integral of a soil conservation strategy.

The importance of anthropogenic soil erosion as a cause for the deterioration of surface waters in Norway cannot be traced back so far. Its current priority for environmental policy has its origin in the catastrophic levels reached by algae blooms in the Skagerak and North Sea coastal waters in 1988 (Fig.1.2). In that year, the alga *Chrysochromulina polylepsis* unexpectedly reached levels that proved

FIGURE 1.1: The most important regions for arable production in Norway.

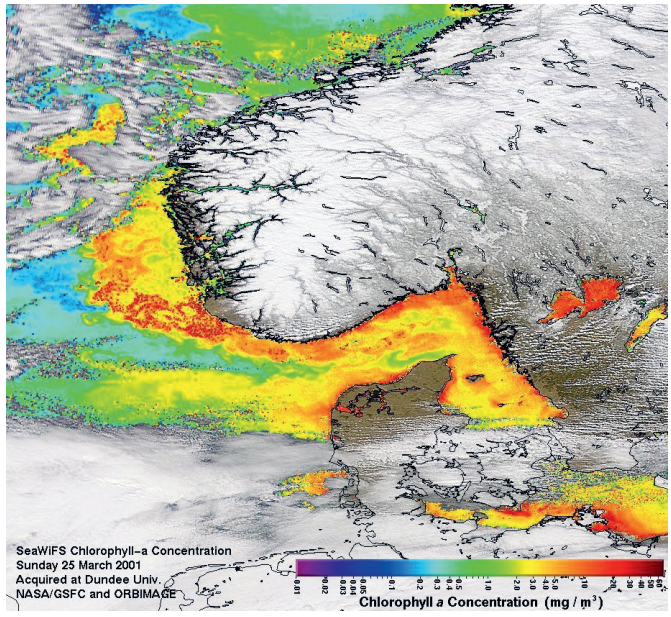

FIGURE 1.2: Annual algae bloom in Norway's coastal waters (source: NASA Earth Observatory, 2001).

detrimental to marine life (Dundas *et al.*, 1989). Realising the severity of the problem of coastal water eutrophication, mitigation strategies, already set out in the 1984 Bremen Declaration, were accelerated by the North Sea countries in an orchestrated manner. In Norway, this has resulted in a framework of rules and incentives that aim at the reduction of sediment and nutrient loads from agricultural soils. The Regional Environmental Programme for Agriculture (Regionalt Miljøprogam for Jordbruket) in 2020 had a total budget of 724 million Norwegian Kroner (€72 million), 33% of which was allocated towards activities to reduce the negative impact of agriculture on surface waters (Landbruksdirektoratet, 2020). Resources are not only allocated to the implementation of mitigation measures, but also for the assessment of their efficacy. The Norwegian Institute for Bioeconomy Research (NIBIO) is one the country's main contributors to the knowledge base on which national and regional regulations are, or should be, based.

The many changes in weather conditions as a result of climate change are likely to exacerbate the detrimental environmental effects of soil erosion at the global scale (Borrelli *et al.*, 2020). In Norway too, climate change results in weather conditions that are likely to increase sediment loading as a result of soil erosion. Driving mechanisms are the changing distribution of precipitation over the year (Hanssen-Bauer *et al.*, 2015), more frequent melt-thaw cycles (resulting in poorer soil aggregate stability) and a less stable snow cover (more melting during winter and early spring (Fig.1.3), resulting in overland flow on frozen soil.

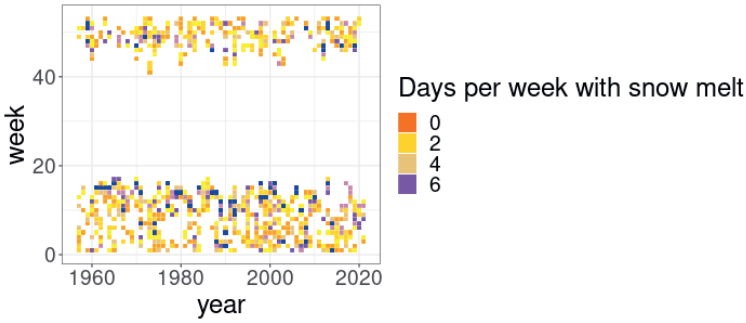

FIGURE 1.3: Weekly number of days with melting snow for the period 1957 - 2021 (town of Ski in southeastern Norway).

The developments briefly represented in the paragraphs above form the context in which soil erosion research in Norway is conducted. While the overall dynamics that drive erosion processes are taken to be well understood (erosion is a function of climate, land use, soil properties and terrain), there are a series of questions that require the expansion of our quantitative understanding in order for society to be able to reduce environmental damage as the result of soil loss from agricultural soils. In Norway, these topics fall in three broad, fuzzy categories. The implications of climate change provide an added dimension to all topics. This objective of this dissertation is to contribute to the matters raised under the topics in bold print.

1. Particle detachment
   (a) **the magnitude of sheet and rill erosion**
   (b) **the magnitude of ephemeral gully erosion**
   (c) the magnitude of matrix erosion (soil loss through the tile drain system)
   (d) the magnitude of streambank erosion
   (e) **the role of tillage in soil erosion**
2. Sediment transport and delivery
   (a) the role of surface drainage inlets in the transport of sediment
   (b) the importance of torrential events for periodic loading
   (c) agriculture's relative importance as a source of pollutants at the scale of larger watersheds

3. Soil conservation
   (a) **the relevance of topography for prioritisation**
   (b) optimised regulations for different detachment and transport processes
   (c) (compound) effectiveness of measures
   (d) economic efficiency of measures
   (e) farm economy: reward and motivation

The consequent research questions cannot be studied in isolation from each other. *E.g.* process understanding is a prerequisite for a revision of the incentives for soil conservation measures, and predictions about sediment loading from gully erosion are not meaningful without understanding hillslope-stream connectivity.

1.2 Soil erosion as a multidisciplinary topic

Soil erosion as a phenomenon is a subject that can only be studied meaningfully in a multidisciplinary way. In order to understand the processes of erosion and sedimentation and to be able to make predictions, knowledge and methodology from several scientific traditions is required. Scientific inquiry in the geophysical aspects of erosion are carried out in the intersection of the disciplines of hydrology (rainfall-runoff modelling), soil physics (infiltration and erodibility) and geomorphometry (topography-runoff interactions). Knowledge and methods of the disciplines of agronomy, (rural)sociology, (farm) economics and political science are required for the analysis of erosion as a function of farming systems. According to Auguste Comte, no one can understand a scientific discipline unless they are' familiar with its history [1]. Considering the range of scientific traditions that erosion research unites, an exhaustive overview will weigh too heavy in this introductory chapter. A few remarks about the history of hydrology and geomorphology, however, are warranted, especially considering the developments of the last decades.

Historiographies of hydrology tend to start in Ancient Greece, either as part and parcel of the nascent deductive tradition on which modern science is based, or as a branch of engineering, pivotal to the development of the city-state, and therefore modern civilisation. Musings about the hydrological cycle are present in the Old Testament:

All streams flow into the sea, yet the sea is never full.
To the place the streams come from, there they return again[2].

[1] *Je pense même qu'on ne connaît pas complètement une science tant qu'on n'eu sait pas l'histoire.* Cours de Philosophie Positiv, 1830.

[2] Ecclesiastes 1.7 (*Nb.* Hellenistic Levant)

Thales and Anaximander of Miletos, 7^{th} century BC proponants of the monist tradition, respectively postulate that the earth floats on water and that water vapour transforms into land (Jones *et al.*, 1963; Latinopoulos, 1999). Bras (1999) states that the explicatory framework of the Classical Period lacked knowledge of three important aspects of the hydrological cycle: conservation of mass, evaporation and infiltration. For many centuries, the driving force behind the hydrological cycle was assumed to be the pressure of the sea, pushing waters up though the earth through the mountains, filtering it into freshwater streams. After the Classical period, scientific hydrology consisted of conjectures, often as part of theological traditions, but did not develop to a mature science before the Age of Enlightenment. Positivism and the consequent mathematisation of physics directed science onto a path that lead directly to humankind's current conceptualisations of physical reality. Important instances during this period are civil servant Pierre Perrault's observations that showed that precipitation explains fluctuation in the discharge of the Seine river[3]. His contemporary Edmé Mariotte provided the first examples of a quantitative comparison of precipitation and river discharge. Polymaths Evangelista Torricelli (1608 - 1647) and Benedetto Castelli (1578 - 1643), both pupils of Galileo, derived the first modern principles of hydraulics. Castelli derived an early formalisation of the continuity equation for river flow, and Torricelli experimented with the relation between pressure and flow rate (Meli, 2007). Domenico Guglielmini's (1655 - 1710) work on hydraulics resulted in the following propositions that could only partially be tested experimentally (Chorley, Dunn, and Beckinsale, 1964):

1. *Streams erode or build up their beds until equilibrium is attained between force and resistance.*
2. *Slope therefore will vary inversely with velocity.*
3. *The less the resistance of the bed materials, the less the slope of the channel.*
4. *Slope varies inversely as the normal discharge.*
5. *A mobile bed is modified to give a longitudinal profile which is concave upwards.*

Nevertheless, it took three centuries to arrive at a description of the hydrological cycle that coincides with our (current) model (Rosbjerg and Rodda, 2019). The developments in physics and mathematics and the increasing role of experimentation as a basis for explanation resulted in ever better descriptions of hydrological processes. In the 18^{th} and 19^{th} centuries, discoveries relevant to hydrology were mostly in the field of hydraulics (Bernoulli, Chézy, Darcy and Manning), whose equations are at the very core of many hydrological models until today. Quantitative understanding of infiltration is a relatively recent addition to the body of hydrological knowledge. Experimentation, *e.g.* analyses of river discharge, remained the primary mechanism behind the growth of hydrological knowledge. In the 1970's, Gray (1973) observes the end of the primacy of empiricism for the

[3] De l'Origine des Fontaines, 1674.

further development of the discipline. Phenomena are studied by means of a combination of deductive (based on physical principles and laws) and inductive (measurements, observations) methods. This shift might have happened gradually, but its implications for the scope and possibilities are nothing less than revolutionary (Gregory and Lewin, 2014).

The lineage of geomorphology as a sub-discipline of geology begins much later than that of hydrology. A notable exception is Leonardo da Vinci (1452 - 1519) who expressed a level of understanding that is remarkable in its aptitude to explain landforms and processes. Quoting McCurdy's 1938 translation:

> *I perceive that the surface of the Earth was from of old entirely filled up and covered over in its level plains by the salt waters, and that the mountains, the bones of the earth with their wide bases, penetrated and towered up amid the air, covered over and clad with much high-lying soil. Subsequently, the incessant rains have caused the rivers to increase, and by repeated washing, have stripped bare part of the lofty summits of these mountains, leaving the site of the earth so that the rock finds itself exposed to the air, and the earth has departed from these places.*

Where hydrology finds its origin in questions about processes (river flow, rainfall), geomorphology questions the state of the landscape. Hydrology requires information about states for the explanation of processes, and geomorphological investigation began as a series of conjectures about the processes that lead to landforms. Two distinct traditions arose more or less simultaneously in Europe. Although the literature on the subject is somewhat limited, continental 19^{th} century geomorphology was what now would be described as orography. Early continental geomorphology, primarily German, was essentially descriptive, although (Sonklar, 1873) does pay considerable attention to the origin of mountainous landforms. In 19^{th} century Britain, however, the discipline was characterised by a focus on process understanding. In the 18^{th} century, the field was dominated by theories that held the deluge of the Old Testament as the primary cause for the diversity of landforms. This catastrophist tradition still thrives in orthodox religious communities the world over. The earliest documented proponent of the uniformitarianist tradition[4], which still is a basic tenet of modern day science, was James Hutton (Chorley, Dunn, and Beckinsale, 1964). In 1795 Hutton published his *Theory of the Earth, with Proofs and Illustration*, in which he presented a unified theory on the formation of rocks and soils, erosion (processes and mass balance), glacial activity and the origin of mountains and valleys (*ibid.*). Charles Lyell, with his monumental *Principles of Geology*, published between 1830 and 1833, continued on the uniformitarianist path and improved on Hutton's conjectures by providing evidence and introducing geological concept of time. The latter half of the 19^{th} saw the rise of quantitative methods in geomorphology (Wooldridge, 1956). The increasing amount of data saw a shift in the debates from

[4]The conviction that physical laws that describe reality now, also hold for other epochs and places, or 'the principle of the permanence of laws' in Russel's words (*On the notion of cause*, 1918).

theoretical to empirical. Geikie (1868) publishes an early attempt to compare the importance of different erosion processes (driven by wind, runoff or tidal forces). Another major advancement in the knowledge of soil-water interactions was the publication of *An Inquiry into the Operation of Running Streams and Tidal Waters* by T.J. Taylor in 1851. This publication introduces the concept of self-organisation, and collects experimental data on the importance of velocity profiles and particle size for erosion and sediment transport along a river. Note that the research that formed the basis for the latter two publications, while considered a part of hydrology by today's definitions, was undertaken to answer geomorphological questions.

The 20^{th} century was not old before the combination of drought and large scale monoculture turned the Great Plains in the central USA into the Dust Bowl. The US Soil Conservation Service (SCS) was established as a result, and in 1980, Kirkby states that:

> Most of our present knowledge of soil erosion mechanisms and rates originates in the work of the US Soil Conservation Service.

The literal validity of this statement is a matter for discussion, especially when process understanding is concerned [5]. The measurements of SCS, however, clearly mark the beginning of the investigation of erosion rates at the hillslope scale. Studies based on these first measurements are among the earliest published investigations into the factors that drive sheet erosion. The earliest peer reviewed publication about the relation between slope degree and erosion rate was published in 1932 (Duley, 1932). In 1940, Zingg investigated the combined effect of slope degree and length on erosion rates (Zingg, 1940). A year later, Smith (1941) added a conservation factor to Zingg's relation. Browning *et al.* (1948) introduced soil erodibility and an agronomic factor to this analysis. Seventeen years later, the combination of driving factors were formalised by Wischmeier and Smith in the Universal Soil Loss Equation (USLE, Wischmeier and Smith, 1965). Erosion studies onward from the 1930s became part of an emerging scientific tradition that focused on the interaction between human activity and the natural environment (see also Chorley, 1969). In contrast to the role that the description of the erosion process played in geomorphological explanation, the field studies became part of an engineering effort to reconcile agricultural production with environmental sustainability.

Soil loss was recognised as a worldwide ecological disaster as early as the 1940s (Graham, 1946). The alarmist idiome that characterises current scientific and political communications about climate change was once reserved for soil loss (*e.g.* De Vries (1948) uses terms like "regional suicide" and compares high erosion rates to "death sentences"). Moreover, erosion was recognised as a threat to the productivity of colonial agriculture (Van Baren, 1947; Schwarz, 1950), and

[5] Kirkby and Carson's *Hillslope Form and Process* came out eight years prior, in 1972.

therefore an engineering problem rather than a piece in a geomorphological puzzle. As such, erosion studies are an early example of Gibbons *et al.*'s shift from 'Mode 1' (theoretical, experimental, discovery oriented and autonomous) science towards 'Mode 2' (application oriented, trans-disciplinary, socially contracted) science (Nowotny, Scott, and Gibbons, 2003).

Parsons (1988) dates the bifurcation of erosion studies somewhat later. His motivation to do so is given by his focus on the methods by which hillslopes are studied; he discerns trends towards quantitative description of hillslope morphology and an increased focus on the erosion process. The spatio-temporal focus of problem-oriented erosion studies required new conceptual frameworks for the description and quantification of soil erosion (Schumm and Lichty, 1965). Process understanding for hillslope-scale, man-induced accelerated erosion cannot be separated from the overland flow process. This shift has pushed erosion studies towards the domain of hydrology and hydraulics. Chorley's 1969 publication 'Water, Earth and Man' (Chorley, 1969) can be considered a monument to a paradigm characterised by transdisciplinarity and the emancipation of the environmental sciences. It includes chapters on hillslope hydrology and erosion (by M.J. Kirkby) and advocates for the basin as the primary spatial unit for investigations into water-soil interactions. In addition, the book highlights the state of the art concerning channel hydraulics, cold climate hydrology, rainfall-runoff relations and climate dynamics. Richard J. Chorley is renowned for his advocacy for systems theory in the field of geography. The system described in 'Water, Earth and Man' and its more integrated follow up 'Physical Geography: A Systems Approach' (1971) turned out to be a blueprint for a synthesis of hydrology and geomorphology that still coincides with the conceptual frameworks of current investigations into erosion and soil loss [6].

1.3 Soil erosion as an elusive process

Accelerated soil loss on agricultural fields is a complex process (Fig. 1.4). On the soil surface, particles are detached by the impact of raindrops and/or overland flow. Once in suspension, particles are transported by the (theoretical) film of water (sheet erosion) or in patterns of concentrated flow. The ability of a raindrop to detach particles depends on the energy of its impact and the stability of the soil aggregate. Concentrated flow occurs when small depressions in the soil surface fill up with water that has not infiltrated and develop into a continuum in the direction of the steepest inclination. Once the force exerted by the flow in these pathways exceeds a certain value, particles will be detached and transported onward. The linear, parallel patterns that develop on hillslopes in this way are usually classified as rill erosion. Rills develop in the direction of flow. When concentrated flow erodes linear features in the thalweg [7], they are called

[6] Agriculture, however, is largely absent, with the exceptions of irrigation and artificial drainage.
[7] A line in the landscape that coincides with interconnected points of low elevation.

gullies. Gullies develop in the uphill direction (headcut) and can have widths from several decimetres to decametres. Large gullies tend to be part of permanent systems, while smaller, ephemeral gullies on agricultural soil can be filled up during standard field operations like ploughing.

Water that infiltrates the soil profile through the matrix and macropores also exerts erosive force. When agricultural soils are drained, suspended particles can be transported rapidly through the tile drain system (drainage erosion).

Soil creep, or solifluction, is the slow mass movement of topsoil in the direction of gravity along a hillslope. This process is driven by alterations of soil freezing and thawing and can be assumed to be more common in colder climates than in regions without seasonal sub-zero temperatures. Tillage erosion is an accelerated form of soil creep. It is the result of the asymmetric impact of ploughing implements, which results in the movement of soil in the direction of the downward slope.

At the level of the hillslope or catchment, none of the processes can be measured directly. The rate and spatial distribution of erosion in a system can therefore only be quantified by measuring and comparing the state of constituent subsystems. The two most informative and widely used subsystems for the quantification of soil loss rates are the soil surface and the watercourse at the system (catchment) outlet. Relevant quantifiers of the state of the soil surface are its elevation and morphology. For the watercourse, this is the concentration of suspended solids in catchment discharge. Stroosnijder (2005) includes methods for the measurement of splash erosion among the directly measurable processes, as well as in-field runoff collection. These methods do give quantitative insight in the detachment phase of the erosion process, but cannot be considered observations of soil loss. Parsons (2019) mentions the use of tracers as one of the methods to estimate erosion rates. He also points out that in order to translate results from tracer experiments to soil loss rates, conversion models are required. The overall challenge with erosion studies is that observations are usually bound to a certain spatio-temporal scale, while the processes leading up to these observations occur at a variety of scales. Erosion rates from runoff plots and laboratory studies yield quantitative insight at a certain phase and locus of the detachment-entrainment-transport process. At the catchment or hillslope scales, the dynamics may be overridden by a multitude of other factors. Observations at this scale (*e.g.* sediment yield from a catchment) are a function of a complex system that is characterised by subsystems that are connected and disconnected by a variety of processes. The categorical difference between erosion measurements at distinct scales has been recognised as a major challenge to researchers since at least five decades, especially with regard to sediment delivery to recipient surface waters (Wolman, 1977; Walling, 1983; Walling, 1999; Collins and Walling, 2004; Bartley *et al.*, 2014).

When soil erosion studies are conducted for process understanding, or to inform

land management decisions, methods need to be deployed that integrate conceptual frameworks and empirical data (*i.e.* information about states) at different spatio-temporal scales.

Some of the factors that determine the rate of the soil loss process (Fig. 1.4) are equally challenging to measure. Overland flow can in theory be measured at any location in a field or on a hillslope, but in practice these measurements are difficult for practical and/or budgetary reasons. The implication of this difficulty is that erosion models are usually constructed around a hydrological core that provides estimates of the amount of overland flow at some resolution in space and time. Soil erodibility is an inverse measure of it's resistance to detachment and can therefore be approximated through standardised, laboratory based, measurements of aggregate stability. Topographical factors (slope inclination and length, contributing area, planform and profile curvature) can be readily derived from a DEM (digital elevation model). DEMs are available at increasingly high spatial resolutions; compare the resolutions described by Moore *et al.* in 1991 (resolutions of several hundreds of metres) with, for example, Norway's current national elevation model (resolution 1m). Microtopography as an input for the derivation of surface depression storage and hydraulic resistance to flow, can be measured with a variety of methods (Thomsen *et al.*, 2015). Vegetation characteristics (density, morphology, stem height) can be measured in-field, and increasingly by means of remote sensing from space (satellites) or by unmanned aerial vehicles (UAV). Quantitative analysis of precipitation consists of measuring precipitation depth at various temporal resolutions, and controlled experiments of the kinetic energy of different types of rain showers.

Researchers are thus presented with the task to combine observations of driving factors and of the changes in system states as a result of erosion. The amount of data on the factors that influence the erosion process appears to be abundant. The usefulness of individual measurements, however, is always limited by the spatio-temporal scale of the measurement, its location and timing and the purpose and the reliability of the data. The incompleteness of both sets of observations (drivers and effects), especially at the hillslope or catchment level, necessitates the use of models. Models, in their various forms (see the Discussion in Chapter 7) are also the only method for meaningful integration of observations across spatio-temporal scales. Models are therefore indispensable for the further development of quantitative and qualitative understanding of the relations between topography and erosion processes.

1.4 Goal and objectives of this dissertation

The goal of this dissertation is to contribute to quantitative understanding of the relation between topography and erosion rates. The objectives concern (A) the effect of erosion on terrain morphology, and (B) the effect of terrain form on erosion rates and patterns. They are formulated as:

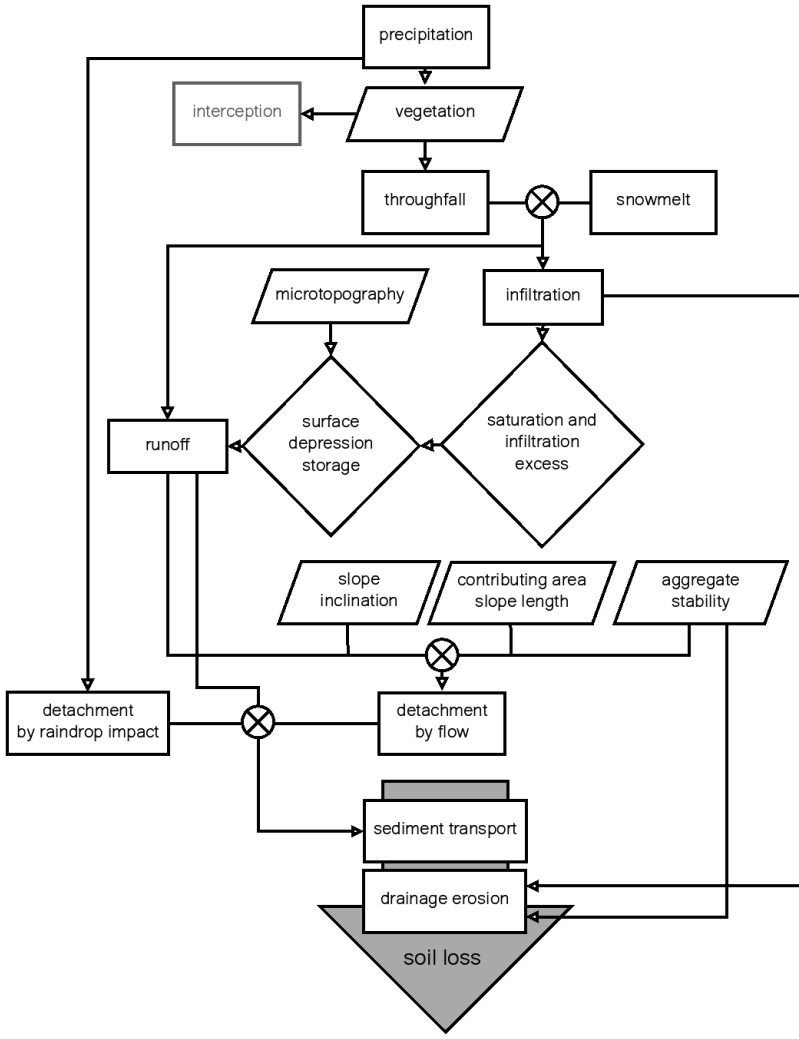

FIGURE 1.4: The erosion process (event/hillslope scale).

(A) The improvement of methods for the measurement of changes to soil surface microtopography as a result of erosion, and

(B) The evaluation of commonly used terrain indices for their correspondence with otherwise estimated erosion and sediment transport rates.

The work presented in Chapters 2, 3 and 4 in this dissertation aim to contribute to objective A. The first two chapters report on the evaluation the aptitude of Terrestrial Laser Scanners (TLS) to accurately measure surface elevation of agricultural soils. The latter chapter describes and tests a methodology to derive net soil loss rates from ephemeral gully erosion at the catchment scale by means of UAV-imagery.

Chapters 5 and 6 present evaluations of two terrain indices for their appropriateness to represent topography in soil erosion models. In Chapter 5, a sediment connectivity index is explored for its applicability for ex-ante evaluations of a soil conservation strategy (stubble cover during winter and early spring). Chapter 6 combines a literature review of the widely used topographical factor (LS) in the USLE with a quantitative comparison to a deterministic, spatially explicit erosion model. Chapter 7, finally, presents a critical evaluation of the conceptual and methodological assumptions that determines all of the choices behind the work presented in Chapters 2 to 6, but that rarely are discussed explicitly. A synthesis of the research and the reflection is presented in Chapter 8.

Chapter 2

Assessment of terrestrial laser scanning technology for obtaining high-resolution DEMs of soils

Abstract

Terrestrial Laser Scanners (TLS) provide a non-contact method to measure soil microtopography of relatively large surface areas. The appropriateness of the technology in relation to the derived Digital Elevation Models (DEM) however has not been reported. The suitability of TLS for soil microtopography measurements was tested on-field for three large soil surface areas in agricultural fields. The acquired point clouds were filtered with a custom cloud import algorithm, and converted into digital elevation models (DEM) of different resolutions. To assess DEM quality, point clouds measured from different viewpoints were statistically compared. The statistical fit between point clouds from different viewpoints depends on spatial resolution of the DEM. The best results were obtained at the higher resolutions (0.02 to 0.04 cm), where less than 5 % of the grid cells showed significant differences between one viewpoint and the next ($p < 0.01$).

Published as: R.J. Barneveld, M. Seeger and I. Maalen-Johansen, 2013. *Assessment of terrestrial laser scanning technology for obtaining high-resolution DEMs of soils*. **Earth Surface Processes and Landforms** 38, p. 90-94.

2.1 Introduction

2.1.1 Background

The role of microtopography in overland flow and related processes like soil particle detachment and deposition, has long been acknowledged (Römkens and Wang, 1987; Mwendera and Feyen, 1992; Katz, Watts, and Burroughs, 1995; Govers, Takken, and Helming, 2000; Darboux and Huang, 2005; Liu and Singh, 2004). Soil roughness measurements or estimates are important for the quantification of sub-grid size processes in spatially explicit erosion models (*e.g.* De Roo, Wesselink, and Ritsema, 1996) as roughness determines hydraulic radius, flow resistance and ponding. Much like the length of a coastline in Richardson's coastline problem (Mandelbrot, 1967), soil surface roughness is a scale dependent parameter. Smaller horizontal distances between surface height observations result in higher roughness estimates (Zhixiong *et al.*, 2005; Alvarez-Mozos *et al.*, 2011). The availability of one dimensional laser profile scanners has provided researchers with an accurate and precise means to study soil roughness (Römkens and Wang, 1987). These scanners have also facilitated measurements of soil detachment and deposition processes at high resolutions by measuring soil surfaces prior to and after a runoff event (Helming, Römkens, and Prasad, 1998; Moritani *et al.*, 2010) Until recently, when Vidal Vázquez *et al.* 2010 and Haubrock *et al.* 2009 undertook three-dimensional field measurements of microtopography, experiences however remained limited to laboratory studies. This is partly due to the lack of methods to obtain accurate three-dimensional terrain data for relatively large surface areas at resolutions higher than 0.10 m.

Jester and Klik (2005) provided a systematic comparison of the available methods to obtain statistical terrain data, mostly roughness parameters. Actual models of a soil surface can only be obtained by means of pin-frame methods, photogrammetry, or laser based methods. Pin-frame methods can provide precise renderings of a soil surface at fairly high resolutions (5 mm, ibid.), but have three important drawbacks. The spatial extent that can be measured is typically not more than one to two meters square. Secondly, measuring and data processing are labour intensive and very time consuming. Thirdly, the method is destructive to the soil surface, or at least the area immediately around it. This prohibits the use of contact methods in field studies that require multiple recordings over time, e.g. for monitoring of erosion. Non-contact measurements like photogrammetry and laser scanning are non-destructive; at least to the direct soil surface under observation. Measurements with one-dimensional, frame mounted, laser scanners have greatly increased the understanding of overland flow dynamics at high levels of spatial detail (Huang and Bradford, 1992; Darboux and Huang, 2005; Aguilar, Aguilar, and Negreiros, 2009).

Like with the pin-frame method, setting up and operation of the required mounting frame however cannot be done without considerable damage to the adjacent

areas. In the field, one-dimensional laser scanners are therefore useful for snapshot measurements, but not for time series when hydrological processes are concerned for larger surface areas.

The restrictions of one-dimensional scanners for sequential recordings of microtopography in the field could be overcome by the use of terrestrial, three-dimensional, laser scanners. Martin and Valeo (2008) used data obtained with a terrestrial laser scanner for the construction of a digital elevation model (DEM) of a forest soil. Haubrock *et al.* (2009) have used the technology for an on-site study of some spatio-temporal aspects of erosion. The equipment used by Martin and Valeo (2008) and Haubrock *et al.* (2009), the Minolta Vivid 900, is designed and typically used for the measurement of dimensions of industrially produced parts. Haubrock *et al.* (2009) recognise this and limit the surface area of their scans to 2.2 m^2. Despite its suitability to study the changes in the soil surface over time, the technology is less suitable for the assessment of soil surface processes at higher spatial scales, e.g. in-field measurement of drainage pattern development and surface depression storage in ridge/furrow systems. High density terrestrial laser scanners (TLS) of the type mainly used in construction and infrastructure surveying may overcome this limitation. Schneider *et al.* (2012) and Schürch *et al.* (2011) provide an example of how TLS can be used for sediment budget calculations on areas covering several hectares. The applicability of the methodology for larger surface areas is not evident for two reasons; the incongruity between the intended and actual use of TLS technology and the fact that soil roughness obstructs lines of view. TLS technology is primarily designed for small incidence angles, whereas large angles dominate when a soil surface is scanned from a tripod, typically 1.5 to 2.0 m above the soil surface. Ridges, soil aggregates and clods, vegetative material and stones obstruct lines of view, especially on tilled agricultural fields. Schneider *et al.* (2012) and Schürch *et al.* (2011) give an overview of measurement error and quantify its subsequent propagation for DEMs with resolutions of 0.5 and 0.2 m, respectively. The objective of the research presented in this article is to assess the suitability of terrestrial laser scanning technology for high resolution (0.02 m) DEM construction of agricultural, tilled, larger soil surfaces (20 to 100 m^2).

2.1.2 Measurement precision and DEM accuracy

For hydraulic simulations on high spatio-temporal resolutions, small differences in slope values can propagate into significant variations in the calculated flow. A microtopography measurement should therefore be (1) precise and (2) accurate and (3) have a substantially complete data coverage: as little spatial data gaps as can be dealt with by means of standard interpolation techniques. Accuracy is the most appropriate parameter to inform users about DEM quality (Kraus *et al.*, 2006; Li, 1993). Precision calculations were performed to assess the suitability of the TLS on highly acute angles. Absolute precision and accuracy for a given device are intrinsic equipment parameters. For the terrestrial laser scanners used in

this study, the accuracy of the range and position measurements is 4 and 6 mm, respectively, within a 50 m range of observation according to the manufacturer's specifications (Leica Geosystems 2007; 2009). Measurement precision within this range, calculated as the standard deviation for the scanners is 2 mm (*ibid.*). Actual measurement precision and accuracy depend on the geometry of the measurement set-up (distance and incidence angle) and ambient circumstances, most notably air temperature gradients, soil moisture and wind. The precision and accuracy of the final output, the DEM, also depends on factors related to the object of measurement, the soil surface. It does so because of the presence of non-terrain points in the obtained point clouds. These non-terrain points are the result of the presence of non-terrain objects in the field (e.g. crop residue, vegetation) and of a structural error source typical for laser scanning technology. This structural error results from the fact that the laser beam has a certain footprint, which can result in a split range measurement where part of the beam is reflected by one surface and another part by the next, a so-called multiple return (Lichti and Skaloud, 2010). As the firmware of the scanners used is not able to recognise and resolve multiple returns, it will ultimately result in the presence of points that float between the real surface and the non-surface entity. To what degree a DEM is precise and accurate therefore depends on the answers to the following questions: (1) are artefacts and non-terrain points excluded, (2) are measurement errors discarded and (3) is the obtained average height value within the raster cell a good estimate of an actual height value?

2.2 Materials and methods

2.2.1 Study areas

The field experiments were undertaken at the locations of Bjørnebekk (+59° 39′ 9.20", +10° 50′ 12.01") and Mørdre (60° 6′ 46.61", +11° 24′ 5.43") in Akershus County, Southern Norway. As tillage is the principal source of roughness for agricultural soils, three typical pre-winter soil surface states were studied: mouldboard ploughed (Bjørnebekk 01), harrowed (Bjørnebekk 03) and winter wheat ready (Mørdre 03; seedbed prepared and wheat in early stage of germination). The mouldboard and harrowed plots are approximately 100 m^2 runoff plots situated on a sandy loam soil. The winter wheat plot is an almost 21 m^2 part of a productive field characterised by a high clay content.

2.2.2 Data collection

Two Leica High Density terrestrial laser scanners were used in this study. For the laboratory study, a Leica ScanStation 2 was used while the field plots were scanned with a Leica ScanStation C10. These scanners issue a pulsed visual green laser beam with an exit width of 4 mm that expands to 6 mm at a range of 50 m. The distance measurement thus acquired (time-of-flight) in combination with

the vertical and trunnion (horizontal) axis angles yields the desired three dimensional vector. The most relevant difference between the two machines is scan control; ScanStation 2 is operated from a laptop computer, whereas the C10 also features stand alone operation. Both scanners have of 360° fields of view in the horizontal plane and 270° in the vertical plane. Each measurement consisted of scans from four or more viewpoints in order to minimise shade and optimise coverage. The scanners were mounted on a standard surveyor's tripod, elevating the scanner 1.7 to 2.0 m above ground level. In order to facilitate the process of combining point clouds from different viewpoints, black/white targets where used around the areas of interest. Four targets were used in the Mørdre scan, whereas the larger runoff plots of Bjørnebekk required 10 targets each.

2.2.3 Data import and filtering

Point cloud pre-processing consisted of registration and clipping. Both procedures were undertaken with Leica's Cyclone cloud processing software, which was also used to operate the ScanStation 2. The registration process overlays point clouds with an algorithm that minimises the residual sum of squares. The registered clouds were then clipped to the area between the targets. Both the registered and individual (viewpoint) clouds were then exported into a non-proprietary xyz format for further processing. These untreated point clouds contain measurements of ground and non-ground points. Kraus and Pfeifer (1998) classify point measurements as terrain points, points that float within an acceptable range or non-terrain points. Filtering is required to reduce the presence of non-terrain observations to a minimum. A combined approach of segment and surface based algorithms was taken for filtering of the raw point clouds while importing them into a raster format for further calculations. Surface based filtering is an iterative procedure that assigns a relative weight to a point for the final average value within a raster cell by determining its deviation from an initial average height value of the indiscriminately imported points (Briese, 2010). These filters require parametrisation, rendering DEM quality the subject of the surveyors expertise. Kraus and Pfeifer (1998) define a weight function for the individual measurement as:

$$w_i = \begin{cases} 1 & \text{if } v_i \leq g \\ \frac{1}{1+(a(v_i-g)^b)} & \text{if } g < v_i \leq g + r_t \\ 0 & \text{if } g + r_t < v_i \end{cases} \tag{2.1}$$

where w_i is the weighing factor for point measurement v_i, g is an offset value (m), r_t is a range tolerance level (m) a and b are filter parameters (no units). A new average value in the grid cell is calculated after all points have been assigned a weight w_i and the procedure is reiterated. Since the primary types of non-ground points are the result of multiple signal returns and vegetation, it was assumed that points below the initial grid cell average were ground points (*i.e.* $g = v$). In

our adaptation of the filter, r_t was set at twice the standard deviation. Based on a series of test runs, we fixed the number of iterations at three. The values of a and b were set at 12 and 2, respectively. Segment based filtering considers the morphology of the scanned surface and discards points according to preliminary values of neighbouring raster cells (Briese, 2010). This is a particularly useful approach when, at higher resolutions, average elevation values within grid cells are dominated by non-ground objects such as vegetative material. These cells were identified by calculating the slope towards the neighbouring cells. When two or more neighbouring cells had a slope tangent greater than 1, the cell average was considered dominated by a non-terrain point. Raster import and filtering algorithms were tested and parametrised for grid resolutions from 0.010 to 0.100 m.

2.2.4 Point cloud analysis

Coverage was defined as the ratio of grid cells in the final DEM that had at least one observation after filtering over the total amount of cells in the grid. Precision was defined as the standard deviation (m) of the observations within a grid cell at the given resolution. Accuracy was defined in this study as one minus the fraction of cells that had an surface elevation estimate that differed significantly ($P<0.01$) from a reference model or other scan. Point clouds from different viewpoints were tested against each other by means of a Welch t.test for samples with an unequal variance. This approach does not provide conclusions about the absolute accuracy of a point cloud from a single viewpoint, but does inform about the accuracy of the combined point clouds. Since all the soil surfaces were scanned from four or more viewpoints, randomly chosen pairs of viewpoints were compared in this study.

2.3 Results and discussion

Table 2.1 provides an overview of the main quantitative aspects of the scans of the field plots. The number of required viewpoints for the two Bjørnebekk scans was 11, while the Mørdre site was scanned from four viewpoints. The reason that Bjørnebekk 01 has a significantly higher point density than the other sites is that it was partially scanned at a higher angular density. It was quickly found that higher densities would take too much time per viewpoint.

On average, a viewpoint was scanned in 20 to 30 minutes. This means that a 100 m² plot could be scanned in a single day. Point cloud registration and clipping took approximately four hours for a 100 m² plot. Filtering and surface model construction was a matter of seconds after the algorithms were programmed, tested and calibrated. Coverage depended much on the type of surface and indeed the resolution of the final surface model. Coverage at a resolution of 0.02 m was as good as full for the harrowed and winter wheat plots and satisfactory for the

TABLE 2.1: Basic statistics of the field plot scans. Coverage, precision and accuracy at 0.02 m resolution.

	Bjørnebekk 01	Bjørnebekk 02	Mørdre
area (m^2)	119	100	21
tillage	mouldboard	stubble	seedbed
total point count	$11.5\ 10^6$	$6.0\ 10^6$	$1.5\ 10^6$
point count per m^2	$97\ 10^3$	$60\ 10^3$	$69\ 10^3$
coverage (0-1)	0.93	1.00	1.00
precision (mm)	7.1	8.1	4.9
accuracy (-)	0.99	0.99	0.99

mouldboard plot. Coverage rates were not spatially uniform, especially on the rough and highly anisotropic surface of the ploughed plot. This can be relevant when coverage becomes irregular and gaps in the dataset emerge. Filling algorithms for instance might predominate in certain areas of the surface model. Fig.**??** illustrates the importance of terrain characteristics for coverage rate by plotting point count per grid cell against slope and aspect. As coverage is also a function of distance to the point of observation, point count values are normalised according to distance to the centre of the plots. It is mainly the highly anisotropic and very rough soil surface of Bjørnebekk 01 that clearly displays concentrated areas of high within-cell count values.

Within-cell standard deviations are lowest at the highest DEM resolution; 7.1, 8.1 and 4.9 mm for the respective plots. For rough surfaces like the cultivated soil, the distribution of the within-cell height measurements depends on surface roughness. To obtain an idea of the precision of the 0.02 m resolution DEM, Fig.2.2 shows the histogram of the observed standard deviations. All three surfaces show a distinct skewed bell shape, although the rougher surfaces appear to peak at lower standard deviations.

Two factors that are likely to display a correlation with precision are distance to the scanner viewpoint and local slope. Regression analysis did not provide conclusive evidence for this, but did seem to indicate that slope is more significant than distance to the scanner (r^2 of 0.01 and 0.18, respectively). Accuracy calculations were performed on the pre- and post-filtered point clouds in order to assess the effect of the filter algorithms and calibration. The graph in Fig.2.3 shows the outcomes of the accuracy calculations. The accuracy is high (more than 0.99) at the highest resolution used in this study. However, it quickly decreases with lower resolutions, and reaches 0.5 as early as a resolution of 0.05 m (Mørdre 03). The reason should, like with progressive precision decline, be sought in sub-grid cell roughness. Soil surface elements with dimensions smaller than the grid length will be observed from one side by one viewpoint, and from another by the next viewpoint. As grid cell size increases, the amount of sub-grid length objects will increase progressively. The simple definition of precision used in this

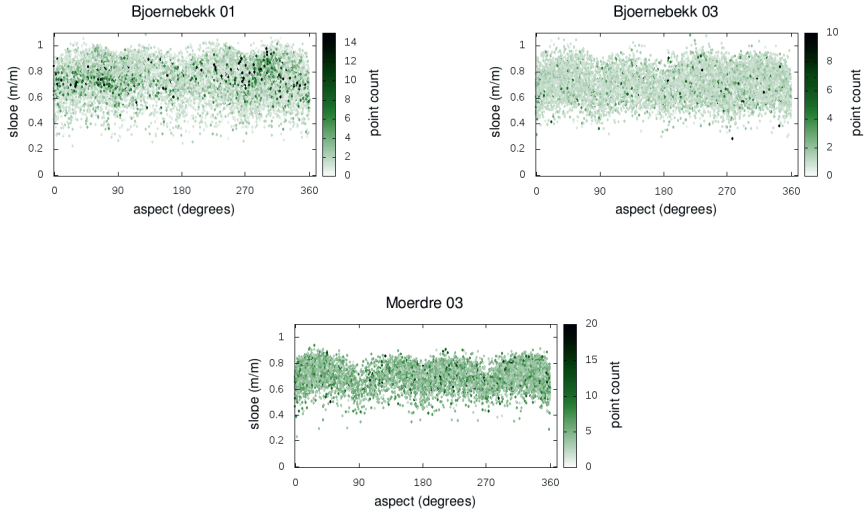

FIGURE 2.1: Average point count per grid cell (resolution 0.02 m) against aspect (°) and slope (m/m). Average point count is represented by shade intensity along a white-green-black scale (varies with field plot).

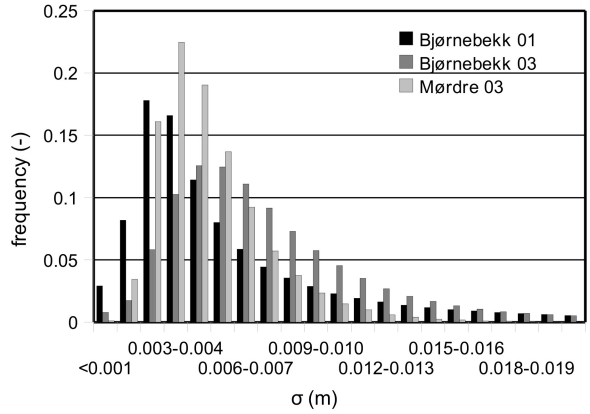

FIGURE 2.2: Grid cell frequency distribution of the precision (m) of the filtered point clouds for the field plots (resolution 0.02 m).

study therefore becomes less meaningful at lower resolutions. Better coverage, from more than one angle, namely, will decrease directional bias of the combined point cloud, but increases the likelihood of a different elevation average for scans from two viewpoints.

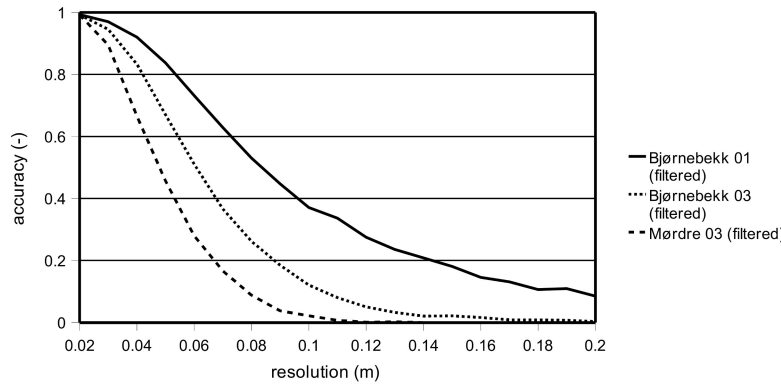

FIGURE 2.3: Accuracy as a function of DEM resolution.

Point cloud filtering proved to improve the accuracy of the final DEM significantly in the domain of higher resolutions. For resolutions up to 0.06 m, the accuracy of the DEMs made with filtered point clouds was up to twice that of the DEMs from the unfiltered point clouds. Absolute differences however were small. The improvement ratio for the Bjørnebekk 01 site is markedly higher than those for the other two plots. This can be explained by 'floating', or non-terrain

points. The higher and steeper the elevation drops in front of and behind a peak or indeed a ridge on the surface, the larger the error as a result of the presence of floating non-terrain points would be.

2.4 Conclusion

The availability of a TLS technology allows for the measurement of a series of relatively large on-field soil surfaces at fairly high resolutions in a way that no other known type of equipment can. Data capture, pre-processing and DEM derivation are rapid and fairly straightforward exercises and are easily automated. When proper care is taken with the parametrisation of the point cloud filtering algorithms, the accuracy of the measurements and final DEM can be considered excellent, especially at higher resolutions. Both precision and accuracy rapidly decline with decreasing resolutions. The presence of sub-grid cell sized roughness elements at the soil surface is the most likely explanation for this structural phenomenon. This implies that when TLS is the sole means of soil surface measurement data, care should be taken with the choice of resolution. The choice for a higher resolution has implications for the operation of the scanner; higher angular densities are required in order to obtain a proper coverage rate. When multi-temporal recordings are undertaken, e.g. for soil roughness dynamics or erosion/deposition processes, viewpoints should be chosen so that the areas of interest, i.e. there where runoff concentrates, are sufficiently covered. Terrain models derived from TLS measurements are generally good, if proper filter settings are applied. The availability of high resolution spatial data further raises the question of how to deal with the non-normal distribution of measured points at lower resolutions. Further work is required to identify and moderate bias as a result of over- and under-represented slope and aspect classes. Finally, when the DEM will be used for hydrological simulations, it is worthwhile exploring the merit of a multi-layer DEM that does not only store average elevation, but also slope, aspect and roughness as derived from the raw instead of interpolated point clouds.

Chapter 3

Quantifying the dynamics of microtopography during a snow melt event

Abstract

Knowledge of soil microtopography and its changes in space and over time is important to the understanding of how tillage influences infiltration, runoff generation and erosion. In this study, the use of a Terrestrial Laser Scanner (TLS) is assessed for its ability to quantify small changes in the soil surface at high spatial resolutions for a relatively large surface area (100 m^2). Changes in soil surface morphology during snow cover and melt are driven by frost heave, slaking, pressure exertion by the snow pack and overland flow (erosion and deposition). An attempt is undertaken to link these processes to observed changes at the soil surface. A new algorithm for soil surface roughness is introduced to make optimal use of the raw point cloud. This algorithm is less scale-dependent than several commonly used roughness calculations. The results of this study show that TLS can be used for multi-temporal scanning of large surfaces and that small changes in surface elevation and roughness can be detected. Statistical analysis of the observed changes against terrain indices did not yield significant evidence for process differentiation.

Published as: R.J. Barneveld, S. E. A. T. M. van der Zee and J. Stolte, 2019. *Quantifying the dynamics of microtopography during a snowmelt event.* **Earth Surface Processes and Landforms** 44, p.2544– 2556.

3.1 Introduction

Soil microtopography can be defined as soil surface morphology at the scales of the aggregate and soil clod, including rills, vegetation and washed on sediments (Ploeg *et al.*, 2011). Soil surface morphology, in particular hydrological connectivity and surface storage, is an important driver for hillslope response to rainfall (Appels, Bogaart, and van der Zee, 2011; Frei and Fleckenstein, 2014; Thompson, Katul, and Porporato, 2010) and snow melt. Its importance for the understanding and simulation of overland flow processes has long been recognised (Römkens and Wang, 1987). As a derived surface morphological characteristic, random roughness (RR, m) is an important variable in many overland flow and erosion models. RR can be used to estimate a roughness factor such as Manning's n (e.g. (De Roo, Wesselink, and Ritsema, 1996; Deng, De Lima, and Singh, 2005; Jinkang *et al.*, 2007)) or as a variable in the energy gradient in hydraulic equations (Fiedler and Ramirez, 2000; Esteves *et al.*, 2000). Some models treat soil surface roughness as a dynamic parameter that changes during an event or simulation period (Loon, 2002; Kirkby *et al.*, 2008). Another derived parameter, depression storage capacity (DSC, m) is used in the water balance of several models to determine a lag period before an area starts to produce overland flow (e.g. (De Roo, Wesselink, and Ritsema, 1996)). Temporary storage and infiltration of overland flow in sinks also determines how hydrological connectivity develops during a runoff event (Darboux and Huang, 2001; Peñuela *et al.*, 2016; Wang *et al.*, 2018). At the plot and field scales, quantitative knowledge of microtopography therefore is a key factor for understanding and simulating overland flow.

Microtopography changes over time due to several processes. On agricultural soils, the most significant of these are tillage, precipitation impact, overland flow, erosion and sedimentation, slaking and, in cold climates, frost heave.

Much work has been done on the quantification of roughness development as a result of rainfall and surface runoff (Zobeck and Onstad, 1987; Cremers and Dijk, 1996; Römkens and Wang, 1987; Haubrock *et al.*, 2009). Surface roughness concerns morphology at the spatial scale of small aggregates down to soil particles. Roughness at this scale is not directly included in catchment scale runoff models, but is relevant for runoff and erosion models developed for simulations at high spatial resolutions, i.e. cm scale (Fiedler and Ramirez, 2000; Esteves *et al.*, 2000). This roughness influences the infiltration process because it is related to surface storage and crust formation and decreased initial infiltration rates as a result thereof (le Bissonnais and Singer, 1992; le Bissonnais and Singer, 1993). Surface roughness and its change over time are also relevant for studies that utilise Synthetic-Aperture Radar (SAR), where they are used to interpret backscatter (Louis *et al.*, 2004; Snapir, Hobbs, and Waine, 2014).

Roughness metrics are strongly dependent on the spatial resolution at which the calculations are carried out (Kamphorst *et al.*, 2000). This can be problematic in multi-temporal measurements if the spatial scope of the expected changes is

unknown. Algorithms that show a high correlation between slope gradient and roughness are less likely to distinguish sub-grid cell roughness elements from the overall slope within this grid cell (see Section 2.3 of this thesis).

Little is reported about roughness development during snow cover and melt (Blackburn, Pierson, and Seyfried, 1990). Slaking, or sloughing, is a process of smoothing out small elements at the soil surface. It is a form of soil structure decline, driven by for example the impact of frost-thaw cycles. No studies were found to report on the magnitude or characteristics of slaking during snow cover and subsequent melt.

The quantification of erosion and sedimentation processes at the level of microtopography has been reported in laboratory studies (Helming, Römkens, and Prasad, 1998; Rieke-Zapp and Nearing, 2011; Moritani *et al.*, 2010; Bogner *et al.*, 2012) and field studies at limited spatial scales (Vidal Vázquez, Miranda, and Paz-Ferreiro, 2010; Haubrock *et al.*, 2009). (Eltner, Maas, and Faust, 2018) use a combination of Unmanned Aaerial Vehicles (UAV) and TLS to quantify erosion and sedimentation at the hillslope scale.

When conditions are characterised by frost and high soil moisture conditions, the process that is likely to have the largest impact on surface elevation change is frost heave. Frost heave rates can be several orders of magnitude higher than erosion and sedimentation rates. Beskow (Black and Hardenberg, 1991) reports road heave values in Sweden of 0.6 m. The same study indicates that frost heave rates can be 0.1 mm per hour in a fine sandy soil. Bronfenbrener (Bronfenbrener, 2009) reports values of 3.7 mm/day for the same medium in an experimental set up. Hermannson (Hermannson and Spencer Guthrie, 2005) measured maximum heave values between 0.20 and 0.25 m during a winter season at a field site. While progress in the theoretical understanding and modelling of frost heave is ongoing (Peppin and Style, 2013), the spatial heterogeneity of the driving forces and soil physical parameters limits the possibilities for simulations at high spatial resolutions in and for field conditions.

Typical for most soil roughness and erosion and sedimentation studies is that the processes affecting microtopography are isolated or that the magnitude of the lesser processes is assumed small in comparison to the main process studied. In field studies where the comparative magnitudes are unknown, no conclusions about the contribution of the individual processes to surface morphology dynamics can be drawn without explicitly addressing process differentiation. With the exception of Eitel *et al.* (2011), Vidal Vázquez *et al.* (2010) and Kaiser *et al.* (2018), little is known about the correlation between the changes to microtopography over time and their correlations with the processes that drive them.

Obtaining quantitative information about changes in soil surface morphology can only be undertaken by means of multi-temporal georeferenced measurements of a certain area of interest. Soil microtopography can been studied with several

different technologies, ranging in resolution from pin-frames (several centimeters) to terrestrial laser scanners (TLS, sub-centimeter, citeauthorJester2005, 2005). More recently, Thomsen *et al.* (2015) provide a comparison of these methods with regard to their ability to quantify surface roughness. Photogrammetric methods, most notably Structure-from-Motion (SfM) techniques, are increasingly being used to quantify soil surface roughness on agricultural soils (Gilliot, Vaudour, and Michelin, 2017) and its development over time (Snapir, Hobbs, and Waine, 2014; Bauer *et al.*, 2015; Hänsel *et al.*, 2016). One-dimensional laser scanners have been in use for almost thirty years (Huang and Bradford, 1992), and continue to do so (Martinez-Agirre, Álvarez-Mozos, and Giménez, 2016), but their frame mounting limits the spatial extent of the measurable object. Most other methods to obtain three-dimensional datasets are either intrusive or can only cover limited surface areas. They are therefore not suited for multi-temporal measurements at the larger plot scale.

Terrestrial laser scanners have been used to characterise soil surfaces at different resolutions. Barneveld *et al.* (2013) and Nield *et al.* (2013) indicated that TLS can be used to obtain high-resolution digital elevation models (DEM) of good quality for areas over 100 m^2. Eitel (2011) correlated TLS measured soil roughness values with runoff characteristics and the quantification of erosion and deposition for artificial runoff events. The maximum value of surface lowering obtained in their study was 6.0 10^{-2} m. Overland flow velocities as a result of snow melt during early spring in southern Norway are likely to be much smaller than in Eitel's study. The effects on microtopography can therefore be expected to be smaller too. Examples of gully erosion monitoring with multi-temporal TLS can be found in (Goodwin *et al.*, 2016) and (Perroy *et al.*, 2010). (Hohenthal *et al.*, 2011) provide an overview of how airborne and terrestrial laser scanning can be used to monitor river bed dynamics. Gully development and fluvial dynamics, however, result in relatively large changes to the soil surface or stream profile (0.01 m and over). (Eltner and Baumgart, 2015) report that small elevation changes as a result of erosion and deposition can be detected by multi-temporal TLS. The smallest changes detected reliably in their study are 1.5 10^{-2}m. With the exception of (Marx *et al.*, 2017), no studies of TLS measurements of surface elevation changes smaller than a centimeter have been found for on-field experiments.

Data quality in any multi-temporal measurement must be such that errors and uncertainties are smaller than the expected changes to be observed (Williams, 2012). Errors that can be expected with the use of TLS for creating DEMs of Difference (DoD) can be classified broadly into measurement inaccuracies, misalignment of subsequent terrain models and miscellaneous errors. Measurement accuracy and precision primarily dependent on the equipment used. Misalignment between elevation models occurs when reference points move during the time between measurements. The most notable miscellaneous error that may influence the quality of the DoD for soil surfaces can be vegetation growth.

The objective of this study was to quantify changes to the surface of an agricultural soil at the plot scale in field conditions typical for the spring climate of southern Norway. The main challenge with comparing DEMs is that fixed reference points for calibration and quality assurance are usually not available on agricultural soils. As a consequence, there is no fully reliable method to differentiate measurement bias and noise from actual soil surface changes. This study hypothesises that changes in soil surface elevation and roughness reflect the processes that have driven these changes. Slaking, erosion and deposition and frost heave are typically not randomly distributed over the surface area of an agricultural field. The primary objective of this study is to correlate changes in the DEM to the processes that drive these changes locally. The secondary objective is to define an algorithm for RR that is less sensitive to spatial resolution and local slope.

3.2 Materials and methods

3.2.1 Experimental site and event

The experiment was carried out on a runoff plot situated at Bjørnebekk (+59° 39′ 9.2″, +10° 50′ 12.01″) in Akershus County, southeastern Norway. The soil type at the location is a silty clay loam. Since tillage is the principle source of roughness for agricultural soils, a mouldboard ploughed surface, typical for wheat fields in Norway, was studied. The plot is 5.5 m wide and 21 m long, in the direction of the slope. The slope shape is largely linear, with an average inclination of 12.4%. Tillage was undertaken in late September 2010, in the parallel to the slope. In the course of the winter 2010-2011, a snow cover of 0.52 m of depth on average, or 0.147 m snow water equivalent (SWE, m), accumulated. Snow melt occurred between March 17^{th} and April 9^{th}. Peak melting rates occurred between March 22^{nd} and 24^{th}. During this period, the development of the snow pack was monitored by taking snow depth and SWEmeasurements at around 12:00 AM. Depth was monitored with a ruler, while SWE was measured by taking and weighing cores of a known volume. Both the depth and SWE of the snowpack were spatially homogeneous throughout the winter and melting periods. Tipping bucket counts of the runoff collector of the plot were taken simultaneously (Fig.3.1). The maximum melting rate recorded was 1.9 mm hr^{-1} (SWE) on March 24^{nd} at 1:30 PM. The maximum runoff rate on the same day was 3.6 mm hr^{-1} at 3:00 PM. Note that the soil temperature drops considerable after the bulk of the snow pack melted on March 24^{th}. Melting continued gradually without inducing runoff in the same order of magnitudes as on March 24^{th}.

3.2.2 Soil surface elevation

The study plot was scanned in mid October 2010, several weeks before the first snow. No precipitation occurred between scanning and the beginning of snow

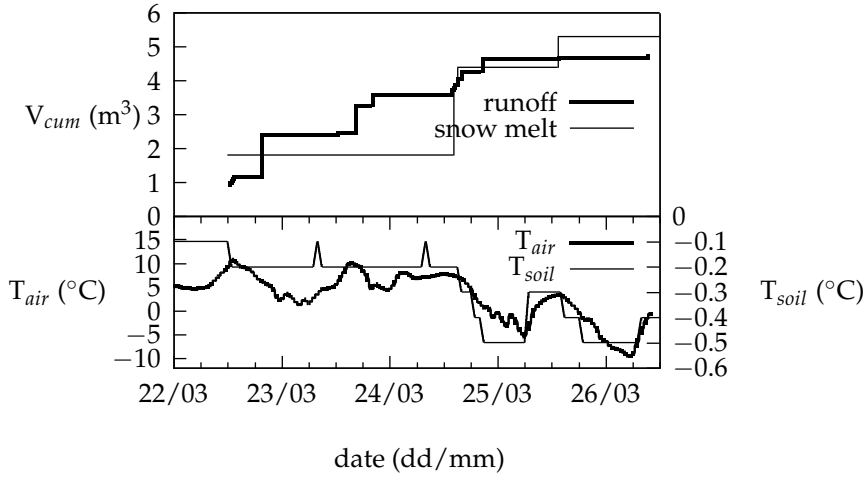

FIGURE 3.1: Observed cumulative snow melt and plot runoff and air temperature dat 2.0 m above ground and soil temperature at 0.10 m depth. The spikes in soil temperature on March 23^{rd} and 24^{th} reflect the resolution of the thermometer (0.1°C) rather than actual events.

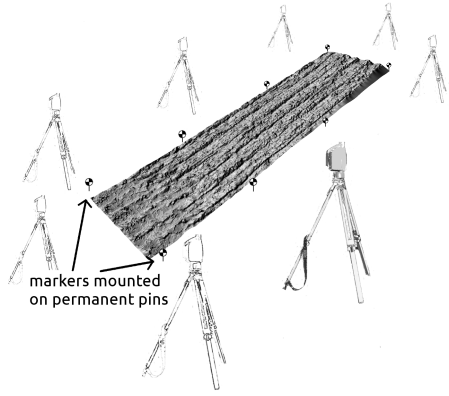

FIGURE 3.2: TLS field set up, with the pin-mounted markers on the boarders of the runoff plot and six of the eight view points.

cover. A next scan was carried out less than a week after all snow had melted completely in the second week of April 2011. Again, no precipitation occurred between the completion of the melting process and the TLS scan.

Soil surface elevation data were obtained with a Leica ScanStation2 terrestrial laser scanner (TLS). This scanner issues a pulsed green laser signal to measure distance (time-of-flight). It records a single return signal and this, combined with a vertical and horizontal angle, yields a three-dimensional vector (Vosselman and Maas, 2010). Its maximum scan rate is 50,000 points per second (Leica Geosystems, Inc., 2007). The scanner was mounted on a tripod, so that the effective scanning height was between 1.7 and 2.0 m above ground level (Fig.3.2). A series of scans from eight view points around the plot were required to ensure sufficient coverage to create a reasonably fine DEM with a grid cell length of 0.02 m. With the eight viewpoints, shading due to the ploughing ridges could be minimised. Milenkovic, Pfeifer, and Glira, 2015 quantify the importance of scan geometry, and conclude that roughness features smaller than 5.0 10^{-2} are underrepresented when a soil object is covered by only a single scan. Georeferencing the viewpoints and the DEMs at the different points in time was carried out by installing 10 iron pins of 0.60 m length along the sides of the plot. The pins were driven into the ground for at least 0.40 m to avoid frost deformation or displacement. It was confirmed that the pins were not bent or otherwise disturbed after snow melt. In the absence of any unmoveable structures in the direct vicinity of the runoff plots, changes in the exact positions of the pins could not be ruled out. Detachable, high contrast visual targets were mounted on the pins during the TLS measurements. The total plot size was 115.5 m^2 and the number of points of the combined point clouds totals 11.5 million. The average point density therefore was 10.0 points cm^{-2}.

3.2.2.1 Point cloud registration and error analysis

The goal of this study was to quantify differences in elevation and surface roughness between two terrain models. The ability to detect these differences depends on their magnitude relative to the errors associated with data capture and post-processing. The precision and accuracy of the TLS depend on the equipment used, atmospheric and light conditions, the scanning geometry and the object of the measurement (Soudarissanane *et al.*, 2011). The principle sources of error are mixed pixels, where the laser beam gets multiple returns because of partially reflecting objects, errors in co-referencing multiple scans, and inaccuracies in the time-of-flight recordings.

The raw point clouds were registered with Leica Cyclone (v. 7.0, Leica Geosystems, Inc.). Point cloud registration generally consists of two steps: coarse and fine registration. Coarse registration in the Cyclone software package consists of a transformation of successive point clouds, so that they have a consistent geometry in a certain coordinate system. The parameters for these transformations are calculated by manually identifying common features in the paired point clouds. In our case, these were the cross-points in the reference targets that were placed along the boundary of the plot. Fine registration is then undertaken by a bundle adjustment algorithm (Triggs *et al.*, 2000), during which further local transformations are undertaken until the residual error between paired point clouds reaches a minimum. A similar sequence of transformations is undertaken for the registration of the multi-temporal point clouds. Here, the possibility that the reference targets have moved in four months between the measurements introduces an additional potential source of errors. The algorithms for accuracy assessment used in Cyclone were not known to the authors at the time of writing. Moreover, it is unclear how the accuracy metrics generated by the software are influenced by the complex geometry of the soil surface. A registration accuracy assessment is therefore proposed that takes into account the effect of grid cell size and the roughness of the terrain. The method is based on two premises:

1. The average horizontal distance between points within a grid cell is a function of the cell dimensions, or resolution, and
2. The average vertical distance between points within a grid cell is a function of the surface roughness.

As a logical consequence, the average point-to-point distance (d_{P2P}, m) in a grid cell of size zero without roughness is equal to zero.

The final point clouds, i.e. including the measurements from all the viewpoints, were tested for their residual error in the following way. First, the average d_{P2P} within a grid cell and the standard deviation of the elevation (σ_z^2, m) were calculated. This was done for grid cell lengths between 0.01 and 0.10 m, with 0.01 m increments. The results for the different cell sizes were combined into a single file, with the average d_{P2P} as the dependent variable and σ_z^2 and the cell size as

the independent variables. A non-linear regression was carried out in the R statistical package (R Development Core Team, 2008). The model to be fitted was given by:

$$\overline{d}_{P2P} = \epsilon + a \cdot l_{grid} + (\sigma_z^2)^b \tag{3.1}$$

Following the premises 1 and 2, ϵ was taken to be the compound error as a result of data capture and post-processing. The regression was carried out by assigning grid size-dependent weights, since the amount of observations decreases quadratically with increasing grid sizes. The regression model was then compared to the terrain indices, described in Section 3.2.3 in order to test for any spatial bias.

3.2.2.2 Point cloud filtering

The raw point cloud contains non-ground points that are the result of the presence of vegetative material and mixed pixels. The registered point clouds were filtered to discard these. Non-ground points were identified by the iterative application of an algorithm proposed by (Kraus and Pfeifer, 1998). The algorithm is designed for filtering vegetation from LIDAR data of forested areas, but is also able to remove mixed pixels, vegetation and other non-ground elements in a TLS point cloud. The algorithm assigns a weight to individual points proportional to the vertical distance to an initial estimate of the ground surface level (Eq. 3.2). This estimate is then used in the next iteration for the new vertical distance of each point to the new average.

$$w_i = \frac{1}{1 + (a(z_i - \sigma_z)^b)} \tag{3.2}$$

where w_i is the weight assigned point measurement z_i, σ_z is the standard deviation of the vertical distances within the grid cell (m) and a and b are dimensionless parameters. The values of a and b were set at 12 and 2, respectively. For b the value is based on the original research by (Kraus and Pfeifer, 1998). The value of a was set at 12, which is higher than the value proposed by (*ibid.*) who used 4. This ensures a sharper vertical cutoff in Eq. 3.2, which makes the algorithm faster on surfaces with sparse vegetation. Points lower than the initially estimated average elevation within the grid cell, and those higher than $\bar{z} + 2 \cdot \sigma_z$ are discarded in order to reduce the number of iterations. Filtering was undertaken by means of a raster grid with a cell length of 0.02 m. Iteration stops when the difference between the current and the new estimated average surface elevation is below a certain threshold. The number of iterations typically required in the absence of vegetative material is two to four (Barneveld, Seeger, and Maalen-Johansen, 2013).

TABLE 3.1: Parameters for process differentiation

process	*index*	*change*
slaking	slope, aspect, ridge/furrow	ΔRR<0
overland flow	catchment area, ridge/furrow	Δz<0
snow pack pressure	slope	ΔRR<0
frost heave	-	Δz >0
erosion/deposition	flow convergence index	Δz
	sedimentation index	Δz
	ridge/furrow	Δz

3.2.3 Process differentiation

Without the presence of a reference surface, a direct distinction between observed changes and measurement error cannot be made. Besides the random error of the measurement itself, the main error source for multi-temporal comparisons of a soil surface is expected to be caused by misalignment of the DEMs at the different moments. Errors in vertical georeferencing would result in overestimations of erosion or deposition values across the entire surface area. Referencing errors in the horizontal plane would result in patterns that do not match terrain characteristics like local slope and catchment area. Differentiating measurement errors from actual changes in soil surface therefore requires a conceptual model of what these changes entail and where in the runoff plot they are expected to be more pronounced. For this purpose, a series of structural topographic indices were calculated for comparison with the observed changes in surface elevation and roughness and the quantification of frost heave (Table 6.1). These indices are calculated for each grid cell in the DEM and then compared to the observed changes in surface elevation and roughness in that particular cell. The DEM used for the calculations of the indices was created by importing the filtered point cloud into a raster grid in SAGA GIS (Conrad, 2001), with a cell length of 0.02 m. The correlations between terrain index and observed roughness or elevation change were tested by means of linear regression analysis in R (R Development Core Team, 2008), and the coefficients of determination of these linear functions.

3.2.3.1 Surface roughness development

In the absence of any impact of rain drops, the development of surface roughness during snow cover and melt is driven by slaking (Blackburn, Pierson, and Seyfried, 1990), overland flow and possibly the pressure exerted by the snow pack. All three are expected to lead to a reduction in surface roughness, although (Eitel *et al.*, 2011) suggest the emergence of new roughness elements in zones of concentrated flow, mainly due to new incisions in the soil surface.

Surface roughness is a scale-dependent quantity (Vidal Vázquez, Vivas Miranda, and Paz González, 2005). The scale at which the relevant changes in roughness

occur cannot always be defined precisely. Govers *et al.* (Govers, Takken, and Helming, 2000) classify four scales for microtopography, where soil roughness is in the range of the individual soil aggregate. However, the order of magnitude would vary between several millimetres and several centimetres. Choosing a spatial resolution is required by all methods for the calculation of soil roughness. The sensitivity of the final result to this choice, however, varies with the method. A much used roughness parameter, random roughness (Doren and van Linden, 1986), is defined as a comparison of the elevation value in a central cell with the values in the eight neighbouring cells. This method is sensitive to the resolution at which the calculations are done and can be expected to correlate strongly with the local slope. Local slope gradients in a high resolution DEM of a ploughed agricultural soil can be well over 100 %. The implication is that roughness elements smaller than the slope multiplied by the grid cell length will not be recognised. The roughness calculations in this study therefore were based on the vertical distance of the individual points of the filtered point cloud to an fitted reference plane, rather than average values within the limits of a raster cell.

In order to minimise the scale-dependency of the calculation, three methods to define a reference plane were tested for their scale dependency. All three use the point cloud and are based on the standard deviation of residual topography (Brubaker *et al.*, 2013), where the average distance from the points to a reference level is a measure for roughness. The algorithms were programmed in C++.

First, a maximum scale is chosen and used as the cell size for the calculations. Any roughness feature larger than this scale will be ignored, or at least underrepresented. The average distance of the individual points within a grid cell to a reference plane is defined to be a measure for the local soil roughness. In the first method, the reference plane is defined as a horizontal plane with the same elevation as the geometric centroid of the points contained by the grid cell (Fig.3.4a), and random roughness is given by:

$$RR = \frac{1}{n}\sqrt{\sum_{i=1}^{n}(z_i - \bar{z})^2} \tag{3.3}$$

where RR is random roughness, z_i is the elevation of point i (m), n is the number of observations, and $\bar{z}$ is the elevation of the centroid (m).

In the second method, the reference plane is defined by the vectors between the centroid C and two points in the point cloud (Fig.3.4b). These two points, A and B, are identified by first searching for point with the largest horizontal distance to the centroid. After that, the point with the largest distance to the centroid in the adjacent quadrant (in the x or y direction) is identified (Fig.3.3). Point pairs were selected from adjacent quadrants rather than diagonals in order to minimise the likelihood that they are situated on the same line (i.e. in opposite directions from the centroid). The vectors $\vec{CA}$ and $\vec{CB}$ are then used to calculate the point-normal

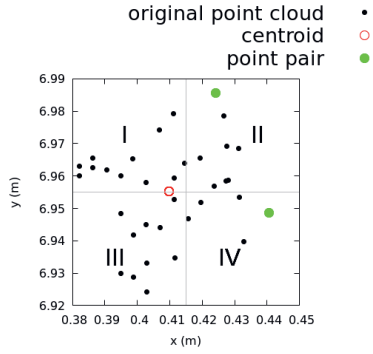

FIGURE 3.3: Selection of points in a 5 by 5 cm grid cell to define a single reference plane per grid cell. Initially, the furthest point is identified in quadrant I. The second furthest in an adjacent quadrant is identified in quadrant IV.

equation of the reference plane in the form of:

$$ax_i + by_i + cz_i + D = 0 \tag{3.4}$$

where a,b, c and D are constant for the thus defined plane, on which point (x_i, y_i,z_i) is situated (Fig.3.4b). The proposed measure for soil roughness is the orthogonal distance from point i in the point cloud to this projected plane, given by:

$$RR = \frac{1}{n}\sum_{i=1}^{n}(\hat{z} - z_i) = \sum_{i=1}^{n}\frac{c_x(x_i - A_x) + c_y(y_i - A_y) + D}{-c_z} \tag{3.5}$$

where $\hat{z} - z_i$ is orthogonal distance between the plane and the point, and $(c_x\ c_y\ c_z)$ is the dot product of $\vec{CA}$ and $\vec{CB}$.

The third method is similar to the second, but selects four pairs of points in each grid cell quadrant, and subsequently defines four separate reference planes (Fig.3.4c). Eq.3.5 and 3.4 are then applied to all of the four planes, depending on the position of point i within the grid cell. This method is expected to follow the actual point cloud more closely than the method with a single equation of a plane, and therefore to be less scale-dependent.

The three methods were applied at grid cell lengths from 0.01 to 0.10 m (0.01 m increments) and 0.12 to 0.20 m (0.02 increments) in order to quantify their sensitivity to scale and dependence of local slope.

The magnitudes of the effect of slaking, overland flow and pressure are not expected to be spatially homogeneous. Slaking is expected to be more pronounced on steeper slopes, where the centre of gravity of the aggregate or clod has a large lateral offset from the overall slope plane. Increased exposure to the sun increases

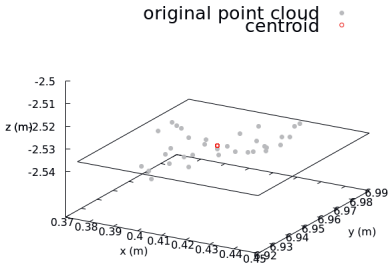

(A) Average elevation

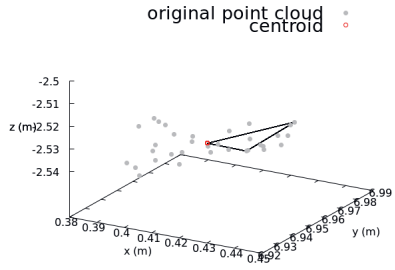

(B) One inclined plane

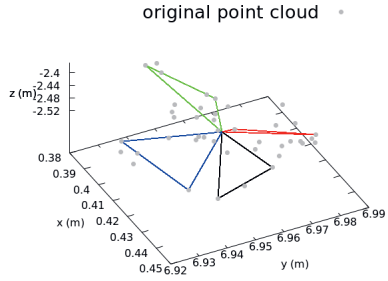

(C) Four inclined planes.

FIGURE 3.4: Three methods to define a plane for reference elevation. Fig (a) shows a horizontal plane, based on the elevation of the centroid, (b) shows the vectors used to define a single plane and (c) shows the vectors for the definition of four separate planes.

the amplitude of diurnal frost-thaw cycles, and is expected to accelerate the slaking process.

Runoff processes occur everywhere, but higher shear stress values are expected to result in smoother surfaces. Only in situations were small, i.e. sub grid cell size, incisions would occur, roughness would increase. The weight of the snow pack is expected to result in higher shear stress values on aggregates protruding from steeper slope segments. The changes in roughness over time (ΔRR) were compared to local slope values, an index that describes the relative position in the plough ridge/furrow system, and an aspect indicator. Local slope values S (m m^{-1})were calculated as follows:

$$S = \sqrt{{S_x}^2 + {S_y}^2} \tag{3.6}$$

Where the slope in the x-direction S_x is given by:

$$S_x = \frac{1}{n} \sum_{i=1}^{n} (\frac{z_i - \bar{z}}{dx_i}) \tag{3.7}$$

Where z_i the elevation in neighbouring cell i, $\bar{z}$ is the average elevation in a 3 by 3 cell window and dx_i is the horizontal distance from the centre of the window to the centre of the ith cell. S_y is calculated in a similar way. The position in the ridge-furrow system is a comparative predictor for the amount of runoff that can be expected to pass a grid cell.

The DEM was used to calculate the dimensionless Ridge Furrow Index, I_{RF}, a topological indicator that compares the elevation values within a moving window to the value of the central cell. In this study, the index is used to describe a location's position in the ridge-furrow system typical for mouldboard plouging. I_{RF} is calculated as:

$$I_{RF} = n_{higher}/n_{lower} \tag{3.8}$$

where n_{higher} is the number of cells with higher elevation values and n_{lower} the number of lower values within the window. The window size should be chosen so that it covers the full ridge and furrow system only once. In this study, the size of the moving window was set at 0.30 m. In this way, grid cells on the ridges get values close to one, while those in the bottom of the furrows get values close to zero. The I_{RF} algorithm was implemented in a C++ programme.

Since slaking is a frost/thaw driven process (Kværnø and Øygarden, 2006), a grid cell's orientation towards the sun will determine the daily temperature amplitude and maximum value. The Ridge Furrow index is expanded to include a categorical aspect index. The Ridge Furrow index (I_{RF},) differentiates between north and south facing slopes in combination with the position either on the plough ridge or in the furrow, to correct for exposure to sunlight. It is determined by classifiying the terrain model into four classes: north or south facing and on the ridge or

in the furrow, so that:

$$I_{RF} \begin{cases} furrow \cap north & 1 \\ furrow \cap south & 2 \\ ridge \quad \cap north & 3 \\ ridge \quad \cap south & 3 \end{cases} \tag{3.9}$$

Locations with I_{RF} values below 0.5 were classified as furrows, and higher then 0.5 as ridges.

The sub-sets were analysed for normality and variance. Two-tailed analyses of variance and paired t-tests for samples with equal variance were carried out in the R statistical package (R Development Core Team, 2008) to assess whether the ΔRR was different for the four I_{RF} classes.

3.2.3.2 Frost heave

What is known about frost heave is that it is unlikely to occur in small restricted areas. Although no literature was found on the minimum extent at which the process is observable, it can be assumed that heave patterns on a mouldboard ploughed surface occur at scales similar to or larger than the ridge-furrow topography in our experimental plot. The most appropriate procedures to differentiate smaller from larger scale processes in terrain analysis is DEM de-trending or, the opposite, smoothing (Vieux, 1993). The lower limit of an appropriate window size is given by which topographical features are to be ignored. The ridge-furrow system as a result of tillage is the largest feature to be smoothed out. The window size therefore should be 0.50 m or larger. The presence of ridges and furrows creates a boundary effect when a moving window is applied. Preliminary tests with artificial data showed that the magnitude of this boundary effect is in the order of centrimeters. This is larger than the expected changes in surface elevation. A field margin with a width of half the window size was therefore ignored in the final calculations. In order to rule out effects of scale, detrending was carried out with different moving window sizes (0.5 m to 2.5 m with 0.5 m increments).

To obtain the magnitude of frost heave, the detrended DEM of October 2010 was subtracted from the detrended DEM of April 2011. To rule out the possible effects of sedimentation, only the plough ridges ($I_{RFA} = 1$ and $I_{RFA} = 2$) were used in the calculation. Peppin and Style (2013) show that all explanatory and predictive models of frost heave pressure have water content as the principal variable; either directly or through a water pressure term. Several studies (McNamara *et al.*, 2005; Grayson, Western, and Chiew, 1997) report a soil moisture gradient at the end of a wet season that is positive in the direction of the slope. Soil water content in the experimental plot was not measured. It can however be assumed that, under the wet conditions of autumn 2010, soil water content would show a positive trend in the downward direction.

3.2.3.3 Soil detachment and deposition

The quantification of the erosion and deposition process at the spatial resolution used in this study by means of simulation would require dynamic hydraulic modelling. In order to obtain an accurate sediment budget for a simulation at plot scale, such a model would require meticulous calibration against measured data (e.g. (Fiedler and Ramirez, 2000; Esteves *et al.*, 2000)). At plot scale, the spatial variability of the parameters that drive soil surface deformation can be expected to be considerable. Instead of attempting a comprehensive simulation of the runoff and erosion processes, two terrain indices, a convergence and a sedimentation index, are proposed to link the observed change in soil surface elevation with overland flow. Each of the indices is based on a characteristic assumption. The first index is based on the assumption that sediment is more likely to be deposited in cells where overland flow is diverged. Sediment transport capacity of overland flow is an exponential function of flow depth and velocity (Singh, 1997), so when runoff is distributed over a larger plane, the amount of particles it can carry is reduced. Positive values of the convergence index, CI (unitless), indicate converging flowlines, while negative values diverging lines. Therefore, a negative correlation is expected between CI and surface elevation change, e.g. the more flow diverges, the more likely is sedimentation to occur. CI was calculated with the Convergence Index module of SAGA GIS (Conrad, 2001). The second index looks at the vertical profile along the stream lines. Deposition is more likely to be predominant on concave sections with a small slope and erosion is more likely on convexities with larger slopes. A sedimentation index, SI ($^{\circ}m^{-1}$) was defined based on the assumption that sedimentation is more likely to occur at less steep slopes and in slope segments with decreasing slopes. SI was therefore defined as the product of S (here in $^{\circ}$) and slope curvature, S' ($^{\circ}m^{-1}$).

$$SI = -S' \cdot S \tag{3.10}$$

Figure 3.5 shows the general principle of the sedimentation index on a unitless slope. Besides CI and SI, the correlations between both slope and curvature and surface elevation change were also determined. Since a large part of the surface area consists of sinks, the calculations were carried out for sink and non-sink cells in the DEM. The terrain indices were used only in the non-sink areas. For the sink areas, the net surface elevation change was calculated. A positive value is expected since the reduced flow velocities would result in decantation during the snow melt event. The net change in surface elevation $\Delta_n z$ was calculated as the measured difference in surface elevation minus the change in elevation that resulted from frost heave. Correlations between observed net elevation change and the terrain indices were expressed as the Pearson correlation coefficient, r, and by means of fitting linear regression functions.

Finally, the DEMs were analysed for concentrated forms of erosion. Overland flow is likely to result into incisions in the soil surface that will shorten the average length of flow paths. These changes were detected by comparing average

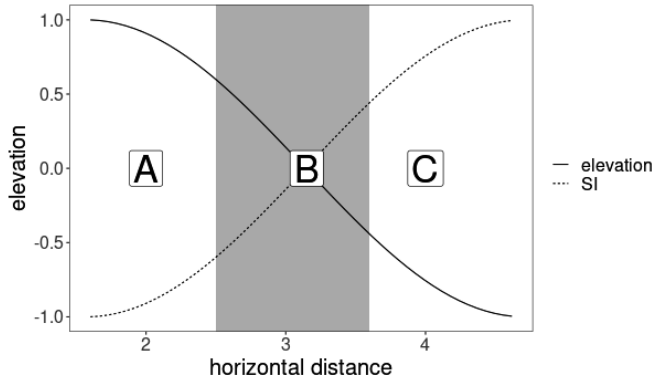

FIGURE 3.5: The general principle of the sedimentation index, SI. A designates an erosive zone, B a transitional zone and C a sedimentation zone.

flow length values and local changes in catchment area. Since the erosive force of runoff is a function of flow velocity and discharge, these incisions are expected to be more pronounced towards the lower end of the runoff plot.

3.3 Results

3.3.1 Point cloud co-registration and filtering

The number of points that were discarded during the filtering processes amounted to 34.1% for the October scan, and 34.2% for the April scan. The subsequent decrease in residual error of the final DEMs is given in Table 3.2. Eq.3.1

TABLE 3.2: Residual errors (ϵ) before and after filtering.

scan	ϵ before filtering	ϵ after filtering
October	$6.2\ 10^{-4}$ m	$6.0\ 10^{-4}$ m
April	$9.0\ 10^{-4}$ m	$3.7\ 10^{-4}$ m

was used to map the predicted residual error $E[\epsilon]$ as a function of d_{P2P} and $\sigma 2_z$ for $l_{grid} = 0.02\,m$, with the corresponding fitted parameters a and b, so that:

$$E[\epsilon] = d_{P2P} - 9.20 \cdot 10^{-3} - (\sigma_z^2)^{1.169} \tag{3.11}$$

The Pearson correlation coefficient r of $E[\epsilon]$ with the terrain indices SI and RF, roughness RR and point cloud density (number of observations per grid cell, n) was calculated in order to test for spatial bias in the residual error. While there

was some degree of correlation with RR (-0.17), the r values for SI (-0.05), RF and n (both 0.00) were much lower.

3.3.2 Frost heave

A profile was extracted by calculating the average surface level change (m) and elevation for each row of grid cells in the 0.02 m DEM. Figure 3.6 shows the average surface level change after the winter period as a function of elevation. The profile is characterised by a clear negative correlation between elevation and frost heave rate. At the bottom of the slope however, corresponding to the lower 2.0 m of the runoff plot, the trend is disturbed.

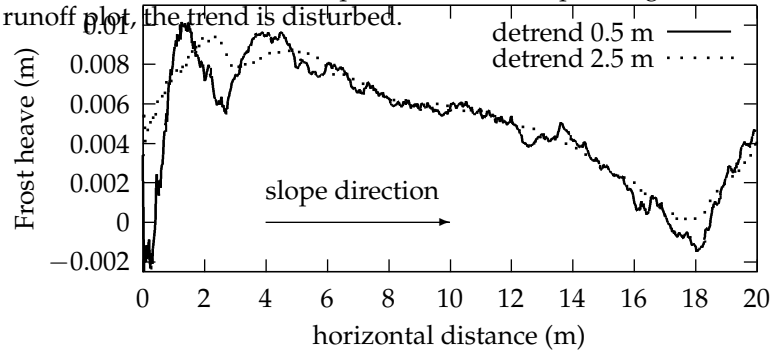

FIGURE 3.6: Frost heave (m) as a function of elevation and distance along the profile (two moving window sizes).

3.3.3 Surface roughness

3.3.3.1 Compared sensitivity of roughness calculations

The comparison of the methods to define the reference plane for the determination of random roughness indicates that fitted planes decrease the overall average RR in comparison to using the average elevation of the grid cell. Compared to a single plane per grid cell, average RR is smaller when four planes are defined. The increase in RR between a cell size of 0.01 and 0.20 m for the horizontal plane method is 14.0 10^{-3} m, 13.0 10^{-3} m for the single plane and 9.5 10^{-3} m for the four plane method (see Fig.3.7.a).

The comparison of the methods for the effect of local slope on RR shows that the dependence of RR on local slope is largest when the grid cell average elevation is used as the reference plane. Fig. 3.7.b shows the Pearson correlation coefficient (r) as a function of the spatial resolution. The difference between the horizontal reference and four-plane methods is smaller, but RR by the four-plane method is less dependent on local slope than when one reference plane is used as the reference elevation.

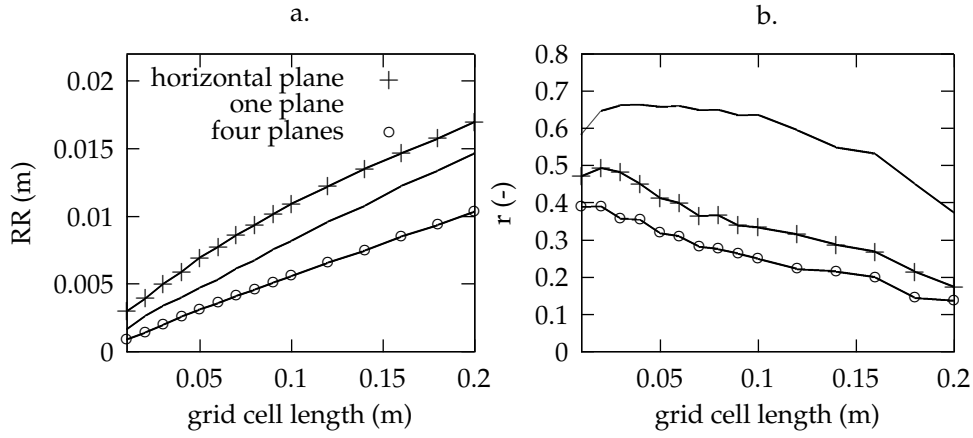

FIGURE 3.7: Sensitivity of the *RR* algorithms to scale and slope. Figure a. shows the relation between average *RR* for the entire plot and the grid cell size for each of the three methods. Figure b. shows the Pearson correlation coefficient *r* between *RR* and local slope as a function of cell size.

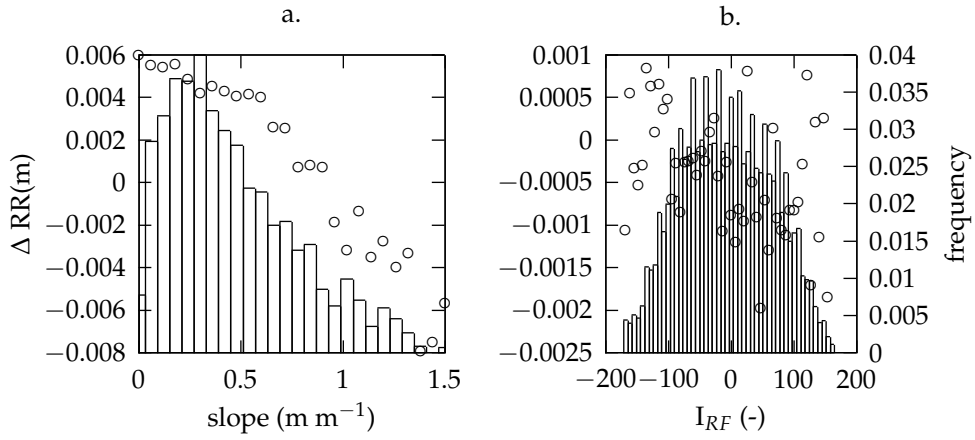

FIGURE 3.8: Soil roughness decrease as a function of a. slope and b. Ridge/furrow position. The bar graphs indicate the relative frequency.

Further roughness calculations were based on the four-plane method, at a grid cell length of 0.02 m. At this resolution, the correlation between local slope and RR is still considerable, but this cell size was chosen because it allows for the identification of changes in the soil surface that are small in comparison to the soil aggregate. At this resolution there also is a sufficient number of point measurements available per grid cell ($n = 36$ on average, after filtering).

3.3.3.2 Effect of topography on roughness decrease

The overall mean random roughness decreased from 1.30 10^{-3} m to 1.19 10^{-3} m during the winter and snow melt event ($p < 0.001$). This general smoothing was more pronounced in the non-sink areas ($\Delta RR = -1.9\ 10^{-4}$ as opposed to -1.3 10^{-4} m within the sinks) when absolute values are regarded. However, RR in the sink areas was less than in the non-sink areas in the pre-winter situation (by a mere 8.0 10^{-5} m). The relative decrease in the sink areas is somewhat higher: 33% in the sinks, as opposed to 21% outside.

The decrease in RR was more pronounced in concavities than in convexities; -3.0 10^{-4}m and -2.4 10^{-4}m, respectively. Similarly, areas facing north showed a larger decrease (-4.0 10^{-4}m) than south facing slopes (-1.0 10^{-4}m). Table 3.3 gives an overview of the average decrease of random roughness in each of the I_{RF})

TABLE 3.3: Results of ΔRR for the I_{RF} classes.

I_{RF}	n	*average* ΔRR (10^{-3} m)
1: north, convex	3.00 10^4	-0.39
2: south, convex	2.51 10^4	-0.06
3: north, concave	2.21 10^4	-0.42
4: south, concave	1.66 10^4	-0.15
convex	5.51 10^4	-0.24
concave	3.87 10^4	-0.30
north	5.21 10^4	-0.40
south	4.17 10^4	-0.10

classes. The ANOVA significance test on I_{RF} against ΔRR showed that all four aspect categories have different magnitudes of the decrease in random roughness (p <0.001). A Tukey Honest Significant Differences test further revealed all four I_{RF} categories have different average ΔRR values (p <0.001).

3.3.4 Erosion and deposition

The Figures 3.9 .a to 3.9 .d show the outcomes of the average change in surface elevation as a function of the various topographic indices. Due to the large number of grid cells, merely plotting the point clouds of observed elevation differences against the respective topographic indices results in visually amorphous scatter plots. Instead, average surface elevation change values, $\Delta_n z$, were calculated for classified topographic index values. Average net change in surface elevation in classes with relative frequencies under 0.01 were found to be dominated by outliers and are not included. The frequency distributions of both SI and CI indicate a normal distribution. Slope and curvature show positive skewness. The graphs for curvature, SI and CI also indicate that the exclusion of the sinks in this part of the data analysis does not mean that all deposition is neglected: a considerable volume of soil is distributed in non-sink areas: deposition occurs on 46% of the surface area not classified as sinks. The apparent trends of the classified data cannot be confirmed by the linear regression. The coefficients of determination, r^2, for surface elevation change as a function of slope, curvature and the convergende index were 0.09. For the sedimentation indices, r^2 was 0.08. Pearson correlation coefficient for slope was -0.04. Slightly better correlations were established for the convergence index (r=0.20), curvature (r=-0.21) and sedimentation index (r=0.24). All of these weak correlations are significant, with $p \ll 0.001$.

Fig. 3.10b gives an overview of where soil erosion and deposition occur within the runoff plot. The observed net surface elevation change was calculated for sink and non-sink areas. The average $\Delta_n z$ for the sink areas (6.30 m^2) was 2.78 10^{-3} m. For the non-sink areas (56.49 m^2) this was -0.67 10^{-3} m. Note that the total area

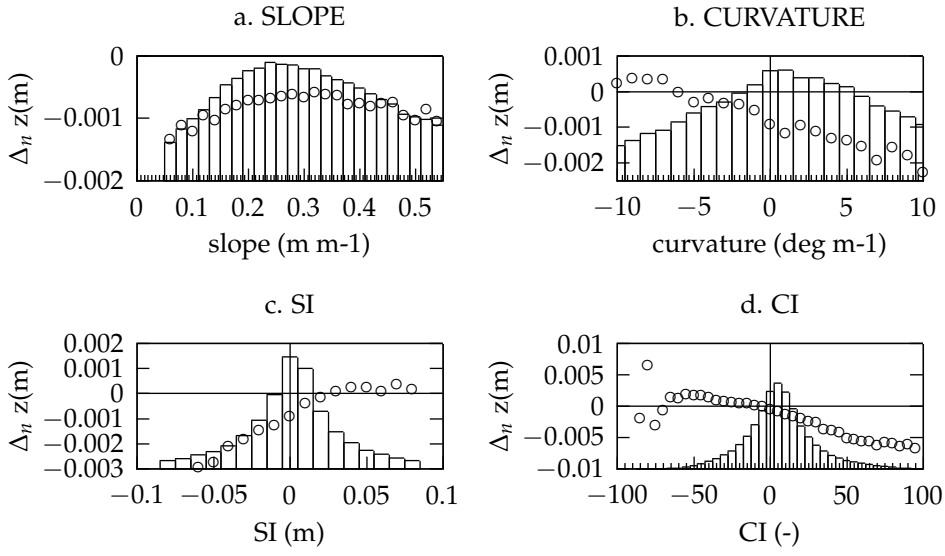

FIGURE 3.9: Soil surface elevation change as a function of the different topographic indices. The bar graphs indicate the relative frequencies of the classes.

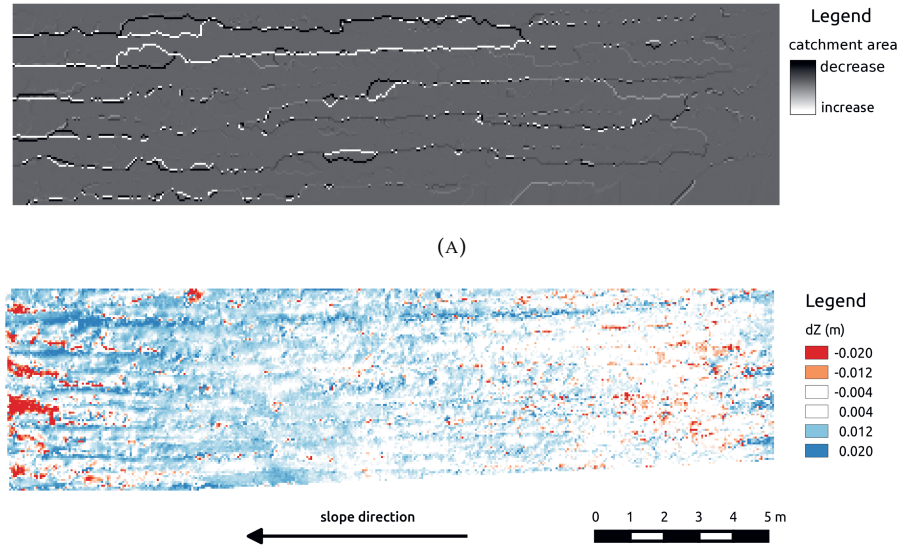

FIGURE 3.10: Changes in soil surface, (a) showing the changes in catchment area and (b) the net surface elevation change.

(62.79 m^2) is less than the total area of the runoff plot due to boundary effects of the moving window for the calculation of frost heave. At plot scale, the volume of detached soil is 3.79 10^{-2} m^3, while 1.75 10^{-2} m^3 is deposited. Assuming a bulk density of 1.52 10^3 kg m^{-3} (Skøien, Børresen, and Bechmann, 2012a) this would correspond to a net erosion rate of 4.83 tonnes ha^{-1}.

To illustrate the significance of soil loss and local redistribution for the hydrological behaviour of this soil surface, the pre-winter contributing areas for individual cells were compared to those after snow melt. The average difference of all the runoff plot's grid cells is 0.066 m^2. Fig.3.10a shows this difference in contributing area for the runoff plot. Similarly, the average length of the flowpath from the individual cells to the runoff collector at the bottom or any other sink decreased from 0.301 m to 0.286 m during the melting event.

3.4 Discussion

The magnitude of frost heave was expected to be larger in the lower parts of the plot, where soil water content can be assumed to be higher. The general trend in Fig.3.6 confirms this expectation, with the exception of the lower two or so meters. A possible explanation for this would be the collapse of the plough ridges

as a result of saturation after thawing and runoff. Visual inspection of the ridges did indeed reveal signs of severe structural deterioration in the lower part of the plot. The effect of soil moisture content on aggregate stability under freeze-thaw cycles has been documented by e.g. (Staricka and Benoit, 1991; Oztas and Fayetorbay, 2003; Kværnø and Øygarden, 2006). The magnitude of this change could be larger than the effect of frost heave, but no metrics were derived from the data to confirm this.

At the upper plot boundary, frost heave is more pronounced than would be expected. The area immediately above the plot is under a permanent grass cover. The observation therefore could be explained by higher soil moisture conditions at the top of the plot compared to areas closer to the centre. Since no soil moisture content measurements were undertaken during the experiment, this explanation could not be confirmed by field data.

Data analysis confirmed the assumption that the four plane method was less sensitive to the choice of a cell size (Fig.3.7). Without exact prior knowledge about the size of the features that are affected by the processes studied, relative scale independency is an important quality of any metric used. In most cases, however, the choice of a spatial resolution is still more significant for for the magnitude of *RR* than the choice for any of the three methods applied in this research.

Both the single and four planes methods show a gradual decrease with increasing resolutions. This is likely due to the fact that slope values decrease with increasing resolution, while *RR* is more likely to increase due to the presence of more roughness elements, like cavities and protruding aggregates. The horizontal plane shows an initial increase and this could be the result of the compound effect of scale and the poorer fit of the horizontal plane to the actual point cloud.

This reduction in the correlation between local slope gradient and *RR* resembles the statistics presented by (Chu, Yang, and Chi, 2012). They apply a less scale-dependent *RR* algorithm, developed by (Hansen and Sibbesen, 1999), but reduce slope dependency on tilled soils by DEM preprocessing.

The overall reduction in *RR* during snow cover and melt is in accordance with all studies that quantify this change, e.g. (Römkens and Wang, 1987; Haubrock *et al.*, 2009; Wang *et al.*, 2018). The decrease in *RR* in this study is an order of magnitude smaller than studies that characterised by intense runoff, like (Eltner, Maas, and Faust, 2018). Some studies (Haubrock *et al.*, 2009; He *et al.*, 2018) report local increases in *RR* as a result of rill formation; locally or towards the lower boundary of a runoff plot. These local increases could not be quantified in this study. This can either be because of the limited extent of rill formation, or its more homogeneous distribution over the runoff plot (Fig. 3.10a). North-facing areas show a larger reduction in *RR* than those facing south. This is contrary to the expectation that the larger daily temperature amplitudes on south facing slopes would result in a more marked reduction in soil roughness. This could

be explained by a difference in water content. Before the onset of winter, north-facing areas can be expected to evaporate less of their moisture due to the smaller amount of incoming solar energy.

The difference between the average reduction in RR between the concave and convex is small (0.30 and 0.24 10^{-3} m, respectively), but statistically significant. This could be explained by the fact that concave areas where material is deposited can be expected to smoothen during an erosive event. The correlation between curvature and net elevation change (Fig.3.9.b) confirms this presumption: concave areas are more likely to accumulate sediment.

Despite the apparent trends in Fig.3.8, neither the linear regression nor the (Pearson) correlation coefficients were significant for both slope and I_{RF}. A possible explanation for this apparent independency could be that I_{RF} does not perform well as a hydrological terrain index. Overland flow can be expected to concentrate in the furrows, but its ability to reshape the soil surface will also depend on the force it exerts. This force will depend on the catchment area of each particular point in the furrow rather than on the ridge/furrow index.

The derived net soil loss rate for this spring period is at a realistic level. Although only representative for the spring season, this value compares favourably to the average measured value at Bjørnebekk for the autumn ploughed plots between 1994 to 2004, which is approximately 6.00 tonnes $ha^{-1}year^{-1}$ (Skøien, Børresen, and Bechmann, 2012a)).

The effect of soil redistribution during snow cover and melt on the plot's hydrological characteristics is in accordance to the changes reported for rainfall events. (Darboux and Huang, 2001) quantify the reduction in surface storage capacity as the result of soil deposition in sinks during consecutive rainfall events. Average deposition in the sinks in this study was indeed positive (2.78 10 m^{-3}). Average flow path length in the study plot decreased, while the average contributing area increased. This observation is in accordance with the conclusion by e.g. (Peñuela *et al.*, 2016; Wang *et al.*, 2018) that hydrological connectivity increases during a sequence of runoff events.

3.5 Conclusion

The first objective of this research was to correlate small changes in soil microtopography during a winter/spring interval by means of TLS technology. Several observations did indicate that the error associated with data acquisition and pre-processing is small in comparison to the actual changes that occurred. Most notably, the residual error is distributed over the runoff plot independent of the observed changes. The decreasing roughness, and its spatial distribution in the runoff plot, is a clear quantification of a general smoothing of the soil surface that can be expected during a runoff event. In a similar fashion, the quantification of net accumulation of soil material in the depressions in the terrain, compared to

the net soil loss from the areas in between, can be regarded as a confirmation that TLS is able to changes in the same order of magnitude of the residual error. After correcting for frost heave, the calculated changes to the soil surface at the scale of the runoff plot yield results that are both consistent with our understanding of how overland flow, the pressure of the snow pack and freeze-thaw cycles affect soil surface morphology. The derived erosion and deposition rates are realistic when compared to long-term sediment measurement series.

With regard to soil surface roughness, TLS technology can be applied to quantify the kind of minute changes that occur during a single event. The difference in surface roughness decrease in the plough furrows and on the ridges was small, but significant. This outcome corresponds to the expectation that roughness decrease is more pronounced areas where flow processes are the main driver for a change in surface roughness.

Since no ground truth was available to evaluate the observed surface elevation changes against, secondary terrain indicators had to be developed and applied. Each of these terrain indicators is connected to a certain understanding of the different processes leading to changes in microtopography. Most of the indicators displayed some degree of correlation with the observed dynamics in microtopography when presented as class average values. The large variance of the data within the classes complicated the objective confirmation of these trends. Additional research might investigate the appropriateness of non-continuous terrain indices for better linking surface dynamics to processes. This research has shown that categorical distinctions, like I_{RF} and sink/non-sink, provided unambiguous confirmations that soil surface changes can be observed when linked to their respective locations in the runoff plot.

The categorical indices used in this study, I_{RF} but also the distinction between sink and non-sink areas, provided much less disputable correlations than continuous indices like slope, curvature and the Sedimentation Index.

A question that was not addressed in this research is how the decrease in surface roughness is correlated to surface elevation change. On average, their orders of magnitude are roughly the same. In erosive zones, flow processes may result in both elevation and roughness decrease, while deposition zones can expected to display elevation rise and roughness decrease. Further quantification of this correlation could provide useful information in situations where measurements have lower spatial resolutions. Understanding the link between roughness decrease and surface elevation change then could complement understanding about the process of soil redistribution at the very local scale. Of the roughness metrics tested in this study, the four plane method proved to be least sensitive to both spatial resolution and local slope. As such, it is a useful method to calculate random roughness in situations when the spatial scale of the expected changes is not clearly defined. It also provides an alternative to DEM pre-processing (detrending) in order to minimise the effect of local slope. This also is a matter of

scale, especially on agricultural surfaces where local slopes are a composite of general topography (hillslope) and microtopography (tillage ridges).

Chapter 4

Estimating ephemeral gully erosion rates in a Norwegian agricultural catchment, using low-altitude UAV imagery

Abstract

Ephemeral gully erosion occurs regularly on Norwegian agricultural soils. Few observation based estimates are available for the assessment of its relative contribution to soil loss at the catchment scale. Measurement of ephemeral gully erosion dimensions is traditionally done by determining profile cross sections or manual depth and width evaluations with certain intervals along the gully's length. More recently, methods to obtain three-dimensional data have become available to researchers that allow for the constructions of high-resolution Digital Elevation Models (DEM). The availability of Unmanned Aerial Vehicles (UAV), equipped with digital cameras, has significantly improved the potential of stereophotography for mapping at the field and hillslope scales. Processing high-resolution DEMs for the estimation of gully volumes by means of monotemporal imagery consists of two phases: delineation and the construction of a, pre-event, reference surface. Several methods exist for the delineation of gullies, and methods for reference surface construction are limited to spline-based approaches. This study presents a delineation and a soil surface reconstruction algorithm that are almost parameter free. Its robustness for parametrisation and for the spatial resolution of the input DEM is assessed. The tests show little sensitivity to both these factors. The method is then applied to measured ephemeral gullies for an agricultural catchment in southeastern Norway. The contribution of

ephemeral gully erosion as a fraction of the total seasonal soil loss varies between 7% (2019) and 30% (2021).

Submitted for review to **Catena** as: R.J. Barneveld, J.Stolte and S.E.A.T.M van der Zee. Estimating ephemeral gully erosion rates in a Norwegian agricultural catchment, using low-altitude UAV imagery. (*under peer review*)

4.1 Introduction

Soil loss from arable land is a worldwide threat to sustainable food production and ecosystem quality. In Northern Europe, soil erosion is less severe than in the (sub)tropical or Mediterranean climate zones (Grimm, Jones, and Montanarella, 2001; FAO and ITPS, 2015), but sediment loss from agriculture does affect surface water quality (Wenng *et al.*, 2021). Soil erosion is a natural phenomenon, but anthropogenic factors can increase its order of magnitude (Nearing *et al.*, 2017). The mechanisms by which arable cropping aggravates rates of soil erosion and sediment transport are diverse. While wind is a significant driver for particle detachment and transport in many areas in the world, water is the most significant force in the areas dominated by arable cropping in Scandinavia. The main mechanisms that connect agricultural land use with surface waters are sheet erosion, gully erosion and matrix (drainage) erosion (Barneveld *et al.*, 2019). Stream bank erosion can be an important process as well, but is less directly related to seasonal farm operations. Tillage erosion can have long term effects, especially in Norway's fragmented arable production landscapes. Since net transport occurs only very locally, its effects on surface water quality can assumed to be negligible. Rill erosion is an intermediate form of erosion between sheet ('inter-rill') erosion and ephemeral gully erosion. In this study, ephemeral gullies are defined as linear erosion features that occur in talwegs. Additionally, they are small enough to be levelled out by means of regular tillage operations (Nachtergaele, Poesen, and Govers, 2002). The dimensions of ephemeral gullies in the study area are typically not more than 1 m wide and 0.5 m deep. Rills are generally smaller and occur on hillslope segments rather than in talwegs. In contrast to ephemeral gullies, rills often develop in parallel to each other.

In Norway, measures to control the detrimental effect of soil erosion on the aquatic environment have been in place since the 1980s. Considerable resources are directed towards no-till during the winter season (Landbruksdirektoratet, 2020). Mouldboard ploughing is a common tillage operation during autumn. While some of the subsidies in this regulatory framework are aimed at the reduction of erosion resulting from concentrated overland flow, its monetary weight is directed towards measures against sheet erosion (most notably the maintenance of a stubble cover during winter). Poesen *et al.* (2003) observe that sheet and rill erosion have been the focus of most erosion studies in the 20^{th} century. Monographs on soil erosion published in the last decades of the period hardly mention gully erosion (Morgan, 1996) or are restricted to rill erosion (Kirkby and Morgan, 1980). Vanmaercke *et al.* (2021) reiterate Poesen *et al.*'s observation of 2003 nearly two decades later. The importance of ephemeral gully erosion for surface water quality, relative to other mechanisms is still largely unknown. Multiple studies show that it is likely to be a major process for particle detachment and sediment delivery (see Poesen *et al.*, 2003). Øygarden *et al.* (2003) report episodic erosion rates from rill and gully erosion that are several orders of magnitude larger than

what is generally expected from sheet erosion (in exceedence of 30 Mg ha^{-1} compared to the 1 to 2 Mg ha^{-1} as a result of sheet erosion). Barneveld *et al.* (2019) arrive at contributions of between 30 and 60 % of ephemeral guly erosion to total annual soil loss from two agricultural headwater catchments for longer term averages (two decades).

The estimates by Øygarden (2003) are based on episodic losses during a catastrophic year and Barneveld *et al.*'s (2019) numbers are based on a sediment balance that is derived from physically based and phenomenological models. The question of how much ephemeral gully erosion contributes to annual sediment loads from predominantly agricultural headwater catchments in Norway requires more empirical data than currently available. The relevance of the question is not only theoretical, but also practical with regard to the priority of erosion control in Norwegian environmental policy making.

Standard field methods for estimating soil loss from ephemeral gully erosion are transects (Morgan, 1996), regular grids (Bug and Mosimann, 2012) and gully profile descriptions (Øygarden, 2003 or combinations according to the local density of erosion patterns (Edwards *et al.*, 1998). Rill and gully cross section areas can be estimated by measuring a typical depth and width for consecutive rill sections, or be measured by profile meters. Contact methods (pin-boards) have been used since the 1950s (Kuipers, 1957; Burwell, Allmaras, and Amemiya, 1963). Pin-boards were improved on during the 1970s and 1980s (Radke *et al.*, 1981; Podmore and Huggins, 1981; Römkens, Singarayar, and Gantzer, 1986), but the advent of laser scanners improved the accuracy and spatial resolution of the derived soil surface elevation models substantially (Huang and Bradford, 1992). While the use of rail-mounted laser scanners is largely restricted to the laboratory or to limited surface areas in the field, Terrestrial Laser Scanners (TLS) facilitated detailed data acquisition for larger areas (Barneveld, Seeger, and Maalen-Johansen, 2013). Photogrammetry expanded the possibilities to acquire detailed information about soil surface morphology at a lower cost (Jester and Klik, 2005; Thomsen *et al.*, 2015). The increased availability of off-the-shelf unmanned aerial vehicles (UAV) has advanced the importance of image based digital terrain construction (structure from motion, SfM). There is a substantial volume of documented research assessing the comparative reliability the non-contact methods that emerged in the last two decades. Milenković (2016) assess the suitability of imagery from a UAV for the estimation of soil roughness. Eltner *et al.* (2013) use UAV imagery to observe small changes in the soil surface through multi-temporal recordings. Both studies use TLS generated DEMs as the reference model for the actual soil surface and conclude that the accuracy and precision of UAV derived DEMs are sufficient for their respective purposes. Onnen *et al.* (2020) develop and test a routine that uses UAV imagery to monitor the development of soil roughness under a cereal crop throughout the growing season. Meinen *et al.* (2020) use UAV imagery to estimate the volume of sediment plumes. While the use of UAVs at present is not sufficient to measure inter-rill erosion, it has become a powerful

method to monitor phenomena in with sizes in the order of magnitude of rill and ephemeral gully erosion.

The availability of DEMs with high spatial resolutions (raster grids with a spacing in the order of centimetres or smaller) of larger areas with varying degree of complexity, also renewed the need for an appropriate method to deduct rill and gully volumes from these DEMs. Volume calculations require two derivate geospatial datasets: a delineation in the horizontal plane and a reference elevation. The difference of the reference elevation within the boundary of the rill or gully is equivalent to the local soil loss. Cross section areas are very sensitive to the delineation in the horizontal plane (Fig.4.1a). Casalí *et al.* (2015) point out that the definition of a reference surface is not trivial, especially for relatively small phenomena like rills and ephemeral gullies. They provide an example of how the choice of a delineation method can result in cross section areas with a factor two difference.

(A) Two possible gully delineations, depending on where the ridge on the left is defined.

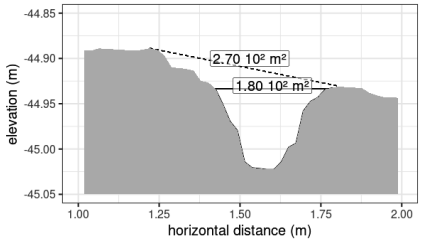

(B) Reference surface defined by a straight line (solid) compared to the real, pre-event surface.

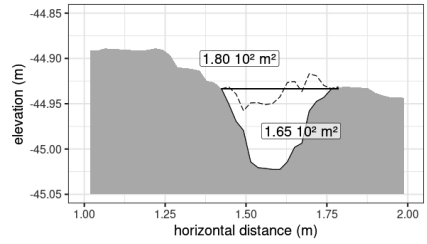

FIGURE 4.1: The importance for the calculation of cross section area of feature delineation (a) and reference surface definition (b).

Several methods for the delineation of linear erosion features have been used since the emergence of high resolution DEMs. Changes in soil surface elevation can only be observed directly at high spatial resolutions if consecutive recordings can be geo-referenced precisely by means of immobile ground control points (GCP) or fixed terrain features. On agricultural soils, it often is not feasible to install GCPs and fixed terrain features might not be available in the vicinity of the areas of interest. Besides this, rills and ephemeral gullies can develop in fields not previously surveyed and GCPs can not be part of such *ad hoc* mapping exercises. In situations where multi-temporal imagery is unavailable, delineation and profile depth are to be derived from data from a single recording. Di Stefano *et al.* (2017) provide an overview of the different approaches that can be taken for gully delineation on a DEM. They categorise existing methods as curvature based (Pirotti and Tarolli, 2010; Tarolli, Sofia, and Dalla Fontana, 2012; Sofia *et al.*, 2011), slope based (Vinci *et al.*, 2015), and those based on the Canny operator (Canny,

1986; Eltner and Baumgart, 2015). Bazzoffi (2015) delineate rills by combining approaches based on curvature and contributing area. Morphometric methods like the ones based on slope and/or curvature identify grid cells that are likely to be part of rill or gully walls within a moving window.

The literature on how a reference surface can be reconstructed in studies without multi-temporal imagery is limited. Reference surfaces are generally constructed by linear interpolation between the rill or gully edges (Carollo *et al.*, 2015; Báčová *et al.*, 2019). Di Stefano *et al.* (2017) derive rill volumes from gypsum casts in a laboratory experiment. Here too, the original surface is approximated by a line, although its straightness is a function of the viscosity of the plaster. While the reference surfaces of one-dimensional cross sections do not require any further processing, this is not the case for the construction of reference surfaces on DEMs. Here, the delineated area requires interpolation with the elevation values at the outer side of the ridges as boundary conditions. Interpolation of this sort, generally referred to as gap filling, can be linear or based on spline based algorithms. The latter result in smoothed but not necessarily flat surfaces. With the exception of Vinci *et al.* (2015), who construct Triangular Irregular Networks, the studies referenced to in this section do not describe which methods were used for this interpolation. Fig.4.1b illustrates that the form of the (pre-event) reference surface can have a significant effect on cross section area estimates, and thereby on the estimates of total gully volumes.

The objective of this study is to develop an algorithmic approach to ephemeral gully delineation and volume estimation with the goal to estimate the contribution of gully erosion as a fraction of the total soil loss from a predominantly agricultural headwater catchment in southeastern Norway. The hypotheses underlying the objective is that ephemeral gully erosion is a significant mechanism behind soil loss at the catchment level and that ephemeral gully volume estimates can be arrived at by less parameter-dependent methods than those described in the introduction.

4.2 Materials and methods

4.2.1 Study area and weather

The study was carried out in Skuterud catchment in southeastern Norway (outlet located at 59.685° N, 10.831° W). The catchment has a surface area of 4.5 km^2, of which 2.7 km^2 are used for cereal production, 1.9 km^2 consists of mixed deciduous and coniferous forest and the remaining 0.9 km^2 is used for residential area, roads and farmyards. The soils in the catchment predominantly have a silty clay texture, with a higher sand content in the higher situated areas near the divide. The climate in the study area is a Warm Summer Continental (Köppen *Dfb*, Fig.4.2). The average length of the growing season is 202 days (Wenng *et al.*, 2020), starting in late April or early May and ending in September. Skuterud is

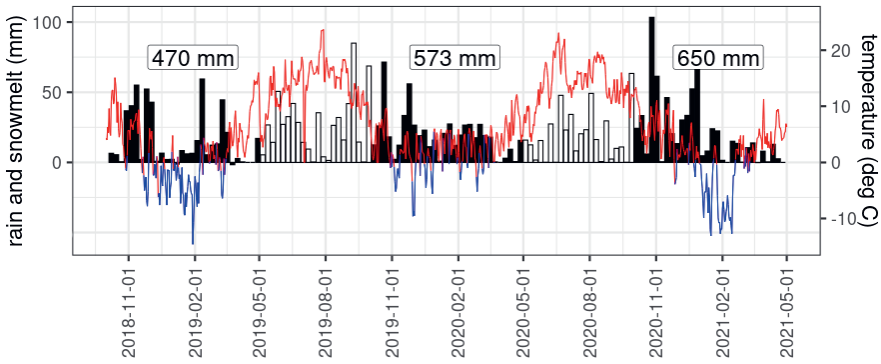

FIGURE 4.2: Weather conditions in Skuterud catchment during the study period: precipitation and snowmelt (weekly totals) and temperature (daily average; above 0°C in red, below in blue). The dark columns represent the period of ephemeral gully formation (cumulative precipitation and snowmelt depths indicated by the labelled values). Source: seklima.met.no.

one of thirteen agricultural headwater catchments that are monitored by NIBIO's Agricultural Environmental Monitoring Programme (JOVA; NIBIO, 2020).

4.2.2 Catchment scale soil loss

The JOVA programme monitors catchment discharge from Skuterud catchment continuously, taking mixed samples at uneven time intervals (NIBIO, 2020). The average soil loss per agronomic year (May to April) from the catchment in the period from 2009 to 2021 was 2.31 Mg ha^{-1}. Ephemeral gully formation occurs in the period between the last post-harvesting operations in October and tillage for seedbed preparation in May. Table 4.1 show the annual and seasonal soil loss values for the study period (spring 2019 to spring 2021). Much of the annual

TABLE 4.1: Annual and seasonal soil loss from Skuterud catchment in the study period per agronomic year (Mg ha^{-1})

year	annual	seasonal (winter)
2018/2019	0.82	0.71
2019/2020	2.39	2.09
2020/2021	2.53	2.23

soil loss occurs during winter and early spring, most notably because of the poor soil cover at the onset winter and the snow and ice melt induced runoff of the spring period, often concurring with rainfall. Occasionally, rill and gully formation occur directly after seedbed preparation in May, and during the early stages

of vegetation cover development. Torrential rainfall can then result in the rapid formation of deep and long gullies that cause significant soil loss and damage to infrastructure and roads. No such event occurred during the study period in Skuterud catchment.

Sediment fluxes measured at the catchment outlet are the result of a variety of sources, through many different pathways. Equation 4.1 represents the composition of the sediment balance.

$$SS_{tot} = SS_{sheet,rill} + SS_{eph.gully} + SS_{drainage} + SS_{streambank} \tag{4.1}$$

The total amount of suspended solids (SS_{tot}, Mg a^{-1}), as measured at the catchment outlet, is the sum of sheet and rill erosion ($SS_{sheet,rill}$), ephemeral gully erosion ($SS_{eph.gully}$, the subject of this study), drainage erosion ($SS_{drainage}$) and stream bank erosion ($SS_{streambank}$). Drainage erosion, soil loss through the soil matrix towards the tile drainage system, is of significance for Norwegian agricultural soils. Lundekvam (1998) report values at levels equal to or higher than those for sheet erosion. Stream bank erosion can be observed in the form of the gradual movement of soil, sometimes resulting in structural collapse. No measured data are available to assess the contribution of the process to the total soil loss from the catchment.

4.2.3 DEM acquisition and preprocessing

UAV imagery from areas with ephemeral gully erosion in Skuterud catchment was acquired during three consecutive spring periods (2019 - 2021). Locations with a high likelihood of gully formation are well known in the catchment (Kværnø *et al.*, 2020). Landowners in the area were notified in March of each year, and their agreement to take aerial imagery was confirmed for each property during the campaigns. Aerial photographs were taken with a DJI Mavic Pro quadcopter at altitudes between 25 and 40 m above the lowest point in the region of interest. Flights were planned with the DroneDeploy mobile app in the advanced 3D mode that supplements perpendicular images with oblique photos at an angle of 65° (DroneDeploy, 2022). Standard settings for frontal and lateral overlap were used (75% and 65%, respectively). The images were processed in Agisoft Metashape Professional (Agisoft LLC, 2019). The DEMs were set to have a grid size of 2 cm. The choice for 2 cm was considered optimal for both computational performance and representation of terrain form.

4.2.4 Gully delineation

Gully areas were delineated in two steps. The initial step is based on the fact that gullies have a lower elevation than their immediate surroundings. The DEMs

were first detrended by subtracting the elevation of each grid cell from the average elevation in a 1 by 1 m moving window.

$$z_{rel,x,y} = (\frac{1}{n} \sum_{x=-w}^{w} \sum_{y=-w}^{w} z_{x,y}) - z_{x,y} \tag{4.2}$$

where $z_{rel,x,y}$ is the relative elevation, or prominence, (m) at position [x,y], $z_{x,y}$ the original elevation (m.a.s.l.), w equivalent to half the window size (0.5 m) and n the number of elevation values within the moving window. Detrending is necessary to differentiate variations in surface elevation due to the presence of the gully channel from larger variations in the surrounding topography (Fig. 4.4b). The first gully area mask is then produced by selecting all grid cells for which $z_{rel} < 0.05$ is true. The area thus selected includes all depressions in the DEM. Within the gully area, only the central, deeper part of the channel is selected, and the mask needs to be expanded laterally in order to cover the gully walls as completely.

This is done in the consecutive step, during which the mask is extended iteratively by testing bordering grid cells for the product of the local slope s (m m^{-1}) and z_{rel} (Fig. 4.4c). Preliminary results showed that if bordering cells were tested for the validity of $s \cdot z_{rel} < -1.5 \cdot 10^{-3}$m, the gully area was covered while the mask did not extend to other depressions. The mask is then vectorized, viewed in a GIS and the polygon that covers the gully is selected manually. This polygon is then used as a mask for a DEM that serves as the input to the surface reconstruction phase (Fig. 4.4d).

The effect of DEM resolution on delineation was investigated for grid sizes between 1.7 and 3.0 cm with 0.1 cm increments. The lower limit of this domain was given by the highest obtained resolution of a UAV-derived DEM. The upper limit is a subjective value above which the representativeness of the DEM is assumed to deteriorate.

The results obtained by the delineation algorithm will vary with the values assigned to parameters used in the initial and expansion stages of gully delineation. The sensitivity of the method to these two parameters and the DEM grid size was tested by calculating delineated areas for three 20 m long test segments of randomly selected gullies at a resolution of 2 cm (Appendix A).

4.2.5 Gully volume calculation

A method was developed to generate a reference soil surface that represents the topography prior to gully incision. The premise of the method is that the morphology of the soil surface before gully development is similar to that of the (unaffected) area around the gully. The masked areas in the DEM are gradually filled with elevation values that are based on the autocorrelation of the elevation values in the area surrounding the gully. An algorithm was written in C++ that moves through the DEM by alternating between the x and y directions. Whenever a

masked grid cell is encountered, the width of the gap in the masked DEM in the direction of movement is calculated. Next, the semivariogram of the elevation along the direction of algorithm movement is calculated in a 0.50 m range at both sides of the gap. The algorithm then assigns a value to the grid cell in the middle of the identified gap. This value is generated by means of the following formula (in the x-direction).

$$\dot{z}_{x,y} = 0.5 \cdot (z_{x-dx,y} + z_{x+dx,y}) + f(\mu, \sigma^2) \tag{4.3}$$

where $\dot{z}_{x,y}$ is the generated elevation (m) at the midpoint between the points with readily assigned or original elevation, $z_{x-dx,y}$, $z_{x+dx,y}$. The width of the gap in the masked DEM is equivalent to $2 \cdot dx$ (m). A Gaussian random number generator, $f(\mu, \sigma 2)$, yields values around the mean μ (the average of the elevation on the edge of the gap) and a standard deviation σ^2, which is taken from the semivariogram of the surrounding area. In the first round, the algorithm moves through the masked DEM with spatial intervals of 64 grid cells in the x-direction, then with 64 grid cell intervals in the y-direction. It then proceeds by repeating the alternation with decreasing intervals of 32, 16, 8, 4, 2 and 1 grid cells until all gaps in the DEM are filled. The process is illustrated for a 2 m gully segment in Fig.4.3. The surfaces generated in this way have the same variation in elevation and spatial autocorrelation as the surrounding area (Fig. 4.4e). Gully volumes were then calculated as the difference of the detrended DEM and the reconstructed surface (Fig. 4.4f).

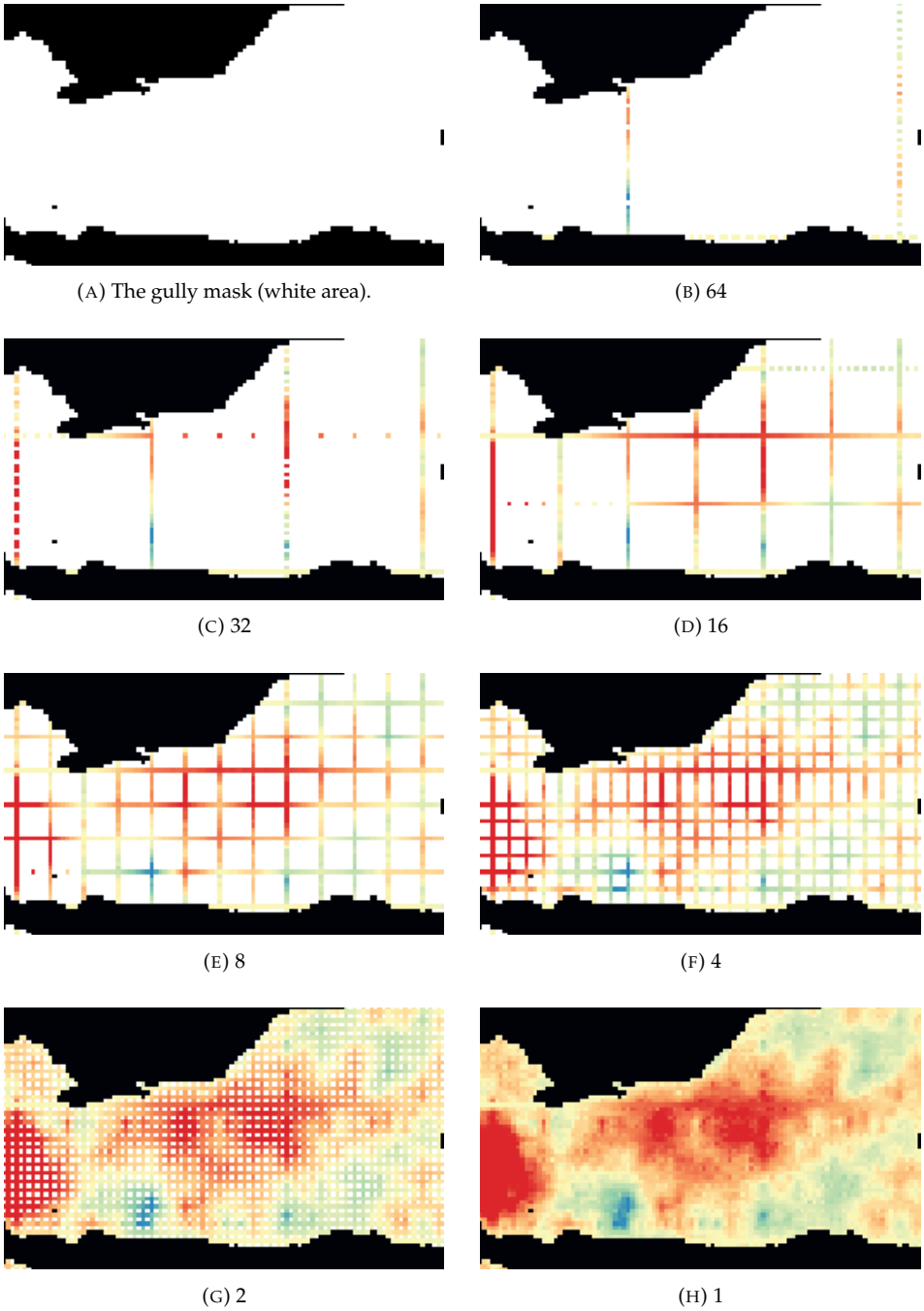

(A) The gully mask (white area).

(B) 64

(C) 32

(D) 16

(E) 8

(F) 4

(G) 2

(H) 1

FIGURE 4.3: Consecutive stages of applying the midpoint algorithm (figure captions indicate the iteration interval, expressed in number of grid cells). The width of the depicted gully segment is 2 m and the color scale corresponds to elevation (m).

The presence of a random number generator implies that the generated surfaces are different each time, as well as the estimated gully volume. The variation between generated surfaces was used to determine the minimum number of generations required to obtain a representative estimate. Three 20 m long segments of gullies were used to generate 20 surfaces. The set of 20 associated gully volume estimates was used to parametrise the Cochran formula for minimum representative sample size (Cochran, 1977).

$$n_{min} = \frac{Z^2\sigma^2(1-\sigma^2)}{e} \tag{4.4}$$

where n_{min} is the minimum representative sample size (rounded up to the nearest integer), Z is the standard score (associated with a certain confidence interval) for a normally distributed sample, σ^2 the standard deviation of the set of 20 gully volumes (m^3), and e the acceptable relative error (-). The test was performed for the 90% confidence interval and an acceptable error of 10% of the estimated volume.

The relation between grid size and estimated gully volume was investigated for the three 20 m test segments by applying the same algorithm for volume calculation on grid sizes between 1.7 cm and 3.0 cm with 0.1 cm increments. Spearman (rank) correlation coefficients r_s (-) were calculated to test for the effect of DEM resolution on estimated gully volume.

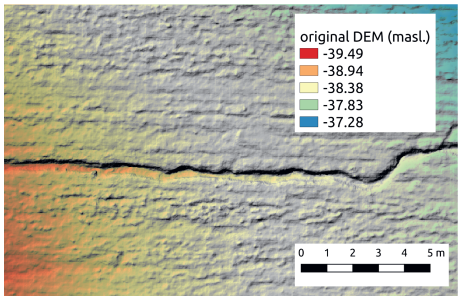

(A) original DEM

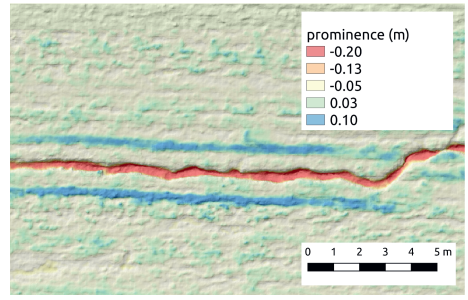

(B) relative elevation after detrending

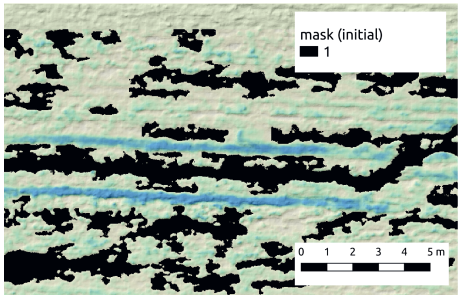

(C) mask of all depressions

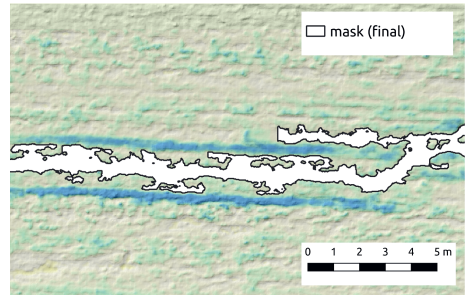

(D) masked DEM after isolation of the gully area

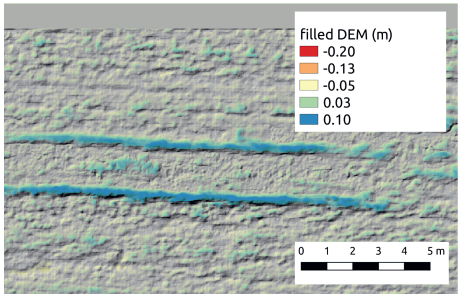

(E) prominence after surface reconstruction

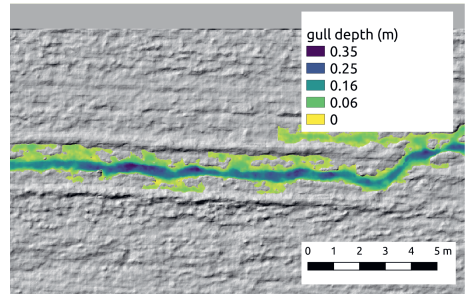

(F) gully depth

FIGURE 4.4: The six map layers generated during soil surface construction and volume calculation. The original DEM (4.4a) is first detrended (4.4b) and all depressions are selected (4.4c) and polygonised. The polygon that represents the gully area is selected and used to mask de detrended DEM (4.4d). The masked area is filled with the surface construction algorithm (4.4e) and the depth of the gully is calculated (4.4f).

4.3 Results

4.3.1 Algorithm sensitivity: delineation

The effect of DEM grid size on the identified gully surface area was assessed for values in the range between 1.7 and 3.0 cm. Fig.4.5 shows the results of this assessment for the three 20 meter long gully segments (Appendix A). The largest reduction in detected gully surface area is 1.7 % (segment 1).

The sensitivity of the gully area delineation algorithm was also investigated for the initial and the expansion phases. Initial delineation is a function of a threshold value for the relative elevation of the detrended DEM, z_{rel}. Threshold values between -0.05 and -0.10 m were tested for a DEM with a 2 cm grid size and no effect on the estimated gully surface area was discerned.

The threshold value during the expansion phase evaluates the product of the slope s and z_{rel} iteratively. Fig.4.6 shows the relation between the threshold value and the estimated gully surface area. Sensitivity for the expansion threshold value differed between the three sample gullies and ranged between 2 and 5% for gully 2 and 3. The discontinuity displayed by gully 1 is the result of a sudden connection between the gully surface area and adjacent soil surface depressions that can not be considered part of the gully area. Values in the less restrictive range of the tested threshold values ($s \cdot z_{rel} < 1.0 \cdot 10^{-3}$s) resulted in expansion of the delineated area outside of the gully channel.

4.3.2 Algorithm sensitivity: reconstruction

The dependence of the soil surface reconstruction algorithm on the spatial resolution of the DEM was tested for grid cell dimensions between 1.7 and 3.0 cm. The DEMs of the three sample gullies were resampled with 0.1 cm increments, resulting in fourteen generations per gully. The Pearson correlation coefficients for the gullies were 0.20, -0.06 and 0.00, with p-values outside of the 95% confidence interval.

Fig.4.7 illustrates the similarities and differences between four renditions of reconstructed soil surfaces for a 2.5 m long gully section. The minimum number of soil surface reconstructions required for representative gully volumes was estimated by analysing 20 generated surfaces for each of the three test segments. The segments had surface areas of approximately 200 m^2, and contained between 20 and 22 m of gully length (Appendix A). The number of reconstructions required for a maximum relative error of 10% at the 10% confidence interval was 12 for two of the surfaces and 13 for the third.

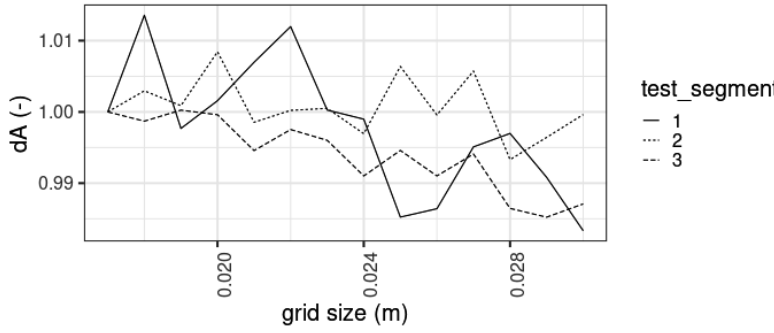

FIGURE 4.5: Algorithm sensitivity to DEM grid size (m). The delinated gully areas on the vertical axis (dA) are presented relative to the smallest attainable grid size (1.7 cm).

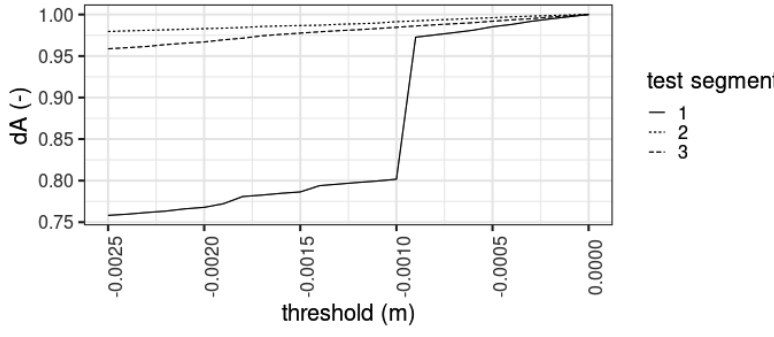

FIGURE 4.6: Algorithm sensitivity to the treshold value in the expansion phase ($s \cdot z_{rel}$). The estimated surface areas on the vertical axis (dA) are presented relative to the estimated area with a threshold value of 0.00 m.

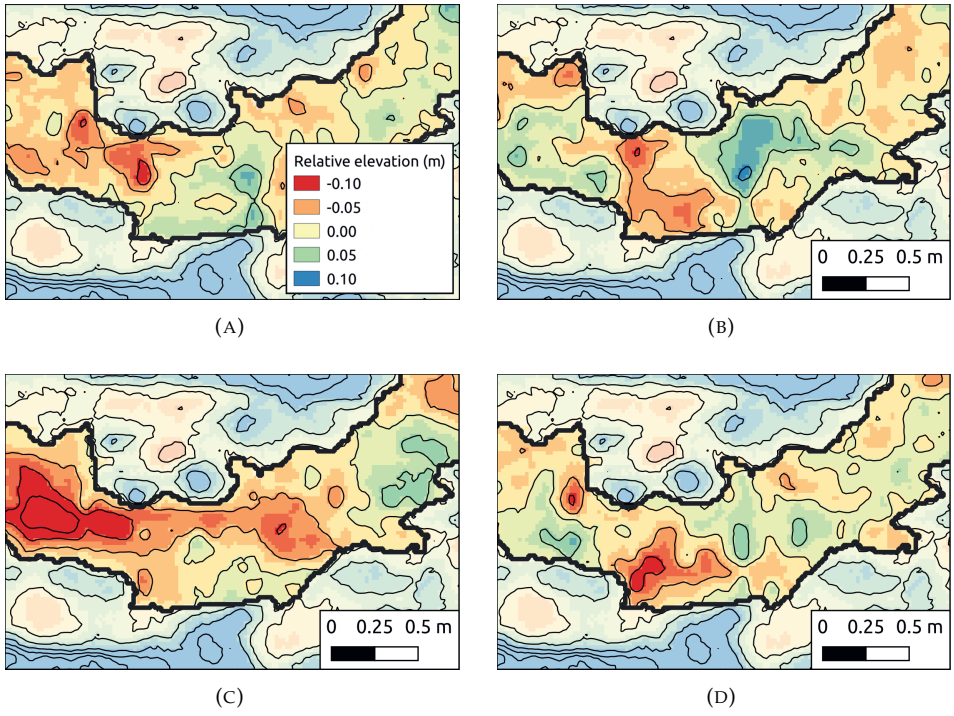

(A) (B)

(C) (D)

FIGURE 4.7: Four examples of reconstructed soil surfaces: different renditions of the algorithm. The reconstructed surface is delineated by the black lines.

4.3.3 Ephemeral gully erosion at the catchment level

The surveys and UAV campaigns in April of 2019, 2020 and 2021 covered all ephemeral gully prone areas in Skuterud catchment. During the study period, all gullies were recorded by UAV, except one in 2021. This gully had lead to damage to property and had been filled up again and levelled by the land owner before the area could be surveyed. In April 2019, 3 gullies were observed and recorded, 15 in 2020 and 13 in 2021. One of the 15 gullies in 2020 and two of the 13 in 2021 were too small for further analysis. The majority of the landowners asked for anonymity in the presentation of the processed data. Due to this constraint, maps of observed gullies within the catchment can not be presented here. Two morphometric characteristics of the observed gullies, area and volume, are summarised in Fig.4.8. The gully volumes were multiplied with a BD value of 1.5 Mg m^{-3} (Starkloff and Stolte, 2014) for the conversion to mass. Fig.4.9 compares

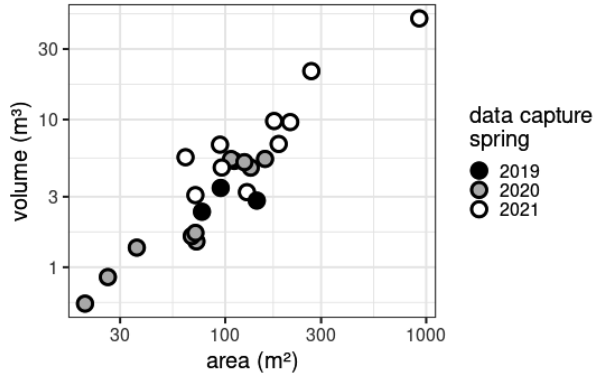

FIGURE 4.8: Estimated gully volume as a function of estimated area (log scale) for the observed spring periods.

the measured soil loss from ephemeral gully erosion to the overall, seasonal soil loss from Skuterud catchment as measured at the outlet. In the winter and early spring of 2018/2019, gully erosion was estimated to make up 7% of the the total catchment soil loss (0.05 out of 0.71 Mg ha^{-1}). In 2019/2020, this was 11% (0.23 out of 2.09 Mg ha^{-1}) and 30% in 2020/2021 (0.67 out of 2.23 Mg ha^{-1}).

4.4 Discussion

The assessment of the effect of grid size on gully delineation and volume calculation showed that the algorithms are robust. The range of the sensitivity analysis (1.7 to 3.0 cm) in this study, however, is limited in comparison to other studies (Lu *et al.*, 2017; Li, McNelis, and Washington-Allen, 2020). It compares favourably to Lu *et al.* (2017), who report a 24% decrease in the detected rill area when the grid

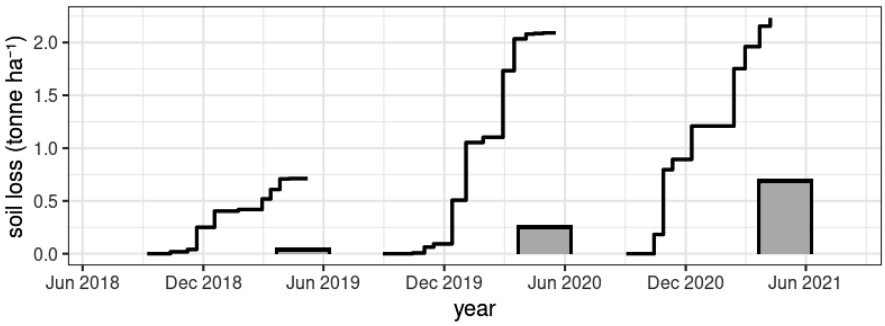

FIGURE 4.9: Cumulative soil loss from Skuterud catchment (solid line) and estimated ephemeral gully erosion (Mg ha^{-1})

size is increased from 1 to 2 cm. The features they extract from the terrain model are somewhat larger than the ephemeral gullies in this study and the range of their sensitivity analysis extends to a grid size of 30 cm. The shape of the sidewalls in their study is more gradual and this might explain the higher sensitivity to grid size. Li *et al.* (2020) report a reduction in the detected erosional area of an existing gully of 25% when the grid size was increased from 2 to 4 cm. The dimension of the gully in their analysis, however, is an order of magnitude larger than than the gullies measured in Skuterud.

The gully delineation algorithm is parametrised by two threshold values; the first for the identification of the gully bottom, and the second for the expansion of the selection towards the gully wall. The gully bottom algorithm's sensitivity was tested in the range of -0.10 m to -0.05 m of the relative elevation in the detrended DEM. The Pearson correlation test between the threshold value and the delineated area showed that the method is robust within this range. The reason for the independency is likely to be the fact that only the central, lowest areas in the DEM are isolated in the initial delineation phase. The range between -0.10 and -0.05 m is somewhat restricted and based on typical depths of the gullies encountered during the measurement campaigns in Skuterud in 2019 to 2021. Gullies that are deeper, especially in comparison to the roughness of the soil surface in the surrounding terrain, are more easily differentiated from other depressions in the DEM and the algorithm can be expected to be useful in their identification. Smaller features however, like rills, might be more superficial than the upper value of the domain of the sensitivity test and are therefore less likely to be isolated from other depressions.

The algorithm for expansion and identification of the outer gully edge depends on a single threshold value for the product of the local slope and the relative elevation. Sensitivity to this parameter was shown to be somewhat higher in the tested range of $-2.5 \cdot 10^{-3}$ and 0 m. The upper limit of zero represents a gully

wall expansion towards all surrounding area that is either without any slope inclination or exactly at a relative elevation of 0 m. In high resolution DEMs, low slope values do not occur frequently, so the upper parameter of 0 m represents an implementation in which all areas for which $z_rel < 0$ m is true. The size of the moving window used in the detrending phase therefore has to be large enough. Window sizes that are too small will increase the likelihood that grid cells that actually belong to the gully area will have positive relative elevation values, and therefore not identified correctly.

The sensitivity in the expansion phase was limited in comparison to other methods. The method described by Bazzoffi (2015) delineates rills by selecting grid cells in the DEM based on planform curvature values but sensitivity is not reported. Vinci *et al.* (2015) present a comparison of different algorithms, but their investigation is focused on rill recognition rather than delineation. Báčcová *et al.* (2019) report volumetric errors to 15% as a consequence of the parametrisation used in their delineation algorithm. Eltner *et al.* (2015) report underestimations of rill width between 17 and 24% when the Canny operator is used.

The performance of the algorithms is likely to depend on the morphometric characteristics of the soil surface surrounding the gully. Soil surfaces with larger, tillage induced, features like furrows and ridges will complicate the delineation phase of the calculation. The usefulness of the presented method is restricted to situations were gullies are at least twice as deep as the random depressions in surrounding terrain.

The comparison of the accumulated ephemeral gully volumes with seasonal soil loss at the catchment level indicates that the values are significant for the two more erosive seasons (2019/2020 and 2020/2021). The method developed and applied in this study is not designed for the mapping of sediment transport pathways. The presented percentages of the contribution of gully erosion to catchment scale soil loss therefore depend on the assumption that losses from gully development are transported towards the permanent stream network. The absence of sediment fans between the lower gully boundaries and adjacent open waterways was assumed to be a sufficient basis for the assumption that the recorded gullies contributed directly to soil loss at the catchment level.

Poesen (2003), in their overview of the contribution of (ephemeral) gully erosion to overall soil loss report values between 10 and 60% for northern Europe. They further state that the relative contributions depend on the size of the study area. The estimated importance of ephemeral gully erosion in this study can therefore not be readily compared with published surveys. The estimated contribution of gully soil loss in this study is somewhat lower than the values simulated by Barneveld *et al.* (2019) for the same catchment, that ranged from 30 to 60%. Their study, however, covered a longer period that included several years with more erosive rainfall.

The significance of this contribution should be considered against the fact that the observed gullies only make up a fraction of the total surface area used for arable cropping in the catchment (less then 0.1% in 2021). Total annual soil loss from Skuterud catchment in the study period was somewhat lower than the long term average. Episodic soil loss during torrential rain in the early stages of crop development can lead to erosion at levels that are an order of magnitude larger. In combination with the established efficacy of grassed waterways (Fiener and Auerswald, 2003; Fiener and Auerswald, 2006; Verstraeten *et al.*, 2002) this study suggests that soil conservation measures on a small proportion of agricultural land, have the potential to reduce soil loss substantially.

4.5 Conclusion

In this study, exhaustive mapping of gullies by means of mono-temporal UAV imagery was combined with a novel algorithm for the estimation of gully volume to evaluate the significance of ephemeral erosion at the catchment scale. Within the tested range, the algorithm for gully delineation is robust with regard to the grid size of the input DEM with a maximum reduction of 1.5% within the tested grid size range. The range, however, was limited (grid sizes between 1.7 to 3.0 cm), and the results are likely to vary for courser DEMs. The algorithm is somewhat sensitive to the parameter that determines the upper edge of the gully wall, with an error range of up to 5% of the delineated area. The volume estimations by means of the soil surface reconstruction algorithm showed little sensitivity to grid size. The algorithm itself is parameter-free. At least twelve replicate executions of the algorithm are required to obtain a robust, representative average volume estimate. This study shows that gully volumes can be estimated by the set of algorithms by means of a single parameter when a DEM with a grid size of at most 3 cm is available.

Further testing is required to assess the versatility of the algorithms and their potential for improvement. Special attention will need to be paid to tillage induced microtopography. Mouldboard ploughing results in ridges and furrows with variations in elevation of at least 0.30 m. Due to their loose structure, these soil surfaces tend to be susceptible to gully formation. Further development of the algorithms presented in this study will therefore be beneficial to comprehensive mapping of ephemeral gullies on agricultural soils.

The total soil loss from ephemeral gully erosion at the catchment level varied between the years during which gullies were analysed. The minimum value during the study period was 0.05 Mg ha^{-1} (2019) and the maximum 0.67 Mg ha^{-1} (2021). During the observed seasons 2019/2020 and 2020/2021, ephemeral gullies contributed to 7 and 30% of the total, catchment scale soil loss, respectively. The assumption that all soil that is lost from gullies is transported towards the stream network and the catchment outlet requires the development of methods

to describe the functioning of these pathways. The estimated annual contributions of ephemeral gully erosion in this study is restricted to a single Norwegian headwater catchment. Further investigation is required to investigate the importance of gullies in Norway, most notably in areas with different soil and weather conditions.

4.6 Gully test segments

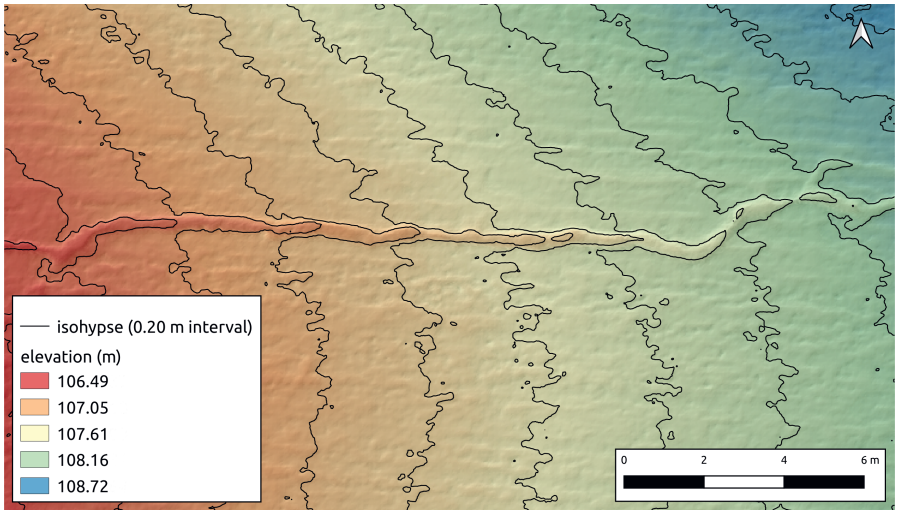

FIGURE 4.6.1: Test segment 1

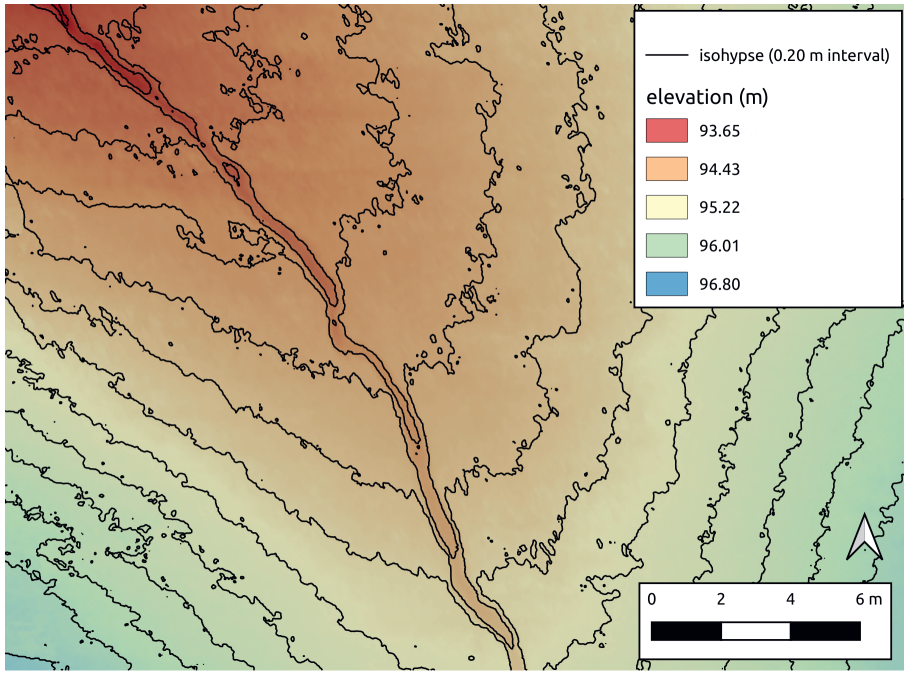

FIGURE 4.6.2: Test segment 2

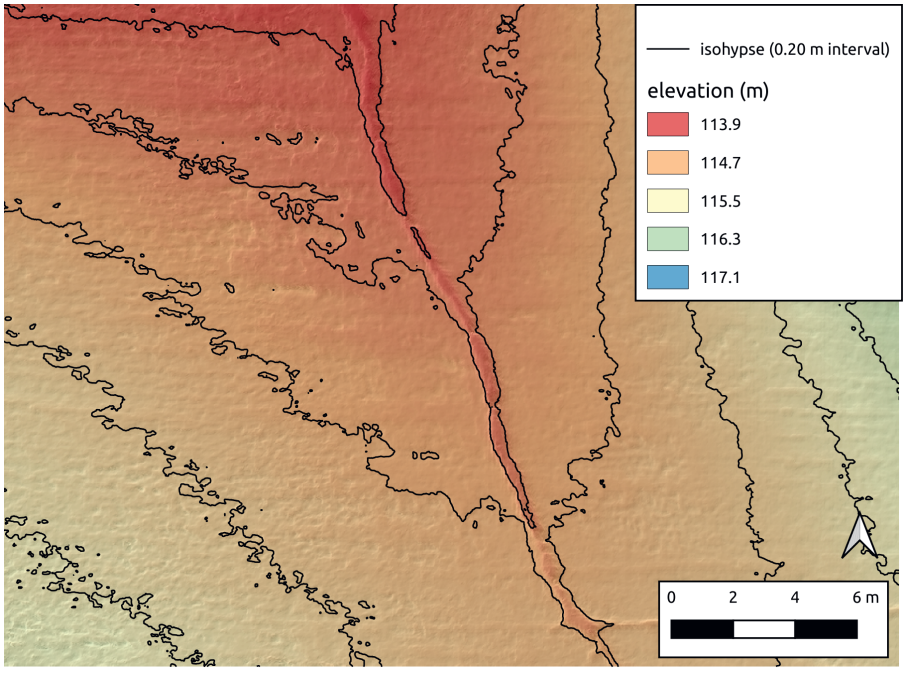

FIGURE 4.6.3: Test segment 3

Chapter 5

Prioritising areas for soil conservation measures in small agricultural catchments in Norway, using a connectivity index

Abstract

Measures designed to control erosion serve two purposes: on site (reduce soil loss) and off site (reduce sediment delivery to streams and lakes). While these objectives often coincide or at least are complementary, they could result in different priority areas when spatial planning is concerned. Prioritising for soil loss reduction at the field level will single out areas with high erosion risk. When sediment flux at the catchment scale is concerned, sediment pathways need to be identified in ex ante analyses of soil conservation plans. In Norway, different subsidy schemes are in place to reduce the influx of solutes and sediments to the freshwater system. Financial support is given to agronomic measures, the most important of which is reduced autumn tillage where areas with higher erosion risk receive higher subsidies.

The objectives of this study are (1) to assess the use of an index of connectivity to estimate specific sediment yields, and (2) to test whether conservation measures taken in critical source areas are more effective than those taken at where erosion risk levels are highest. Different modelling approaches are combined to assess soil loss at catchment level from sheet and gully erosion and soil losses through the drainage system. A calibration on two parameters gave reasonable results for annual soil loss. This model calibration was then used to quantify the

effectiveness of three strategies for spatial prioritisation: according to hydrological connectivity, sheet erosion risk level and estimated specific sediment yield. The latter two strategies resulted in a maximum reduction in total soil loss due to reduced autumn tillage of 10%. Both model performance and the effectiveness of the different prioritisation strategies varied between the study catchments.

Published as: R.J. Barneveld, S.E.A.T.M. van der Zee, I. Greipsland, S.H. Kværnø, J. Stolte, 2019. *Prioritising areas for soil conservation measures in small agricultural catchments in Norway, using a connectivity index.* **Geoderma** 340, p. 325-336.

5.1 Introduction

Soil erosion is a threat to agro-ecological systems worldwide. It's negative impacts can be categorised as on-site and off-site. In areas where agricultural production is limited by nutrient inputs, the on-site effect of soil quality deterioration often is the main reason to implement soil conservation measures. In the Nordic countries, however, the main problem associated with runoff and soil erosion is the delivery of nitrogen and phosphorus to the freshwater system (Ulén *et al.*, 2012). The need for pro-active and orchestrated policy making was acknowledged by the North Sea countries as far back as 1984 (the Bremen Declaration). Norway, as an EEA country, has started implementing the EU Water Framework Directive (WFD) in 2007. A system of regulations and economic instruments to encourage farming practices that would reduce non-point pollution from agriculture was put into place in Norway between 1980 and 1990. Subsidies were given to hydro-technical measures, changed tillage methods and vegetative measures like catch crops and grassed water ways. The traditional soil tillage method in Norway until 1990 was autumn ploughing in combination with spring wheat. Autumn ploughing is shown to increase soil and phosphorus losses compared to spring tillage (Bechmann *et al.*, 2001; Skøien, Børresen, and Bechmann, 2012b). Between 1990 and the present state the area with autumn tillage has been significantly reduced. In 2013, the area with cereals ploughed in autumn covered 46% of the total cereal area in the country, compared to approximately 86% in 1990 (Bechmann *et al.*, 2016). Despite the introduction of numerous measures in recent years, problems with eutrophication still remain (Skarbøvik *et al.*, 2016). In both research and policy making, there has been much focus on erosion risk at field level. For sediments to reach the freshwater system however, pathways from source to sink have to be present. Identifying areas with high erosion risk and a high connectivity to surface waters (critical source areas, CSA), is essential to develop an effective strategy for mitigation measures.

At the catchment level, several approaches may be adopted to quantify the contribution of specific areas to sediment fluxes to the freshwater system. These methods are either based on sediment source tracing or on distributed risk and transport mapping. Sediment source tracing techniques rely on mineralogical and geochemical characterisation of suspended solids, isotopic signatures, or other trace elements like pollen (Walling, 2005). These techniques require intensive field measurements, and are generally unable to quantify delivery ratios towards the stream network (ibid.). The costs of the acquisition and analysis of the required samples and associated mapping of the parameter throughout a catchment, prohibit a wide application in Norway. Transport risk mapping can be carried out by process simulation, terrain analysis or a combination of both. Process simulation through physical, empirical or stochastic models is not always feasible due the lack of either input data or the measurements that are needed to parametrise, calibrate and validate the model. Besides this, calibrated parameter sets of these models sometimes show equifinality, while little is known about the

fate of sediments between source and sink (Starkloff and Stolte, 2014)

Methods that rely on terrain analysis include network approaches, like the application of graph theory on sediment cascades in alpine catchments (Heckmann and Schwanghart, 2013), the network definitions by Czuba and Foufoula-Georgiou (2014) and Phillips, Spence, and Pomeroy (2011) and the measurements by Masselink *et al.* (2016). Many topographic indexes describing hydrological and sediment connectivity are based on the wetness index by Beven and Kirkby (1979). Examples include the rainfall-runoff-phosphorus model by Lazzarotto et al. (2006) and the Network Index as defined by Lane et al. (2004) and as applied for the identification of sediment source areas by Reid et al. (2007) and Reaney et al. 2011). Borselli, Cassi, and Torri, 2008 propose a spatial index that combines a characterisation of the contributing area of a location with that of the flow path down to a sink. Vigiak et al. (2012) showed that this Index of Connectivity (IC) is a scale independent terrain index that improved the estimation of specific sediment yields for a large catchment (3,300 km^2) in Australia. In this study the hypothesis is tested that IC can be scaled and used as a multiplier to derive specific sediment yields from soil erosion risk rates at point or field level. The specific sediment yield of an area in a catchment will, besides depending on topography and weather conditions, be a function of vegetative cover. Vigiak *et al.* (2012) used a crop factor to calculate connectivity as a function of land use. No other studies were found where connectivity was differentiated over time. When connectivity is defined as a function of vegetative cover, it can be expected to show a seasonal trend, especially so in catchments dominated by agriculture. Understanding of the temporal aspect of sediment yields is therefore of great relevance for the identification of CSAs, but also for the *ex-ante* evaluation of soil conservation measures like reduced tillage.

The objectives of this research were; (1) To assess the suitability of an index of connectivity for estimating time variable specific sediment yields, and (2) to evaluate the relative efficiency of reduced tillage according to different spatial prioritisation rationales.

5.2 Materials and methods

5.2.1 Study areas

The analysis was carried out for two catchments in the south-east of Norway: Skuterud and Mørdre (Fig.**??**). The two catchments are part of the JOVA agricultural monitoring programme (Hauken and Kværnø, 2013) and have been monitored for water quality since 1992. In the JOVA catchments, farmers provide information on their management practices. This includes the date and nature of every agronomic operation carried out, including tillage, fertilisation, pesticide use, sowing and harvesting dates and yields. More information can be found in Bechmann and Deelstra, 2013.

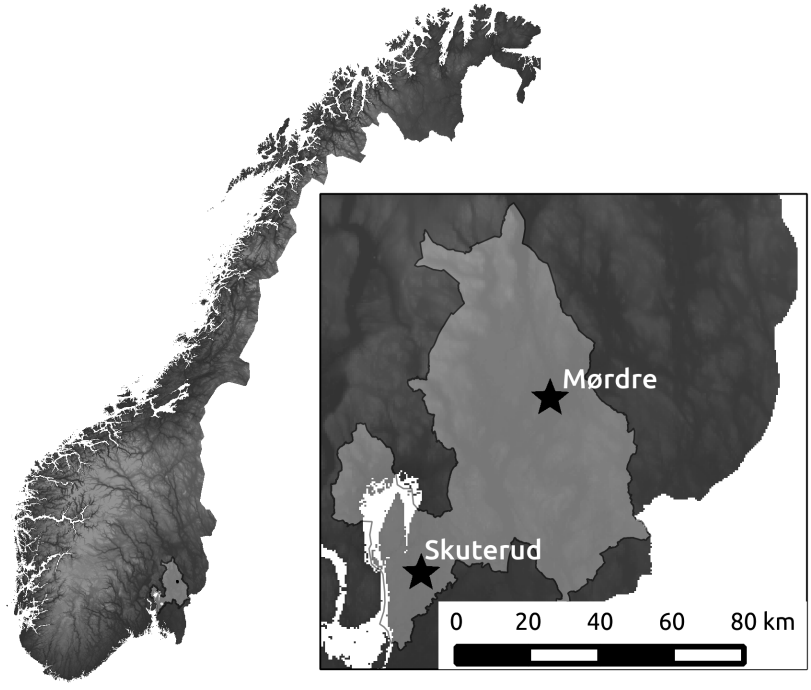

FIGURE 5.1: Locations of the study catchments in Akershus county. The outlet of Skuterud at 59°41′05.6"N+10°49′52.0"E and of Mørdre at 60°06′33.7"N+11°24′03.8"E

TABLE 5.1: Key catchment descriptors.

	Skuterud	Mørdre
area (km^2)	4.49	6.42
% arable land	61	65
average slope (%)	5.9	14.5
average channel slope (%)	5.1	6.1
drainage density (m km^{-2})	2.8	5.3
Annual precipitation (mm)	1023	716

The Skuterud catchment covers 4.5 km^2 in the south-eastern part of Norway. The growing season is relatively long (194 days) and the elevation ranges between 91 to 150 meters asl. The soils primarily originate from marine deposits, with textures ranging from coarse sand to silty clay loam. The main reference soil groups according to the classification system WRB (World Reference Base for Soil Resources) on arable land are classified as Epistagnic Albeluvisols (Siltic), Luvic Stagnosols and Endostagnic Cambisols (Dystric) (Hauken and Kværnø, 2013). The agricultural area is used for cereal and oilseed production (90%) and grass cultivation (10%). The agricultural area is used for cereal and oilseed production (90 %) and grass cultivation (10 %). Winter wheat (32 %), oats (30%) and barley (19 %) are the dominating cereals crops. The upper parts of the catchment are covered by the outskirts of a residential area and forest. Soil tillage has been subject to major variation during the monitoring period and the area with stubble during the winter period has ranged from 3 to 72% of the agricultural area. The years 1995 to 2009 were chosen for further study.

The Mørdre catchment area is also located in the south-eastern part of Norway and covers 6.8 km^2. The climate is continental, and the growing season is 180 days long, the elevation ranges between 130 to 230 m asl. The soils are predominantly composed of 50 to 90 cm thick silt to silt loam glaciolacustrine sediments overlaying silty clay loam marine sediments. Many talwegs of secondary ravines were artificially levelled 1960s in order to increase the area suitable for cereal production and to facilitate mechanisation. In these ravines the silty clay loam soil is exposed. The main reference WRB soil groups on arable land are classified as Haplic Stagnosols (Ruptic, Siltic) and Anthropic Regosols (Hauken and Kværnø, 2013). Arable land is mainly used for cereal production (85%), with oats (40%) and barley (33%) as the main crops. The area with stubble during the winter period has ranged from 19 to 75% of the agricultural area. In Mørdre the measuring procedures were changed in 1998 and therefore the years from 2000 to 2016 were used for model calibration and validation for this catchment.

5.2.2 Measured discharge and sediment load

Discharge in the study catchments is measured by a continuous recording of the water level in combination with a datalogger. Composite water quality samples are taken automatically on a volume proportionate basis, collected every 14 days and analysed for total nitrogen (TN), nitrate (NO_3-N), total phosphorous (TP), dissolved phosphate (PO_4-P), suspended solids (SS), loss of ignition (SR), turbidity, electrical conductivity and pH. For both catchments, data from the period 1993 to 2016 were available.

5.2.3 Soil loss

Suspended solids as measured at the catchment outlets can originate from sheet, or inter-rill, erosion, rill and gully erosion, soil losses through the tile drain system and stream bank erosion. The latter term is ignored in this study, since no quantitative estimates or models are available.

5.2.3.1 Sheet erosion

Monthly sheet soil erosion (SS_s, tonne ha^{-1}) at the field level was estimated by the Pan-European Soil Erosion Risk Model (PESERA, Kirkby *et al.*, 2008) with an implementation that uses long term climatic data and a worst-case land use configuration (i.e. clean post-harvest tillage in autumn in combination with spring wheat). The model was re-configured to run on irregularly shaped soil type polygons in stead of on a regular grid like in the original version. A two-phase model calibration was carried out for the soil physical parameters that drive runoff generation and particle detachment. Time series of measured runoff (Q_s) and sediment load from seven runoff plots in the south-east of Norway were used to calibrate for scale depth and the effective soil water storage capacity, and erodibility. The required soil physical parameters were either taken from the soil map of Norway (NIBIO, 2016), or derived by pedotransfer functions (Riley, 1996; Kværnø and Haugen, 2011) performed on these data. Monthly weather statistics for the catchments were derived from daily temperature and precipitation maps with a 1 x 1 km resolution, provided by the Norwegian Meteorological Institute.

A new country wide erosion risk map for Norway, currently developed by NIBIO, will also be based on PESERA. PESERA is able to simulate for different crops and tillage dates. In this study, where the focus is on the efficiency of reduced autumn tillage, fields were classified as either winter wheat or spring wheat. The tillage date for winter cereal was set at October 1st, and April 1st for spring cereal. This holds true for 85% (Mørdre) to 90% (Skuterud) of the catchments at any given time. Local variations in both crop type and tillage date occur in each of the study catchments. The dates will not deviate more than a month

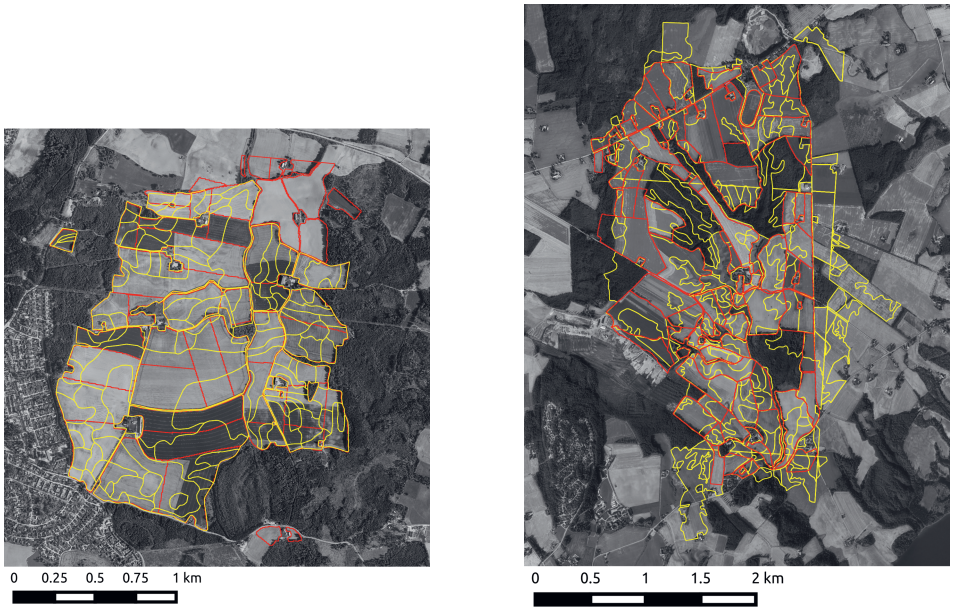

FIGURE 5.2: Field (red) and soil unit (yellow) boundaries in the study catchments.

Model input was generated such that it fully reflected all combinations of agronomy (field boundaries) and soil physical parameters (soil map units) as illustrated in Fig. 6.2.

5.2.3.2 Drainage soil loss

Depending on soil type and the tillage regime and history, soil loss rates through preferential flow towards the tile drainage system can by higher than those of surface erosion (Øygarden, Kværner, and Jenssen, 1997). Soil loss through the tile drainage network (SS_d, tonne ha^{-1}) was calculated by an empirical model, developed by Kværnø (2016, unpublished). The monthly estimate of SS_d is given by:

$$SS_d = 2.2396 \cdot exp^{0.0226 \cdot \phi} \cdot log(Q_d) \cdot Q_d \cdot exp^K \cdot (1 + \frac{1}{exp^S}) \cdot 1.667 \cdot 10^{-6} \quad (5.1)$$

where ϕ is the total porosity of the soil profile (-), Q_d is an estimate of the drainage discharge (mm), K is the same erodibility factor as used for surface erosion in PESERA (-) and S the slope gradient (%). Q_d is estimated by a simple water balance:

$$Q_d = P - Q_s - ET_A \quad (5.2)$$

where P is precipitation, Q_s is surface runoff as calculated by PESERA and ET_A the actual evapotranspiration (all in mm). ET_A was taken from monthly maps derived from satellite data from the MODIS project (Mu *et al.*, 2007; NTSG (The Numerical Terradynamic Simulation Group), 2016). This model was tested on three runoff plots in south-east Norway, but not validated at the catchment scale. SS_d was also simulated with monthly time steps.

5.2.3.3 Gully erosion

Øygarden (2003) report that the contribution of gully erosion to overall annual soil loss can be up to and even over 50%. No physical gully erosion model was available for the study areas, so this study relied on an empirical approach to the estimation of monthly soil losses due to gully erosion. The model is based on a topographic threshold for gully initiation (Vandekerckhove *et al.*, 1998), with the typical form:

$$a \cdot S \cdot A^b \tag{5.3}$$

where A is the slope (m/m), A is the catchment area and a and b are calibration parameters. Gully initiation can be expected at locations where Eq. 5.3 exceeds a certain value. In this study, monthly dynamics are simulated and this cannot be accomplished by merely using the catchment area. Instead, the accumulated monthly overland flow from PESERA were used. Overland flow was routed with a single outflow algorithm (Q_{acc}, mm). Gully initiation was assumed on locations where

$$S \cdot Q_{acc}^{1.2} > 2.2 \cdot 10^6 \tag{5.4}$$

Once gully initiation locations were marked, all downstream cells in the DEM were marked as gully as well. This sequence obtains linear elements that resemble instances of ephemeral gullies in the study areas. The threshold value of $2.2 \cdot 10^6$ (mm) was chosen after visual inspection of the monthly gully maps generated in this way. These were compared to field records, images, aerial imagery and the authors' knowledge of the study areas. While this method obtains likely locations for gullies, it is not a quantification of gully soil loss as such. The amount of soil lost and transported is a function of the average cross section of a typical ephemeral gully. This value is one of the two calibration parameters of the total sediment mass balance (m_g in Eq.5.8 in Section 5.2.6).

5.2.4 Crop factor

In the JOVA catchments, farmers provide information on their management practices. This includes the date and nature of every agronomic operation carried out, including tillage, fertilisation, pesticide use, sowing and harvesting dates and yields. The agronomic index used in this study to represent the crop stand's protection against particle detachment and transport is an USLE type cover, or crop, factor C. Consequently, a value of 1 represents a worst case situation (clean autumn tillage) and 0.01 representing an undisturbed vegetation cover. Since C

TABLE 5.2: Initial and final C values (-).

operation	initial	final
ploughing	1	0.8
ploughing (contour)	0.9	0.8
ploughing (up/down)	1	1
chemical weeding	1	0.8
cultipacking	0.8	0.8
cultivation	0.8	0.8
harrowing	0.8	0.8
direct drilling	0.2	0.01
sowing	0.85	0.01
harvesting	0.2	0.1
direct drilling	0.65	0.1
stubble harrowing	0.8	0.8
fresing	0.8	0.8

appears in the divisor in the the calculation of IC (Eq. 5.7), C was set not to assume values lower than 0.01. The values used for various operations are shown in Table 5.2 and were based on those used in ERONOR, a Norwegian empirical erosion model that was developed and calibrated for arable land in the south-east of the country (Lundekvam, 2002). In this study, the C factor does not directly determine the level of soil erosion risk. It provides a quantitative estimate of the impact of tillage and crop growth on sediment transport. Each agronomic operation was assigned an initial C value and a final one. The development of the value of C after planting or sowing was driven by the cumulative day-degrees with a threshold of 5 $^{\circ}C$ (T_{over5}), thus allowing for a realistic approximation of the plant growth process. Analysis of all the growing cycles recorded between 1992 and 2012 in the study areas indicated that the median value of the cumulative degree-day is 1082, irrespective of the sowing date (i.e. winter or spring wheat). The decline of the C factor throughout the crop growth period subsequently was calculated as a linear function of T_{over5}.

Manual inspection revealed that the tillage records were largely without gaps. In Skuterud, one field with an area of 7.1 ha (or 0.6% of the total agricultural area of the catchment) was left out of further analysis because of structural gaps in the sowing and harvesting dates. Several field records appeared to lack harvesting dates, while sowing dates were present. In this case, a maximum was set on the time for the crop to develop. A maximum of 390 days was used, based on the maximum recorded length of the growing season.

5.2.5 Connectivity index

For the characterisation of the catchment's hydrological and sediment connectivity over time, the Index of Connectivity (IC, unitless) as proposed by Borselli

et al. (2008), was used. Several studies have proven this index to be relatively scale-independent (Vigiak *et al.*, 2012), it is easily calculated and allows for the introduction of a weighing factor that facilitates the representation of seasonal variations in the connectivity of the catchment. The Index of Connectivity provides a spatially distributed estimate of the likelihood that a particle (water or sediment) is transported from location k towards a predefined sink by characterising its contributing area and the subsequent flowpath towards the sink as in Eq. 5.5.

$$IC = log_{10}(\frac{D_{up,k}}{D_{dn,k}}) \tag{5.5}$$

where

$$D_{up,k} = \overline{W}_k \cdot \overline{S}_k \cdot \sqrt{A_k} \tag{5.6}$$

and

$$D_{dn,k} = \sum_{i=k,n_k} \frac{d_i}{W_i S_i} \tag{5.7}$$

where $D_{up,k}$ (m) and $D_{dn,k}$ (m) are the respective upstream and downstream components of equation Eq. 5.5, $\overline{W}_k$ is a the average value of a weighing factor for the contributing area of point k (-), $\overline{S}_k$ the average slope ($m\ m^{-1}$) of this area, and A its surface area (m^2). In the downslope equation (Eq. 5.7), W_i and S_i are the corresponding values, accumulated along the pathway down to the sink, and d_i the flow length (m). Sinks in this study were defined as the permanent stream network and the, monthly variable, gully network as described in section 5.2.3.3. This is a simplification, since gullies typically are expected to have lower transport capacities than permanent streams. Ephemeral gully development is observed to occur in the spring period with snow melt and/or rainfall on (partially) frozen soil, and in summer and autumn during intensive precipitation. Sediment transport rates in ephemeral gullies can therefore be assumed to be considerably larger than those for sheet flow. The weighing factor W represents the the terrain's ability to convey water and particles. In order to be able to compare the values of m for both catchments, IC was ultimately scaled down to range from 0 to 1. In our study, the C factors as derived from the farm records were used. The calculation of D_{up} was carried out in a GIS (GRASS 6.4.4; GRASS Development Team, 2014), while a simple algorithm, written in C++, was used for the D_{dn} calculations. For both the D_{up} and D_{down} terms a deterministic 8 (D8, single outflow) flow routing routine was used; runoff is directed to, and only to, the neighbouring cell with the steepest slope.

5.2.6 Calibration of the catchment sediment mass balance

Total soil loss at the catchment scale is given by Eq. 5.8

$$SS_{tot} = \sum_{i=1}^{n} A_i(m_{s,i} \cdot SS_{s,i} + m_{d,i} \cdot SS_{d,i} + m_g \cdot SS_{g,i}) \tag{5.8}$$

where SS_{tot} is the catchment total monthly or annual soil loss rate (tonne ha^{-1}), summated for n spatial units or polygons, A_i is the surface area (ha) of polygon i, $SS_{s,i}$ is the sheet erosion rate as calculated by PESERA, and $SS_{d,i}$ the rate of soil loss through the tile drainage system from Eq. 5.2 and $SS_{g,i}$ is the gully erosion rate (tonne ha^{-1}), each for polygon i. The multipliers $m_{s,i}$ and $m_{d,i}$ account for particle transport from source to outlet, and effectively are sediment delivery ratios. The multiplier and $m_{g,i}$ for gully erosion represents both sediment delivery ratio and average gully cross section. The term to summate in Eq.5.8 is the specific sediment yield (SSY, tonne ha^1) per polygon, or agronomic unit, in the catchment.

In this study, it was assumed that all suspended solids in the tile drain system will be transported to the surface water network. The multiplier m_d for drain erosion was therefore set at 1 for all times and locations.

The suitability of the Index of Connectivity as an approximation for sediment delivery ratio (SDR) was tested by assessing two calibrations of the model in Eq. 5.8: the first by assuming that all fields have equal SDR values at all times, and the second by assuming that SDR is a function of connectivity and thus variable in space and time. In the latter model, local monthly SS_s values are multiplied by their corresponding connectivity values. Formally, specific sediment yield from an individual field i is estimated by

$$SSY_i = m_s \cdot SS_{s,i} + SS_{d,i} + m_s \cdot SS_{g,i} \tag{5.9}$$

in the static model, and by

$$SSY_i = m_s \cdot IC \cdot SS_{s,i} + SS_{d,i} + m_s \cdot SS_{g,i} \tag{5.10}$$

in the dynamic model version. These values were calculated on the 5 by 5m raster grid before field averages were taken.

The model was calibrated for m_s and m_g on a randomly selected subset (70%) of the monthly values and validated on the full series. The optimisation parameter consisted of the two Nash-Sutcliffe model efficiency values (NSE; Nash and Sutcliffe, 1970) of the monthly and annual SS_{tot} values against the observed sediment loads at the catchment outlets. Annual model performance was expected to outperform monthly performance, so the total efficiency of a calibration was quantified as:

$$NSE = 5 \cdot NSE_{monthly} + NSE_{annual} \tag{5.11}$$

Based on this score, the optimal model fit was chosen from five thousand iterations of selection, calibration and validation.

5.2.7 Scenarios

An assessment was made of the effect of reduced tillage, specifically the spatial prioritisation, on soil loss originating from sheet erosion at the catchment scale. Reduced tillage is defined as the maintenance of a stubble cover between harvesting (autumn) and sowing (spring) of the cereal crop. The baseline for the assessment is sowing (May 1st), harvesting (September 15th) and ploughing (October 1st). The *C* factors of Table 5.2 were used to calculate the average monthly *C* value for each polygon, and *IC* was calculated subsequently. The calibrated model in Eq. 5.8 is the product of the local erosion risk level, the surface area of the polygon, and the multipliers m_s and m_g. The latter term represents the sediment delivery ratio, and the entire product is by definition the specific sediment yield (SSY, tonne $^{-t}$) of a polygon. The scenario analysis was performed by changing the *C* factors, which are the basis for the calculation of *IC* and a configuration of the PESERA model runs. This combination of increased sheet erosion rates and connectivity is expected to results in higher sediment delivery ratios.

Three approaches to spatial prioritisation were compared; 1) polygons with high average *IC* value; 2) polygons with high erosion risk rates; 3) polygons with high specific sediment yield. The changed tillage were applied on the top ranking 25%, 50% , 75% and 100% polygons in each category in the catchments' agricultural area.

5.3 Results and discussion

5.3.1 C factor and IC

The monthly and annual area weighed *C* factors and the index of connectivity are given in Fig. 5.3. The development of the monthly index values over time closely followed the *C* factor (R^2 of 0.88 and 0.87 for Skuterud and Mørdre, respectively). This confirms the presumption that time-differentiated connectivity calculations reflect the seasonality of the connectivity in the small agricultural catchments in this study. Similarly, the range of *IC* values per polygon were expected to be a function of their levels. Despite low R^2 values (0.38 and 0.19 for Skuterud and Mørdre, respectively) the results, displayed in Fig. 5.6, indicate that this is indeed the case. This shows that the scale of the effect of seasonal changes in the crop factor on *IC* depends on the location in the catchment. The marginal effect of reduced tillage on the sediment delivery ratio increases with hydrological connectivity.

The seasonal development of *C* (and as a consequence IC), averaged over the period of investigation, is illustrated by Fig. 5.5. The trend is characterised by

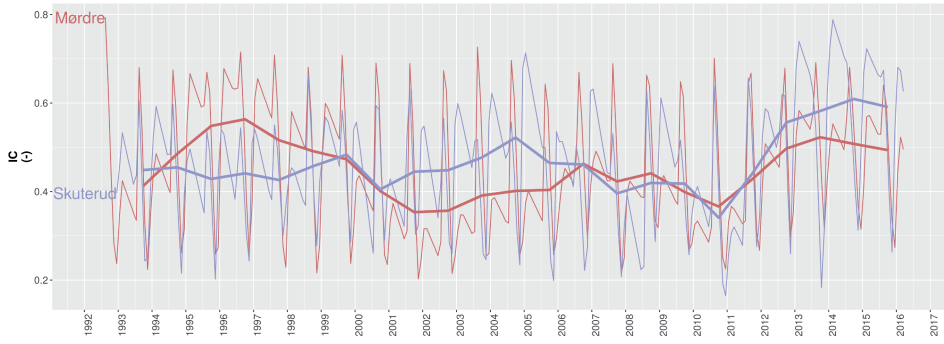

FIGURE 5.3: Monthly and annual *C* factors for Skuterud and Mørdre (thin and thick lines, resp), averaged for the arable surface area.

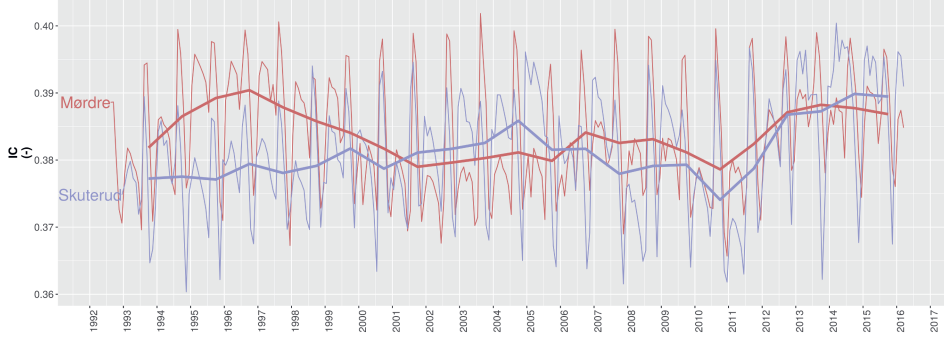

FIGURE 5.4: Monthly and annual *IC* factors for Skuterud and Mørdre (thin and thick lines, resp), averaged for the arable surface area.

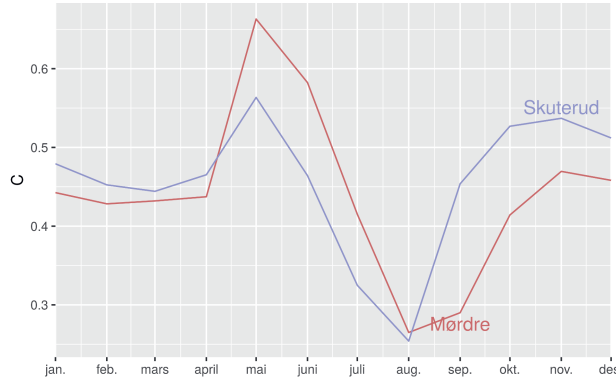

FIGURE 5.5: Monthly *C* factors for Skuterud and Mørdre, averaged for the period of investigation and the arable surface area.

sowing in March and April, marked by a sudden increase in *C*, the subsequent development of the crop cover, and a sharp rise again in August and September, after harvesting. The decrease during winter is explained by the development of either winter corn and weeds. In Mørdre, which is located more to the north and more inland, the lower temperatures result in slower growth rates and a lag in comparison to Skuterud. The difference in the overall level of the *C* factors between the catchments is a result of the different distributions of land use.

In Skuterud, the catchment average *C* factor showed a weak decline in the period 1993-2011, from 0.43 to 0.36, with a sharp rise from 2012 and onwards. In Mørdre, downward trend halted in 2002 and shows a gradual rise after that year. No explanation for either of these trends is available, but both weather and the farmers' individual priorities will influence tillage practise and choice of crops.

The development of the monthly *IC* values over time closely followed the *C* factor (R^2 of 0.80 and 0.87 for Skuterud and Mørdre, respectively). This confirms the asssumption that time-differentiated *IC* calculations reflect the seasonality of the connectivity in the small agricultural catchments in this study.

5.3.2 Erosion rates and sediment delivery ratios

In both catchments, the calibrations for the model with or without spatio-temporally variable sediment delivery ratios performed equally well (Table 5.3). Model performance was poor for the monthly time series of Mørdre catchment. Somewhat better were the monthly results for Skuterud. The annual NSE values for both catchments were considerably better. The model fit for Skuterud was better for the annual and monthly series. This could be explained by the contribution of gully erosion to the total amount of soil loss, as predicted by Eq.5.8.

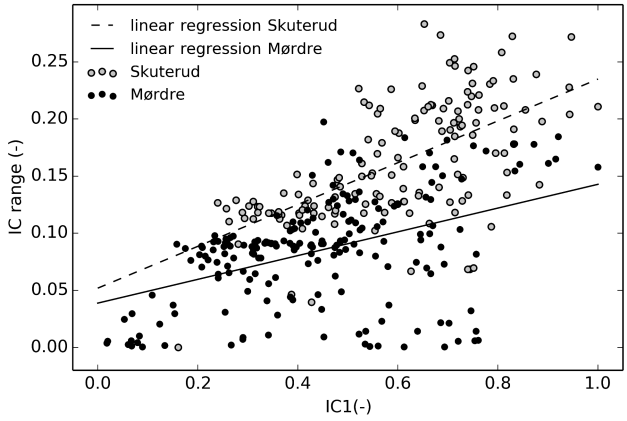

FIGURE 5.6: Range of *IC* values (-) per polygon as a function of *IC* level.

TABLE 5.3: Final values of the calibration parameters and NSE coefficients for Mørdre and Skuterud.

	Mørdre			
SDR	m_s	m_g	$NSE_{monthly}$	$NSE_{monthly}$
static	0.062	$2.30\ 10^{-4}$	0.00	0.25
dynamic	0.138	$2.33\ 10^{-4}$	0.00	0.25
	Skuterud			
SDR	m_s	m_g	$NSE_{monthly}$	$NSE_{monthly}$
static	0.076	$4.17\ 10^{-5}$	0.17	0.37
dynamic	0.195	$4.18\ 10^{-5}$	0.17	0.37

While the average annual contribution of gully erosion in Skuterud is 32%, this is 66% for Mørdre. This difference corresponds to qualitative field observations and available records for the catchments. The contribution of sheet erosion to the observed sediment loss at the outlet is 42% for Skuterud, making this the main source of soil loss. In Mørdre, this value was 22%. The average annual contribution of soil loss through the drainage system for Skuterud and Mørdre is 26% and 12%, respectively.

Other processes might periodically be significant or even predominant. A major source of soil loss is gully erosion (Øygarden, 2003). Channel bed dynamics, stream bank erosion and re-mobilisation of sediments may also contribute. This is especially the case for Mørdre catchment, where the main creek has a broad (5 to 10 m) bed with active meandering. These processes were not taken into consideration because no measurements or models were available to quantify them.

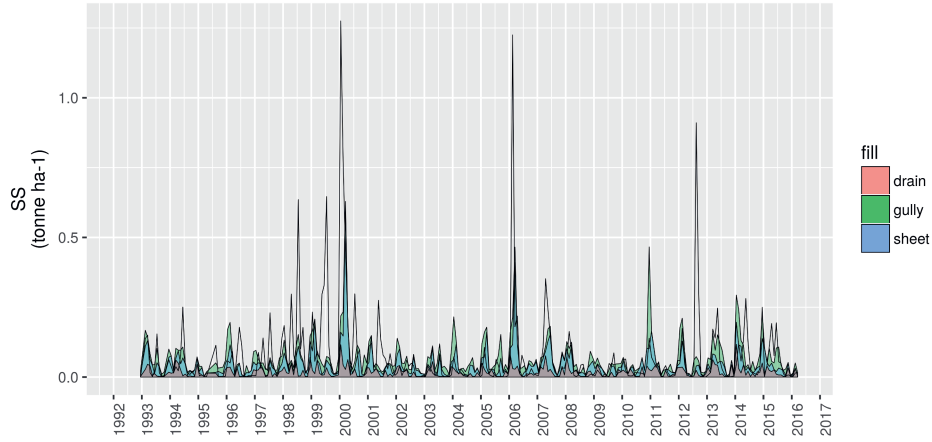

FIGURE 5.7: Model performance (solid black line) against model results per sediment source: monthly soil loss for Skuterud.

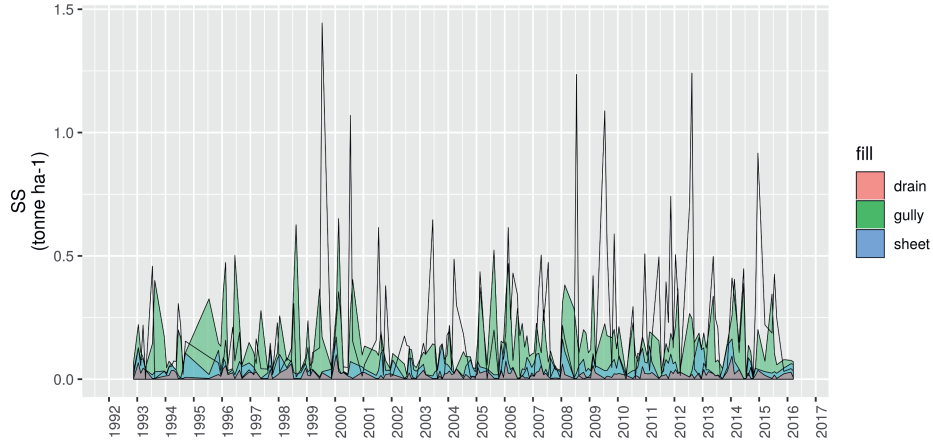

FIGURE 5.8: Model performance (solid black line) against model results per sediment source: monthly soil loss for Mørdre.

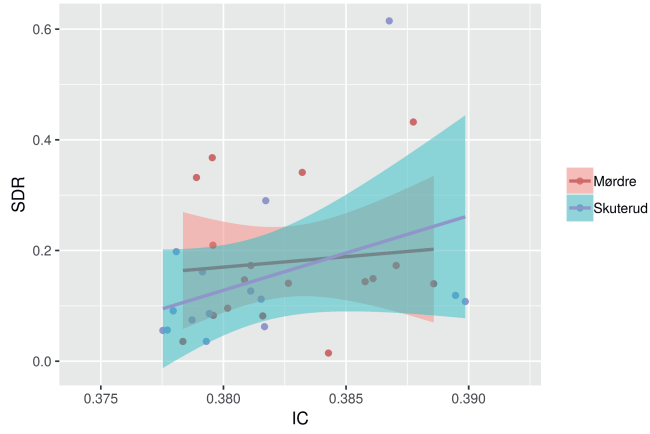

FIGURE 5.9: Annual sheet erosion sediment delivery rates as a function of catchment average connectivity (bands indicate the 95% confidence interval).

The NSE values for the annual time series were considered good enough and further calculations are based on annual values.
The annual data were tested by comparing the annual catchment average IC values to the sediment delivery ratios of the sheet erosion component of total catchment soil loss. SDR in this case is defined as:

$$SDR_s = \frac{SS_s}{SS_{JOVA} - SS_{ssg} - m_g \cdot SSg} \tag{5.12}$$

The denominator in this equation is an estimator of the proportion of sheet erosion in the observed soil loss. SS_{JOVA} is the soil loss as observed at the catchment outlet in the JOVA monitoring programme and m_g is the calibrated multiplier for gully erosion. Note that the multiplier for sheet erosion is not used here, since the numerator represents soil loss at field level.
In both catchments, the simulated sediment delivery ratios were sometimes negative. This could be ascribed to other processes, most likely stream bank erosion and meandering, but there are no data available to confirm this hypothesis. The result of the comparison of annual sheet erosion SDR and IC is given in Fig.5.9.

The coefficients of determination (r^2) for both were low (0.15 for Skuterud and 0.01 for Mørdre). The steeper regression line for Skuterud implies that a equal increase in catchment connectivity has a larger impact on sediment delivery rate than in Mørdre. This is explained by the generally lower slope gradients in Skuterud; sediment transport occurs through temporary channels or otherwise

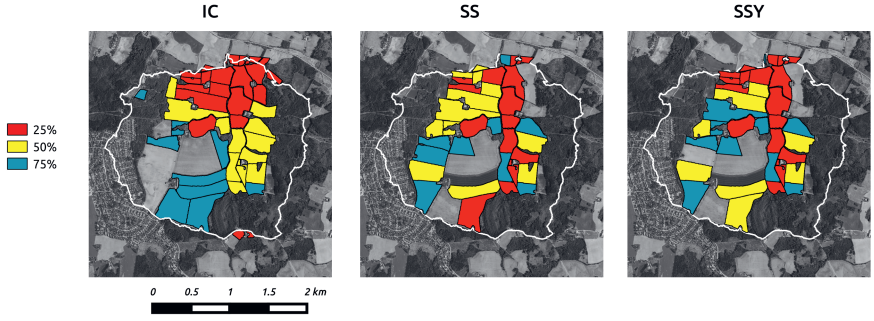

(A) Skuterud

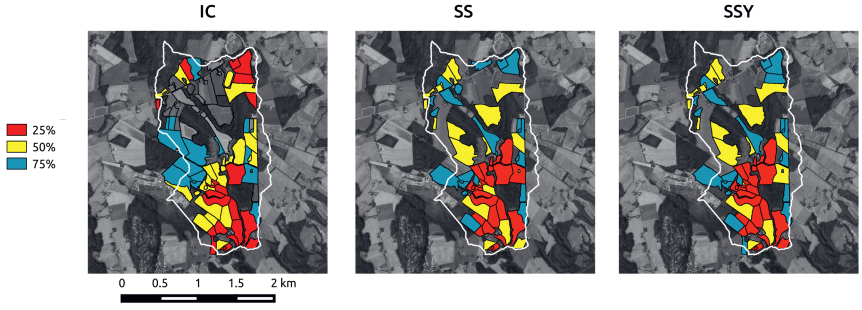

(B) Mørdre

FIGURE 5.10: Coverage of reduced tillage according to the three prioritisation schemes: (a) Skuterud and (b) Mørdre.

concentrated flow, rather than at the hillslope as a whole. Due to the low r^2 values, statistical proof of the catchments' differences in behaviour under different tillage and weather regimes could not be produced.

5.3.3 Scenarios

The maps in Fig. 5.10 show the selections of fields with reduced tillage for the three prioritisation rationales with increasing spatial coverage. In Skuterud, the selection varies significantly for the three rationales, while in Mørdre this was less the case. This is explained by the fact that the areas with the highest erosion risk level in the latter largely coincide with the most hydrologically connected areas. In Skuterud, the highest erosion risk rates are generally found halfway the hillslope. Linear regression for *IC* and erosion risk level indeed showed a low value for Skuterud (0.03) and a higher value for Mørdre (0.34).

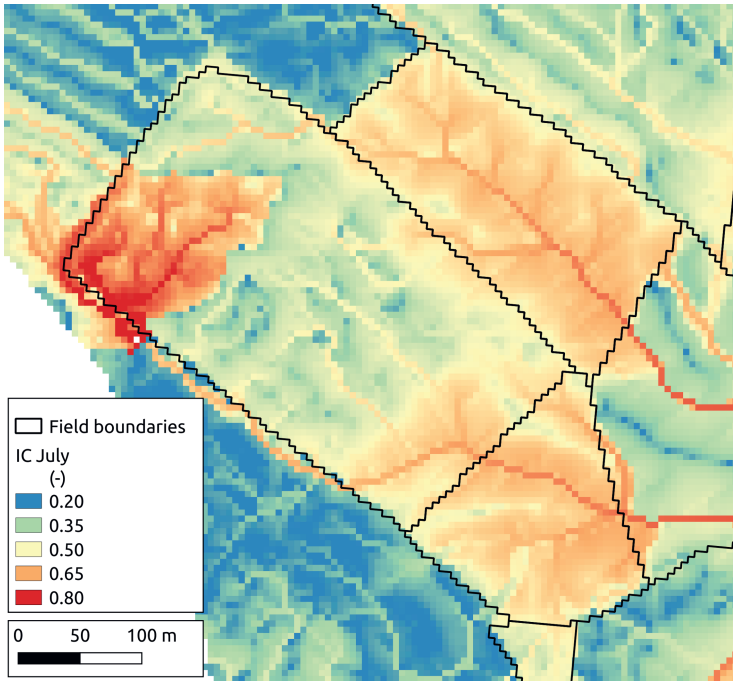

FIGURE 5.11: Spatial variability and resolution of *IC*: an example of how local differences in sediment connectivity are averaged out at field level. The four field polygons in the centre of this map have very similar average *IC* values (example from Mørdre catchment).

Table 5.4 gives an overview of the impact on the catchment sediment balance as a function of prioritisation rationale and coverage. The maximum impact of reduced tillage was a reduction in sheet erosion risk for Skuterud of 24% and for Mørdre of 45%. The reduction of total soil loss is 10 and 9.9%, respectively. The reason for the difference in the efficiency for sheet erosion reduction between the catchments is given by the generally higher levels in Mørdre.

For Mørdre, the largest marginal effect is observed when the first 25% of the agricultural area is covered by reduced tillage. Marginal gains continue to decrease up to full coverage. From 75% to full coverage however, the marginal reduction increases. For Skuterud, the marginal efficiency remains constant up to 50%, and then decreases.

With regard to which of the strategies is chosen, no marked differences were found between prioritising areas according to sheet erosion risk level or specific sediment yield. The reason for this observation might be given by the fact that the spatial variability of the sediment connectivity is leveled out at field level (Fig.**??**.)

TABLE 5.4: Indexed annual reductions in soil erosion risk rates for the reduced tillage scenarios.

	Skuterud			Mørdre		
coverage	IC	SS_s	SSY	IC	SS_s	SSY
25%	0.07	0.09	0.08	0.14	0.20	0.20
50%	0.14	0.17	0.16	0.25	0.28	0.28
75%	0.19	0.21	0.20	0.28	0.31	0.31
100%	0.24	0.24	0.24	0.45	0.45	0.45

The outcomes of the scenarios do not warrant generic conclusions about the effect of different prioritisation rationales. Whether selection based on erosion risk level, connectivity or a combination of both matters for the expected reduction in sediment yield, depends on the terrain. In the undulating terrain of Skuterud, where erosion risk rates comparatively independent of their connectivity, the prioritisation strategy will have a larger effect than in Mørdre.

A similar observation can be made with regard to the marginal effect of increased spatial coverage of reduced tillage. While this decreased for Mørdre, it was almost constant for Skuterud. This does however show that for topographies similar to Mørdre, the extra impact of reduced tillage decreases with increased spatial coverage. If, however, a conservation measure like reduced tillage is planned on smaller fractions of the total surface area in a catchment where erosion risk rate and connectivity are unevenly distributed, the choice of a prioritisation rationale does affect the impact.

5.4 Conclusion

A combination of approaches to quantify the origin of sediment losses at catchment level resulted in a model that could be calibrated against 25 years of measured data on only two parameters. The outcome of the model, monthly estimates of three different sources of soil loss (sheet, gully and drain) might help land use planners to evaluate the suitability and relevance of soil conservation measures. Combating sheet erosion is more relevant to soil loss reduction at catchment level in Skuterud than in Mørdre. In the latter, a focus on the reduction gully erosion risk appears to be more effective.

The first objective of this study was to test the suitability of the Index of Connectivity as a basis for the calculation of sediment delivery ratios and yields of individual fields throughout the year. It is important that IC adequately reflects variations in both time and space, and that it can be incorporated into a calculation of soil loss. The mass balance of the calibrations presented in this study show that the inclusion of IC as a multiplier to upscale sheet erosion at field to

sediment losses at catchment level does not perform better than a uniform, static multiplier.

The principal unit of investigation was the farm field. Much of the spatial variability of topographic factors is leveled out at this scale. Since *IC* and the subsequent calculations were carried out at a spatial resolution of 5m, it is likely to have more added value for the ex-ante evaluation of soil conservation measures at a smaller spatial extent. Similarly, since it depends on flow routing, it will be able to predict the effect of measures that affect the runoff process much more locally, e.g. ditches and barriers to overland flow. At this scale, it can be used to assess the impact of a soil conservation measure like reduced tillage in explicitly in time and space. This enables planners to estimate the effect of measures taken on specific locations on sediment yield at the catchment level at specific times in the year.

The simulations carried out in this study indicate that reduced tillage will decrease soil loss at catchment scale by maximum 10%. Depending on local circumstances, the prevention of other forms of erosion might be a more effective and resource efficient strategy to reduce sediment and solute fluxes to freshwater systems. Transferring experimental results obtained at (runoff) plot level to the catchment scale cannot be done without addressing the question of how much sediment is lost, will actually reach recipient like rivers and lakes.

All of the results and conclusions in this study are at least partially based on a calibrated reservoir model, PESERA, for the estimation of monthly and annual soil loss. But the conclusions about the identification of critical source areas are drawn based on comparisons to a baseline level of erosion risk. This implies that CSA identification is not so much depending on absolute soil loss rates, but on relative values within the space of a catchment. Ultimately, this could mean that a much simpler erosion risk model, even in an uncalibrated configuration, that is able to differentiate risk levels over space, could perform equally well. This was not an objective in this study, but might prove to be a way forward to a robust and data extensive tool for land use planners.

Chapter 6

Comparative performance of methods to calculate the USLE topographical factor (LS)

Abstract

The topographic factor of the Universal Soil Loss Equation (USLE) is a combination of the multipliers for slope length (L) and inclination (S) or an integration of the two. The USLE model and it derivates are have been widely used since the 1960s for the assessment of soil erosion risk rates and *ex-ante* evaluations of soil conservation measures. Erosion at the landscape level typically shows a much higher degree of complexity than at the runoff plot level, for which the USLE originally was developed. Many different methods to calculate the topographic factor have been developed in 50 years since the inception of the USLE. Some of these methods have been calibrated at plot level, while many are deductive in nature and have not been tested at the level of the hillslope or landscape. In this article, soil loss rates are simulated with a physical, spatially explicit model, and compared to the values of the topographic factor as calculated by several established methods. The results show that the performances of the methods differ and that the differences can partially be ascribed to constituent parameters that represent terrain (slope inclination and length). The results also show that none of the methods are able to represent the spatial complexity of the erosion and sedimentation processes.

Submitted for review to **Earth Surface Processes and Landforms as: R.J. Barneveld, S.E.A.T.M van der Zee and J. Stolte. Comparative performance of methods to calculate the USLE topographical factor (LS). (*under revision for re-submission*)**.

6.1 Introduction

Soil erosion is a world wide threat to agricultural productivity and environmental quality that comes with great costs to society (Panagos *et al.*, 2018). Erosion risk maps are developed to quantify the seriousness and spatial distribution of the problem and for *ex-ante* evaluations of conservation strategies. Examples of such exercises on the large, near continental, scale level area described by (FAO, 1979) for North Africa and the Middle East, (Grimm, Jones, and Montanarella, 2001; Kirkby *et al.*, 2008) for Europe, and (Claessens *et al.*, 2008; Nill *et al.*, 1996) for Africa. One of the most widely used models to quantify erosion risk is the Universal Soil Loss Equation (USLE). The model, an empirical equation, is the product of six factors that estimate the erosion risk level for a given period (Wischmeier and Smith, 1965).

$$E = R \cdot K \cdot L \cdot S \cdot C \cdot P \tag{6.1}$$

where E is predicted erosion rate (M L^{-2} T^{-1}), R is the rainfall erosivity factor (E L^{-1} T^{-2} or M L^{-1} T^{-4}), K is the soil erodibility factor (-), L is the slope length factor, S is the slope steepness factor (-), C is the cover management factor (-) and P is a factor to account for erosion control practices (-). The magnitudes of these factors are relative to a worst-case land use scenario (a ploughed, bare soil) on a slope of a standard length (22.13 m) and with an inclination of 9 %. The standard slope length is inherited from the dimensions of the ten first runoff plots established in the 1930s. Their area was set at 1% of an acre while the width for practical reasons was set at 1.83 m (USDA, 2016). The effect of different crops, measures, soil and climatic conditions is quantified by the analysis of the 10,000 records of measured annual soil loss from runoff plots (Morgan, 1996). The validity domain of the original USLE is limited to the pedo-climatic zones found east of the Rocky Mountains (Wischmeier, 1976). Despite this theoretical limitation to its use outside the USA, it is still one of the most applied models, with between 50 to 90 new studies published annually in the last decade. More recent measurements supplement the American data set by new C factors for additional crops and P factors for additional conservation measures, e.g. (Gabriels *et al.*, 2003; Guo *et al.*, 2015). A rainfall erosivity map for Europe, based on collated data from 1541 weather stations, was developed by (Panagos, Borrelli, and Meusburger, 2015a). Several offshoots of the USLE were developed in the decades following its publication. Williams (1975) replaced the rainfall erosivity factor by a runoff energy factor in the Modified Universal Soil Loss Equation (MUSLE). Kinnel and Risse (1998) adapted the orginal equation in a similar fashion, but incorporated the runoff ratio in the rainfall erosivity factor (USLE-M). The Revised Universal Soil Loss Equation (RUSLE Renard *et al.*, 1991), is the most commonly used USLE derivative. RUSLE includes revised methods for several of the factors, including a new rainfall erosivity term, a sub-factor approach for the cover management term and an LS factor that accounts for more complex terrain.

Common to the listed USLE-type models is that topography is represented by a factor that accounts for slope gradient, S, and local slope length, L, often combined in the topographic factor LS. Wischmeier and Smith (1978) define slope length as the distance from the point of origin of overland flow to the point where deposition begins, or where overland runoff starts to concentrate into channeled flow. Several algorithms have been developed to calculate the slope length and steepness factors. These algorithms can be classified by their dimensionality: some, including the original, algorithms are based on slope length, while many more recent definitions use the contributing area or a combination of the two.

6.1.1 Original definition

The original equation used to quantify the dimensionless slope factor S (Wischmeier and Smith, 1965) is:

$$S_{W65} = \frac{0.43 + 0.30s + 0.043s^2}{6.613} \tag{6.2}$$

where s is the slope gradient (%). Renard *et al.* (1997) developed two equations for slope gradients above and below 9%, so that:

$$S_{R97} = 10.8 \cdot \sin\theta + 0.03 \qquad \text{for slopes} < 9\% \tag{6.3a}$$

$$S_{R97} = 16.8 \cdot \sin\theta - 0.5 \qquad \text{for slopes} \geq 9\% \tag{6.3b}$$

where θ is the slope gradient (°). While Eqs.6.2 and 6.3 are based on slope gradients less than 22%, Nearing (1997) derives a single logistic equation for the USLE and RUSLE that is suitable for gentle and steep slopes alike.

$$S_{N97} = -1.5 + 17/\left[1 + \exp(2.3 - 6.1\sin\theta)\right] \tag{6.4}$$

In the original USLE formulation (Wischmeier and Smith, 1965), the slope length factor is given by:

$$L_{W65} = \left(\frac{\lambda}{22.13}\right)^m \tag{6.5}$$

where λ is the slope length (m) and the exponent m is an empirical parameter, derived from field data. While a nomogram is presented in the original publication, the developers include some recommendations for the value of m in the revised handbook (Wischmeier and Smith, 1978). m is 0.5 for slopes steeper than 5%, 0.4 on slopes between 3.5 and 4.5%, 0.3 on slope between 1 and 3 and 0.2 when gradients are less than 1%. Foster, Meyer, and Onstad (1974) relate the value of m to the ratio β between rill and inter-rill erosion, so that:

$$m = \frac{\beta}{1 + \beta} \tag{6.6}$$

where β is defined as:

$$\beta = \frac{\sin\theta / 0.0896}{3.0 \cdot (\sin\theta)^{0.8} + 0.56} \tag{6.7}$$

6.1.2 Definitions derived for complex terrain

Foster *et al.* (1974) derive an equation for *LS* for non-uniform slopes by dividing the hillslope into sections. Assuming a constant value of m, they calculate the combined slope length and steepness factor as:

$$LS_{F74} = \left[\frac{\sum_{j=1}^{n} (S_j \lambda_j^{1.5} - S_j \lambda_{j-1}^{1.5})}{\lambda_e (22.13)^{0.5}} \right] \tag{6.8}$$

where n is the number of hillslope segments, λ_j is the distance from the upper to the lower limits of segment j, λ_{j-1} the slope length of the upslope segment, and S_j and S_{j-1} are the slope factors for segment j and the upslope segment, respectively. λ_e is the total slope length.

Moore and Burch (1986) derive an *LS* equation from unit stream power theory, with the form:

$$LS_{MB86} = \left(\frac{a \cdot \lambda}{22.13} \right)^{0.4} \cdot \left(\frac{\sin\theta}{0.0896} \right)^{1.3} \tag{6.9}$$

where a is a catchment shape parameter given by Eq.6.10, which represents diverging (a<1) and converging (b>1) catchments.

$$a = A / b\lambda \tag{6.10}$$

where A is the contributing area (m^2) and b the effective contour width (m). The contour width can be derived from the DEM in several ways (Gallant and Hutchinson, 2011). Examples of two commonly used methods are aspect based methods (Eq.6.11a; Mitasova *et al.*, 1996) and methods based on flow routing (Eq.6.11b; Quinn *et al.*, 1991).

$$b_{M96} = D \cdot (|\sin\alpha| + |\cos\alpha|) \tag{6.11a}$$

$$b_{Q91} = \begin{cases} 0.5 \cdot D & \text{for the cardinal directions} \\ 0.354 \cdot D & \text{for the diagonal directions} \end{cases} \tag{6.11b}$$

where D is the grid cell size (m) and α the aspect direction (°), given by:

$$tan\,\alpha = \frac{-s_y}{-s_x} \tag{6.12}$$

where s_x and s_y are the slope gradients in the cardinal (west-east and south-north)

directions. Moore and Burch (1986) further derive Eq.6.13 to account for rill erosion.

$$LS_{MB86} = \left(\frac{\lambda}{22.13}\right)^{0.4} \cdot \left(\frac{\sin\theta}{0.0896}\right)^{1.3} \cdot Z \tag{6.13}$$

where Z is a rilling factor given by $Z = (c/e)^{0.4}$, in which c and e are constants that represent the frequency and dimensions of rills. Renard *et al.* (1997) rewrite the L factor for a segmented, non-uniform, slope as:

$$L_{R97} = \frac{(\lambda_i^{m+1} - \lambda_{i-1}^{m+1})}{(\lambda_i - \lambda_{i-1}) \cdot 22.13^m} \tag{6.14}$$

A slope segment is a unit of length on a hillslope that displays some degree of uniformity with regard to certain properties. A cell in a regular raster grid like a DEM can be perceived as a slope segment, where its upper and lower boundaries are described by the elevations of the neighbouring cells (Schmitt, 2009; Bagherzadeh, 2014).

While Eq. 6.9 is designed to differentiate between hillslope segments with converging and diverging flow patterns, it cannot be considered a two-dimensional definition of the slope length factor. The same can be said about the method proposed by (Flacke, Auerswald, and Neufang, 1990), who cascade information about slope steepness and length over the segments of a Triangular Irregular Network (TIN). The first instance of an algorithm that replaces one-dimensional slope length by contributing area is included in the mathematical derivation of *LS* by (Moore and Wilson, 1992). Here, the specific catchment area (A_s, $m^2\, m^{-1}$) replaces λ of Eq. 6.9. They also differentiate the exponents of Eq. 6.9, so that:

$$LS_{MW92} = \left(\frac{A_s}{22.13}\right)^m \cdot \left(\frac{\sin\theta}{0.0896}\right)^n \cdot (m+1) \tag{6.15}$$

where A_s is the contributing area per contour width, or the specific catchment area ($m^2\, m^{-1}$). Note that the exchange of a one-dimensional parameter (λ) for a two-dimensional (A_s) is characteristic of the phenomenological nature of *LS* equations. The recommended range for the slope length exponent m is between 0.4 and 0.6, and between 1.2 and 1.3 for the slope steepness exponent n. Foster (1992) in his comments on Moore and Wilson, 1992 points out that this approach is not equivalent to the original definition of *LS*, because it represents erosion limited by transport capacity rather than by detachment rate.

Mitasova *et al.* (1996) present an algorithm to calculate the specific catchment area as:

$$A_s = \frac{1}{b} \sum_{i=1}^{n} \mu_i D_i^2 \tag{6.16}$$

where b is the effective contour length (Eq.6.11), i is one of the n grid cells contributing to the point of interest. The unitless weighting factor μ is included to

account for the volume of the runoff generated in the catchment area. When no information is available, μ is set to be 1.

Desmet and Govers (1996) present a definition of L where A_s is included implicitly.

$$L_{DG96} = \frac{(A_{i,j-in} + D^2)^{m+1} - A_{i,j-in}^{m+1}}{D^{m+2} \cdot b^m \cdot 22.13^m} \tag{6.17}$$

where L_{DG96} is the slope length factor for one segment or grid cell and $A_{i,j-in}$ the contributing area of the grid cell i (m^2). Note that $A_{i,j-in}$ and A_s differ by the area of grid cell i, which is excluded in the former and included in the latter. Panagos (2015) applied Eq.6.17 for the derivation of a new LS map for Europe.

Slope length λ itself in terrain with converging and diverging flow patterns is most commonly calculated as presented by Hickey (2000). In this method, local slope lengths (λ_i), *i.e.* within grid cell i, are 0.5·(cell size) at locations on the divide of a catchment (no inflow), 1.0·(cell size) when the input cell is in a cardinal direction and $\sqrt{2}$·(cell size) when the input cell is situated diagonally. When flow-paths merge, the highest λ value is assigned and continued. In this way, the maximum flow-path length is calculated (Gallant and Wilson, 2000). Slope length according to Hickey's algorithm is further referred to as λ_{H00} (m). Zhang *et al.* (2017) correct the internal flow-path length within the cell (CSL, m) by defining it as:

$$CSL = 0.5 \cdot D \qquad \text{if } \theta = 0 \tag{6.18a}$$

$$CSL = D \cdot a \cdot (|\sin\alpha| + |\cos\alpha|) \qquad \text{if } \theta \neq 0 \tag{6.18b}$$

where a is value of distance transforms in the orthogonal direction (0.962, (Butt and Maragos, 1998)). This transformation is reported to better approximate the actual length of linear elements over a regular raster grid, like a DEM (Paz *et al.*, 2008). They then calculate the Distribution Watershed Erosion Slope Length (DWESL or λ_{Z17}) by accumulating the CSL values with a multiple flow direction (MFD) flow routing algorithm. While the described algorithms for slope length (λ) and contributing area (A) follow the flowpath in the downward direction, Mitasova *et al.* (1996) utilise an algorithm that progresses upward. Flow lines in their algorithm are generated uphill in the direction of the gradient, based on the aspect.

Finally, all the above methods can be applied with or without dividing the hillslope by means of cutoff slope angles. Cutoff slope angles can be defined as threshold values to identify locations where discontinuities in the transport of suspended solids can be expected. One way of defining these sedimentation and transition zones is to set a threshold value for the decrease in slope from one grid cell or hillslope segment to the next. While Hickey (2000) points out that the threshold value will depend on the amount of runoff and/or sediment that passes through a location, Remortel, Hamilton, and Hickey (2001) and Rodriguez

and Suarez (2010) find relatively robust values of around 0.5 (*i.e.* a decrease in slope gradient of 50 %) for slopes equal to or greater than 5%. For slopes gentler than 5%, they use a value of 0.7 as the default in their tool (*ibid.*).

LS algorithms have been improved in several ways in the past five decades, with the objective to better represent topography. In combination with the increasing availability of accurate and high-resolution digital elevation data (Alewell *et al.*, 2019), *LS* algorithms should become better at estimating the effect of slope inclination and length on erosion. The variety of methods to calculate the topographic factor *LS* and its constituent variables warrants a comprehensive evaluation. Several studies have compared different methods (Hoffmann Oliveira *et al.*, 2013; Zhang *et al.*, 2013) but do not relate the obtained *LS* values to measurements or model outcomes. Other studies compare measurements with *LS* factors to assess the suitability of the approaches (Liu *et al.*, 2000; Bagarello, Ferro, and Pampalone, 2013; Hrabalíková and Janeček, 2017). In these studies, calculated LS factors are compared to measurements from runoff plots. These runoff plots have a simple geometry and have a linear profile curvature. The runoff plots in the cited publications are also restricted in size (maximum 15 m wide and 60 m long). Successful calibrations and validations of particular methods do not necessarily hold for larger spatial scales, even less so to catchments with relatively complex topographies. Measurements of sheet erosion to quantify the isolated effect of any of the USLE factors at catchment scale are challenging, if not impossible (Stroosnijder, 2005). The suitability of the different *LS* algorithms could, however, be tested by comparing them to simulated erosion rates.

The objectives of this study are (1) to test the most commonly used *LS* methodologies against simulated erosion rates for three one-dimensional hillslopes with idealised morphologies, and (2) to use the results of these tests to quantify where and under which circumstances the different methods to calculate *LS* are best suitable to predict soil erosion on complex terrain.

6.2 Materials and methods

6.2.1 Selected LS factor algorithms and their constituent parameters

In view of the diversity of methods and algorithms to calculate the constituent parameters for *LS*, most notably slope gradient and length, flow routing and effective contour length, a choice had to be made in order to understand the consequences on the final value of *LS*. The parameters used in this study, and the associated algorithms, are given in Table 6.1.

Slope gradient s can be calculated in many different ways (Zevenbergen and Thorne, 1987), and the choice of a method can have a significant impact on the final result (Dunn and Hickey, 1998; Nakil and Khire, 2016; Zhou and Liu, 2004).

TABLE 6.1: Overview of the topographic factors and their variations, evaluated in this study. The subscript refers to the original reference of the algorithm.

parameter	*short description*	*reference*	*Eq.*
slope steepness factor (S)	original definition	S_{W65}	Eq.6.2
	differentiated for steep and gentle slopes	S_{R97}	Eq.6.3
	logistic function	S_{N97}	Eq.6.4
slope length factor (L)	original definition	L_{W65}	Eq.6.5
	specific catchment area	L_{DG96}	Eq.6.17
	hillslope segments	L_{R97}	Eq.6.14
topographic factor (LS)	unit stream power theory, 1-dimensional	LS_{MB86}	Eq.6.13
	unit stream power theory, 2-dimensional	LS_{MW92}	Eq.6.15
slope steepness (s)	third-order finite element	s_{S69}	Eq.6.19
	slope towards steepest neighbour	s_{H00}	*see text*
slope length (λ)	1-dimensional, longest	λ_{H00}	*see text*
	2-dimensional, accumulated	λ_{Z13}	*see text*
contour length (b)	contour length based on aspect	b_{M96}	Eq.6.11a
	contour length based on flow routing	b_{Q91}	Eq.6.11b

For the *LS* methods based on unit catchment area, slope steepness was calculated by means of the third-order finite difference method (Sharpnack and Akin, 1969), Eq.6.19.

$$s_{x,S69} = (z_7 - z_1 + z_8 - z_2 + z_9 - z_3)/6D \tag{6.19}$$

where $s_{x,S69}$ is the slope steepness in the x direction according to the method by Sharpnack and Akin (*ibid.*), $z_7 - z_1$, $z_8 - z_2$ and $z_9 - z_3$ are the elevation differences (m) in the x direction in a 3x3 window. s_y is calculated by performing the same operation on the three columns in the window. The maximum downhill slope method (Hickey, 2000) was used in the 1-dimensional algorithms and is referred to as s_{H00}. Contributing area, too, can be calculated in different ways. In the research presented here, flow accumulation along a single-neighbour path (D8) was calculated by propagation along the maximum downhill slope direction. Where flow was divided over multiple neighbouring cells (MFD), a slope-proportional method was used (Quinn *et al.*, 1991).

A selection of (combinations of) parameters had to be made in order to evaluate the resulting values of LS against simulated erosion rates. The parameters and factors from Table 6.1 were combined to calculate 36 different LS maps in six groups. The premise of the combinations as listed below, is conceptual consistency. The most notable categorisation is the dimensionality. One-dimensional (cumulative slope length) methods are rooted in the empirical basis of the USLE: soil loss measured from runoff plots. Since the original model was developed for the comparison of different agronomic practices, *LS* in its original sense can be considered a multiplier that helped to harmonise soil loss data from different

runoff plots. Two-dimensional methods (specific catchment area) are developed within the framework of applying the USLE to real, complex, landscapes.

I. *L* as in the original definition by (Wischmeier and Smith, 1965). Slope steepness and length are calculated 1-dimensionally and along the steepest neighbouring cell. *L* is combined with the three *S* methods from Table 6.1.
   (a) $\mathbf{L_{W65}S_{W65}}$ S according to the original definition (Wischmeier and Smith, 1965)
   (b) $\mathbf{L_{W65}S_{R97}}$ S according to (Renard *et al.*, 1997)
   (c) $\mathbf{L_{W65}S_{N97}}$ S according to (Nearing, 1997)

II. *L* for 1-dimensional hillslope segments according to (Renard *et al.*, 1997)
   (a) $\mathbf{L_{R97}S_{W65}}$ S according to (Wischmeier and Smith, 1965)
   (b) $\mathbf{L_{R97}S_{R97}}$ S according to (Renard *et al.*, 1997)
   (c) $\mathbf{L_{R97}S_{N97}}$ S according to (Nearing, 1997)

III. *LS* based on stream power theory (Moore and Burch, 1986) 1-dimensional
   (a) $\mathbf{LS_{MB86}}$

IV. *LS* based on stream power theory (Moore and Wilson, 1992) 2-dimensional
   (a) $\mathbf{LS_{MW92}}$

V. *L* based specific catchment area (Desmet and Govers, 1996) 2-dimensional, *s* calculated with (Sharpnack and Akin, 1969) and *b* with (Mitasova *et al.*, 1996) or (Quinn *et al.*, 1991).
   (a) $\mathbf{L_{DG96}S_{W65}}$ S according to (Wischmeier and Smith, 1965)
   (b) $\mathbf{L_{DG96}S_{R97}}$ S according to (Renard *et al.*, 1997)
   (c) $\mathbf{L_{DG96}S_{N97}}$ S according to (Nearing, 1997)

VI. *L* based on 2-dimensional accumulated flow-path length (Zhang *et al.*, 2013).
   (a) $\mathbf{L_{Z13}S_{W65}}$ S according to (Wischmeier and Smith, 1965)
   (b) $\mathbf{L_{Z13}S_{R97}}$ S according to (Renard *et al.*, 1997)
   (c) $\mathbf{L_{Z13}S_{N97}}$ S according to (Nearing, 1997)

The 14 listed *LS* methods were all calculated with and without defining cutoff points in the landscape. These versions of the LS factor are marked with a superscript **X**, so that, for example, the original definition by Wischmeier with cutoff points is denoted as $\mathbf{L^X_{W65}S_{65}}$. Since the definition of cutoff points depends on the rate of change of the slope gradient, it depends on the slope algorithm used.

Cutoff points for the 1-dimensional *LS* methods are defined by the steepest neighbour method. For the 2-dimensional methods, the specific catchment areas were calculated while incorporating the cutoff routine proposed by (Zhang *et al.*, 2013). Here, flow accumulation halts when the slope flattens out. Contour length b for the calculation of A_s (Eq.6.16) in the 2-dimensional methods was determined by both the aspect and flow routing method (b_{M96} and b_{Q91} in Table 6.1), where the latter is marked by a q (e.g. $\mathbf{L^{X}_{DB96,q}S_{W65}}$).

6.2.2 Modeling erosion rates

Testing the performance of the *LS* methods required a spatially distributed estimate of erosion rates. Since point or sub-field measurements of this kind were not available, an erosion model was used to provide estimates. The revised Morgan, Morgan and Finney model (MMF) for soil erosion risk was adapted and parametrised to estimate annual soil erosion rates (Morgan, Morgan, and Finney, 1984; Morgan, 2001) at a 5 x 5 raster grid. The original MMF model simulates the runoff phase by estimating saturation excess at daily time intervals. Erosion and deposition are then calculated by empirical equations for splash detachment and sediment transport by overland flow. The revised MMF model also simulates detachment by overland flow. In this study, the model was enhanced by including a soil water balance module, simplifying the approach taken by Choi *et al.* (2017). Inclusion of the soil water balance was deemed important because it enabled the model to mimic spatial differentiation with regard to infiltration and re-infiltration. This allows for the simulation of sedimentation and re-entrainment of particles during subsequent erosive precipitation episodes.

The daily water balance for the effective hydrological depth (EHD, mm) is given by

$$V_{EHD} = I - ET - D \tag{6.20}$$

where V_{EHD} is the volumetric soil water content, I the daily infiltration, ET the daily evapotranspiration (mm) and D the daily drainage to deeper soil layers (mm). Infiltration depends on the available pore space compared to the daily precipitation P (mm, rainfall and/or snow melt).

$$I = \begin{cases} P, & \text{if } \Phi \geq P \\ \Phi, & \text{if } \Phi < P \end{cases} \tag{6.21}$$

where Φ is the available pore space within the EHD (mm). On days with an air temperature of less than 0 °C, infiltration was assumed to be zero. Drainage was not modelled explicitly, but expressed as a daily rate, equivalent to 25 % of free water in the EHD profile.

$$D = (\theta - \Phi) \cdot 0.25 \tag{6.22}$$

The model does not account for delays in runoff production due to surface depression storage: excess precipitation or snow melt will result in surface runoff.

Flow accumulation assumes instantaneous redistribution for the daily time steps. In concordance with the LS calculations, overland flow is routed by a *D*8 algorithm for the 1-dimensional model runs. Similarly, a slope proportional *MFD* algorithm is applied for the 2-dimensional simulations. Particle detachment and transport are governed by the equations described by Morgan (1996). Detachment by rainfall is given by:

$$F = K \cdot KE \cdot 10^{-3} \tag{6.23}$$

where F is the daily splash detachment rate (kg $m^{-2}day^{-1}$), K the erodibility of the soil (g J^{-1}) and KE the kinetic energy of the effective rainfall (J m^{-2}). Leaf drainage was ignored in this model run, and only direct precipitation was taken into account.

$$KE = P \cdot (11.9 + 8.7 \cdot \log_{10}(I)) \tag{6.24}$$

where I is the precipitation intensity, typical for erosive rainfal in a temperate climate (10 mm h^{-1}, Morgan, 2001. Detachment by runoff (H, kg $m^{-2}day^{-1}$) is given by

$$H = Z \cdot Q^{1.5} \cdot sin(s) \cdot 10^{-3} \tag{6.25}$$

where Q is the daily runoff (mm), and Z a soil cohesion factor, set at 1 in this simulation. Particle detachment rates are compared to the daily sediment transport capacity, evaluated as

$$TC = C \cdot Q^2 \cdot sin(s) \cdot 10^{-3} \tag{6.26}$$

where TC is the sediment transport capacity (kg $m^{-2}day^{-1}$). If the sum of detachment and incoming sediment in a raster cell is greater than TC, the surplus is deposited. Otherwise, the sediment is routed further down. Sediment routing is simulated by the same equations for the conservation of mass as for runoff.

The model was evaluated for its ability to produce results that were reasonable with regard to their absolute quantities and variance. No attempt was undertaken to calibrate it against measured data. Model evaluation consisted of comparing output to measurements of local θ and discharge and sediment load at catchment level. The Nash-Sutcliffe model efficiency coefficient (NSE) (Nash and Sutcliffe, 1970) was used to this purpose.

6.2.3 Terrain data

6.2.3.1 Gryteland catchment

Gryteland, is a 0.27 km^2 headwater catchment in Southeastern Norway, ca. 30 km south of Oslo (outlet located at 59°40'12.2", 10°50'2.9"). A monitoring station that measures overland flow discharge is situated at its outlet. Land use in the catchment consists of agriculture (55%), mixed forest (45%) and farm infrastructure (1%). Agricultural land use consists of arable cropping, primarily wheat cultivation. The climate is a warm humid continental, (Köppen Dfb), with

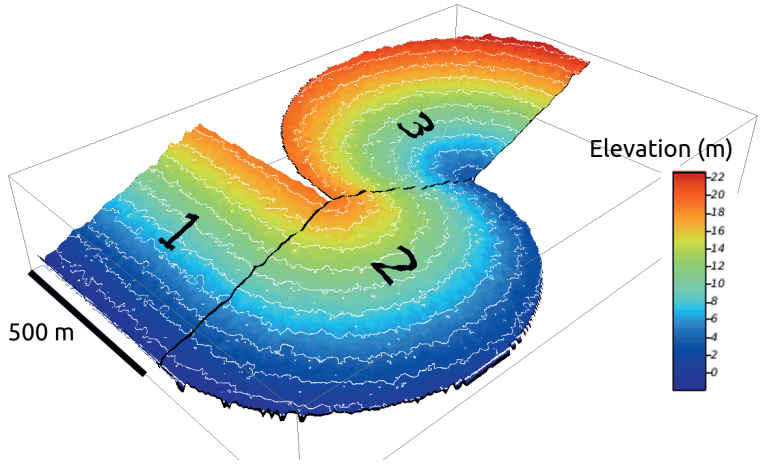

FIGURE 6.1: Artificial DEM (linear profile curvature); (1) parallel flow, (2) divergent flow and (3) convergent flow.

snow in winter and a distinct melting period in March-April. The landscape is undulating, with forest covering the higher parts and agriculture dominating the foothill. The DEM with a grid size of 5 m was derived from Norway's 1x1 m national elevation model (Kartverket, 2022). This DEM, covering most of Norway's landmass, is based on LIDAR measurements with a point density of at least 1.5 points m^{-1}.

6.2.3.2 Artificial DEMs

DEMs were generated with a general hillslope form (macrotopography) and a mesotopography that allows for the local routing of overland flow (Appels, Bogaart, and Zee, 2017) that resembles the Gryteland catchment as representative for Norwegian agricultural soil surfaces. The DEMs used for the erosion modelling and LS calculations should represent the primary hillslope forms. Nine hillslope forms were generated by combining three planform curvatures (convergent, divergent and parallel flow) with three profile curvatures (convex, linear and concave). For computational ease, the three planform curvatures were combined into one DEM as depicted in Fig. 6.1. The spatial resolution of the DEMs was set at 5 m. This resolution is suitable for the modified MMF model, and allows for the representation of local flow patterns. The maximum slope length (euclidean) was set at 500m. This distance was chosen in order to cover all slope lengths up to the recommended 1,000 ft for the *LS* factor in USLE and RUSLE (Wischmeier and Smith, 1978; Water Research, 2002). The average slope gradient in the Gryteland microcatchment is 3.82%. The artificial DEMs were given a similar mean slope gradient, so that the elevation difference from top to bottom of the hillslope was 19.1m.

Slope steepness and especially slope length as hydrological terrain metrics at the level of the grid cell are not only a function of macrotopography (*slope form*), but also of how overland flow diverges and concentrates from grid cell to grid cell. In this study, the variation in elevation at the scale of the grid cell is referred to as mesotopography (as compared to microtopography; soil roughness, or variation at the scale of the soil aggregate). To this purpose, a soil surface was generated by the diamond-square algorithm introduced by (Fournier, Fussell, and Carpenter, 1982). This is a midpoint displacement technique that enables the generation of surface models with a certain autocorrelation and roughness. The initial step consists of assigning random Gaussian numbers to the corners of a 5 by 5 grid. Diagonal, or diamond, steps are then alternated with square steps until all positions in the grid are assigned an elevation value.The magnitude of the Gaussian variation in elevation is scaled according to the distance in between points, so that

$$z_{i,j} = 0.25 \cdot \underbrace{(z_{i-1,j} + z_{i+1,j} + z_{i,j-1} + z_{i,j+1})}_{\text{readily assigned elevations}} + \underbrace{f(\mu, \sigma^2)}_{\text{Gaussian}} \cdot \underbrace{dx}_{\text{scaling}} \tag{6.27}$$

where $z_{i,j}$ = is the generated elevation (m) at the midpoint between the points $z_{i-1,j}$, $z_{i+1,j}$, $z_{i,j-1}$, $z_{i,j+1}$, i and j are the relative positions in the x and y directions, respectively, $f(\mu, \sigma 2)$ is a function that generates values according to a normal distribution with mean μ and standard deviation σ^2, and dx is the horizontal distance between zi, j and $z_{i-1,j}, z_{i+1,j}, z_{i,j-1}, z_{i,j+1}$. This pattern is repeated until a raster grid with the same dimensions as the DEM containing the macrotopography is filled.

The semivariogram of the Gryteland microcatchment was assumed to characterise a typical agricultural mesotopography. Subsequently, a mesotopography was generated so that nugget, sill and range were within the range of those of Gryteland sub-catchment (Fig. 6.2a). The hydrological-morphometric realism of these DEMs finally was tested by comparing the tortuosity (τ, unitless) of the flowpaths of the generated mesotopography to that of the Gryteland microcatchment. Tortuosity was calculated by:

$$\tau = \frac{l_H}{l_E} \tag{6.28}$$

where l_H is the hydrological flow path length (m), calculated with the D8 algorithm, and l_E the Euclidean distance (m) between the first and final points in a certain flowpath. Both lengths were calculated in the horizontal plane. Flowpath tortuosity depends on slope, flow-path length and mesotopography. In order to isolate the effect of mesotopography of the generated DEMs, tortuosity was expressed as a function of the product of flowpath length and slope, s. A regression was performed on a series of the generated mesotopography superimposed on planes with inclinations between 0.01 m m^{-1} and 0.10 m m^{-1}, with 0.01 m m^{-1}

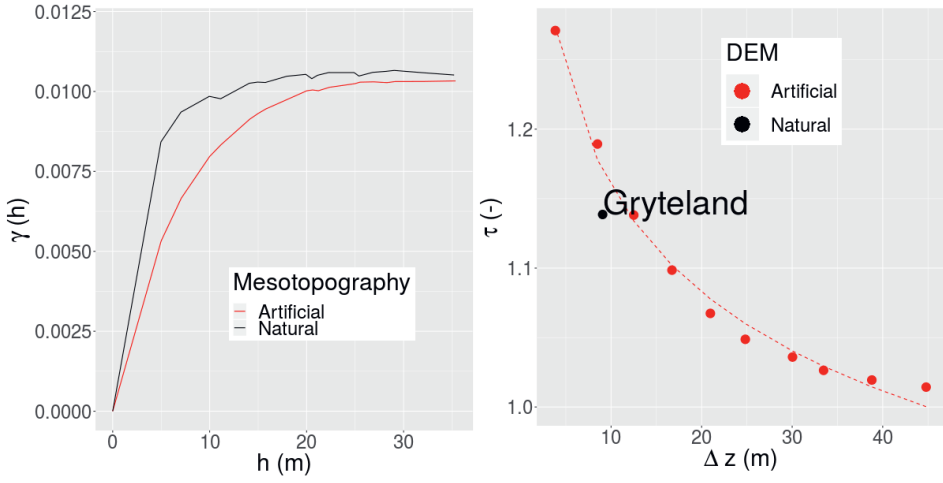

(A) semivariogram (B) tortuosity

FIGURE 6.2: Comparison of mesotopography of Gryteland catchment and the artifically generated DEM.

increments (Fig. 6.2b). In each increment, the sinks in the generated soil surfaces were filled with the algorithm by Planchon and Darboux (2001) in SAGA GIS. As a final evaluation, the tortuosity and semivariograms of the artificial DEMs were compared to those of the Gryteland microcatchment (Fig. 3).

While the semivariogram of the artificial surface (Fig.3a) has a slightly smaller gradient, the range and sill are in the correct order of magnitude. Figure 3b shows that the tortuosity of the artificial surface is within reasonable range of the characteristic value for Gryteland. The final DEMs were created by adding the generated mesotopography to the nine macrotopographies (Fig. 1).

6.2.4 Algorithm performance

The algorithms to calculate the LS factor were tested for their ability to produce quantitative and spatial similarity to the erosion model run. The MMF model, configured with the same input parameters as for the runs on the artificial DEMs, was run on a Wischmeier plot. The standard erosion rate with this configuration at the bottom of the 22.13 m long plot, i.e. $LS = 1$, was compared to the erosion rates on the DEMs. The ratio of these values to the standard erosion rate is then the observed LS value. The observed values were compared to the results from the 18 algorithms. The 1-dimensional, slope length based, LS algorithms were compared to the 1-dimensional, D8, MMF runs. The 2-dimensional, catchment based, algorithms were compared to the MMF runs that used multiple flow direction for flow routing.

Being a spatial index, *LS* was tested by assessing both its quantitative and spatial qualities. In this study, a multiple-component performance metric is used as the one described by Koch, Demirel, and Stisen (2018). Their Spatial Efficiency metric (SPAEF) consists of three parts, so that:

$$SPAEF = 1 - \sqrt{(\alpha - 1)^2 + (\beta - 1)^2 + (\gamma - 1)^2} \tag{6.29}$$

Here, α is the Pearson correlation coefficient between *LS* as calculated by the 18 algorithms and as derived from the erosion model runs. β represents the variation, expressed as the ratio between the coefficients of variation of *LS* values based on the algorithms to those on the model run. γ, finally, is a comparison of the spatial variability, calculated as the intersection of the histograms of the normalised *LS* values as in the following equation;

$$\gamma = \frac{\Sigma_{j=1}^{n} min(LS_{algorithm}, LS_{model})}{\Sigma_{j=1}^{n} LS_{model}} \tag{6.30}$$

where n is the number of bins in the histogram. The SPAEF metric thus integrates a comparison of the absolute values, the overall variance and the spatial variability. It is therefore considered a suitable, unified metric to express *LS* algorithm performance.

The *LS* algorithms with the most favourable SPAEF scores were investigated further by identifying areas in the terrain where they perform particularly good and bad.

A comparison of the algorithms' performance on the artificial DEMs were compared for the different planform and profile slopes. Statistical difference between the slope forms were tested pairwise by t-tests or Kruskal-Wallis' tests, according to the normality of their distributions.

6.3 Results

6.3.1 Primary topographic attributes

Different algorithms for slope and specific catchment area yield different results. Table 6.2 shows the average values of topographic attributes on which the *LS* equations are based. The figures show that slope form affects the magnitude of these attributes significantly, despite the DEMs equal overall length and slope gradients. Slope gradients calculated towards the steepest neighbouring cell (s_{H00}) are higher than those taking account all neighbouring cells (s_{S69}). Similarly, the calculated LS values based on algorithms that calculate the specific catchment area by means of Mitasova (1996; b_{M96}]) are consistently lower than those that include Quinn's SCA method (1991; b_{Q91}).

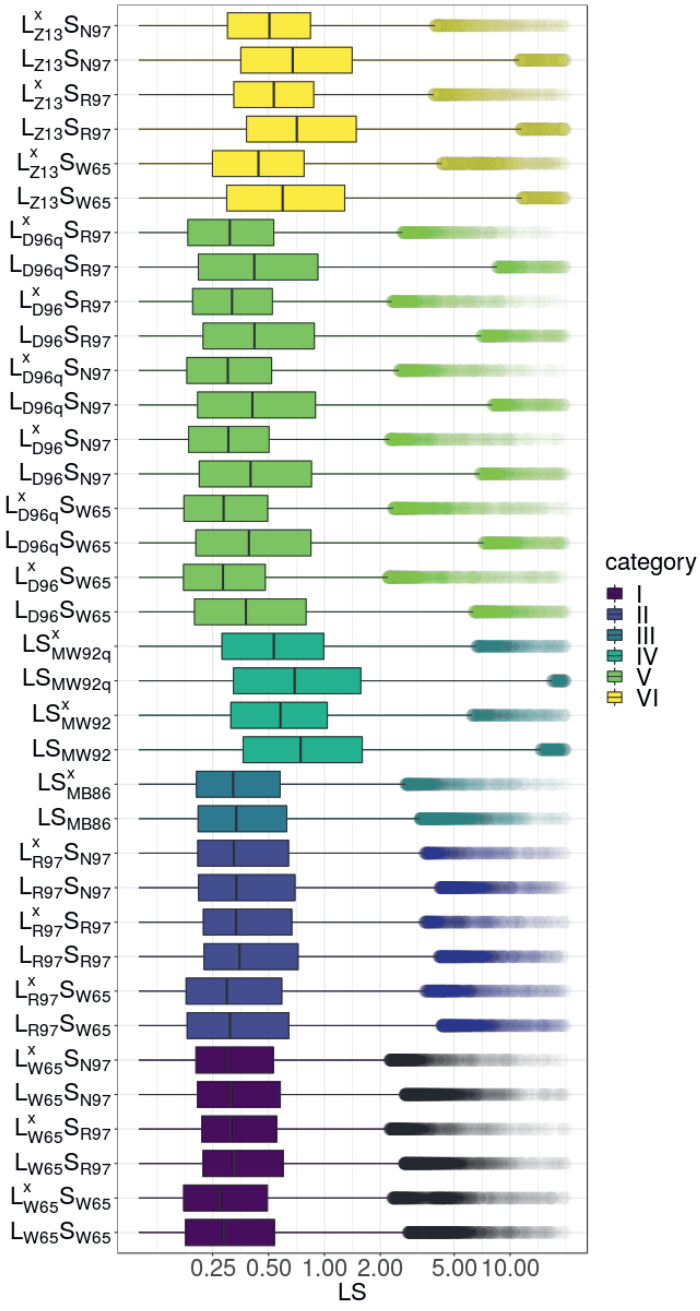

FIGURE 6.3: Quantiles and outliers for the LS factors for each algorithm. The points within the interquartile range are represented by the boxes, while the individual outliers in the right-hand tail are plotted by transparent dots. The data are colour coded according to the categorisation described in Section 6.2.1.

TABLE 6.2: Average values of primary terrain attributes of the artificial DEMs and Skuterud catchment.

		slope H_{00} (m/m)	slope S_{69} (m/m)	slope length (m)	catchment area (m^2)	SCA Q_{91} (m)	SCA M_{96} (m)
linear	parallel	0.081	0.062	201	1609	420	258
	divergent	0.074	0.055	188	1090	288	170
	convergent	0.062	0.051	228	2338	647	369
convex	parallel	0.081	0.062	211	1639	401	265
	divergent	0.082	0.063	188	1025	241	160
	convergent	0.054	0.045	214	2278	626	360
concave	parallel	0.080	0.062	206	1604	447	256
	divergent	0.066	0.049	190	1299	389	202
	convergent	0.070	0.059	228	2401	675	380
Skuterud		0.057	0.058	54	1499	259	239

6.3.2 Erosion model

The Nash-Sutcliffe Efficiency coefficient for daily discharge at the catchment level for the period 1994-2015 for Skuterud was 0.51. The NSE for daily soil moisture in the same period was 0.34. The winter periods were excluded from the performance evaluation because no reliable measurements of soil moisture content were available for frozen soil. Fig.6.4 shows the model results and the measured time series for the year 2010. Average annual soil loss for the period 1994-2016 in the Skuterud catchment was 0.28 kg m^{-2} for the D8 version of the erosion model, and 0.17 kg m^{-2} for the MFD version. The average annual simulated erosion rate from a Wischmeier plot for the simulation period was 8.02 10^{-2} kg m^{-2}. The average erosion rates on the artifical DEMs are given in Table 6.3.

6.3.3 LS factors

Fig.6.3 illustrates how the choice for (a combination of) algorithms determines the magnitude of the final topographic factor LS. The median values on the linear artificial DEMs range from 0.27 to 0.70 for the different algorithms, while the maximum values range from 64 to 938. When aggregated by their respective main groups, the algorithms based on Zhang *et al.* (2013) give the highest median values (0.65 on average for the three variants), while the original definition (Wischmeier and Smith, 1965) has the lowest medians (0.30). As expected, the versions for each algorithm that included a cutoff point for maximum slope length are consistently lower than the those without limitations on the slope length. The effect of cutoff points is markedly stronger in the groups of 2-dimensional algorithms (LS_{MW92}, L_{D96} and L_{Z13}, with reductions from 22 to 25 %) than in the

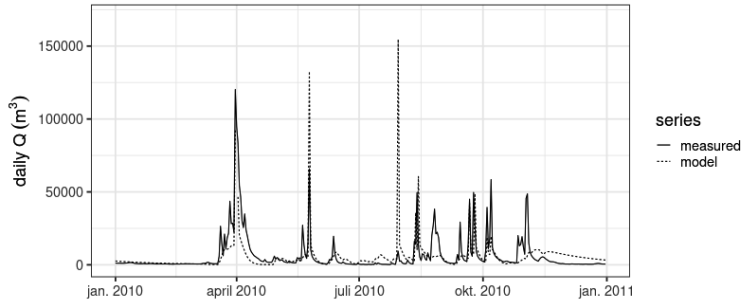

(A) Modeled and measured daily discharge from Skuterud catchment for the year 2010. Discharge as measured at the catchment outlet.

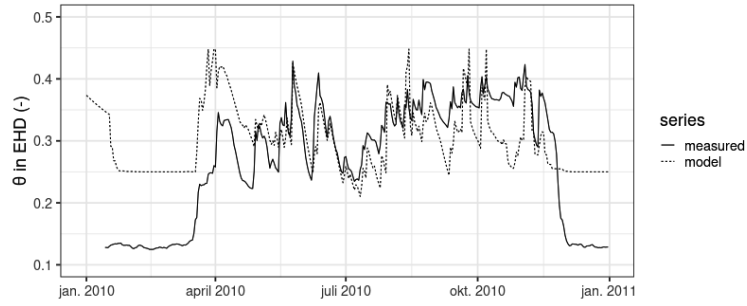

(B) Modeled and measured daily volumetric soil moisture content in the EHD. Measurements taken in the Gryteland sub-catchment.

FIGURE 6.4: Modeled and measured discharge and soil moisture for the year 2010.

TABLE 6.3: Average detachment, deposition and soil loss rates for the MFD and D8 runs of the MMF model on the artificial DEMs (kg m^{-2} $year^{-1}$)

		MFD			D8		
		detachment	deposition	soil loss	detachment	deposition	soil loss
linear	parallel	0.62	0.19	0.43	0.58	0.20	0.38
	divergent	0.62	0.17	0.45	0.58	0.19	0.39
	convergent	0.72	0.19	0.53	0.62	0.19	0.44
convex	parallel	0.61	0.19	0.42	0.57	0.19	0.37
	divergent	0.67	0.17	0.50	0.61	0.19	0.42
	convergent	0.62	0.18	0.45	0.57	0.18	0.39
concave	parallel	0.61	0.19	0.42	0.56	0.19	0.37
	divergent	0.56	0.17	0.40	0.54	0.17	0.36
	convergent	0.80	0.20	0.60	0.65	0.18	0.46
Skuterud		0.69	0.52	0.17	0.63	0.34	0.28

1-dimensional groups with a reductions between 2.5 and 3.5 %. These reductions are independent of planform and profile curvature.

6.3.4 Comparison of LS with simulated erosion rates

The SPAEF scores for the artificial DEMs are given in Table 6.4. All algorithms have Spatial Efficiency scores below 0.5 (the overall maximum value is 0.488). Two-way analysis of variance shows that algorithm performance depends on planform curvature ($p < 0.001$) but not on profile curvature. Calculated LS shows better correspondence with simulated soil loss on divergent slopes than on parallel or convergent slopes.

Some algorithms perform well or badly across the board, while others' SPAEF scores vary with slope form. The largest range is recorded for $L_{Z13}W_{S65}$, with a score of 0.65 on concave convergent slopes and 0.31 for linear divergent slopes. Most algorithms show a marked difference in performance between their versions with and without the inclusion of a cutoff point. The algorithm with the smallest range, or most consistent performance on the artificial DEMs, is LS_{MB86} with scores of 0.00 (concave divergent) to 0.07 (convex divergent).

The use of a cutoff point decreases algorithm performance slightly but not significantly, except for $LS_{MW92,Q}$. The 1-dimensional methods outperform the 2-dimensional methods. The mean SPAEF score of the 1-dimensional methods is significantly higher ($p < 0.005$) than those of the 2-dimensional methods (0.23 and 0.01, respectively). However, the interquartile range (IQR) of the SPAEF scores for the 2-dimensional methods is more than four times larger than the IQR of the 1-dimensional methods (0.24 and 0.07, respectively).

The three algorithms and their SPAEF scores that show the best correspondence with the erosion model on the artificial DEMs are $L_{W65}S_{W65}$ (0.35), $L_{DG96}S_{N97}$ (0.31) and $L_{R97}S_{W65}$ (0.31).

The SPAEF scores for Skuterud show a different distribution and ranking (Table 6.5). The four best performing algorithms here are $LS_{MW92,Q}$ (-0.24), LS_{MW92} (-0.25) $L_{Z13}S_{R97}$ (-0.26) and $L_{R97}S_{W65}$ (-0.26). The difference in performance between algorithms with and without cutoff points is similar to what was observed for the artificial DEMs. For Skuterud, the 1-dimensional algorithms perform slightly better than the 2-dimensional methods (-0.319 and -0.289, respectively, with $p < 0.05$).

algorithm	LINEAR PAR	LINEAR DIV	LINEAR CONV	CONVEX PAR	CONVEX DIV	CONVEX CONV	CONCAVE PAR	CONCAVE DIV	CONCAVE CONV
$L_{DG96}S_{N97}$ (2D)	0	0.16	0.09	−0.14	0.16	−0.18	0.16	0.19	0.23
$L^{X}_{DG96}S_{N97}$ (2D)	0.46	0.47	0.41	0.42	0.49	0.42	0.41	0.43	0.42
$L_{DG96}S_{R97}$ (2D)	−0.04	0.13	0.06	−0.16	0.13	−0.2	0.12	0.14	0.19
$L^{X}_{DG96}S_{R97}$ (2D)	0.36	0.38	0.32	0.33	0.4	0.33	0.32	0.34	0.34
$L_{DG96}S_{W65}$ (2D)	−0.2	−0.03	−0.07	−0.35	−0.01	−0.41	0.02	0.01	0.11
$L^{X}_{DG96}S_{W65}$ (2D)	0.43	0.47	0.44	0.35	0.43	0.46	0.35	0.46	0.41
$L_{DG96,Q}S_{N97}$ (2D)	−0.27	−0.13	−0.14	−0.32	−0.08	−0.31	−0.14	−0.07	−0.02
$L^{X}_{DG96,Q}S_{N97}$ (2D)	0.36	0.44	0.43	0.33	0.36	0.44	0.28	0.44	0.39
$L_{DG96,Q}S_{R97}$ (2D)	−0.28	−0.14	−0.15	−0.33	−0.1	−0.33	−0.15	−0.11	−0.04
$L^{X}_{DG96,Q}S_{R97}$ (2D)	0.31	0.38	0.35	0.28	0.33	0.36	0.23	0.35	0.34
$L_{DG96,Q}S_{W65}$ (2D)	−0.52	−0.41	−0.36	−0.56	−0.3	−0.57	−0.33	−0.35	−0.17
$L^{X}_{DG96,Q}S_{W65}$ (2D)	0.24	0.34	0.36	0.19	0.23	0.4	0.15	0.38	0.33
$L_{R97}S_{N97}$ (1D)	0.25	0.29	0.27	0.13	0.23	0.09	0.26	0.29	0.31
$L^{X}_{R97}S_{N97}$ (1D)	0.3	0.3	0.3	0.3	0.35	0.28	0.3	0.27	0.33
$L_{R97}S_{R97}$ (1D)	0.21	0.24	0.23	0.09	0.19	0.05	0.22	0.24	0.25
$L^{X}_{R97}S_{R97}$ (1D)	0.26	0.24	0.23	0.25	0.29	0.23	0.25	0.21	0.27
$L_{R97}S_{W65}$ (1D)	0.22	0.29	0.27	0.07	0.18	−0.04	0.22	0.3	0.3
$L^{X}_{R97}S_{W65}$ (1D)	0.33	0.37	0.35	0.32	0.37	0.33	0.31	0.33	0.36
LS_{MB86} (1D)	0.03	0.06	0.05	−0.06	0.02	−0.1	0.02	0.03	0.06
LS^{X}_{MB86} (1D)	0.05	0.05	0.03	0.04	0.07	0.02	0.04	0	0.05
LS_{MW92} (2D)	−0.56	−0.39	−0.39	−0.69	−0.35	−0.76	−0.39	−0.41	−0.19
LS^{X}_{MW92} (2D)	−0.09	−0.02	0.02	−0.15	−0.06	−0.02	−0.16	−0.06	0.03
$LS_{MW92,Q}$ (2D)	−0.86	−0.75	−0.68	−0.89	−0.6	−0.93	−0.7	−0.77	−0.45
$LS^{X}_{MW92,Q}$ (2D)	−0.21	−0.11	−0.04	−0.26	−0.17	−0.07	−0.3	−0.14	−0.03
$L_{W65}S_{N97}$ (1D)	0.3	0.32	0.32	0.22	0.3	0.2	0.32	0.3	0.35
$L^{X}_{W65}S_{N97}$ (1D)	0.28	0.25	0.25	0.31	0.34	0.25	0.3	0.22	0.31
$L_{W65}S_{R97}$ (1D)	0.26	0.27	0.26	0.18	0.24	0.16	0.27	0.25	0.29
$L^{X}_{W65}S_{R97}$ (1D)	0.24	0.2	0.19	0.26	0.27	0.19	0.25	0.17	0.25
$L_{W65}S_{W65}$ (1D)	0.31	0.36	0.35	0.2	0.29	0.15	0.32	0.35	0.38
$L^{X}_{W65}S_{W65}$ (1D)	0.34	0.33	0.33	0.35	0.39	0.33	0.35	0.31	0.37
$L_{Z13}S_{N97}$ (2D)	−0.18	0	−0.08	−0.31	0.01	−0.38	0.01	0.01	0.09
$L^{X}_{Z13}S_{N97}$ (2D)	0.28	0.3	0.25	0.28	0.34	0.29	0.27	0.27	0.28
$L_{Z13}S_{R97}$ (2D)	−0.21	−0.02	−0.1	−0.33	−0.01	−0.4	−0.03	−0.02	0.05
$L^{X}_{Z13}S_{R97}$ (2D)	0.21	0.24	0.2	0.21	0.28	0.23	0.2	0.21	0.23
$L_{Z13}S_{W65}$ (2D)	−0.41	−0.22	−0.28	−0.55	−0.17	−0.65	−0.15	−0.23	−0.05
$L^{X}_{Z13}S_{W65}$ (2D)	0.26	0.31	0.27	0.2	0.28	0.29	0.21	0.27	0.26

TABLE 6.4: Spatial Efficiency scores for the *LS* algorithms and their combinations. Deep red shading indicate little similarity between *LS* derived from terrain and from modeled erosion. Dark green indicates favourable comparison. Each column contains the SPAEF scores for a combination of planform (PARallel, DIVergent, CONvergent) and profile curvature (LINEAR, CONVEX, CONCAVE). The algorithms printed in bold are the two best performing methods and will be reviewed in more detail.

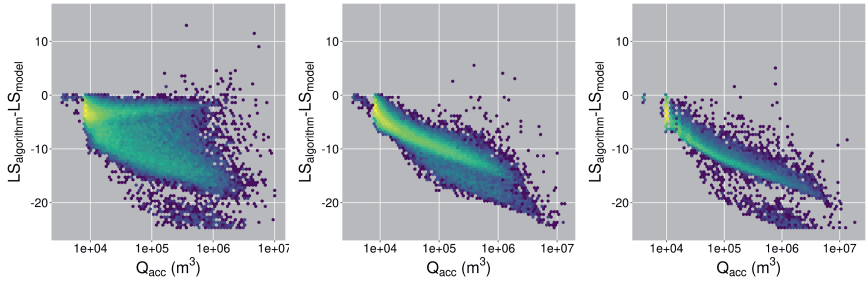

(A) $L_{W65}S_{W65}$ (B) $L_{DG96}S_{N97}$ (C) $L_{R97}S_{W65}$

FIGURE 6.5: Scatter density plot that plot *LS* as calculated by selected algorithm (y-axis) against *LS* as derived from the erosion model (x-axis) for the three best performing algorithms.

6.4 Discussion

6.4.1 Algorithm performance for different slope forms

The α component of the SPAEF (Eq.6.29) is the parameter with the lowest scores for the artificial DEMs and Skuterud catchment. Its values are smaller for the 1-dimensional algorithms than for the 2-dimensional algorithms. For Skuterud, the average α for the 1-dimensional algorithms is 0.05 (β is 0.32 and γ is 0.47). The corresponding value for the 2-dimensional algorithms is 0.12 (β is 0.29 and γ is 0.33). This is an indication of the importance of the spatial aspect for the algorithms' performances. Since divergent planform curvature showed the better correspondence, the effect of accumulated runoff, as a hybrid functional and structural landscape property, was investigated further. The relevance of runoff accumulation was confirmed by comparing it's Pearson correlation coefficient (r) to those of other terrain properties. For $L_{W65}S_{65}$, Pearson r for the difference between LS calculated by the algorithm and derived from the erosion model with accumulated runoff was -0.51. For $L_{DG96}S_{N97}$ this value is -0.44 and for $L_{R97}S_{W65}$ -0.51. The graphs in Fig.6.5 show the densities of the raster cell-wise comparison for these three algorithms. The next most relevant terrain parameter is planform curvature. This reinforces the likelihood that the performance of the LS algorithms in the landscape largely depends on the degree of concentration of overland flow. The larger the accumulated overland flow in the toposequence, the larger the underestimation of the LS factor by the best performing methods.

The algorithms furthermore show a structural underestimation of the *LS* factor in comparison to what the erosion model indicates.

algorithm	*Skuterud*
$L_{DG96}S_{N97}$ (2 D)	−0.32
$L^{X}_{DG96}S_{N97}$ (2 D)	−0.38
$L_{DG96}S_{R97}$ (2 D)	−0.32
$L^{X}_{DG96}S_{R97}$ (2 D)	−0.37
$L_{DG96}S_{W65}$ (2 D)	−0.33
$L^{X}_{DG96}S_{W65}$ (2 D)	−0.38
$\mathbf{L_{DG96,q}S_{N97}}$ (2 D)	−0.31
$L^{X}_{DG96,q}S_{N97}$ (2 D)	−0.36
$L_{DG96,q}S_{R97}$ (2 D)	−0.3
$L^{X}_{DG96,q}S_{R97}$ (2 D)	−0.36
$L_{DG96,q}S_{W65}$ (2 D)	−0.32
$L^{X}_{DG96,q}S_{W65}$ (2 D)	−0.37
$L_{R97}S_{N97}$ (1 D)	−0.27
$L^{X}_{R97}S_{N97}$ (1 D)	−0.28
$L_{R97}S_{R97}$ (1 D)	−0.26
$L^{X}_{R97}S_{R97}$ (1 D)	−0.27
$L_{R97}S_{W65}$ (1 D)	−0.26
$L^{X}_{R97}S_{W65}$ (1 D)	−0.27
LS_{MB86} (1 D)	−0.3
LS^{X}_{MB86} (1 D)	−0.31
LS_{MW92} (2 D)	−0.25
LS^{X}_{MW92} (2 D)	−0.3
$\mathbf{LS_{MW92,q}}$ (2 D)	−0.24
$LS^{X}_{MW92,q}$ (2 D)	−0.3
$L_{W65}S_{N97}$ (1 D)	−0.3
$L^{X}_{W65}S_{N97}$ (1 D)	−0.32
$L_{W65}S_{R97}$ (1 D)	−0.3
$L^{X}_{W65}S_{R97}$ (1 D)	−0.31
$L_{W65}S_{W65}$ (1 D)	−0.3
$L^{X}_{W65}S_{W65}$ (1 D)	−0.31
$L_{Z13}S_{N97}$ (2 D)	−0.26
$L^{X}_{Z13}S_{N97}$ (2 D)	−0.35
$\mathbf{L_{Z13}S_{R97}}$ (2 D)	−0.26
$L^{X}_{Z13}S_{R97}$ (2 D)	−0.34
$L_{Z13}S_{W65}$ (2 D)	−0.27
$L^{X}_{Z13}S_{W65}$ (2 D)	−0.34

TABLE 6.5: Spatial Efficiency scores for the *LS* algorithms and their combinations for Skuterud catchment (*cf*. Table 6.4).

6.4.2 Selected LS algorithms in Skuterud catchment

Three algorithms were selected for further analysis of their performance on the artificial DEMs and Skuterud catchment. The two best performing methods were that by Moore and Wilson (1992) for the combined *LS*, with contour length calculated by either Quinn *et al.* (1991) or Mitasova *et al.* (1996), with SPAEF scores of -0.24 and -0.25 respectively. The third best, with a score of -0.26, was *L* by Zhang *et al.* (2013) in combination with *S* by Renard *et al.* (1997). Because of its wide acceptance and application in erosion models, the original Wischmeier definition of 1965 was also included in this analysis, ranked 12^{th} with a score of -0.30).

As for the artificial DEMs, the difference between *LS* values calculated by the algorithms and derived from the erosion model is best explained by accumulated overland flow and planform curvature. A visual inspection of the *LS* maps after algorithm and erosion model illustrates where in the landscape the differences are most pronounced (Fig.6.6). The overall impression that the algorithms underestimate erosion rates on the artificial DEMs is reinforced in the more realistic terrain of Skuterud catchment. The reason for this should be sought in the origin of the topographic factor of the USLE; a means of harmonising data from experimental runoff plots. These plots are by definition simpler in their topography, as they are generally designed as linear slopes with parallel planform curvatures. They are also shorter than the slope lengths typically found in real terrain.

These differences in topography result in two non-linearities relevant in this context. The first is the relation between accumulating overland flow and particle detachment. Its exponential nature is well established empirically, *e.g.* Govers, 1990, and analytically, *e.g.* Singh, 1997. Comparing results from experimental (flume or plot based studies) and analytical equations to field measurements of particle detachment and transport rates is challenging for many reasons. Generalising results from such a study would be equally difficult. This is an old problem; Wischmeier 1965 calls for revision of the original definition (Eq.6.5) for slope lengths over 300 feet ($\approx$100 m). The exact value of the maximum slope length can be expected to be a function of the terrain and hydrological conditions and will depend on which *LS* algorithm is used. The gradual decline in the spatial correlation between model derived and algorithmic *LS* can be illustrated by investigating the relation between the spatial efficiency scores and contributing area. SPAEF analyses were performed on subsets of the Skuterud area by selecting raster cells with flow accumulation values under a certain threshold. The results are depicted in Fig.6.7.

The performance of the LS_{MW92} (Moore and Wilson, 1992) algorithms peak at a contributing area of 50 m^2, LS_{Z13} (Zhang *et al.*, 2013) at around 80 m^2 and $L_{W65}S_{W65}$ (Wischmeier and Smith, 1965) at around 100 m^2. After these maxima, the curves display a harmonic decline.

The second non-linearity concerns the complexity of the topographical sequence of detachment, transport and deposition. At the annual time scale, temporary

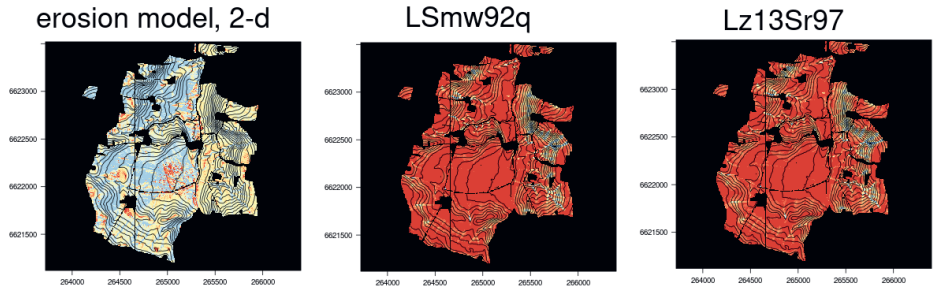

(A) 2-dimensional erosion model and algorithms.

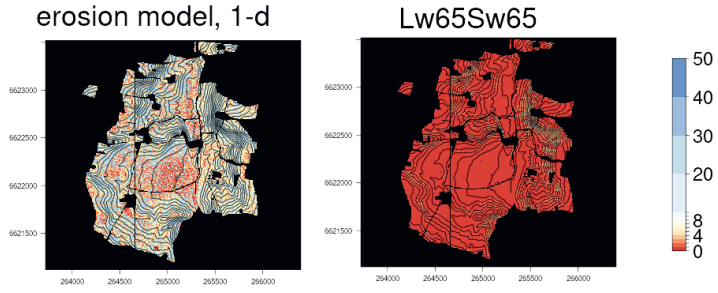

(B) 1-dimensional erosion model and algorithm.

FIGURE 6.6: *LS* as derived by the erosion model and the highest ranking algorithms. Isohypses presented as black contour lines.

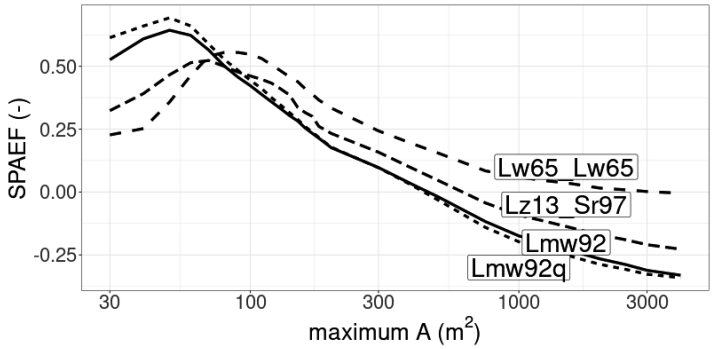

FIGURE 6.7: SPAEF scores of subsets of Skuterud catchment, selected with increasing contributing areas, for the four *LS* algorithms.

sediment storage and re-entrainment increase the complexity of the erosion process. The original definition of the *LS* factor does not represent erosion as a process with a complex spatio-temporal dimension. It was not intended to do so, as re-iterated by Wischmeier (1976). The *LS* algorithms tested in this research are unable to predict deposition, unless they were used in combination with a mass balance (*e.g.* flow routing, approximations of sediment transport capacity). In Skuterud catchment, this problem is especially apparent in the central part. Here, a relatively flat area is situated at the foot of the steeper areas. There is better correspondence between the model derived and algorithm based *LS* values in the sloping areas than in the flatter parts. Net soil loss in these areas mainly tends to occur in the form of ephemeral gully erosion. The talwegs in these flatter areas will, if not incised by gullies, be characterised by signs of particle deposition in the form of sediment fans or dispersed areas in the transitional zones. The definition of cutoff points for the calculation of slope length or contributing area is intended to account for spatial discontinuities in the particle detachment phase of the erosion process. In practice, the concept appears to be unable to bridge the spatial scales of the runoff plot and the catchment.

6.5 Conclusion

Since the inception of the USLE in the 1960s (Wischmeier and Smith, 1965), a variety of methods to derive the topographic factor *LS* have been developed. These methods differ in their representation of the terrain by slope length or contributing area, and their estimation of the effect of terrain on soil loss. The different combinations of algorithms for the slope gradient (S) and the slope length (L) factors were assessed for their ability to predict soil erosion rates by comparing them to an adaptation of the Morgan, Morgan and Finney (1984) erosion model.

While the majority of the algorithms performed reasonably well in homogeneous terrain, *i.e.* artificially generated DEMs, their performance in the more complex terrain of a real catchment is problematic.

LS algorithms are under-dimensioned for the accurate representation of the process of particle detachment, transport and deposition. The analysis of their spatial efficiency in representing the erosion process shows that their appropriateness is limited to the spatial scale of the typical runoff plot, with areas up to 100 m^2. Fields and catchment with surface areas larger than this value will be characterised by a much more intricate complex of processes and their interactions.

The USLE is explicit in its limitation to the prediction of sheet erosion. The applicability of the maximum slope length of 300 m, suggested by Wischmeier and Smith (1965), depends on too many static and dynamic factors to be considered generic. As a result, it should be concluded that the topographic factor, irrespective of its method of calculation, represents the erosion process in a limited domain of a catchment. The spatial analysis presented in Section 6.4.2 shows that this domain has its upper limit at hydrological discontinuities, such as the divide of a catchment. Its lower limit is less well defined, but the data generated in this research indicate that algorithm performance deteriorates in the transitional zone. A hard lower limit is the discontinuity between sheet and (ephemeral) gully erosion. The nature of this boundary is dynamic in time; a function of climate, soil physical conditions and agronomy and, in its essence, chaotic.

These conclusions indicate the need for a reassessment of the topographic factor for its use in complex terrain at higher spatial resolutions, *i.e.* orders of magnitude in the range of meters. A point of departure for this reassessment could be a return to the original concept of the topographic factor, but at the scale of the watershed, *i.e.* relating soil erosion rates to catchment morphometry. This would entail the collection and harmonisation of catchment scale sediment loads across a variety of climates, topographies and land use.

6.6 Acknowledgement

The measurements for the assessment of the performance of the erosion model were provided by NIBIO's JOVA programme for monitoring of agricultural catchments (NIBIO, 2020).

Chapter 7

Landform and erosion as subjects of scientific inquiry

> *If you should do philosophy, you should do philosophy, and if you should not do philosophy, then you should do philosophy. Therefore in every case you should do philosophy. For if philosophy exists, then positively we are obliged to do philosophy, since it truly exists. But if it does not truly exist, even so we are obliged to investigate how it is that philosophy does not truly exist. But by investigating we would be doing philosophy, since to investigate is the cause of philosophy.*[1]

7.1 Introduction

The study of water, soil and their interactions does not happen in isolation from other scientific and philosophical traditions, practices, attitudes and convictions. Researchers rarely have the opportunity to reflect on the conventions and assumptions that prescribe so much of our daily tasks. This means that most decisions with regard to the objects of study, the methods applied and the means of communicating findings, are made without reflecting on how they are influenced by exterior factors.

Researchers involved in the humanities are generally more conscious of their attitudes. Social scientists are, to a degree, the subject of their own investigations. Acknowledgment of the relevance of the relation between the observer and the observed has given rise to a relativist attitude towards knowledge (Raven, 2015). Perspectives matter, and people, groups and structures appear different to different observers. The definitions required to describe the objects of their research can generally be characterised as constructs (Hayek, 1952).

[1] From Aristotle's Protrepticus, in: Hutchinson and Johnson, 2017.

To a certain degree, this can also be said of the realm of theoretical physics. Models about the nature of matter, time and space appear to require ever smaller atomic units, that, for either theoretical or practical reasons, cannot be observed directly. Linkages between theoretical physics and philosophical questions are part of a tradition that started with Aristotle and had its most recent impetus by the discoveries about the nature of matter, space and time at the onset of the 20^{th} century. The interchange of ideas about method and reality has inspired historians of science ever since. Examples of such explorations are Mion (2019) and Penco (2010), who explore Einstein's discoveries with Wittgenstein's analysis of language, Howard and Giovanelli's overview of Einstein's contributions to the philosophy of science (Howard and Giovanelli, 2019) and the writings of Werner Heisenberg (*e.g.* 1958).

In erosion studies, the evaluation of the relation between the researcher and the object of inquiry appears to be less relevant to the quality and direction of the investigations. While interactions between the natural and human spheres usually are part of the scope of environmental research, they are present as boundary conditions, inputs and outputs of the system under investigation. Environmental physics, chemistry and biology may be rooted in the European scientific tradition, but can hardly be characterised as subjective with regard to the individual researcher or their cultural background. As a result, textbooks on the philosophy of physical geography are almost non-existent. Inkpen and Wilson's *Science, Philosophy and Physical Geography* (2013) and Castree *et al.*'s *Questioning Geography: Fundamental Debates* (2005) are the exceptions that confirm the rule. There also is a body of literature on critical theory in the environmental sciences on how they are influenced by the wider socio-political context (*e.g.* Rhoads, 1999; Lave *et al.*, 2014; Blue and Brierley, 2016; Lane, 2017).

In the field of hydrology, philosophical considerations about methodology amount to a more considerable volume. The literature, however, is fragmented. The reason for this is that the publications in this category tend to be highly focused on particular topics. Examples are Hoffman and Hoffman 1992 on the value of a phenomenological relationship like Darcy's Law for structural explanation in hydrology and Nearing *et al.* (2016) on the role of probability theory in the definition of ontological and epistemological uncertainty. Here again, there are exceptions, *e.g.* Beven's monograph on uncertainty in hydrological modelling, *Environmental Modelling: An Uncertain Future* (Beven, 2009).

The scarcity of harmonised philosophical reflection on the standards for the advancement of knowledge about erosion and its relation to the structure of the earth's surface, warrants the concise inventory in this chapter. The boundaries of the overview presented here are given by three fundamental questions that drive environmental research (paraphrasing Joseph Margolis, 1995):

1. What do we take to be the nature of environmental systems and why do we do so?

2. What do we take to be the extent of our ability to have knowledge of these systems?
3. How should we interact with them, and why?

The first question concerns ontological considerations; what do we consider to be the objective of our investigation? The second question concerns epistemology; how do observations contribute to improved understanding of the world around us? In the case of the environmental sciences in the (post)industrial era, the third question adds a normative dimension to the first two: how much environmental decline is acceptable and what measures should be deployed to stay below that threshold? The questions raised by Margolis are generic and scalable; they apply to research communities as well as individuals. The undertaking presented in this chapter is an attempt to describe the current standards for scientific investigation against which the methods developed and applied in the previous chapters could be measured. These standards, if indeed there are any, are the outcome of debates on ontology and epistemology that have driven the western philosophical and scientific traditions for at least 25 centuries. In this chapter, the assumptions about the researcher's relation to the study object are identified and briefly discussed. Rather than giving exhaustive historical overviews of the different philosophical considerations in the natural sciences, it contains a reflection on a selection of basic, usually implicit, foundations of the methods presented in the previous chapters. Where relevant, the implications of alternative definitions and attitudes are explored in thought experiments. The chapter is loosely organised according to Margolis' categorical questions. Section 7.2 concerns matters of ontology by presenting systems thinking as the current paradigm for the environmental sciences, erosion studies included. Section 7.3 concerns questions about how we acquire new knowledge about environmental systems, their structures, functions and behaviours. In the next section, environmental systems are presented as having a societal purpose, thereby accentuating teleology as an inherent property of environmental systems. Attention will be paid to the drivers of scientific progress and the relevance of the current social contract between the environmental research community and society as a whole. In the last section, some conclusions are drawn that, to some, could be read as recommendations.

The chapter includes several 'thought experiments' that are less generic and more technical than the body text. They are included for their illustrative value, or, if nothing else, for the joy of it.

7.2 Ontology: a world of systems

7.2.1 Systems thinking in the environmental sciences

A system might be defined as a delineated set of elements and their connections. An open system relates to its environment by means of input and output, either

material (*e.g.* matter, energy) or immaterial (*e.g.* information). A system consisting of a single element is usually referred to as a 'black-box'; the inner workings are not know or not relevant. The discovery and description of relations between system elements or subsystems can be considered the objective of all scientific research. They are described by the laws, theories and conjectures that take the form of testable hypotheses. Of all its properties, a system's boundary might be the most defining for any investigation into its nature and functioning. It reflects the purpose and determines the scope of the investigation. Gerard (1946) summarises it as 'entitation is more important than quantification'.

It is difficult to imagine erosion research without a worldview based on systems. Scientific inquiry beyond (statistical) description relies on the fact that subsystem relations are of a causal nature (see Section 7.2.2). These generic characteristics of systems are intuitive to anyone engaged in, or familiar with environmental research. Systems thinking has been an integral part of hydrology and geomorphology since the 1960s. Gregory and Lewin (2014) provide a concise overview of the introduction of systems thinking in geomorphology, a process in which R.J. Chorley has played an important role (Chorley, 1969; Chorley and Kennedy, 1971; Bennett and Chorley, 1978). It should be noted that the ideal of scientific multi-disciplinarity in geography can be dated back to the period in the wake of the publication of Darwin's Origin of Species. Davis advocates collaboration between physiography and ontography[2] (Davis, 1902).

Not all reactions to systems thinking were immediately positive. Chisholm (1967) reacted to General Systems Theory in its formulation by Ludwig Von Bertalanffy (GST, *e.g.* 1972) by disqualifying it as 'common sense'. Wilson (1972) is milder in his assessment and points out that General Systems Theory is not a paradigm, but that it belongs to the realm of methodology. Von Bertalanffy's publications are not characterised by an abundance of modesty, and this might explain some of the early reactions to the expansion of GST into (physical) geography. In hindsight, Von Bertalanffy might best be remembered as a chronicler of scientific developments who had a wide scope of interest. As for the environmental sciences: neither Von Bertalanffy nor GST are mentioned in any of Chorley's monographs of the 1960's and 1970's [3]. Systems thinking has also been criticised for its formalisation of natural systems as controlled systems (Gregory, 1980). This criticism will be part of the discussion of system functioning in Section 7.4. Despite this early scepticism, systems thinking nowadays provides the framework to probably all scientific investigations into environmental problems.

In hydrology, systems thinking gained dominance during the same period. In

[2]Davis' own neologism; the study of the relations between the responses of living organisms to their environment. The term as such did not catch on.

[3]Chorley does acknowledge Von Bertalanffy's identification of the role of entropy in open and closed systems in an earlier report (Chorley, 1962)

1965, UNESCO initiated an programme to the international advancement of hydrology. While its original intentions were focused on measurement and the harmonisation of international data gathering (Nature, 1965), Vemuri (1970) observes that the effort will 'relieve the empiricism [in hydrology]', thereby juxtaposing systems thinking with empiricism.

While the definition of systems can be given in intuitive terms, an answer to the question of where systems exist in the deductive-inductive cycle can not. There are, broadly speaking, two sorts of answers to this question. In the tradition of (ontological) realism, systems are part of physical reality, *i.e.* independent of our perception. At the other side of the spectrum, idealists argue that systems are the product of human imagination, however well informed. Note that in both instances, systems 'exist', the difference being that the latter lacks the attribute of actuality in space and time (Quine, 1948). In the idealist understanding, any instance of a system is one of infinitely many possible systems. This view coincides with the arbitrariness that characterises the definition of system boundaries and composition (see the Though Experiment in this section).

The debate between ontological realists and idealists has been ongoing since the Classical Period, with Aristotle's worldview firmly embedded in the former attitude, and Plato's cave in the latter. It is unlikely to be resolved anytime soon, and the intricacies of the debate are too many and too technical to be summarised here. Orthodox realism can be characterised as naive, because it is based on the assumed reliability of our sensory system as an intermediary between reality 'as is' and a brain that is wired by thousands of years of natural selection. Extreme idealism on the other hand denies the existence of physical reality. Although it may have strong theoretical grounds (scepticism is hard to refute) it is counter-intuitive and a gateway to cynicism in stead of inquisitiveness. Hawking and Mlodinow (2010) observe that the modern (physical) sciences are based on a hybrid attitude that they call model-dependent realism. They describe this attitude as:

> *...our brains interpret the input from our sensory organs by making a model of the world. When such a model is successful at explaining events, we tend to attribute to it, and to the elements and concepts that constitute it, the quality of reality or absolute truth. But there may be different ways in which one could model the same physical situation, with each employing different fundamental elements and concepts.*

It is a form of ontological pragmatism, because

> *If two such physical theories or models accurately predict the same events, one cannot be said to be more real than the other; rather, we are free to use whichever model is most convenient.*

In this view of reality the distinction between the hard ('real') and soft (cognitive) systems in the classification of (Bennett and Chorley, 1978) is dissolved. A system,

in other words, is the interface between the language of science and some source of impressions (reality) that allows the researcher to organise observations, theories and laws in a testable fashion that allows for explanation and prediction. Incidentally, this is one way of defining a model (see section 7.3.2 for the role of models in erosion research). The truth claim of system models is never absolute, and usually reduced to its ability to predict, rather than explain. This non-realist attitude is commonly referred to as instrumentalism, a term coined by Pierre Duhem [4]. In this view the standard against which scientific results are measured is empirical adequacy, rather than a (realist) truth claim.

7.2.2 Systems functioning: causation

Perhaps the most fundamental of all assumptions on which science relies, is the conviction that any phenomenon is the result of one or more other phenomena. Without this assumption of causation, there is little ground to analyse regularities in nature. While there is little reason to question the premise of causation, its exact nature has always been subject to debate. In the mechanistic paradigm that dominates the environmental sciences, causation is often equated with a paraphrasing of Newton's third Law: action equals the negative of the reaction. This definition of causal relation, however, is essentially quantitative and does not elaborate of the idea of causation. Krajewski (1982) differentiates four types of causation. (1) Materialist or Hobbesian, (2) phenomenalist, (3) rationalist or apriorist, and (4) spiritualist or voluntarist causation.

The first, materialist, conception of causation is best described by Hobbes' definition of cause-effect relations (Leijnhorst, 1996). Not unlike Aristotle's description of the concept (Aristotle, 2000), causation requires an active agent and a reactive patient. The change that the agent actuates is a change in movement. Hobbes moved away from these absolute positions in his later writings, but they do provide the backdrop for the dominant, mechanistic understanding of causation. An implication of the materialist understanding is necessity in causation.

The second, phenomenalist, conception is perhaps best understood by David Hume's positivist epistemology. Krajewski (1982) sketches Hume's viewpoint by means of five points. The first is the statement that we cannot deduce the nature of the effect by means of the nature of the cause. Secondly, as a consequence, our understanding of causality can only be rooted in experience. Hence (thirdly), necessity is not given in experience. The fourth point is a formal one; Hume states that the cause precedes the effect. And lastly, the actual connection between observation C and its effect E is only formed in the mind. With this analysis, Hume positioned causation at the heart of the positivist attitude towards the acquisition of knowledge.

[4] *A physical theory is not an explanation. It is a system of mathematical propositions, derived from a small number of principles, whose purpose is to represent a set of experimental laws as simply, as completely and as exactly as possible.* Duhem, quoted in Torretti, (1999)

The rationalist conception of causation is characterised by logical necessity. It is the deductive version of the inductive first, materialist position. Understanding about causation is to be derived from logical reasoning. Let C be a cause and E its effect, Mackie (1975) presents two related, but essentially different, logical conceptions of causation.

i. C is a cause of E and only if C and E are actual and C is *ceteris paribus* sufficient for E.

ii. C is a cause of E and only if C and E are actual and C is *ceteris paribus* necessary for E.

Formally, both are represented in the language of propositional calculus as

$$C \rightarrow E \tag{7.1}$$

When D represents the condition *ceteris paribus*, and L the law of nature that governs the relation between C and E[5], then Eq.7.1 can be written as

$$C \,\&\, D \,\&\, L \rightarrow E \tag{7.2}$$

The elaboration into Eq. 7.2 is one of many ways in which the semantic value of the word 'cause' is diluted. If the original C is only one of three preconditions that are necessary for the actuation of the cause-effect relation, the elementary character of the term 'cause' is disputable. The difference between necessity and sufficiency (notions *i* and *ii* above) is not purely semantic, but highlights the role of conditional circumstances and the nature of the laws that govern natural systems (see the thought experiment at the end of this section).

The fourth, voluntarist, conception belongs to a deistic or theistic worldview, where the world of matter is subject to the actions of a numenous, often omnipotent, being. This position is of relevance for historians and philosophers of science, but will not be discussed further here, save one remark about anti-rationalism. Voluntarist attitudes might be the driver behind the rise of alternative theories about matters that were considered to be resolved for centuries. Web-based movements, mostly transatlantic for the time being[6], promote counter-factual empirical observations as disproof for commonly accepted models (gravity, heliocentrism, spheroid earth). Yet another arena where the primacy of the scientific method is disputed is climate change. The magnitude of the stakes in climate change mitigation and prevention (political, economical, financial and social) is probably unprecedented in world history. The price of gaining prominence on political agendas the world round, seems to be a decrease in the general public's confidence in the scientific community. Disinformation and doubt about, for example, IPCC conclusions are usually part of ideological

[5] Any formalised regularity; deterministic or stochastic.

[6] Klaas Dijkstra being a notable European exception with his 'Pleidooi voor een Platte Aarde' (*Argument for a Flat Earth*, 1963).

messages. In other words: belief and subjectivism have never fully yielded since the Age of Reason, and show no sign of doing so in the near future.

The concept of causation has been, is and will continue to be the subject of much philosophical debate. The intricacies of the discourse are far beyond the scope of this chapter. As diverse as the attitudes towards causation may be, all of those touched upon above, have a crucial common feature. Effects derive from their causes (Anscombe, 1975), and, by implication, causes can be known through their effects if, and only if, the conditions and governing laws are known. Cause-effect relations form the core of scientific inquiry. A thought experiment is presented as an illustration of the significance of how cause-effect relations are formalised in empirical research.

Thought experiment: Efficacy of soil conservation measures

Chapters 5 and 6 of this thesis illustrate the importance of knowledge of erosion processes for the design and evaluation of soil conservation measures. The expansion of process knowledge, however, should run parallel to the acquisition of empirical data. The complexity of sediment dynamics and its environmental and agronomic drivers can not always be described mathematically (*e.g.* with process based models). The most important challenge in quantifying the effect of winter stubble is its limitedness in comparison to the intra-annual weather variability. Several reports indicate that there is likely to be a positive effect of winter stubble on autumn and spring soil loss, but none are able to present statistically significant evidence. The cause-effect models at the basis of these reports all presume the primacy of changed tillage regimes (*i.e* the cause), while the weather is considered the necessary condition for a certain stochastic regularity.

Consider then the following model:

$$E = \alpha P + \beta T + C \tag{7.3}$$

where E is annual erosion, P is precipitation, T is the tillage state of the soil in autumn (binary yes/no), C is some unknown factor and α, β are multipliers. An instance E_i of a catchment in a certain climate (Fig.7.1a) is generated by

$$E_i = (0.5 \cdot x_i + 1) p_i \cdot 10^{-3} + 10 t_i \tag{7.4}$$

where x_i is a randomly generated value between 0.4 and 0.6 to account for the unknown conditional in the i^{th} of 30 years. Annual precipitation depths p_i are generated randomly between 800 and 1100 mm. Years with tillage are randomly assigned. The real relative importance of tillage over precipitation was analysed with the Relaimpo package in R (Grömping, 2006). Relative importance (the ratio of variation explained) of tillage is 4%, precipitation

38%, while the remaining 58% cannot be explained from the data (Fig.7.1b).

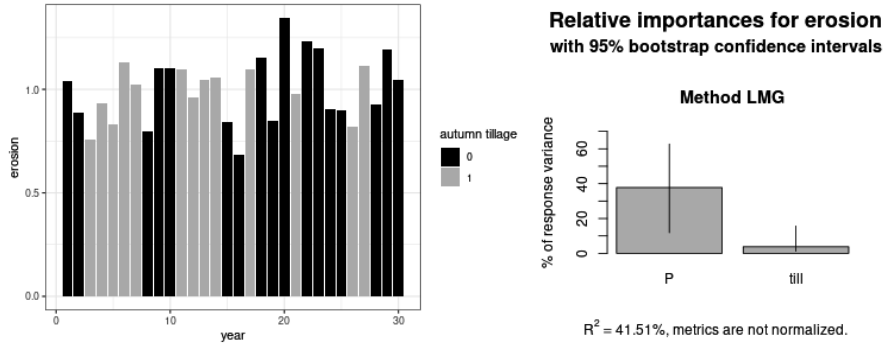

(A) Annual erosion (B) Relative importance

FIGURE 7.1: Stochastic renditions of the erosion model of Eq. 7.3.

Were this system to be analysed on the premises that (1) tillage is the cause of soil erosion, (2) weather is a conditional for this cause and (3) that the governing law is given by Eq.7.3, a typical test would be a comparison of the average erosion rates between year with and without autumn tillage. Erosion rates would be normalised for weather conditions. Normalised annual erosion with tillage is 1.04 tonnes annually, while the value for years without tillage is 0.97. A t-test shows that the difference in this analysis is insignificant ($p > 0.1$). The null hypothesis that there is no difference between years with and without tillage is not rejected.

Alternative premises are that (1) soil erosion is a function of precipitation, (2) tillage is a conditional for this cause and (3) the governing law is the same Eq.7.3). The function describing premise 1 is given by

$$E = \alpha P + C \tag{7.5}$$

Linear regression on the rendered model gives $\alpha = 1.05 \cdot 10^{-3}$ and $C = 1.07 \cdot 10^{-2}$. An additional premise is introduced, namely that the constant C in Eq.7.5 is sufficiently representative of the conditional in the cause-effect relation described by Eq.7.2. This additional premise presupposes the absence of multicollinearity in the data. If tillage were an effective soil conservation strategy, it should be expected that the regression model overestimates erosion rates in years without tillage, and *vice versa*. The confusion matrix shows the outcome of the analysis (bold print mark the occasions were model and expectation coincide).

	tillage	no tillage
predicted < observed	**11**	7
predicted > observed	6	**6**

The proportion of years that confirm the effect of tillage on annual soil loss is 17/30, only slightly more than 50%. A t-test on the data normalised for precipitation now indicates a difference between the years with and without tillage ($p \ll 0.01$).

The thought experiment shows that the choice for a certain formalisation of a relatively simple cause-effect relation can have a qualitative effect on the answer to a research question. It furthermore shows that a formal representation of the internal structure of the research question is not only convenient but also conducive for the identification of new approaches.

Cause-effect relations in environmental systems are often complex and cover multiple spatio-temporal scales. Describing system functioning requires the acceptance and use of general principles (*e.g.* conservation of mass as $q = \rho \cdot v \cdot h$; flow per unit width equals the flow velocity multiplied by the fluid density and water depth) and constituent or phenomenological laws *e.g.* the Manning-Strickler equation. Bertrand Russell stated that by extension, the entire universe should be considered the cause of an event (Russell, 1981). In order to avoid this, physical laws are not to be confused with cause-effect relations (Smith, 2000). An intuitive, simple and versatile concept of causation is presented by Von Wright (1975). His reasoning is based on a temporal sequence of bifurcations of system states. Each bifurcation represents an unaltered and an alternative state. As a consequence, cause is defined as that which makes a system move to an alternative state. In the environmental sciences, this model can be considered the dominant attitude underlying methodologies for scientific inquiry the into human impact on environmental systems.

7.3 Epistemology: induction, deduction, abduction

It was concluded in the introductory chapter of this dissertation that soil erosion is a process that can not be observed directly, and can be only measured on limited spatio-temporal scales. Yet, a century of research has resulted in a substantial amount of process understanding and the ability to predict erosion rates at various scales in all the world's agro-ecological regions. Carson and Kirkby (1972) provide a diagram to illustrate the epistemic cycle ('the inductive-deductive model building process') that is the basis for the ongoing accumulation of process understanding. Fig. 7.2 is based on their representation, but includes some adaptations. The first is the elimination of a direct connection between the real world and measurements. Instead, measurements are undertaken according to a plan that is based on a certain understanding of the real world. A second

alteration is the inclusion of abduction as one of the modes of inference. Abductive inference is difficult to define, but can be thought of as drawing preliminary conclusions from one or more observations. Abductive inferences are tentative and therefore characterised by their inconclusiveness. Abduction was first identified and named by Charles Peirce (see Fann, 1970) and can be illustrated by the following diagram (*ibid.*).

$$Inference \begin{cases} Explicative\ (analytic\ or\ deductive) \\ Ampliative\ (synthetic) \end{cases} \quad \begin{cases} Abductive \\ Inductive \end{cases}$$

Peirce describes abduction in the classical sense as *the process of forming explanatory hypotheses. It is the only logical operation which introduces any new idea* (in: Douven, 2021). Beven (2002) refers to this phase as qualitative understanding in the form of a perceptual model. It is closely related to the lexical phase[7] in Chorley's understanding of geographical systems thinking. This system definition is not based on measurements, but emerges as a formalisation of an perception of reality.

Deductive inference is analytical in nature, *i.e.* the result of the analysis of premises and their combinations. Causal, or process based, models are deductive in their essence. They describe connections between subsystems by means of laws that are established and proven to be reliable. Deduction applies generic principles to arrive at specific instances. Inductive inference moves in the opposite direction and can for simplicity's sake be equated with the statistical analysis of observations. Induction departs from specifics in order to derive generic properties or rules.

The third alteration to Carson and Kirkby's schematic is the representation of where the 'system', as the object of research, resides. The grey box in Fig.7.2 is included to illustrate the place of 'the system', as the object of investigation, woven into the process of theory building. Note that the real world resides outside of the grey box: the system is not an entity that exists in itself: it is part of an interpretation of reality, as described in Section 7.2.1.

7.3.1 Knowledge as justified, meaningful belief

When we study systems (processes or states) we want to generate knowledge. This knowledge can be the first we have of a certain process or state, or it can build on, or refute existing knowledge. Leaving the problem of induction aside for a moment, we are left with the burden of presenting our newly gained observations and explanations in a way that the reader recognises them as such, *i.e.* knowledge. Nozick (1981) aggregates descriptions of knowledge into four conditions that distinguish knowledge from mere belief. They are (paraphrased)

[7] Here understood to be the construction of a conceptual model.

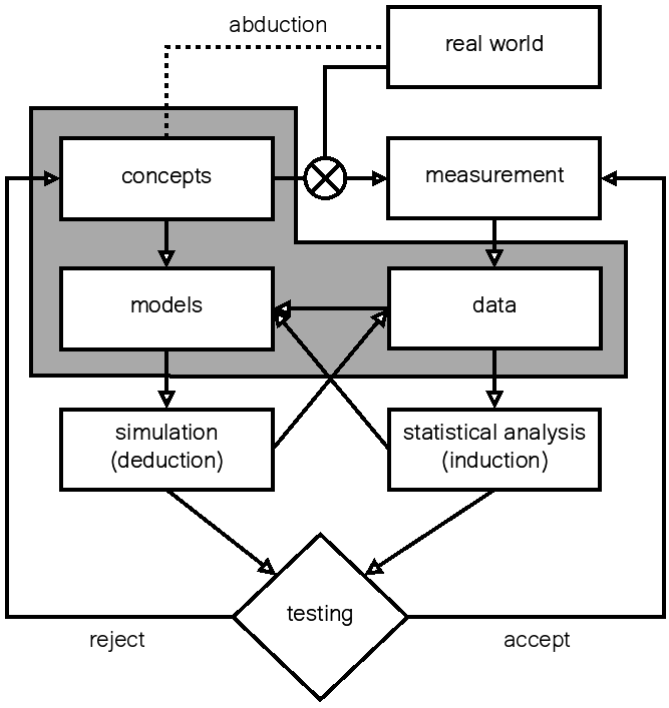

FIGURE 7.2: The process of theory building and testing. The 'system' as the formalisation of the object under investigation is ensemble of the components wihtin the grey box.

1. A preposition p is true.
2. Researcher S believes p to be true.
3. If the preposition weren't true, the researcher wouldn't believe it to be true, and
4. If the preposition were true, the researcher would believe it to be so.

At first glance, the conditions appear to be tautological, but they are not. A statement can be true, and a researcher might believe it to be so, but for the statement to qualify as knowledge (2) has to be the consequence of (1); this is the essence of (4). A counterexample is a researcher's belief that water quality in a certain catchment is a function of agronomic practice. If this is true for that particular catchment, the researcher's belief can only be deemed knowledge if and only if this belief is based on observations or general principles applied to the particular catchment. The truth of condition (1) is an essential qualifier for the distinction between knowledge and belief. Synthetic statements, however, can never be proven to be true (only to be false). Observations can only corroborate statements

by expressing a degree of certainty. The difference between knowledge and belief is therefore a quantitative one and not a qualitative. The distinction between knowledge and belief about a certain phenomenon or occurrence is, according to Nozick's model, in part dependent on the truth of a certain preposition.

Evaluating the truth of a statement is therefore essential for its classification as knowledge or belief. Truth itself is not easily defined without resorting to tautologies. Analytical statements, *i.e.* concerning truth in the domain of the deductive sciences (logic, mathematics) are, at least in theory, generally assumed to be objective and provable. Whether or not this is justified might be a matter for philosophical debate. Gödel's incompleteness theorems seem to have settled the matter by stating that the language of mathematics cannot be the basis for its own consistency. To those at the outside of the domain of mathematical philosophy, analytical truths are absolute. The truth of synthetic statements, i.e. those that include references to physical reality in the form of measurements and other observations, can not be established without a certain amount of uncertainty. The fact that laws and theories cannot be proven to be absolutely true was first reasoned by Hume. In his analysis of the acquisition of knowledge, the relation between cause and effect is a fabrication of the mind. No matter how accurate, precise and consistent the measurements are, the connection between cause and effect is a mental construct. As such, it could also considered part of natural language.

If the truthfulness of a synthetic statement, typical for the environmental sciences, can not be assessed exhaustively, its value should be evaluated by other means. An essential element in any of these alternatives is the concept of justification. Methods that evaluate the justification of a certain belief (in the truthfulness of a statement) are either internalist or externalist. Internalist evaluations of justification focus on personal, internal, processes. A minimum requirement for internalist justification is that the believer has knowledge of, or access to the motivations for her belief. The externalist position is best exemplified by Goldman, an early proponent (1979):

> If a person S's belief in a statement p at time t results from a reliable cognitive process, and there is no reliable ... cognitive process available to S which, had it been used by S in addition to the process actually used, would have resulted in S's not believing p at t, then S's belief in p is justified.

This attitude is known as reliabilism because it pivots around the reliability of the process that leads to a certain belief. Today's standards for scientific publication can be considered reliabilist. They focus on reproducibility of results by means of accurate descriptions of the methods used and the circumstances under which the work was carried out. The peer review process aims at the independent confirmation of the reliability of the results in relation to the methodology. This is the epistemological holism refered to by the influential 20^{th} century analytical philosopher Willard Quine as a 'web of beliefs' (Hylton and Kemp, 2020). Not

all truths in peer-reviewed publications have to be reduced to their inductive of deductive origin in order to be convincing. Arithmetic, algebra and elementary statistics are examples of fundamental elements in a web of beliefs.

A final note in this section about the nature of knowledge is dedicated to the predicate 'meaningful'. The origin of meaningfulness as a necessary condition for scientific knowledge is the logical positivist tradition that emerged on the continent in the early 20^{th} century.

Meaningfulness implies having to be true, false or being able to be assigned a (quantified) likelihood of being true. *'It snows outside'* is a meaningful statement, *'it snows in Mordor'* is not. This requirement, in combination with the problem of induction mentioned earlier, resolves into Popper's falsification principle. Scientific knowledge is distinguished from mere belief through the possibility of refutation. Meaningfulness can also be viewed pragmatically, *i.e.* measured against its usefulness. As such, it is a central concept in evolutionary theories to explain the emergence of language (Skyrms, 1996). Translated to the domain of scientific inquiry, the meaningfulness of a statement is then also given by its explanatory or predictive value.

Meaningfulness in the tradition of systems thinking also implies reference; the 'meaning' of a word consists of its reference to a certain object (or its property and/or function), an action or function. A meaningful preposition about system properties should refer to elements and/or relations that are contained by the system that defines the subject under investigation. In erosion research, this condition for meaningfulness is not always addressed properly. Examples typically concern problems of scale. Chapter 6, for example, addresses the problem of spatial scales in the use of the topographical factor of the USLE in studies that supersede the plot scale. The chapter illustrates how the meaningfulness of the relation between topography and erosion rate is bound by upper limits the slope length or contributing area. Limits to meaningfulness can also be temporal. Farmers perceptions of Norway's erosion risk map, for example, are often characterised by a focus on (historical) event losses, while the risk map presents a value that represents average conditions for a climate period (30 years).

7.3.2 The model as the horizon of knowledge

If our senses would allow us to perceive the physical environment directly, the amount of information would exceed our ability to process it in a meaningful way. We resort to mental images as abstractions that allow us to interact with our environment on a daily basis. A table does not have to be understood as a set of pieces of timber that are connected somehow and able to carry a certain weight. It suffices to perceive it as a flat, elevated area confined to a certain space that can be used for the placement of plates and cutlery. Models in scientific inquiry serve the same purpose and are closely related to the system concept described in

section 7.2.1. Bertels and Nauta (1969) define the model as *a concrete representation of situations and entities from nature and history in a set of symbols*.

In erosion research, there are two common and distinct notions of what a model is. The first is a representation of a system state, the second the representation of system functioning. State models are also referred to as morphological systems (Chorley and Kennedy, 1971), and consist of the properties of phenomena (*ibid.*). Examples of state models are digital elevation models, descriptions of vegetation or microtopography and terrain indices. Functional models on the other hand describe the relations between system components and/or between input and output. In Fig.7.2, the model is presented as a formalisation of a (mental) concept of reality. In the practice of erosion research, the term model usually refers to a series of quantitative variables and parameters that are combined in one or more equations. An example of a model is given in Fig.1.4, which represents a causal model for erosion at the hillslope scale. Causal models are usually referred to as physically based, *i.e.* connections between system components are described by general, physical laws. They are mechanistic representations of processes. If system properties are expressed non-probabilistically, causal models are deterministic. An example of the next category of models, phenomenological models, is the USLE (see the Introduction to Ch.6). This type of models is not characterised by exhaustive process description, but focuses on system behaviour. In erosion studies, they are referred to as empirical models. Empirical, because the parameter values that describe the relations between system input and output are based on measurements. A third, intermediate, category are generally referred to as conceptual models. In conceptual models, system composition is the starting point. The relations between system components in conceptual models can be deterministic or stochastic. Often, models combine physical with conceptual methods for the simulation of the rainfall-runoff-erosion process. An example is the Pan-European Soil Erosion Risk Assessment (PESERA; Kirkby *et al.*, 2008), applied in Chapter 5. PESERA is a hybrid model that combines a physics-based approach to rainfall-runoff simulations with an analytical (*i.e* conceptual) approach for erosion at the hillslope scale.

State and functional models are the pivotal point of contact between the researcher and reality. Researchers involved in erosion research sometimes appear to disagree about the hierarchy of system understanding. Some will argue for the primacy of observations to obtain system understanding, others will argue that measurements are conditioned by some (conceptual) model (compare Fig.1.4). This disagreement might be the result of a narrow definition of what a model is. In the literature, models usually refer to implementations of system dynamics in series of equations, aiming at simulation and prediction. If models were to be understood in the more rigid sense (representations of physical reality) much of the apparent contrast is bound to disappear.

State models, as representations of parts of the physical world, are the basic units

of any system description. A model that is as well known among the general public as it is fundamental to geography is the map. Another example is the Digital Elevation Model. The choice for a functional model determines which state models are included in a scientific inquiry; which subsystems are invoked, how they are connected and which behaviours are included in the chain of cause and effect (see the Thought Experiment at the end of this section). An example of how model development and system delineation can alter research traditions is the identification of the hillslope as the primary unit for the advancement of geomorphological process understanding in the 1960s and 1970s (Young and Saunders, 1986).

The strong correlation between qualitative understanding and static and functional models can be problematic. It is akin to the problem of theory-ladeness of observations as described by Hanson (1958) and Kuhn (1970). Theories, as conceptual models of reality, determine humans' perceptions of that reality. Brewer and Lambert (2001) broaden the domain of where theory-ladeness is of influence by including other phases of scientific investigation in their analysis: attention, acquisition and interpretation of data, memory and communication.

The role of models in erosion research therefore has a paradoxical nature; they are needed to understand and predict processes while habitual use may impede abductive inference and thereby innovation.

Thought experiment: Catchment entitation and erosion modelling

An elementary entity in hydrology and erosion studies is the catchment or drainage basin. Catchments are usually understood to be *the area from which the runoff concentrates in a certain point*, this point being the outlet. Catchments are generally considered real, physical entities; their delineation can be drawn on a map. Moreover, they are considered constant over time. This assumption is crucial in time series analysis of measured sediment concentrations at the outlet of a catchment. Concentrations are converted into loads, and loads are converted into soil loss rates expressed as mass per unit area per unit time.

There is nothing inherent to the definition of a catchment that obstructs a more dynamic interpretation. Connectivity as a system property does not only depend on structural factors (terrain), but also has a functional, and therefore time-dependent, component.

Fig. 7.3a shows the development of the contributing area of Skuterud catchment (described in Chapters 4 and 5) during a precipitation episode. The model used for the simulations is an adapted version of the Morgan, Morgan and Finney model (described in Chapter 4) and the episode depicted has a duration of 3 hours with an intensity of 30 mm hour^{-1}. Areas that are connected to the permanent stream throughout most of the episode are depicted blue, while the extents in red are only connected incidentally or briefly. The

surface area of the effective catchment during this particular episode is about 40% of the structural catchment area. Fig. 7.3b illustrates the sensitivity of sediment yield to the size of the effective catchment area for events with varying intensity and duration. This dependency is exponential in the given model configuration.

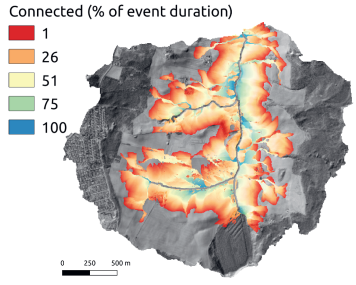

(A) Relative effective contributing area during a precipitation episode.

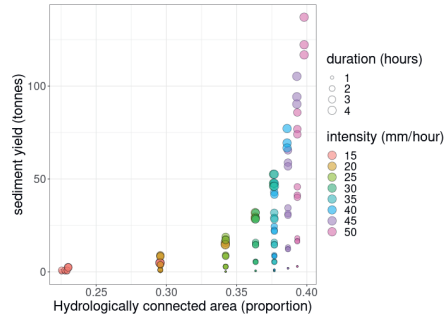

(B) Sediment yield as a function of the proportion of the hydrologically connected area and rainfall intensity and duration. Each dot represents a runoff producing precipitation episode.

FIGURE 7.4: Contributing area as a functional definition of connectivity.

We now have defined and quantified a functional concept of what a catchment is over time. The simulations have also suggested the importance of the extent of the functional catchment area for sediment delivery to the stream. These conjectures were not part of the system description or the conceptual model of Chapter 5. Note that the approach taken in Chapter 4 did not give significant support to the hypothesis that the Index of Connectivity in itself was a better basis for spatial prioritisation than mere erosion risk. Model calibration and the analysis of the results were based on a static, structural, definition of the catchment area. The more process-oriented model used here allows for an analysis by means of a dynamic, function-based, definition of the catchment area. To this purpose, soil conservation measures were introduced in the model by decreasing soil erodibility and the transport capacity of overland flow. The prioritisation strategies of Chapter 4 were used to parametrise model runs, and the results are given in the following table. The numbers represent the indexed sediment yield after implementing soil conservation measures in 25%, 50% and 75% of the agricultural area within Skuterud catchment. Three strategies are explored, where the prioritised areas are identified by the Index of Connectivity, (sheet) erosion risk and estimated specific sediment yield (the product of connectivity and erosion risk). Negative numbers indicate a reduction in sediment yield as compared to the reference situation).

	25%	50%	75%
connectivity	-0.39	-0.43	-0.44
erosion risk	-0.21	-0.41	-0.44
sediment yield	-0.41	-0.41	-0.42

The reductions in soil loss are larger than the values presented in Chapter 4. There, the reductions in the initial 25% of the area for connectivity, erosion risk and sediment yield based strategies were 0.06, 0.09 and 0.18, respectively. The results also show that for the initial 25% of the area, the difference between the strategies is larger than in Chapter 4. The third observation concerns the decreased marginal efficiency when the area of implementation increases.

Results from two models cannot be drawn without taking into account their methodological differences. The higher level of simulated efficiency by the process based model reflects not only the difference between the static and dynamic definition of the catchment, but also the models' different approximation of the sediment transport process.

As a thought experiment, this exercise is an example of how the choice for a modelling approach determines the definition of the system under investigation. System boundaries do not exist outside the domain of conceptual models, and care should be taken in their definition: 'entitation is more important than quantification' (Gerard, 1946).

7.4 Teleology: systems and purpose

As discussed in the Introduction of this dissertation, accelerated erosion as a constituent process of environmental systems is studied as a problem that requires a solution. A problem can be said to occur when there is a difference between the actual and a desired situation. Erosion research, in other words, is carried out because environmental systems do not perform according to some standard. The environmental pressure exerted by agricultural production, for example, is a problem because it is a threat to its own sustainability and to the integrity of lateral systems (nature, water, air, etc.). The basis for standards of proper system functioning vary between stakeholders, times and places. But common to all standards for environmental systems is the fact that they describe desired behaviour. Russel (1981) defines a teleological system as 'one in which purposes are realised'. Agricultural systems differ from other types of ecosystems because they have their origin and sustenance in human intentions; they are purpose-based in their very core. Texts as ancient as the second chapter of Genesis bear witness to this: the first human name shares the root of its meaning with the word for (cultivated) soil [8]. Hannah Arendt phrases it like this: *This future man ... seems to be possessed by a rebellion against human existence as it has been given, ..., which he wishes*

[8] ādām and hā-ădāmāh, respectively.

to exchange for something he has made himself. In this section the relation between systems behaviour, science and the societal contract is briefly examined.

7.4.1 System control: research as part of an engineering effort

Science as an activity solely driven by curiosity and a desire to explore and discover is the privilege of a minority. Nearly all environmental research is aimed at the reduction of anthropogenic pressures on ecosystems. It is perhaps no coincidence that the rise of systems thinking in physical geography coincided with environmentalism's rise to political prominence. The perceptual connection between human activity and environmental decline is by no means a product of modernity. It can be argued that the Epic of Gilgamesh, the world's oldest surviving literary text (~2100 BCE), is about the struggle between man and a vindictive natural environment (Sharif, Mohammad, and Saeed, 2019). Calls for restoration of damages done can be dated back to the period shortly after the Industrial Revolution (*e.g.* Marsh, 1864). The content of some texts of this period sound remarkably similar to the information one might find in contemporary communications of agricultural extension services. A letter from Thomas Jefferson of 1816, cited in an address to the Agricultural Society of North Carolina in 1857, (Sorsby, 1973) says that:

> ...the introduction of the Horizontal Method of Plowing; instead of straight furrows, has really saved this hilly country. It was running off in the valleys with every rain, but by this process we scarcely lose an ounce of soil.

Soil conservation measures, such as contour tillage in this quotation, continue to be the focal point between scientific inquiry and the political background to the societal contract of these research efforts. This implies that the blueprint for any system definition in the environmental systems is the control system as depicted in Fig. 7.5. Here, the system process turns uncontrolled inputs and human action into a variety of outputs. These outputs are compared to some standard or defined target and human action is adjusted in accordance to the expected effect. The urgency of the plethora of environmental problems, exacerbated by accelerated climate change, is recognised by governmental bodies at the national and international levels. The question of whether this is the result of scientific communications, or *vice versa*, will not be addressed here; it suffices to state that the vitality of the environmental scientific tradition depends on problem recognition. Analyses of which drivers shape scientific traditions are expressed in philosophical, sociological, psychological and economic terms, often in combination with each other. Kühn's (1970) concept of the paradigm is rooted in a philosophical approach towards scientific revolutions as sociological events. Bourdieu applies a materialist (dialectic) framework to explain the ever changing structures of the scientific field (Bourdieu, 2004). He analyses the dynamics of scientific fields in terms of scientific capital as based on knowledge and recognition (*i.e.* symbolic

capital). In this view, the state of science reflects a balance between pure scientific capital (based on an agent's position, status and publications) and temporal power within the domain of science (agents that are able to exert authority within the scientific field). This distinction is likely to be intuitive for researchers who earn a wage in exchange for their scientific labour. Lane (2017) arrives at a seemingly similar framework when mapping out the drivers of progress in physical geography when building on Harvey's (1981) analysis of overproduction and expansion. He and Inkpen (2018) sketch a social-evolutionary image of science as a struggle for limited capital (be it monetary or immaterial) by any means available to the researcher, either as an individual or in a group.

These are a mere three of countless conceptual frameworks to understand the dynamics of scientific progress. The shared tenet of, probably, all of them is that the resources that are made available to, and distributed over the scientific community determine much of what is studied and what is not. That is not to say that the scientific community is not able to set the agendas of the donor agencies. In democratic societies, donor preferences reflect widely shared concerns. Concerns raised by the scientific community are part of the latter.

In conclusion; environmental problems are discerned, quantified and put on the political agenda. The scientific community is granted the necessary resources to plan and undertake research into these problems. This is the essence of the societal contract by which researchers and their institutes are bound. Environmental system control is a key element of the societal contract between public agents and the environmental research community and currently can be considered the overall goal of environmental science.

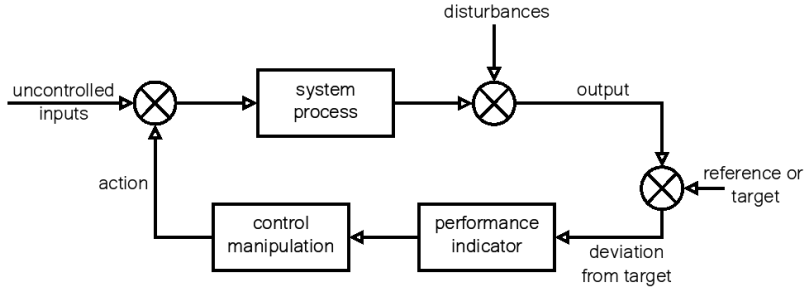

FIGURE 7.5: The control system, after Bennett and Chorley (1978).

7.4.2 Systems services: research as a multifunctional agent

While soil erosion is a natural process, accelerated erosion is the result of human intervention in the natural world. It occurs where forest is harvested, mines are operated and, above all, where food is being produced. Agriculture is a typical

example of the control system of the last section. Bennett and Chorley (1978) ascribe three, embedded interpretations to the control system.

a. as wholly or partly autonomous feedback mechanisms that control the environment;

b. as an extension of the life process of man's conscious control over the environment by means of man-machine systems. Such systems combine in a complex way the capabilities of man and machine for optimal decision-making.

c. as the ability to change the desired output from the existing input.

Gregory (1980) argues that the ideology of control, based on the objectification of natural resources, has a number of undesired consequences. Systems thinking might lead to technocratic approaches to manage the complex interactions between society and the physical environment. Gregory (*ibid.*) summarise this management loop as follows: *the rationalism of systems theory is translated into a realism and ... legitimation is reduced to an empirical inquiry into the adequacy of its modelling.* Another weakness of the control system viewpoint is that undesired outputs and unreliable inputs are considered externalities (see the importance of system boundaries in Section 7.3.2).

One way of overcoming the latter objection to technocratic systems control is the concept of agency. In agency-driven management systems externalities are not passive lateral quantities, but all system components have active representation in a decision-making platform. Ecosystem services (ES) analyses are an example of such agency-based frameworks. Its main tenets are still materialistic, anthropocentric and non-naturalist; the services flow from 'nature' to 'society' (Schröter *et al.*, 2014). Objections against ES often revolve around its anthropocentricity and the primacy of monetary units for the harmonised representation of agents' interests. Nevertheless, the role of the scientist in this environmental management strategy is fundamentally different than in the more technocratic system control strategy. Scientific representation of ecosystem functions is one of multiple voices in the decision making process. Castree (2005) characterise this current role of research as global change research (GCR). Advocacy is an integrated part of GCP; Castree calls for epistemological and political representation as duties of the environmental research community. A similar call was made in an influential article by Lubchenco (1998), which also departs from the principle of ecosystems services. She underlines an established:

1. need to better understand, monitor, and evaluate in order to protect, manage, and restore the environment,

2. need for more effective communication of existing knowledge to the public and policy arenas,

3. desirability to develop new technologies to minimize the ecological footprints of human activities
4. need for better guidance about decision-making in the face of uncertainty

This is the essence of the societal contract that Lubchenco elaborates further in her appeal. Research in this ideology reflects the purposefulness of the socio-ecosystems that it studies.

7.5 Conclusion

The sections above sketch an outline of the wider background to erosion research. Centred around a systems view of the world, the chapter touches upon old philosophical questions about knowledge, its subject and the motivations to develop it. The systems view of the world emerged as the dominant framework for scientific investigation of environmental phenomena in the 1960s. When formulated concisely, its main tenets are unlikely to be disputed by any contemporary environmental researcher.

1. Systems exist in the mind and as reflections of an observer-independent reality that can be known. The independent existence of a (physical) reality is assumed, hardly debated and never proven.
2. Models are useful representations of system states and processes. Models' representativeness is tested by their ability to predict. Their usefulness is derived from this ability; they allow for the evaluation of the effect of change on system behaviour and outputs.
3. The environmental research community competes for resources to identify and study socio-ecosystems and is most likely to succeed when the subject is formalised as a control system.

These characteristics of environmental research are largely implicit and are shared across the research community. As such, they are part of what Kuhn (1970) would characterise as a period of normal science and they can be regarded as a paradigm. The paradigm does not prescribe or canonise the rules and practices of research, but provides a framework for observations, methodologies and models. The systems paradigm that characterises contemporary environmental science has proven its fitness in two important ways during the last 60 to 70 years: it has proven to be able to predict systems' behaviour and to sustain and expand its existence by securing societal backing the form of capital and political support. The systems paradigm enables harmonisation of researchers' attempts to understand socio-ecosystems. The obvious disadvantage of the paradigm is that it tends to trivialise observations and theories that do not coincide with its implicit beliefs and methods. While scientific progresses in periods of normal science (Kuhn), the most significant moments in the history of science were part of paradigm shifts. These shifts are never, and should never be, an objective or goal. Signals

that indicate a paradigm shift are usually met with resistance, disbelief or even mockery. The research community therefore would do well to be aware of its own unwritten rules, and nurture the voices that do not obey these rules.

In a time in which scientific and ideological heads are facing the same direction, scientific disagreement often brings about political unpleasantry. Dissent about the severity, causes and implications of climate change is a typical example of the blurry overlap between science, an impressionable public sector and a private sector that is dominated by powerful multinational holdings. These debates concern the future, and theories and claims that are not in accordance with the systems paradigm can not be evaluated by their truth value. Alternative views and explanations should therefore be assessed according to the diligence and integrity of the groups that produce them and the falsifiability of their claims; without projecting their consequences into the realm of ideology and environmental management.

Debates about the study of landform and soil erosion do not tend to get quite so heated. However, when research results are translated into policy and law, disagreements with other stakeholders are bound to arise. These disagreements are not only of an ideological nature, but often based on practical concerns. The Norwegian farming community, for example, are willing to take measures against soil erosion, but not all agree with the blanket implementation of strategies. Individual farmers have the additional benefit of site or region specific knowledge and experience. This knowledge is not always conform with the generic, often map based, knowledge of the researcher. In these situations, the validity of the claim that models are adequate representations of a variety of circumstances is challenged. Time and location bound situations and management strategies that are based on a 'control system' view of reality are often difficult to harmonise.

All past paradigms were surpassed by alternatives that proved to be a better fit between theory and (new) observations. If the research community is to develop knowledge in the light of an ever increasing body of measurements and improved models, it is obliged to take note of criticism. This also applies when the critique comes from stakeholders whose perception is not determined by a systems view.

Chapter 8

Synthesis

The previous chapters have addressed the relation between terrain form and the erosion process across different spatial and temporal scales. In this chapter, the objectives of the presented research are first summarised. In the section that follows, the results are briefly discussed against the background of the progress that is being made in the environmental sciences. The last section will collate these lessons and reflect on where research will lead from here on and what is needed for erosion research to produce questions and answers that are as relevant within the scientific as they are to the societal contract.

8.1 Research objectives

The objectives of the research presented in this thesis can be divided into two themes. The first of these is the measurement of microtopography (A), the latter is the study of erosion processes at the catchment scale (B).

A Microtopography

- Ch.2 Assessment of the suitability of terrestrial laser scanning technology for high resolution (0.02 m) DEM construction of agricultural, tilled, larger soil surfaces (20 to 100 m^2).
- Ch.3 Establishment of correlations between changes in the DEM and the erosion and deposition processes that drive these changes locally.
- Ch.3 Definition of an algorithm for soil surface roughness (random roughness, RR) that is little sensitive to spatial resolution and local slope.
- Ch.4 Development of an algorithm for ephemeral gully delineation and volume estimation that is little sensitive to spatial resolution.

B Catchment scale

Ch.4 Estimation of the contribution of gully erosion as a fraction of the total soil loss from a predominantly agricultural headwater catchment in southeastern Norway.

Ch.5 Assessment of the suitability of an index of connectivity for estimating time variable specific sediment yields.

Ch.5 Evaluation of the relative efficiency of reduced tillage according to different spatial prioritisation rationales.

Ch.6 Evaluation of the most commonly used methodologies to calculate the (USLE) topographic factor (LS) against simulated erosion rates for three one-dimensional hillslopes with idealised morphologies.

Ch.6 Assessment of where and under which circumstances the different methods to calculate LS are best suitable to predict soil erosion on complex terrain.

8.1.1 Microtopography

The objectives that concern the measurement of microtopography are driven by the availability of new technologies (terrestrial laser scanning, TLS, and unmanned aerial vehicles, UAV). These technologies were not developed for (any specific) scientific use. TLS was, and continues to be, developed for mainly surveying purposes (Wu *et al.*, 2022). Its precision and accuracy is unprecedented, and its application includes urban surveying and multi-temporal monitoring of structures that are at risk of movement or deformation as a result of, for example, soil subsidence. TLS measurements in this type of environment are undertaken at angles that are not too far off the normal vector of the scanned surface (Soudarissanane *et al.*, 2011). On agricultural soils, this is often not possible due to the low altitude of the scanner's viewpoint (unless a tower or elevated tripod is used, *e.g.* by Eltner, Mulsow, and Maas (2013) or Martinez-Agirre, Álvarez-Mozos, and Giménez (2016)). The footprint of the laser beam, *i.e.* its surface area upon hitting the target surface, increases with the distance and the difference of the scan angle with the target surface normal. On unevenly shaped surfaces, the problem of non-surface points ('floating' measurements) is aggravated because the part of the beam is reflected, while the remainder travels further and is reflected by another object. Chapters 2 and 3 of this thesis investigated whether a sufficient amount of points of view, in combination with filtering of the point cloud, yields a DEM that can be assumed to be representative of the real soil surface. The difficulty in this assessment is hidden in the fact that knowledge of the exact morphology of the soil surface is impossible. In other words: there is no reference surface available that can be assumed 'real' and that can be expressed in the same numerical terms as the TLS measurements. Chapter 3 circumnavigates this difficulty by assuming a singularity that is obtained by a, theoretical, grid cell size of 0 m (Eq. 3.1).

In Chapter 4, measurements of changes in the soil surface in another order of magnitude are investigated. Ephemeral gully erosion results in changes in elevation of the soil surface that are a hundred times larger than those measured in Chapters 2 and 3. This makes detection easier, and reduces the requirements to the type of equipment that is used. UAV-borne photogrammetry is a technology that has recently (during the last decade) become available to the geophysical research community. While the development of winged UAVs might have been driven and funded by military industrial agents, quadcopters emerged as consumer grade products after electronic components and batteries became light enough to be integrated on airborne platforms. The fact that quadcopter UAVs currently have such a broad range of applications might be a direct result of this lack of intent in the development phase. Quadcopters do not require the budget that TLS does, and produce DEMs with a grid size in the order of a centimetre, or even less, for reasonably large areas (typically several 100 m²). The availability of this tool inspired and facilitated a NIBIO project that focused on the detection of ephemeral gullies in a monitoring framework [1]. In contrast to the changes that were detected in Chapter 3, the premise of Chapter 4 was that ephemeral gullies can be identified and delineated by means of a measurement at a single point in time. The research presented in this chapter focused on challenges in the analysis of the UAV-derived DEMs; gully delineation and the construction of a reference, pre-event, soil surface. The overall goal of the chapter was a quantification of soil loss as a result of gully erosion. The quality of the final result would ideally be tested against some reference, but, as in Chapter 2, no such reference exists. The real soil surface, existing independent of any observation, is a continuous three-dimensional shape. Photogrammetry and DEM creation take an optic signal from this shape and process it into the series of regularly spaced numbers that is a raster grid. This operation is trivial from a methodological point of view, but also represents a profound and implicit epistemological attitude that is characterised by unquestioned trust in representation of reality in mathematical terms and quantities.

8.1.2 Catchment scale

While the research objectives presented in the previous section are largely of an inductive nature, the objectives in the chapters about catchment scale analysis depart from deductive premises. Process knowledge is used to predict rates of particle detachment and transport at scales and levels beyond where they would, or could, be observed directly. The background to both Chapter 5 and 6 has a practical and an academic aspect. Practical questions related to the presented work concern the negative impact that soil loss from agriculture has on water quality in Norway. The academic interest is given by the problem of (quantifying) sediment transport. This is one of the main challenges in erosion research, and has been so for at least four decades (Walling, 1983; Walling, 1999; Collins and Walling, 2004).

[1] MetFure, funded by the Norwegian Agriculture Agency.

The problem, phrased very briefly, is that the current state of knowledge about the particle detachment and transport processes at the plot scale has not resulted in satisfactory processes understanding at the catchment level. It is a problem of scale, both in time and in space. The spatial aspect of the problem is the result of the fact that exhaustive measurement of sediment transport at the hillslope level is impossible, especially when sheet erosion is concerned. Measurements of sheet erosion are undertaken on runoff plots that have simple geometries and modest spatial extents (the length of a standard, 'Wischmeier', plot is 22.13 m). The interest in how topography affects erosion and sediment transport is not only academic. The overall goal of the research in Chapter 4 is the design of efficient soil conservation strategies. Chapter 5 set out to assess the suitability of different algorithms to calculate the USLE slope length factor by comparing them to (simulated) erosion and soil loss rates.

The objectives of Chapter 5 were developed against the impetus that the concept of hydrological and sediment connectivity gained in the last 15 years. The connectivity of a spatial unit like a hillslope or a catchment describes its ability to convey water and/or sediment from source to some recipient. It has a structural and a functional aspect; connectivity is a spatially distributed quantity that varies in time. The hypothesis in Chapter 4 is that knowledge of local particle detachment rates and the spatially distributed likelihood that sediments are transported will allow for the identification of sediment yield hotspots in the landscape. This in turn enables researchers to evaluate the efficiency of soil conservation measures according to their locations.

The development of a national erosion risk map for Norway, undertaken by NIBIO between 2012 and 2019, formed the background to the research in Chapter 6. The spatial scale of a risk mapping exercise for Norway prohibits a purely process based approach. The PESERA model was chosen because it utilises data sources that represent Norway's diverse soil and climate conditions, while taking a number of computational short cuts. The model is designed to run at the continental scale, and uses a coarse representation of topography in its concept. The Norwegian erosion risk map was to give information at the level of soil polygons and these are much smaller than the advised minimal grid size for PESERA (100 m). The slope length factor was chosen to represent terrain morphology in the national risk map. However, the available methods to calculate the factor had not been analysed for their performance in terrain that is more complex than the largely linear and short experimental plots.

8.2 Main findings

Chapters 2, 3 and 4 present studies about microtopography and are carried by inductive methods. They present measurements of soil surface morphology as the basis for the advancement of process understanding and quantification. Chapters 5 and 6 are about catchment scale process understanding and are deductive in

their essence; they depart from conceptual system descriptions. In Chapter 5 observations are used to corroborate the results obtained by the deductive method, while the methodology in Chapter 6 is fully theoretical.

Slaymaker (2017) states that methods in physical geography are characterised by rigid positivism. According to them, the importance of processes that cannot be measured or seen are therefore underestimated or ignored completely. The chapters in this thesis provide counter examples to Slaymaker's broad sweep: they cover several erosion related quantities that can neither be measured nor observed directly.

8.2.1 Microtopography

The work presented in these Chapters 2 and 3 provided sufficient evidence for the hypothesis that TLS-derived DEMs are realistic for larger areas (100 m²). The precision obtained by the combination of data acquisition by TLS and post-processing by means of filtering and rasterisation gave rise to the hypothesis that small changes to the soil surface as a result of erosion are detectable. This hypothesis contains a hidden paradox: detectable changes are smaller than the average accuracy of the measurement of individual points. Chapter 2 places the precision of the final DEM, defined as the standard deviation of the measured elevation within the 2 by 2 cm grid cell, in the range of several millimetres (Fig. 2.2). The changes in soil surface that were quantified in Chapter 4 are roughness (Fig.3.8) and elevation (Fig. 3.9). Typical values for decreases in soil surface roughness were found to be in the same order of magnitude as the measurement accuracy. Changes in elevation are smaller with an average value of approximately 1 mm. Despite the low significance levels, correlations between changes in soil surface morphology and topology were discerned. The high density of the TLS derived point cloud compensates for the inaccuracy of the individual point measurement (*i.e.* the Central Limit Theorem in statistics).

The methods for gully delineation and volume estimation, presented in Chapter 4, were applied at different spatial resolutions. Raster grids with different cell dimensions are essentially different mathematical representations of the real soil surface. The obtained consistency of the results of the calculations at different grid sizes is therefore a strong indication of the aptitude of the methods to produce realistic estimates of ephemeral gully volumes.

The statistical methods used in the post-processing of the data derived from the high-resolution DEMs in the Chapter 2, 3, and 4 were applied on large data sets. They only verify the validity of the conclusions at the aggregated level. The results of Chapter 3 are valid as averages for the runoff plot. In a similar manner, the validity of the volume estimates is confirmed for the entire gully channel.

8.2.2 Catchment scale

The index of connectivity (IC) of Chapter 5 and the topographic factor (LS) of Chapter 6 both represent a relation between terrain form and the erosion process. The hypothesised ability to provide quantitative information beyond the directly observable is rooted in an instrumentalist attitude towards the acquisition of knowledge of the real world. The challenge posed by this hypothesis is that it cannot be falsified by direct observation. In Chapter 5, the usefulness of index of connectivity is assessed by means of spatial aggregation. The index is calculated in a raster grid (10 by 10 m), and its behaviour is assessed at the catchment level. The solution to the problem of falsification in Chapter 6 was a comparison to another analytical method: simulation by a process based model.

The index of connectivity (Borselli, Cassi, and Torri, 2008) used in Chapter 5 was published a few years prior to a period during which the concept of connectivity gained significant momentum. Prior to that, the concept was applied for the characterisation of hydrologicl processes at the plot scale (Darboux and Huang, 2001), or to characterise sub-grid cell processes that lead to runoff generation (Darboux, Davy, and Gascuel-Odoux, 2002). Reid *et al.* (2007) and Lane, Reaney, and Heathwaite (2009) applied the concept to the catchment scale and indicated that the concept can improve the results of sediment transport modelling, and that is useful for the identification of source areas in a certain catchment. A significant volume of publications has followed these developments, some of which are theoretical explorations of the concept (Fryirs, 2012; Bracken *et al.*, 2015), others attempts to harmonise hydrological process knowledge and topography (Phillips, Spence, and Pomeroy, 2011; Shore *et al.*, 2013), others again to explore its usefulness for planning soil and water conservation measures (Alder *et al.*, 2015; Poeppl *et al.*, 2020; Kalantari *et al.*, 2021). The body of empirical data that would confirm the suitability of the various indices to represent process related quantities, however, is not growing with equal pace. In order to confirm the appropriateness of connectivity concepts for catchment scale studies, this lack of measurements will have to be resolved. One of the conclusions of Chapter 5 was that the index of connectivity, even when given a functional dimension (tillage over time), might not provide the right information to discern critical source areas in the relatively small headwater catchments that were studied (several km² in size). One reason for this finding is the ratio between study area size and the spatial resolution of the analysis. Connectivity analyses are scalable in their spatial resolution and therefore able to utilise the increasingly detailed terrain information generated by airborne platforms (Baartman *et al.*, 2020). This will enable modellers to explicitly define processes that are considered sub-grid cell parameters in models with coarser spatial resolutions. Here, care should be taken in translating hydrological concepts into systems of hydraulic equations. This development will increase the demand for knowledge of physics and 'low level' physical models in projects that take in this type of data.

The challenge of hypothesis testing in an instrumentalist approach is even greater

in the case of Chapter 6. Here, the topographic index of the USLE is assumed to provide quantitative estimates of erosion rates at a number of locations that exceeds even the most optimistic estimate of what is practically possible. The intrusive nature of overland flow measuring and sampling also renders the method theoretically impossible, even at much coarser resolutions and more restricted spatial extents. The USLE is being used with raster data with ever decreasing grid sizes. Djodjic and Markensten (2019), for example, use a USLE-type approach to map erosion risk for a relatively large area (> 200,000 km²) at a high spatial resolution (2 m grid size). They use observations at two spatial scales (headwater catchment and experimental fields) to evaluate model performance and the model performs equally well at both scales. Model performance at the grid cell level however, required for the identification of critical source areas at the (sub-)field level, is not assessed so readily. The comparison between calculated LS and a processed based spatially explicit erosion and deposition model of Chapter 6 is an example of how scales could be bridged in the absence of high resolution observations.

8.3 Directions of and for further research

8.3.1 The societal contract

Sustainability, as an ideological term, has characterised research efforts since the 1990s. Characterisation here means that the term was a point of contact between the research community and broader society (or at least the part of society involved in setting research agendas). It was augmented, or replaced, by a focus on climate change in the first decades of the the 21^{st} century. Krishna (2014) names climate change as one of three drivers for scientific progress in the 21^{st} century, besides globalisation and the industrial and post-industrial society. One has to search long and hard to find an equivalent to the contemporary agreement on the issue between the scientific community, political institutions and popular opinion. Combating climate change, causes and effects, has all the characteristics of a war. Nuances are vulnerable in times of conflict and statements about reality are easily evaluated in terms of morality, rather than of epistemology. Societal and political concerns over climate change have resulted in a strong research focus on the issue and this situation is likely to continue. For erosion research, this implies a continued focus on the spatial and temporal discontinuities in knowledge, models and system definitions. The research community will be required to define answers to questions about soil conservation that will take climate dynamics into consideration. For northern Europe, this will imply a continued focus on the impact of higher average temperatures and changes in the distribution and characteristics of precipitation. Two important questions that are driven by climate change are (1) what is the importance of episodic soil losses (in comparison to annual loads), and (2) how do changing conditions at the onset and end of winter affect sediment delivery to the freshwater system?

Castree's proposal for relevant global change research (2005) also applies to the national, more thematic scale of Norway's agricultural and natural resource management agents. He argues for better communication ('clearly, honestly and without fear') and a move beyond 'physical dimensions' and towards 'actionable research'. These imperatives continue to be relevant for the environmental sciences. For erosion research, this means that research questions are to be developed on platforms of open exchange of ideas, observations and agendas by stakeholders from across the agro-ecosystem. Agents that represent the farming community, agents for ecological quality and public agencies are common participants in these platforms. Soil, however, is currently lacking the same level of advocacy. Soil quality as an autonomous, independent interest would attain the same status of being worthy of protection as surface waters.

In Norway, the environmental research community operates independent from the political decision making process. Funding proposals have to pass standards with regard to methodology, but topics are not restricted to a set agenda. Exchange of ideas between governmental agencies and the research community is facilitated by networks that are largely informal. The current situation facilitates open discussion but is also at risk because of its informality. The research community will have to remain aware of their responsibility to not only formulate answers (in the forms of products) but also questions and concerns that might not be part of society's current agenda. Lubchenco (1998) acknowledges the fact that fundamental research has a vulnerable position in the current societal contract. Its relevance and importance in an age of 'post-academic' science (Ziman, 1996) will have to be acknowledged independent of the cycle of research need identification and methodological innovation.

8.3.2 Generic scientific questions

Blöschl *et al.* (2019) undertook a participatory exercise at different physical and online platforms to map out twenty-three unsolved questions in hydrology. Eleven of these apply to erosion research in the Nordic countries without much interpretation. They are (partly shortened and paraphrased):

1. What causes spatial heterogeneity and homogeneity in runoff and sediment fluxes, and in their sensitivity to their controls (e.g. snow fall regime, antecedent soil moisture, reaction coefficients)?
2. What are the laws that govern sediment transport at the catchment scale and how do they change with scale?
3. Why, how and when are rain-on-snow events erosive?
4. What are the processes that control hillslope–riparian–stream– groundwater interactions and when do the compartments connect?

5. What factors contribute to the long-term persistence of sources responsible for the degradation of water quality?
6. How can we use innovative technologies to measure surface and subsurface properties, states and fluxes at a range of spatial and temporal scales?
7. What is the relative value of traditional hydrological observations vs soft data (qualitative observations from lay persons, data mining etc.), and under what conditions can we substitute space for time?
8. How can we extract information from available data on human and water systems in order to inform the building process of agro-hydrological models and system definitions?
9. How can erosion models be adapted to be able to extrapolate to changing conditions, including changing weather dynamics?
10. How can the (un)certainty in hydrological predictions be communicated to decision makers and the general public?

Slaymaker (1997, cited in Slaymaker, 2009) declares the sediment budget as the core theme of geomorphology. Chapters 4, 5 and 6, and to a certain degree 3, all depart from the goal of understanding sediment flow through a certain space during a certain time; be it with varying degrees of success. The sediment budget, *i.e.* a balance between measured losses and quantitative estimates or measurements of the different sources, is likely to remain the essence of many research activities for some time to come.

8.3.3 Technological developments

While the investment required for the acquisition of TLS currently still inhibits broader application in soil and water research, the development of new sensors and open-source firmware and software is likely to change this earlier rather than later. UAV-borne laser scanners have recently become off-the-shelf technology that can be used by scientists and surveying experts alike. TLS and UAV are increasingly used to detect small changes in the soil surface. The work done by Meinen and Robinson (2020) and Cândido *et al.* (2020) marks an important moment in the study of the dynamics of microtopography. Their reported ability to detect and quantify sheet erosion and sediment fans on agricultural soil surfaces has the potential to study sheet erosion under field, *i.e.* non-experimental, conditions. The magnitude of the observed changes in their study was large in comparison to the reported accuracy of the applied technologies (UAV and TLS). Chapter 3, however, shows that small changes can be detected if analysed in combination with their topography. This development is likely to shed new light on sheet erosion at the field and hillslope scales.

The new data acquisition methods yield large amounts of data in the form of high-resolution DEMs. The analyses provided in this thesis are fully supervised

methods; they build on assumptions. Non-parametric methods have gained momentum with the advent of Big Data [2] in other disciplines and will do the same in the environmental sciences. Image analysis for the detection of erosion and risk mapping is a task that can only be carried by methods based on machine learning. Automated learning can yield unexpected results, but also confirm an implicit bias. Methods based on informatics will only provide true insight if they are accompanied by process understanding.

Catchment scale process understanding is likely to benefit from the increased availability of ever growing time series of satellite imagery. The European Space Agency's Sentinel 1 and 2 satellites are steadily compiling imagery at a high spatio-temporal resolution. It already allows for fairly detailed classification and mapping of agronomic factors like crop type and development. The synthetic aperture radar (SAR) data of Sentinel-1 are already used to map soil moisture content in at the regional scale. The resolution of these analyses can be expected to increase with better availability of imagery.

These developments will in turn result in new types of model input data. A new focus on empirical modelling can be expected in the wake of this development. At the same time, the computational capacity available to an environmental researcher is at a level where it does not any longer restrict process based simulations at high spatio-temporal resolutions at large scales (*e.g.* daily, 10x10 m for Norway). Epple *et al.* (2021) argue for the improvement of existing models to better utilise the now available high-resolution remote sensing data. This is more challenging for purely process-based models and it can therefore be expected that empirical models will progress significantly in the years to come.

The advent of new methods in the acquisition and processing of (large amounts of) data provides opportunities, but also new challenges. With it comes an increasing demand on individual researchers' ability to assess and control data quality. Data from new methods cannot always be compared with data from established techniques, and data quality assessment will therefore have to be integral to the broader adaptation of new methods. Technology also brings about the risk of division between those who have the capacity to invest time and resources and those that do not. Inkpen (2018) analyses the advance of geomorphology in a dialectic way when describing technology as one of the means of production of scientific knowledge. As such, it is a scarce commodity that will follow the same path of accumulation as monetary resources would in a capitalist economy. Care will have to be taken not to let the competition (inter- and intra-institutional) for these means of production to inhibit progress towards meaningful, ever improving and shared understanding of the world around us.

[2] Defined here as characterised by being large and having a dimensionality beyond human intuition.

8.4 The case for curiosity and pride

The work described in this thesis can be placed in a seemingly endless variety of sociological, philosophical, technological and economical frameworks. These explanations are meaningful in their respective contexts, and even in holistic analyses of the progress of human knowledge. But an often overlooked factor in these deterministic lattices is the heterogeneity of the group of human individuals that engage in scientific research. At the level of the individual, there are a number of factors that are not so easily explained in contextual analyses. And yet, they may be the most essential of all drivers behind the advancement of knowledge. Curiosity and pride are psychological drivers that require encouragement and control; this applies to adults as much as it does to children. While curiosity is often valued higher in name than in practice, the opposite is true of pride. Curiosity is appreciated within limits; reporting on set objectives is usually the final phase of a research project. Pride is a vice in the judeo-christian ethics of our time, but is also very closely related to the symbolic capital that enables researchers to secure status and funds. As such, it is an important personal driver for testing the boundaries of existing theories and the identification of alternative hypotheses. Professional curiosity will continue to require nourishment in the form of human interaction, preferably informal and in the field.

Bibliography

Agisoft LLC (2019). *Agisoft Metashape User Manual: Professional Edition*. Version 1.5, p. 145.

Aguilar, M. A., F. J. Aguilar, and J. Negreiros (2009). "Off-the-shelf laser scanning and close-range digital photogrammetry for measuring agricultural soils microrelief". In: *Biosystems Engineering* 103.4, pp. 504–517. ISSN: 15375110. DOI: 10.1016/j.biosystemseng.2009.02.010.

Alder, S., V. Prasuhn, H. Liniger, K. Herweg, H. Hurni, A. Candinas, and H. U. Gujer (2015). "A high-resolution map of direct and indirect connectivity of erosion risk areas to surface waters in Switzerland—A risk assessment tool for planning and policy-making". In: *Land Use Policy* 48, pp. 236–249. ISSN: 02648377. DOI: 10.1016/j.landusepol.2015.06.001.

Alewell, C., P. Borrelli, K. Meusburger, and P. Panagos (2019). "Using the USLE: Chances, challenges and limitations of soil erosion modelling". In: *International Soil and Water Conservation Research* 7.3, pp. 203–225. ISSN: 20956339. DOI: 10.1016/j.iswcr.2019.05.004.

Alvarez-Mozos, J., M. A. Campo, R. Gimenez, J. Casali, and U. Leibar (2011). "Implications of scale, slope, tillage operation and direction in the estimation of surface depression storage". In: *Soil and Tillage Research* 111.2, pp. 142–153. ISSN: 01671987. DOI: 10.1016/j.still.2010.09.004.

Andel, T. H. V., E. Zangger, and A. Demitrack (1982). "Land use and soil erosion in prehistoric and historical Greece". In: *Journal of Field Archaeology* 17.4, pp. 379–396.

Anscombe, G. E. M. (1975). "Causality and determination". In: *Causation and Conditionals*. Ed. by E Sosa. Oxford University Press. Chap. 5, p. 202.

Appels, W., P. Bogaart, and S. van der Zee (2011). "Influence of spatial variations of microtopography and infiltration on surface runoff and field scale hydrological connectivity". In: *Advances in Water Resources* 34, pp. 303–313.

Appels, W. M., P. W. Bogaart, and S. E. van der Zee (2017). "Feedbacks Between Shallow Groundwater Dynamics and Surface Topography on Runoff Generation in Flat Fields". In: *Water Resources Research* 53.12, pp. 10336–10353. ISSN: 19447973. DOI: 10.1002/2017WR020727.

Aristotle (2000). *Physics*. URL: http://classics.mit.edu/Aristotle/physics.mb.txt (visited on 09/19/2019).

Baartman, J. E., J. P. Nunes, R. Masselink, F. Darboux, C. Bielders, A. Degré, V. Cantreul, O. Cerdan, T. Grangeon, P. Fiener, F. Wilken, M. Schindewolf, and

J. Wainwright (2020). "What do models tell us about water and sediment connectivity?" In: *Geomorphology* 367, p. 107300. ISSN: 0169555X. DOI: 10.1016/j.geomorph.2020.107300.

Báčová, M., J. Krása, J. Devátý, and P. Kavka (2019). "A GIS method for volumetric assessments of erosion rills from digital surface models". In: *European Journal of Remote Sensing* 52.sup1, pp. 96–107. ISSN: 22797254. DOI: 10.1080/22797254.2018.1543556.

Bagarello, V, V Ferro, and V Pampalone (2013). "A new expression of the slope length factor to apply USLE-MM at Sparacia experimental area (Southern Italy)". In: *Catena* 102, pp. 21–26. ISSN: 0341-8162. DOI: 10.1016/j.catena.2011.06.008.

Bagherzadeh, A. (2014). "Estimation of soil losses by USLE model using GIS at Mashhad plain, Northeast of Iran". In: *Arabian Journal of Geosciences* 7.1, pp. 211–220. ISSN: 18667511. DOI: 10.1007/s12517-012-0730-3.

Barneveld, R. J., S. E. A. T. M. van der Zee, I. Greipsland, S. Kværnø, and J. Stolte (2019). "Prioritising areas for soil conservation measures in small agricultural catchments in Norway, using a connectivity index". In: *Geoderma* 340. ISSN: 00167061. DOI: 10.1016/j.geoderma.2019.01.017.

Barneveld, R., M. Seeger, and I. Maalen-Johansen (2013). "Assessment of terrestrial laser scanning technology for obtaining high-resolution DEMs of soils". In: *Earth Surface Processes and Landforms* 38, pp. 90–94.

Bartley, R., Z. T. Bainbridge, S. E. Lewis, F. J. Kroon, S. N. Wilkinson, J. E. Brodie, and D. M. Silburn (2014). "Relating sediment impacts on coral reefs to watershed sources, processes and management: A review". In: *Science of the Total Environment* 468-469, pp. 1138–1153. ISSN: 18791026. DOI: 10.1016/j.scitotenv.2013.09.030.

Bauer, T., P. Strauss, M. Grims, E. Kamptner, R. Mansberger, and H. Spiegel (2015). "Long-term agricultural management effects on surface roughness and consolidation of soils". In: *Soil and Tillage Research* 151, pp. 28–38. ISSN: 01671987. DOI: 10.1016/j.still.2015.01.017.

Bazzoffi, P. (2015). "Measurement of rill erosion through a new UAV-GIS methodology". In: *Italian Journal of Agronomy* 10.1s. ISSN: 1125-4718. DOI: 10.4081/ija.2015.708.

Bechmann, M., D. Collentine, F. Gertz, M. Graversgaard, B. Hasler, J. Helin, K. Jacobsen, K. Rankinen, and K. Refsgaard (2016). *Water Management for Agriculture in the Nordic Countries - Background document for NJF-seminar 487. NIBIO Report Vol. 2 Nr. 2.* Tech. rep.

Bechmann, M. and J. Deelstra, eds. (2013). *Agriculture and Environment - Long Term Monitoring in Norway*. Trondheim: Akademikaforlaget, Trondheim, Norway, p. 393.

Bechmann, M., S. H. Kværnø, S. Skøien, L. Øygarden, H. Riley, T. Børresen, and T. Krogstad (2001). *Effekter av jordarbeiding på fosfortap- sammenstilling av resultater fra nordiske forsøk. Bioforsk Report 6 (61)*. Tech. rep. Bioforsk, p. 73.

Bennett, R. J. and R. J. Chorley (1978). *Environmental Systems: Philosophy, Analysis & Control*. London: Methuen Co. Ltd., p. 624.

Bertels, K and D Nauta (1969). *Inleiding to het Modelbegrip*. Bussum: Uitgeveij De Haan, p. 183.

Beven, K. J. (2002). "Towards a coherent philosophy for modelling the environment." In: *Proceedings of the Royal Society A Mathematical, Physical Engineering Sciences* 458, pp. 2465–2484. ISSN: 1364-5021.

Beven, K. J. and M. J. Kirkby (1979). "A physically based, variable contributing area model of basin hydrology". In: *Hydrological Sciences Bulletin* 24.1, pp. 43–69. ISSN: 0303-6936. DOI: 10.1080/02626667909491834.

Beven, K. (2009). *Environmental Modelling: An Uncertain Future?* Chichester: Routledge, London and New York, p. 310.

Black, P. and M. Hardenberg (1991). *Historical Perspectives in Frost Heave Research*. Tech. rep. US Army Corps of Engineers.

Blackburn, W., F. Pierson, and M. Seyfried (1990). "Spatial and temporal influence of soil frost on infiltration and erosion of sagebrush rangelands". In: *Journal of the American Water Resources Association* 26, pp. 991–997.

Blöschl, G. *et al.* (2019). "Twenty-three unsolved problems in hydrology (UPH)–a community perspective". In: *Hydrological Sciences Journal* 64.10, pp. 1141–1158. ISSN: 21503435. DOI: 10.1080/02626667.2019.1620507.

Blue, B. and G. Brierley (2016). "'But what do you measure?' Prospects for a constructive critical physical geography". In: *Area* 48.2, pp. 190–197. ISSN: 14754762. DOI: 10.1111/area.12249.

Bogner, C., M. Mirzaei, S. Ruy, and B. Huwe (2012). "Microtopography, water storage and flow patterns in a fine-textured soil under agricultural use". In: *Hydrological Processes* 27.12, pp. 1797–1806.

Borrelli, P., D. A. Robinson, P. Panagos, E. Lugato, J. E. Yang, C. Alewell, D. Wuepper, L. Montanarella, and C. Ballabio (2020). "Land use and climate change impacts on global soil erosion by water (2015-2070)". In: *Proceedings of the National Academy of Sciences of the United States of America* 117.36, pp. 21994–22001. ISSN: 10916490. DOI: 10.1073/pnas.2001403117.

Borselli, L., P. Cassi, and D. Torri (2008). "Prolegomena to sediment and flow connectivity in the landscape: A GIS and field numerical assessment". In: *Catena* 75.3, pp. 268–277. ISSN: 03418162. DOI: 10.1016/j.catena.2008.07.006.

Bourdieu, P. (2004). *Science of Science and Reflexivity*. The University of Chigago Press, p. 129.

Bracken, L. J., L. Turnbull, J. Wainwright, and P. Bogaart (2015). "Sediment connectivity: a framework for understanding sediment transfer at multiple scales". In: *Earth Surface Processes and Landforms* 40.2, pp. 177–188. ISSN: 01979337. DOI: 10.1002/esp.3635.

Bras, R. L. (1999). "A brief history of hydrology: The Robert E. Horton lecture". In: *Bulletin of the American Meteorological Society* 80.6, pp. 1151–1164. ISSN: 00030007. DOI: 10.1175/1520-0477-80.6.1151.

Brewer, W. F. and B. L. Lambert (2001). "The theory-ladenness of observation and the theory-ladenness of the rest of the scientific process". In: *Philosophy of Science* 68.3 SUPPL. Pp. 176–186. ISSN: 00318248. DOI: 10.1086/392907.

Briese, C (2010). "Extraction of digital terrain models". In: *Airborne and terrestrial laser scanning*. Ed. by G Vosselman and H. G. Maas. Whittles Publishing. Chap. 4.

Bronfenbrener, L. (2009). "The modelling of the freezing process in fine-grained porous media: Application to the frost heave estimation". In: *Cold Regions Science and Technology* 56, pp. 120–135.

Browning, G. M., R. A. Norton, A. G. McCall, and F. G. Bell (1948). *Investigation in erosion control and the reclamation of eroded land at the Missouri Valley Loess Conservation Experiment Station, Clarinda, Iowa, 1931-42. Technical Bulletin No. 959*. Tech. rep. Soil Conservation Service, USDA, p. 88.

Brubaker, K. M., W. L. Myers, P. J. Drohan, D. A. Miller, and E. W. Boyer (2013). "The Use of LiDAR Terrain Data in Characterizing Surface Roughness and Microtopography". In: *Applied and Environmental Soil Science* 2013, pp. 1–13.

Bug, J. and T. Mosimann (2012). "Lineare Erosion in Niedersachsen - Ergebnisse einer elfjährigen Messreihe zu Ausmaß, kleinräumiger Verbreitung und Ursachen des Bodenabtrags". In: *Bodenkultur* 63.2-3, pp. 63–75. ISSN: 00065471.

Burwell, R. E., R. R. Allmaras, and M. Amemiya (1963). "A Field Measurement of Total Porosity and Surface Microrelief of Soils". In: *Soil Science Society of America Journal* 27.6, pp. 697–700. DOI: 10.2136/sssaj1963.03615995002700060037x.

Butt, M. A. and P. Maragos (1998). "Optimum design of Chamfer distance transforms". In: *IEEE Transactions on Image Processing* 7.10, pp. 1477–1484. ISSN: 10577149. DOI: 10.1109/83.718487.

Cândido, B. M., J. N. Quinton, M. R. James, M. L. Silva, T. S. de Carvalho, W. de Lima, A. Beniaich, and A. Eltner (2020). "High-resolution monitoring of diffuse (sheet or interrill) erosion using structure-from-motion". In: *Geoderma* 375.May, p. 114477. ISSN: 00167061. DOI: 10.1016/j.geoderma.2020.114477.

Canny, J. (1986). "A Computational Approach to Edge Detection". In: *IEEE Transactions on Pattern Analysis and Machine Intelligence* PAMI-8.6, pp. 679–698. ISSN: 01628828. DOI: 10.1109/TPAMI.1986.4767851.

Carollo, F. G., C. Di Stefano, V. Ferro, and V. Pampalone (2015). "Measuring rill erosion at plot scale by a drone-based technology". In: *Hydrological Processes* 29.17, pp. 3802–3811. ISSN: 10991085. DOI: 10.1002/hyp.10479.

Carson, M. A. and M. J. Kirkby (1972). *Hillslope Form and Process*. Cambridge: Cambridge University Press, p. 476.

Casalí, J., R. Giménez, and M. A. Campo-Bescós (2015). "Gully geometry: What are we measuring?" In: *Soil* 1.2, pp. 509–513. ISSN: 2199398X. DOI: 10.5194/soil-1-509-2015.

Castree, N., A. Rogers, and D. Sherman, eds. (2005). *Questioning Geography: Fundamental Debates*. Blackwell Publishing Ltd., p. 314.

Chisholm, M (1967). "General Systems Theory and Geography". In: *Transactions of the Institute of British Geographers* 42, pp. 45–52.

Choi, K., S. Arnhold, B. Huwe, and B. Reineking (2017). "Daily based morgan-morgan-finney (dmmf) model: A spatially distributed conceptual soil erosion model to simulate complex soil surface configurations". In: *Water* 9.4. ISSN: 20734441. DOI: 10.3390/w9040278.

Chorley, R. J. (1962). *Geomorphology and General Systems Theory*. Tech. rep. Washington DC, p. 14.

Chorley, R., ed. (1969). *Water, Earth and Man*. London: Methuen Co. Ltd., p. 588.

Chorley, R., A. Dunn, and R. Beckinsale (1964). *The History of the Study of Landforms or The Development of Geomorphology. Volume One: Geomorphology Before Davis*. John Wiley & Sons. Inc., p. 678.

Chorley, R. and B. Kennedy (1971). *Physical Geography: A Systems Approach*. London: Prentice-Hall International Inc., p. 370.

Chu, X., J. Yang, and Y. Chi (2012). "Quantification of soil random roughness and surface depression storage: Methods, applicability and limitations". In: *Transactions of the ASABE* 55.5, pp. 1699–1710.

Claessens, L., P. Breugel, A. Notenbaert, M. Herrero, S., and J. van de Steeg (Jan. 2008). "Mapping potential soil erosion in East Africa using the Universal Soil Loss Equation and secondary data". In: *IAHS-AISH Publication* 325.

Cochran, W. G. (1977). *Sampling Techniques*. 3rd. New York: John Wiley & Sons, p. 428.

Collins, A. L. and D. E. Walling (2004). "Documenting catchment suspended sediment sources: Problems, approaches and prospects". In: *Progress in Physical Geography* 28.2, pp. 159–196. ISSN: 03091333. DOI: 10.1191/0309133304pp409ra.

Conrad, O. (2001). *Convergence Index*. http://sourceforge.net/apps/trac/saga-gis/wiki/ta_morphometry_1. [Online; accessed 17-January-2014].

Cremers, N. H. D. T. and P. M. v. Dijk (1996). "Spatial and temporal variability of soil surface roughness and the application in hydrological and soil erosion modelling". In: *Hydrological Processes* 10, pp. 1035–1047.

Czuba, J. A. and E. Foufoula-Georgiou (2014). "A network-based framework for identifying potential synchronizations and amplifications of sediment delivery in river basins". In: *Water Resources Research* 50.5, pp. 3826–3851. ISSN: 19447973. DOI: 10.1002/2013WR014227.

Darboux, F., P. Davy, and C. Gascuel-Odoux (2002). "Effect of depression storage capacity on overland-flow generation for rough horizontal surfaces: Water transfer distance and scaling". In: *Earth Surface Processes and Landforms* 27.2, pp. 177–191. ISSN: 01979337. DOI: 10.1002/esp.312.

Darboux, F and C Huang (2001). "Evolution of soil surface roughness and flowpath connectivity in overland flow experiments". In: *Catena* 46, pp. 125–139.

Darboux, F. and C.-h. Huang (2005). "Does Soil Surface Roughness Increase or Decrease Water and Particle Transfers?" In: *Soil Science Society of America Journal* 69.3, pp. 748–756. ISSN: 1435-0661. DOI: 10.2136/sssaj2003.0311.

Davis, W. M. (1902). "Systematic Geography". In: *Proceedings of the American Philosophical Society* 16.170, pp. 235–259.

De Roo, A. P. J., C. G. Wesselink, and C. Ritsema (1996). "LISEM: a single-event physically based hydrological and soil erosion model for drainage basins: theory, input and output". In: *Hydrological Processes* 10, pp. 1107–1117.

De Vries, E (1948). *De Aarde Betaalt: De Rijkdommen der Aarde en Hun Betekenis Voor Wereldhuishouding en Politiek*. 's Gravenhage: Uitgeverij Albani, p. 244.

Deng, Z., J. L. M. P. De Lima, and V. P. Singh (2005). "Transport rate-based model for overland flow and solute transport: parameter estimation and process simulation". In: *Journal of Hydrology* 315, pp. 220–235.

Desmet, P. J. J. and G Govers (1996). "A GIS procedure for automatically calculating the USLE LS factor on topographically complex landscape units". In: *J. Soil and Water Cons* 51.5, pp. 427–433.

Di Stefano, C., V. Ferro, V. Palmeri, and V. Pampalone (2017). "Measuring rill erosion using structure from motion: A plot experiment". In: *Catena* 156.November 2016, pp. 383–392. ISSN: 03418162. DOI: 10.1016/j.catena.2017.04.023.

Djodjic, F. and H. Markensten (2019). "From single fields to river basins: Identification of critical source areas for erosion and phosphorus losses at high resolution". In: *Ambio* 48.10, pp. 1129–1142. ISSN: 16547209. DOI: 10.1007/s13280-018-1134-8.

Doren, D. and D. van Linden (1986). "Parameters for Characterizing Tillage-induced Soil Surface Roughness." In: *Soil Sci. Soc. Am. J.* 50, pp. 1–6.

Douven, I. (2021). "Abduction". In: *The Stanford Encyclopedia of Philosophy*. Ed. by E. N. Zalta. Summer 2021. Metaphysics Research Lab, Stanford University.

DroneDeploy (2022). *Drone mapping software: Drone mapping app: UAV mapping: Surveying software*.

Duley, F. L. (1932). "The effect of the degree of slope on run-off and soil erosion". In: *Journal of Agricultural Research* 45.6, pp. 349–360.

Dundas, Johannessen, Berge, and Heimdal (1989). "Toxic Algal Bloom in Scandinavian Waters, May–June 1988". In: *Oceanography* 2.1, pp. 9–14. ISSN: 10428275. DOI: 10.5670/oceanog.1989.24.

Dunn, M. and R. Hickey (1998). "The effect of slope algorithms on slope estimates within a GIS Matthew Dunn Robert Hickey". In: *Cartography* 27.1, pp. 9–15. ISSN: 00690805. DOI: 10.1080/00690805.1998.9714086.

Edwards, L., G. Richter, B. Bernsdorf, R. G. Schmidt, and J. Burney (1998). "Measurement of rill erosion by snowmelt on potato fields under rotation in Prince Edward Island (Canada)". In: *Canadian Journal of Soil Science* 78.3, pp. 449–458. ISSN: 00084271. DOI: 10.4141/S97-053.

Eitel, J. U. H., C. J. Williams, L. A. Vierling, O. Z. Al-Hamdan, and F. B. Pierson (2011). "Suitability of terrestrial laser scanning for studying surface roughness effects on concentrated flow erosion processes in rangelands". In: *Catena* 87, pp. 398–407.

Eltner, A. and P. Baumgart (2015). "Accuracy constraints of terrestrial Lidar data for soil erosion measurement: Application to a Mediterranean field plot". In: *Geomorphology* 245, pp. 243–254. ISSN: 0169555X. DOI: 10.1016/j.geomorph.2015.06.008.

Eltner, A., C. Mulsow, and H.-G. Maas (2013). "Quantitative Measurement of Soil Erosion From TLS and UAV Data". In: *The International Archives of the Photogrammetry, Remote Sensing and Spatial Information Sciences* XL-1/W2.November 2014, pp. 119–124. ISSN: 1682-1750. DOI: 10.5194/isprsarchives-xl-1-w2-119-2013.

Eltner, A., H. G. Maas, and D. Faust (2018). "Soil micro-topography change detection at hillslopes in fragile Mediterranean landscapes". In: *Geoderma* 313.October 2017, pp. 217–232. ISSN: 00167061. DOI: 10.1016/j.geoderma.2017.10.034.

Epple, L., A. Kaiser, M. Schindewolf, and A. Eltner (2021). "Can the models keep up with the data? Possibilities of soil and soil surface assessment techniques in the context of process based soil erosion models – A Review". In: *SOIL Discussions* August, pp. 1–23. ISSN: 2199-3971. DOI: 10.5194/soil-2021-85.

Esteves, M., X. Faucher, S. Galle, and M. Vauclin (2000). "Overland flow and infiltration modelling for small plots during unsteady rain: numerical results versus observed values". In: *Journal of Hydrology* 228, pp. 265–282.

Fann, K. T. (1970). *Peirce's Theory of Abduction*. Springer Netherlands, p. 62.

FAO UNEP (1979). *A Provisional Methodology for Soil Degradation Assessment*, p. 94.

FAO and ITPS (2015). *Status of the World's Soil Resources*, p. 607. ISBN: 9789251090046.

Fiedler, F. R. and J. A. Ramirez (2000). "A numerical method for simulating discontinuous shallow flow over an infiltrating surface". In: *International Journal for Numerical Methods in Fluids* 32, pp. 219–240.

Fiener, P. and K. Auerswald (2003). "Effectiveness of Grassed Waterways in Reducing Runoff and Sediment Delivery from Agricultural Watersheds". In: *Journal of Environmental Quality* 32.3, pp. 927–936. ISSN: 00472425. DOI: 10.2134/jeq2003.9270.

– (2006). "Seasonal variation of grassed waterway effectiveness in reducing runoff and sediment delivery from agricultural watersheds in temperate Europe". In: *Soil and Tillage Research* 87.1, pp. 48–58. ISSN: 01671987. DOI: 10.1016/j.still.2005.02.035.

Flacke, W, K Auerswald, and L Neufang (1990). "Combining a modified Universal Soil Loss Equation with a digital terrain model for computing high resolution maps of soil loss resulting from rain wash". In: *CATENA vol. 17,* 17.1986, pp. 383–397.

Foster, G. R. (1992). "Comment on "Length-slope factors for the Revised Universal Soil Loss Equation: Simplified method of estimation". In: *J. Soil and Water Cons.* 47.5, pp. 423–428.

Foster, G. R., L. D. Meyer, and C. A. Onstad (1977). "Runoff Erosivity Factor and Variable Slope Length Exponents for Soil Loss Estimates". In: *Transactions of the Asae* 20.4, pp. 683–687. ISSN: 0001-2351. DOI: 10.13031/2013.35628.

Foster, G. R. and W. H. Wischmeier (1974). "Evaluating Irregular Slopes for Soil Loss Prediction". In: *Transactions of the ASAE*, pp. 305–309.

Fournier, A., D. Fussell, and L. Carpenter (1982). "Graphics and Image Processing Computer Rendering of Stochastic Models". In: *Communications of the ACM* 25.6, pp. 371–384.

Frei, S. and J. H. Fleckenstein (2014). "Representing effects of micro-topography on runoff generation and sub-surface flow patterns by using superficial rill/depression storage height variations". In: *Environmental Modelling and Software* 52, pp. 5–18. ISSN: 13648152. DOI: 10.1016/j.envsoft.2013.10.007.

Fryirs, K. (2012). "(Dis) Connectivity in catchment sediment cascades : a fresh look at the sediment delivery problem". In: DOI: 10.1002/esp.3242.

Gabriels, D., G. Ghekiere, W. Schiettecatte, and I. Rottiers (2003). "Assessment of USLE cover-management C-factors for 40 crop rotation systems on arable farms in the Kemmelbeek watershed, Belgium". In: *Soil and Tillage Research* 74.1, pp. 47–53. ISSN: 01671987. DOI: 10.1016/S0167-1987(03)00092-8.

Gallant, J. C. and J. P. Wilson (2000). "Primary Topographic Attributes". In: *Terrain Analysis: Principles and Applications*. Ed. by J. P. Wilson and J. C. Gallant. Wiley. Chap. 3, pp. 51–86.

Gallant, J. C. and M. F. Hutchinson (2011). "A differential equation for specific catchment area". In: *Water Resources Research* 47.5, pp. 1–14. ISSN: 00431397. DOI: 10.1029/2009WR008540.

Geikie, A (1868). "On denudation now in progress". In: *Geological Magazine* 5, pp. 249–254.

Gerard, R. W. (1946). "Intelligence, information, and education". In: *Science* 148, pp. 762–765.

Gilliot, J. M., E. Vaudour, and J. Michelin (2017). "Soil surface roughness measurement: A new fully automatic photogrammetric approach applied to agricultural bare fields". In: *Computers and Electronics in Agriculture* 134, pp. 63–78. ISSN: 01681699. DOI: 10.1016/j.compag.2017.01.010.

Goldman, A. I. (1979). "What is justified belief?" In: *Justification and Knowledge*. Ed. by G. Pappas. Dordrecht: D. Reidel Publishing Company. Chap. 1, pp. 1–23.

Goodwin, N. R., J. Armston, I. Stiller, and J. Muir (2016). "Assessing the repeatability of terrestrial laser scanning for monitoring gully topography: A case study from Aratula, Queensland, Australia". In: *Geomorphology* 262, pp. 24–36. ISSN: 0169555X. DOI: 10.1016/j.geomorph.2016.03.007.

Govers, G., I. Takken, and K. Helming (2000). "Soil roughness and overland flow". In: *Agronomie* 20, pp. 131–146.

Govers, G. (1990). "Empirical relationships for the transport capacity of overland flow". In: *Erosion, Transport and Depostition Processes (Proceedings of the Jerusalem Workshop, March-April 1987)* 189.189, pp. 45–64.

Graham, E. H. (1946). "Soil erosion as an ecological process". In: *The Scientific Monthly* 55.1, pp. 42–51. ISSN: 0036-8075. DOI: 10.1126/science.os-2.57.341-a.

GRASS Development Team (2014). *Geographic Resources Analysis Support System (GRASS) Software*.

Gray, D., C. Gray, N. R. C. of Canada, C. committee for the international hydrological decade, and I. Water Information Center (1973). *Handbook on the Principles of Hydrology: With Special Emphasis Directed to Canadian Conditions in the Discussions, Applications, and Presentation of Data*. A Water Information Center publication v. 1. Water Information Center, Incorporated. ISBN: 9780912394077.

Grayson, R. B., A. W. Western, and H. S. Chiew (1997). "Preferred states in spatial soil moisture patterns: Local and nonlocal controls". In: *Water Resources Research* 33, pp. 2897–2908.

Gregory, D. (1980). "The Ideology of Control : Systems Theory and Geography". In: *Control* 71.6.

Gregory, K. J. and J Lewin (2014). *The Basics of Geomorphology: Key Concepts*. SAGE Publications, p. 248.

Grimm, M, R. J. A. Jones, and L. Montanarella (2001). *Soil Erosion Risk in Europ*. Tech. rep. European Commission Joint Research Centre, p. 38.

Grömping, U. (2006). "Relative Importance for Linear Regression in R: The Package relaimpo". In: *Journal of Statistical Software* 17.1, pp. 1–27.

Guo, Q. K., B. Y. Liu, Y. Xie, Y. N. Liu, and S. Q. Yin (2015). "Estimation of USLE crop and management factor values for crop rotation systems in China". In: *Journal of Integrative Agriculture* 14.9, pp. 1877–1888. ISSN: 20953119. DOI: 10.1016/S2095-3119(15)61097-8.

Hänsel, P., J. Schmidt, A. Eltner, M. Schindewolf, and A. Kaiser (2016). "Feasibility of High-Resolution Soil Erosion Measurements by Means of Rainfall Simulations and SfM Photogrammetry". In: *Hydrology* 3.4, p. 38. ISSN: 2306-5338. DOI: 10.3390/hydrology3040038.

Hansen, B. and E. Sibbesen (1999). "Roughness indices for estimation of depression storage capacity of tilled soil surfaces". In: *Soil and Tillage Research* 52.October 1998, pp. 103–111.

Hanson, N. R. (1958). *Patterns of Discovery*. Cambridge University Press, p. 249.

Hanssen-Bauer, I., E. Førland, I. Haddeland, H. Hisdal, S. Mayer, A. Nesje, J. Nilsen, S. Sandven, A. Sandø, A. Sorteberg, and B. Ådlandsvik (2015). *Klima i Norge 2100*. Tech. rep. 2. Norsk Klimaservicesenter, p. 204.

Harvey, D. (1981). "T he Spatial Fix – Hegel, Von Thunen, and Marx". In: *Antipode* 13.3, pp. 1–12. ISSN: 14678330. DOI: 10.1111/j.1467-8330.1981.tb00312.x.

Haubrock, S. N., M. Kuhnert, S. Chabrillat, A. Güntner, and H. Kaufmann (2009). "Spatiotemporal variations of soil surface roughness from in-situ laser scanning". In: *Catena* 79, pp. 128–139.

Hauken, M. and S. H. Kværnø (2013). "Agricultural management in the JOVA catchments". In: *Agriculture and Environment - Long Term Monitoring in Norway*. Ed. by M. Bechmann and J. Deelstra. Akademikaforlaget, Trondheim, Norway, p. 392. ISBN: 9788232100149.

Hawking, S. and L. Mlodinow (2010). *The Grand Design*. Random House Publishing Group. ISBN: 9780553907070.

Hayek, F. A. (1952). *The Counter-Revolution of Science*. Indianapolis: Liberty Fund Inc., p. 415.

He, S., F. Qin, Z. Zheng, and T. Li (2018). "Changes of soil microrelief and its effect on soil erosion under different rainfall patterns in a laboratory experiment". In: *Catena* 162, pp. 203–215. ISSN: 0341-8162. DOI: 10.1016/j.catena.2017.11.010.

Heckmann, T. and W. Schwanghart (2013). "Geomorphic coupling and sediment connectivity in an alpine catchment - Exploring sediment cascades using graph theory". In: *Geomorphology* 182, pp. 89–103. ISSN: 0169555X. DOI: 10.1016/j.geomorph.2012.10.033.

Helming, K., M. J. M. Römkens, and S. N. Prasad (1998). "Surface roughness related processes of runoff and soil loss: a flume study". In: *Soil Science Society of America Journal* 62, pp. 243–250.

Hermannson, A. and W. Spencer Guthrie (2005). "Frost heave and water uptake rates in silty soil subject to variable water table height during freezing". In: *Cold Regions Science and Technology* 43, pp. 128–139.

Hickey, R. (2000). "Slope Angle and Slope Length Solutions for GIS". In: *Cartography* 29.1, pp. 1–8. DOI: 10.1080/00690805.2000.9714334.

Hoffman, J. and P. Hoffman (1992). "Darcy's Law and structural explanation in hydrology". In: *PSA: Proceedings of the Biennial Meeting of the Philosophy of Science Association*, pp. 23–35.

Hoffmann Oliveira, A, M Aparecida da Silva, M. L. Naves Silva, N Curi, G Klinke Neta, and D. A. Franca de Freitas (2013). "Development of Topographic Factor Modeling for Application in Soil Erosion Models". In: *Soil Processes and Current Trends in Quality Assessment*. Ed. by M. C. H. Soriano. Vol. 2. London: IntechOpen Limited. Chap. 4, p. 64. ISBN: 9789537619992. DOI: 10.5772/32009. arXiv: 9809069v1 [arXiv:gr-qc].

Hohenthal, J., P. Alho, J. Hyyppä, and H. Hyyppä (2011). "Laser scanning applications in fluvial studies". In: *Progress in Physical Geography* 35.6, pp. 782–809. ISSN: 03091333. DOI: 10.1177/0309133311414605.

Howard, D. A. and M. Giovanelli (2019). "Einstein's Philosophy of Science". In: *The Stanford Encyclopedia of Philosophy*. Ed. by E. N. Zalta. Fall 2019. Metaphysics Research Lab, Stanford University.

Hrabalíková, M and M Janeček (2017). "Comparison of different approaches to LS factor calculations based on a measured soil loss under simulated rainfall". In: *Soil and Water Research* 2, pp. 69–77.

Huang, C. H. and J. M. Bradford (1992). "Applications of a laser scanner to quantify soil microtopography". In: *Soil Science of America Journal* 56, pp. 14–21.

Hutchinson, D. S. and M. R. Johnson (2017). *Aristotle, Protrepticus or Exhortation to Philosophy*.

Hylton, P and G Kemp (2020). *Willard Van Orman Quine*.

Inkpen, R. and G. Wilson (2013). *Science, Philosophy and Physical Geography*. 2nd ed. Routledge, London and New York, p. 236.

Inkpen, R. (2018). "New technologies and the political economy of geomorphology". In: *Canadian Geographer* 62.2, pp. 200–211. ISSN: 15410064. DOI: 10.1111/cag.12455.

Jester, W. and A. Klik (2005). "Soil surface roughness measurement - methods, applicability, and surface representation". In: *Catena* 64, pp. 174–192.

Jinkang, D., X. Shunping, X. Youpeng, C. Xu, and V. P. Singh (2007). "Development and testing of a simple physically-based distributed rainfall-runoff model for storm runoff simulation in humid forested basins". In: *Journal of Hydrology* 336, pp. 334–346.

Jones, P., G. Walker, R. Harden, and L. McDaniels (1963). *The Development of the Science of Hydrology Circular No. 63-03*. Tech. rep., pp. 1 –35.

Kaiser, A., A. Erhardt, and A. Eltner (2018). "Addressing uncertainties in interpreting soil surface changes by multitemporal high-resolution topography data across scales". In: *Land Degradation and Development* 29.8, pp. 2264–2277. ISSN: 1099145X. DOI: 10.1002/ldr.2967.

Kalantari, Z., S. Seifollahi-Aghmiuni, H. N. von Platen, M. Gustafsson, O. Rahmati, and C. S. S. Ferreira (2021). "Using Landscape Connectivity to Identify Suitable Locations for Nature-Based Solutions to Reduce Flood Risk". In: *Nature-Based Solutions for Flood Mitigation: Environmental and Socio-Economic Aspects,* ed. by C. S. S. Ferreira, Z. Kalantari, T. Hartmann, and P. Pereira. DOI: 10.1007/698_2021_771.

Kamphorst, E. C., V Jetten, J Guerif, J Pitkanen, B. V. Iversen, J. T. Douglas, and A Paz (2000). "Predicting Depressional Storage from Soil Surface Roughness". In: *Soil Science Society of America Journal* 64, pp. 1749–1758.

Kartverket (2022). *Høydedata*.

Katz, D. M., F. J. Watts, and E. R. Burroughs (1995). "Effects of Surface Roughness and Rainfall Impact on Overland Flow". In: *Journal of Hydraulic Engineering* 121.7, pp. 546–553. ISSN: 0733-9429. DOI: 10.1061/(asce)0733-9429(1995)121:7(546).

Kinnell, P. I. A. and L. M. Risse (1998). "USLE-M: Empirical Modeling Rainfall Erosion through Runoff and Sediment Concentration". In: *Soil Science Society of America Journal* 62.6, p. 1667. ISSN: 0361-5995. DOI: 10.2136/sssaj1998.03615995006200060026x.

Kirkby, M. J., B. J. Irvine, R. J. A. Jones, G Govers, M Boer, O Cerdan, J Daroussin, A Gobin, M Grimm, Y Le Bissonnais, C Kosmas, S Mantel, J Puigdefabregas, and G Van Lynden (2008). "The PESERA coarse scale erosion model for Europe. I. - Model rationale and implementation". In: *European Journal of Soil Science* 59.6, pp. 1293–1306. ISSN: 13510754. DOI: 10.1111/j.1365-2389.2008.01072.x.

Kirkby, M. and R. Morgan, eds. (1980). *Soil Erosion*. 1st ed. John Wiley & Sons, p. 312.

Koch, J., M. C. Demirel, and S. Stisen (2018). "The SPAtial EFficiency metric (SPAEF): Multiple-component evaluation of spatial patterns for optimization of hydrological models". In: *Geoscientific Model Development* 11.5, pp. 1873–1886. ISSN: 19919603. DOI: 10.5194/gmd-11-1873-2018.

Krajewski, W. (1982). "No Title". In: *Polish Essays in the Philosophy of the Natural Sciences*. Ed. by W Krajewski. Dordrecht, Boston, London: D. Reidel Publishing Company. Chap. Four conce, p. 488.

Kraus, K. and N. Pfeifer (1998). "Determination of terrain models in wooded areas with airborne laser scanner data". In: *Photogrammetry & Remote Sensing* 53, pp. 193–203.

Kraus, K., W. Karel, C. Briese, and G. Mandlburger (2006). "Local accuracy measures for digital terrain models". In: *Photogrammetric Record* 21.116, pp. 342–354. ISSN: 0031868X. DOI: 10.1111/j.1477-9730.2006.00400.x.

Krishna, V. V. (2014). "Changing Social Relations between Science and Society: Contemporary Challenges". In: *Science, Technology and Society* 19.2, pp. 133–159. ISSN: 09730796. DOI: 10.1177/0971721814529876.

Kuhn, T. S. (1970). *The Structure of Scientific Revolutions*. 2nd ed. Chicago, London: University of Chicago Press, p. 212.

Kuipers, H (1957). "A relief meter for soil cultivation studies". In: *Netherlands Journal of Agricultural Science* 5.4, pp. 255–262.

Kværnø, S. and L. Øygarden (2006). "The influence of freeze-thaw cycles and soil moisture on aggregate stability of three soils in Norway". In: *Catena* 67.3, pp. 175–182. ISSN: 03418162. DOI: 10.1016/j.catena.2006.03.011.

Kværnø, S. H., R. J. Barneveld, E. S. F. Heggem, M Stratman, and N. I. Søvde (2020). *Beskrivelse av erosjonsrisikokart - metoder, forutsetninger og bruk*. Tech. rep. NIBIO, p. 12.

Kværnø, S. H. and L. E. Haugen (2011). "Performance of pedotransfer functions in predicting soil water characteristics of soils in Norway". In: *Acta Agriculturae Scandinavica, Section B — Soil & Plant Science* 61.3, pp. 264–280. ISSN: 0906-4710. DOI: 10.1080/09064710.2010.490233.

Landbruksdirektoratet (2020). *Landbruksdirektoratets Årsrapport 2020*. Tech. rep. Landbruksdirektoratet, p. 110.

Lane, S. N., C. J. Brookes, M. J. Kirkby, and J. Holden (2004). "A network-index-based version of TOPMODEL for use with high-resolution digital topographic data". In: *Hydrological Processes* 18.1, pp. 191–201. ISSN: 08856087. DOI: 10.1002/hyp.5208.

Lane, S. N., S. M. Reaney, and A. L. Heathwaite (2009). "Representation of landscape hydrological connectivity using a topographically driven surface flow index". In: *Water Resources Research* 45.8, pp. 1–10. ISSN: 00431397. DOI: 10.1029/2008WR007336.

Lane, S. N. (2017). "Slow science, the geographical expedition, and Critical Physical Geography". In: *Canadian Geographer* 61.1, pp. 84–101. ISSN: 15410064. DOI: 10.1111/cag.12329.

Latinopoulos, P (1999). "The dawn of hydrology and water management in Ancient Greece". In: *Transactions on Ecology and the Environment* 26, pp. 547–556.

Lave, R., M. W. Wilson, E. S. Barron, C. Biermann, M. A. Carey, C. S. Duvall, L. Johnson, K. M. Lane, N. McClintock, D. Munroe, R. Pain, J. Proctor, B. L. Rhoads, M. M. Robertson, J. Rossi, N. F. Sayre, G. Simon, M. Tadaki, and C.

Van Dyke (2014). "Intervention: Critical physical geography". In: *Canadian Geographer* 58.1, pp. 1–10. ISSN: 15410064. DOI: 10.1111/cag.12061.

Lazzarotto, P., C. Stamm, V. Prasuhn, and H. Flühler (2006). "A parsimonious soil-type based rainfall-runoff model simultaneously tested in four small agricultural catchments". In: *Journal of Hydrology* 321.1-4, pp. 21–38. ISSN: 00221694. DOI: 10.1016/j.jhydrol.2005.07.038.

le Bissonnais, Y. and M. J. Singer (1992). "Crusting, Runoff, and Erosion Response to Soil Water Content and Successive Rainfalls". In: *Soil Science Society of America Journal* 56, pp. 1898–1903.

– (1993). "Seal formation, runoff, and interrill erosion from seventeen California soils". In: *Soil Science Society of America Journal* 57, pp. 224–229.

Leica Geosystems (2007). *Datasheet Leica ScanStation 2*.

– (2009). *Datasheet Leica ScanStation C10.*

Leica Geosystems, Inc. (2007). *Factsheet: Leica ScanStation 2*.

Leick, G. (2007). *The Babylonian world*. Routledge, p. 591. ISBN: 0203946235. DOI: 10.5860/choice.45-5136.

Leijnhorst, C. (1996). "Hobbes' theory of causality and its Aristotelian background". In: *The Monist* 79.3, pp. 426–477.

Li, Y., J. J. McNelis, and R. A. Washington-Allen (2020). "Quantifying Short-Term Erosion and Deposition in an Active Gully Using Terrestrial Laser Scanning: A Case Study From West Tennessee, USA". In: *Frontiers in Earth Science* 8.October, pp. 1–14. ISSN: 22966463. DOI: 10.3389/feart.2020.587999.

Li, Z (1993). "Theoretical Models of the Accuracy of Digital Terrain Models : an evaluatoin and some observations". In: *Photogrammetric Record* 14.82, pp. 651–660.

Lichti, D and J Skaloud (2010). "Registration and Calibration". In: *Airborne and terrestrial laser scanning*. Ed. by G Vosselman and H. G. Maas. Whittles Publishing. Chap. 3.

Liu, B. Y., M. A. Nearing, P. J. Shi, and Z. W. Jia (2000). "Slope Length Effects on Soil Loss for Steep Slopes". In: *Soil Science Society of America Journal* 64, pp. 1759–1763.

Liu, Q. Q. and V. P. Singh (2004). "Effect of Microtopography, Slope Length and Gradient, and Vegetative Cover on Overland Flow through Simulation". In: *Journal of Hydrologic Engineering* 9.5, pp. 375–382. ISSN: 1084-0699. DOI: 10.1061/(asce)1084-0699(2004)9:5(375).

Loon, E. V. (2002). "Overland flow: interfacing models with measurements". PhD thesis. Wageningen University.

Louis, J., N. Floury, M. Davidson, E. Attema, and M. Borgeaud (2004). "Surface roughness characterization for SAR applications". In: *2003 IEEE International Geoscience and Remote Sensing Symposium*. Ed. by IEEE Geoscience and Remote Sensing Society. Vol. 7, pp. 1408–1410. ISBN: 0780379292. DOI: 10.1109/igarss.2003.1294125.

Lu, X., Y. Li, R. A. Washington-Allen, Y. Li, H. Li, and Q. Hu (2017). "The effect of grid size on the quantification of erosion, deposition, and rill network". In: *International Soil and Water Conservation Research* 5.3, pp. 241–251. ISSN: 20956339. DOI: 10.1016/j.iswcr.2017.06.002.

Lubchenco, J. (1998). "Entering the century of the environment: A new social contract for science". In: *Science* 279.5350, pp. 491–497. ISSN: 00368075. DOI: 10.1126/science.279.5350.491.

Lundekvam, H. (2002). *ERONOR/USLENO - Empirical erosion models for Norwegian conditions.* Tech. rep. Ås: Agricultural University of Norway, p. 42.

Lundekvam, H and S Skøien (1998). "Soil erosion in Norway. An overview of measurements from soil loss plots". In: *Soil Use and Management* 14, pp. 84–89.

Mackie, J. L. (1975). "Causes and conditions". In: *Causation and Conditionals*. Oxford University Press. Chap. 1, p. 202.

Mandelbrot, B (1967). "How long is the coast of Britain? Statistical self-similarity and fractional dimension". In: *Science* 156, pp. 636–638. ISSN: 22977007. DOI: 10.4414/sanp.2016.00418.

Margolis, J. (1995). *Historied Thought, Constructed World: A Conceptual Primer for the Turn of the Millennium.* Berkeley, Los Angeles, Oxford: University of California Press, p. 378.

Marsh, G. P. (1864). *Man and Nature*. Ed. by D Lowenthal. 1965th ed. Seattle and London: University of Washinton Press, p. 432.

Martin, Y., C. Valeo, and M. Tait (2008). "Centimetre-scale digital representations of terrain and impacts on depression storage and runoff". In: *Catena* 75.2, pp. 223–233. ISSN: 03418162. DOI: 10.1016/j.catena.2008.07.005.

Martinez-Agirre, A., J. Álvarez-Mozos, and R. Giménez (2016). "Evaluation of surface roughness parameters in agricultural soils with different tillage conditions using a laser profile meter". In: *Soil and Tillage Research* 161, pp. 19–30. ISSN: 01671987. DOI: 10.1016/j.still.2016.02.013.

Marx, S., K. Anders, S. Antonova, I. Beck, J. Boike, P. Marsh, M. Langer, and B. Höfle (2017). "Terrestrial laser scanning for quantifying small-scale vertical movements of the ground surface in Artic permafrost regions". In: *Earth Surface Dynamics Discussions* August, pp. 1–31. ISSN: 2196-6338. DOI: 10.5194/esurf-2017-49.

Masselink, R. J. H., T. Heckmann, A. J. A. M. Temme, N. S. Anders, H. P. A. Gooren, and S. D. Keesstra (2016). "A network theory approach for a better understanding of overland flow connectivity". In: *Hydrological Processes*. ISSN: 10991085. DOI: 10.1002/hyp.10993.

McCurdy, E. (1938). *The Notebooks of Leonardo Da Vinci*. Milwaukee Academy of Medicine Collection v. 1. Reynal & Hitchcock.

McNamara, J. P., D. Chandler, M. Seyfried, and S. Achet (2005). "Soil moisture states, lateral flow, and streamflow generation in a semi-arid, snowmelt-driven catchment". In: *Hydrological Processes* 19, pp. 4023–4038.

Meinen, B. U. and D. T. Robinson (2020). "Where did the soil go? Quantifying one year of soil erosion on a steep tile-drained agricultural field". In: *Science of the*

Total Environment 729, p. 138320. ISSN: 18791026. DOI: 10.1016/j.scitotenv.2020.138320.

Meli, D. (2007). *Thinking with Objects: The Transformation of Mechanics in the Seventeenth Century*. Baltimore: The Johns Hopkins University Press, p. 389.

Milenković, M., W. Karel, C. Ressl, and N. Pfeifer (2016). "A comparison of UAV and TLS data for soil Roughness assessment". In: *ISPRS Annals of Photogrammetry, Remote Sensing and Spatial Information Sciences* III-5.July, pp. 145–152. DOI: 10.5194/isprsannals-iii-5-145-2016.

Milenkovic, M., N. Pfeifer, and P. Glira (2015). "Applying terrestrial laser scanning for soil surface roughness assessment". In: *Remote Sensing* 7.2, pp. 2007–2045. ISSN: 20724292. DOI: 10.3390/rs70202007.

Mion, G. (2019). "On Certainty: Wittgenstein and Einstein". In: *Philosophical Investigations* 42.2, pp. 163–170. ISSN: 14679205. DOI: 10.1111/phin.12232.

Mitasova, H, J Hofierka, M Zloka, and L. R. Iverson (1996). "Modelling Topographic Potential for Erosion and Deposition Using GIS." In: *International Journal of Geographical Information Systems* 10.5, pp. 629–641. DOI: 10.1080/02693799608902101.

Moore, I. D. and G. J. Burch (1986). "Physical basis of the length-slope factor in the Universal Soil Loss Equation". In: *Soil Sci. Soc. Am. J.* 50, pp. 1294–1298.

Moore, I. D., R. B. Grayson, and A. R. Ladson (1991). "Digital terrain modelling: A review of hydrological, geomorphological, and biological applications". In: *Hydrological Processes* 5.1, pp. 3–30. ISSN: 10991085. DOI: 10.1002/hyp.3360050103.

Moore, I. D. and J. P. Wilson (1992). "Length-slope factors for the Revised Universal Soil Loss Equation: Simplified method of estimation". In: *J. Soil and Water Cons.* 47.5, pp. 423–428.

Morgan, R. P. C. (1996). *Soil Erosion & Conservation*. 2nd. Harlow, UK: Addison Wesley Longman Ltd., p. 198.

Morgan, R. P., D. D. Morgan, and H. J. Finney (1984). "A predictive model for the assessment of soil erosion risk". In: *Journal of Agricultural Engineering Research* 30.C, pp. 245–253. ISSN: 00218634. DOI: 10.1016/S0021-8634(84)80025-6.

Morgan, R. (2001). "A simple approach to soil loss prediction: a revised Morgan–Morgan–Finney model". In: *CATENA* 44.4, pp. 305–322. ISSN: 03418162. DOI: 10.1016/S0341-8162(00)00171-5.

Moritani, S., T. Yamamoto, H. Andry, M. Inoue, and T. Kaneuchi (2010). "Using digital photogrammetry to monitor soil erosion under conditions of simulated rainfall and wind". In: *Australian Journal of Soil Research* 48.1, pp. 36–42.

Mu, Q., F. A. Heinsch, M. Zhao, and S. W. Running (2007). "Development of a global evapotranspiration algorithm based on MODIS and global meteorology data". In: *Remote Sensing of Environment* 111.4, pp. 519–536. ISSN: 00344257. DOI: 10.1016/j.rse.2007.04.015.

Mwendera, E. J. and J. Feyen (1992). "Estimation of depression storage and Manning's resistance coefficient from random roughness measurements". In: *Geoderma* 52.3-4, pp. 235–250. ISSN: 00167061. DOI: 10.1016/0016-7061(92)90039-A.

Nachtergaele, J., J. Poesen, and G. Govers (2002). "Ephemeral gullies . A spatial and temporal analysis of their characteristics , importance and". In: *Belgeo* 2.July, pp. 1–23. DOI: 10.4000/belgeo.16167.

Nakil, M. and M. Khire (2016). "Effect of slope steepness parameter computations on soil loss estimation: review of methods using GIS". In: *Geocarto International* 31.10, pp. 1078–1093. ISSN: 1010-6049. DOI: 10.1080/10106049.2015.1120349.

NASA Earth Observatory (2001). *Toxic bloom off the coast of Norway*.

Nash, J. and J. Sutcliffe (1970). "River flow forecasting through conceptual models: Part 1. A discussion of principles." In: *Journal of Hydrology* 10.3, pp. 282–290.

Nature (1965). "The International Hydrological Decade". In: *Nature* 207, p. 920.

Nearing, G. S., Y. Tian, H. V. Gupta, M. P. Clark, K. W. Harrison, and S. V. Weijs (2016). "A philosophical basis for hydrological uncertainty". In: *Hydrological Sciences Journal* 61.9, pp. 1666–1678. ISSN: 21503435. DOI: 10.1080/02626667.2016.1183009.

Nearing, M. A. (1997). "A single, continuous function for slope steepness influence on soil loss". In: *Soil Sci. Soc. Am. J.* 61, pp. 917–919.

Nearing, M. A., Y. Xie, B. Liu, and Y. Ye (2017). "Natural and anthropogenic rates of soil erosion". In: *International Soil and Water Conservation Research* 5.2, pp. 77–84. ISSN: 20956339. DOI: 10.1016/j.iswcr.2017.04.001.

NIBIO (2016). *Kilden*.

– (2020). *JOVA Monitoring Programme Kernel Description*. https://www.nibio.no/en/subjects/environment/the-norwegian-agricultural-environmental-monitoring-programme-jova?locationfilter=true. Accessed: 2020-09-30.

Nield, J. M., J. King, G. F. Wiggs, J. Leyland, R. G. Bryant, R. C. Chiverrell, S. E. Darby, F. D. Eckardt, D. S. Thomas, L. H. Vircavs, and R. Washington (2013). "Estimating aerodynamic roughness over complex surface terrain". In: *Journal of Geophysical Research Atmospheres* 118.23, pp. 12948–12961. ISSN: 21698996. DOI: 10.1002/2013JD020632.

Nill, D, U Schwertmann, U Sabel-Koschella, M Bernhard, and J Breuer (1996). *Soil Erosion by water in Africa*. Tech. rep. Deutsche Gesellschaft für Technische Zusammenarbeit (GTZ), p. 291.

Nowotny, H., P. Scott, and M. Gibbons (2003). "'Mode 2' Revisited: the New Production of Knowledge". In: *Minerva* 41, pp. 179–194.

Nozick, R. (1981). *Philosophical Explanations*. Harvard University Press, Cambridge MA., p. 764. DOI: 10.1111/j.1755-2567.1981.tb00477.x.

NTSG (The Numerical Terradynamic Simulation Group), U. o. M. (2016). *MOD16*.

Onnen, N., A. Eltner, G. Heckrath, and K. Van Oost (2020). "Monitoring soil surface roughness under growing winter wheat with low-altitude UAV sensing: Potential and limitations". In: *Earth Surface Processes and Landforms* 45.14, pp. 3747–3759. ISSN: 10969837. DOI: 10.1002/esp.4998.

Øygarden, L., J. Kværner, and P. Jenssen (1997). "Soil erosion via preferential flow to drainage systems in clay soils". In: *Geoderma* 76.1–2, pp. 65–86. ISSN: 00167061. DOI: 10.1016/S0016-7061(96)00099-7.

Øygarden, L. (2003). "Rill and gully development during an extreme winter runoff event in Norway". In: *Catena* 50.2-4, pp. 217–242. ISSN: 03418162. DOI: 10.1016/S0341-8162(02)00138-8.

Oztas, T. and F. Fayetorbay (2003). "Effect of freezing and thawing processes on soil aggregate stability". In: *Catena* 52, pp. 1–8. DOI: 10.1016/S0341-8162(02)00177-7.

Panagos, P., P. Borrelli, and K. Meusburger (2015a). "A New European Slope Length and Steepness Factor (LS-Factor) for Modeling Soil Erosion by Water". In: *Geosciences* 5, pp. 117–126.

– (2015b). "A New European Slope Length and Steepness Factor (LS-Factor) for Modeling Soil Erosion by Water". In: *Geosciences* 5, pp. 117–126. DOI: 10.3390/geosciences5020117.

Panagos, P., G. Standardi, P. Borrelli, E. Lugato, L. Montanarella, and F. Bosello (2018). "Cost of agricultural productivity loss due to soil erosion in the European Union: From direct cost evaluation approaches to the use of macroeconomic models". In: *Land Degradation and Development* 29.3, pp. 471–484. ISSN: 1099145X. DOI: 10.1002/ldr.2879.

Parsons, A. J. (1988). *Hillslope Form*. London, New York: Routledge, London and New York, p. 212.

Parsons, A. J. (2019). "How reliable are our methods for estimating soil erosion by water?" In: *Science of the Total Environment* 676, pp. 215–221. ISSN: 18791026. DOI: 10.1016/j.scitotenv.2019.04.307.

Paz, A. R. da, W. Collischonn, A. Risso, and C. A. B. Mendes (2008). "Errors in river lengths derived from raster digital elevation models". In: *Computers and Geosciences* 34.11, pp. 1584–1596. ISSN: 00983004. DOI: 10.1016/j.cageo.2007.10.009.

Penco, C. (2010). "The influence of Einstein on Wittgenstein's philosophy". In: *Philosophical Investigations* 33.4, pp. 360–379. ISSN: 01900536. DOI: 10.1111/j.1467-9205.2010.01415.x.

Peñuela, A., F. Darboux, M. Javaux, and C. L. Bielders (2016). "Evolution of overland flow connectivity in bare agricultural plots". In: *Earth Surface Dynamics Discussions* 41.11, pp. 1595–1613. DOI: 10.1002/esp.3938.

Peppin, S. S. L. and R. W. Style (2013). "The Physics of Frost Heave and Ice-Lens Growth". In: *Vadose Zone Journal* 12.

Perroy, R. L., B. Bookhagen, G. P. Asner, and O. A. Chadwick (2010). "Comparison of gully erosion estimates using airborne and ground-based LiDAR on

Santa Cruz Island, California". In: *Geomorphology* 118.3-4, pp. 288–300. ISSN: 0169555X. DOI: 10.1016/j.geomorph.2010.01.009. arXiv: 1020.

Phillips, R. W., C Spence, and J. W. Pomeroy (2011). "Connectivity and runoff dynamics in heterogeneous basins". In: *Hydrological Processes* 25.19, pp. 3061–3075. ISSN: 08856087. DOI: 10.1002/hyp.8123.

Pirotti, F. and P. Tarolli (2010). "Suitability of LiDAR point density and derived landform curvature maps for channel network extraction". In: *Hydrological Processes* 24.9, pp. 1187–1197. ISSN: 08856087. DOI: 10.1002/hyp.7582.

Planchon, O. and F. Darboux (2001). "A fast, simple and versatile algorithm to fill the depressions of digital elevation models". In: *Catena* 46.2-3, pp. 159–176. ISSN: 03418162. DOI: 10.1016/S0341-8162(01)00164-3.

Ploeg, J., W. Appels, D. Cirkel, M. Oosterwoud, J.-P. Witte, and S. van der Zee (2011). "Microtopography as a driving mechanism for ecohydrological processes in shallow groundwater systems". In: *Vadose Zone Journal* 11. DOI: 10.2136/vzj2011.0098.

Podmore, T. H. and L. F. Huggins (1981). "An automated profile meter for surface roughness measurements." In: *Transactions, American Society of Agricultural Engineers* 24.3, pp. 663–665. ISSN: 2151-0059. DOI: 10.13031/2013.34317.

Poeppl, R. E., K. A. Fryirs, J. Tunnicliffe, and G. J. Brierley (2020). "Managing sediment (dis)connectivity in fluvial systems". In: *Science of the Total Environment* 736.May, p. 139627. ISSN: 18791026. DOI: 10.1016/j.scitotenv.2020.139627.

Poesen, J., J. Nachtergaele, G. Verstraeten, and C. Valentin (2003). "Gully erosion and environmental change: Importance and research needs". In: *Catena* 50.2-4, pp. 91–133. ISSN: 03418162. DOI: 10.1016/S0341-8162(02)00143-1.

Quine, W. V. (1948). "On what there is". In: *The Review of Metaphysics* 2.5, pp. 21–38.

Quinn, P., K. Beven, P. Chevallier, and O. Planchon (1991). "The prediction of hillslope flow paths for distributed hydrological modelling using digital terrain models". In: *Hydrological Processes* 5.1, pp. 59–79. ISSN: 10991085. DOI: 10.1002/hyp.3360050106.

R Development Core Team (2008). *R: A Language and Environment for Statistical Computing*. ISBN 3-900051-07-0. R Foundation for Statistical Computing. Vienna, Austria.

Radke, J. K., M. A. Otterby, R. A. Young, and C. A. Onstad (1981). "A microprocessor automated rillmeter." In: *Transactions, American Society of Agricultural Engineers* 24.2. ISSN: 0001-2351. DOI: 10.13031/2013.34264.

Raven, D. (2015). *Relativism, Cognitive*. Second Edition. Vol. 19. Elsevier, pp. 227–232. ISBN: 9780080970875. DOI: 10.1016/B978-0-08-097086-8.32125-0.

Reaney, S. M., S. N. Lane, A. L. Heathwaite, and L. J. Dugdale (2011). "Risk-based modelling of diffuse land use impacts from rural landscapes upon salmonid fry abundance". In: *Ecological Modelling* 222.4, pp. 1016–1029. ISSN: 03043800. DOI: 10.1016/j.ecolmodel.2010.08.022.

Reid, S. C., S. N. Lane, D. R. Montgomery, and C. J. Brookes (2007). "Does hydrological connectivity improve modelling of coarse sediment delivery in upland

environments?" In: *Geomorphology* 90.3-4, pp. 263–282. ISSN: 0169555X. DOI: 10.1016/j.geomorph.2006.10.023.

Remortel, R. D. V., M. E. Hamilton, and R. J. Hickey (2001). "Estimating the LS Factor for RUSLE through Iterative Slope Length Processing of Digital Elevation Data within Arclnfo Grid". In: *Cartography* 30.1, pp. 27–35. DOI: 10.1080/00690805.2001.9714133.

Renard, K. G., G. R. Foster, G. A. Weesies, D. K. McCool, and D. C. Yoder (1997). *Predicting Soil Erosion by Water: A Guide to Conservation Planning With the Revised Universal Soil Loss Equation (RUSLE)*. Tech. rep. USDA, Agriculture Handbook No. 703, p. 404.

Renard, K. G., G. R. Foster, G. A. Weesies, and J. P. Porter (1991). "RUSLE: Revised universal soil loss equation". In: *Journal of Soil and Water Conservation* 46.1, pp. 30–33.

Rhoads, B. L. (1999). "Beyond pragmatism: The value of philosophical discourse for physical geography". In: *Annals of the Association of American Geographers* 89.4, pp. 760–771. ISSN: 00045608. DOI: 10.1111/0004-5608.00176.

Rieke-Zapp, D. and M. Nearing (2011). "Digital close range photogrammetry for measurement of soil erosion". In: *The Photogrammetric Record* 20, pp. 69–87.

Riley, H. (1996). "Estimation of physical properties of cultivated soils in southeast Norway from readily available soil information". In: *Norwegian Journal of Agricultural Sciences* 25.51.

Rodriguez, J. L. G. and M. C. G. Suarez (2010). "Estimation of slope length value of rusle factor l using gis". In: *Journal of Hydrologic Engineering* 15.9, pp. 714–717. ISSN: 10840699. DOI: 10.1061/(ASCE)HE.1943-5584.0000232.

Römkens, M. J. M. and J. Y. Wang (1987). "Soil roughness changes from rainfall". In: *Transactions of the ASAE* 30, pp. 101–107.

Römkens, M. J., S. Singarayar, and C. J. Gantzer (1986). "An automated noncontact surface profile meter". In: *Soil and Tillage Research* 6.3, pp. 193–202. ISSN: 01671987. DOI: 10.1016/0167-1987(86)90454-X.

Rosbjerg, D. and J. Rodda (2019). "IAHS: A brief history of hydrology". In: *History of Geo- and Space Sciences* 10.1, pp. 109–118. ISSN: 21905029. DOI: 10.5194/hgss-10-109-2019.

Russell, B (1981). "On the notion of cause". In: *Mysticism and Logic*. Chap. 9.

Schmitt, L. K. (2009). "Developing and applying a soil erosion model in a data-poor context to an island in the rural Philippines". In: *Environment, Development and Sustainability* 11.1, pp. 19–42. ISSN: 1387585X. DOI: 10.1007/s10668-007-9096-1.

Schneider, A., H. H. Gerke, T. Maurer, S. Seifert, R. Nenov, and R. F. Hüttl (2012). "Evaluation of remotely-sensed DEMs and modification based on plausibility rules and initial sediment budgets of an artificially-created catchment". In: *Earth Surface Processes and Landforms* 37.7, pp. 708–725. ISSN: 01979337. DOI: 10.1002/esp.2274.

Schröter, M., E. van der Zanden, A. van Oudenhoven, R. Remme, H. Serna-Chavez, R. de Groot, and P. Opdam (2014). "Ecosystem Services as a Contested

Concept: A Synthesis of Critique and Counter-arguments". English. In: *Conservation Letters* 7.6, pp. 514–523. ISSN: 1755-263X. DOI: 10.1111/conl.12091.

Schumm, S. A. and R. W. Lichty (1965). *Time, space, and causality in geomorphology*. DOI: 10.2475/ajs.263.2.110.

Schürch, P., A. L. Densmore, N. J. Rosser, M. Lim, and B. W. Mcardell (2011). "Detection of surface change in complex topography using terrestrial laser scanning: Application to the Illgraben debris-flow channel". In: *Earth Surface Processes and Landforms* 36.14, pp. 1847–1859. ISSN: 01979337. DOI: 10.1002/esp.2206.

Schwarz, L. (1950). *Om twintig kostbare centimeters. Landinrichting in Indonesië*. 's Gravenhage - Bandung: Van Hoeve, p. 56.

Sharif, A., B. Mohammad, and I. Saeed (2019). "Nature's Retaliation in the Sumerian Epic Gilgamesh: An Ecocritical Study". In: *Journal of Garmian University* 6.2, pp. 396–403. DOI: 10.24271/garmian.196232.

Sharpnack, D. and G. Akin (1969). "An algorithm for computing slope and aspect from elevations." In: *Photogrammetric Survey* 35, pp. 247–248.

Shore, M, P. N. C. Murphy, P Jordan, P. E. Mellander, M Kelly-Quinn, M Cushen, S Mechan, O Shine, and A. R. Melland (2013). "Evaluation of a surface hydrological connectivity index in agricultural catchments". In: *Environmental Modelling and Software* 47, pp. 7–15. ISSN: 13648152. DOI: 10.1016/j.envsoft.2013.04.003.

Singh, V. (1997). *Kinematic Wave Modelling in Water Resources*. New York: Wiley, p. 848. ISBN: 978-0-471-10948-8.

Skarbøvik, E., S. Haande, M. Bechmann, and B. Skjebred (2016). *Overvåking Morsa 2014-2015. NIBIO Report 42(2)*. Tech. rep., p. 71.

Skøien, S., T. Børresen, and M. Bechmann (2012a). "Effect of tillage methods on soil erosion in Norway." In: *Acta Agriculturae Scandinavica, Section B — Soil {&} Plant Science* 62, pp. 191–198.

– (2012b). "Effect of tillage methods on soil erosion in Norway." In: *Acta Agriculturae Scandinavica, Section B — Soil {&} Plant Science* 62, pp. 191–198.

Skyrms, B (1996). *The Evolution of the Social Contract*. Cambridge University Press, p. 146.

Slaymaker, O. (1997). "A pluralist, problem-focussed geomorphology". In: *Process and form in geomorphology*, pp. 328–339.

– (2009). "The future of geomorphology". In: *Geography Compass* 3.1, pp. 329–349. ISSN: 17498198. DOI: 10.1111/j.1749-8198.2008.00178.x.

– (2017). "Physical geographers' understanding of the real world". In: *Canadian Geographer* 61.1, pp. 64–72. ISSN: 15410064. DOI: 10.1111/cag.12334.

Smith, D. D. (1941). "Interpretation of soil conservation data for field use". In: *Agricultural Engineering* 22.5, pp. 173–175.

Smith, S. R. (2000). "Resolving Russell ' s Anti-Realism About Causation : The Connection Between Causation and the Functional Dependencies of Mathematical Physics". In: *The Monist* 83.2, pp. 274–295.

Snapir, B., S. Hobbs, and T. W. Waine (2014). "Roughness measurements over an agricultural soil surface with Structure from Motion". In: *ISPRS Journal of Photogrammetry and Remote Sensing* 96, pp. 210–223. ISSN: 09242716. DOI: 10.1016/j.isprsjprs.2014.07.010.

Sofia, G., P. Tarolli, F. Cazorzi, and G. Dalla Fontana (2011). "An objective approach for feature extraction: Distribution analysis and statistical descriptors for scale choice and channel network identification". In: *Hydrology and Earth System Sciences* 15.5, pp. 1387–1402. ISSN: 10275606. DOI: 10.5194/hess-15-1387-2011.

Sonklar, C. von (1873). *Allgemeine Orographie: Die Lehre von den Relief-Formen der Erdoberfläche*. Vienna, Austria: Wilhelm Braumüller, p. 254.

Sorsby, N. T. (1973). "Horizontal Plowing and Hill-Side Ditching". In: *Environmental Geomorphology and Landscape Conservation. Volume 1: Prior to 1900*. Ed. by D. R. Coates. Stroudsburg, Pennsylvania: Dowden, Hutchinson & Ross, Inc. Chap. 31, p. 485.

Soudarissanane, S., R. Lindenbergh, M. Menenti, and P. Teunissen (2011). "Scanning geometry: Influencing factor on the quality of terrestrial laser scanning points". In: *ISPRS Journal of Photogrammetry and Remote Sensing* 66.4, pp. 389–399. ISSN: 09242716. DOI: 10.1016/j.isprsjprs.2011.01.005.

Staricka, J. and G. Benoit (1991). "Freeze-Drying Effects on Wet and Dry Soil Aggregate Stability". In: *Soil Science of America Journal* 59, pp. 218–223.

Starkloff, T. and J. Stolte (2014). "Applied comparison of the erosion risk models EROSION 3D and LISEM for a small catchment in Norway". In: *Catena* 118, pp. 154–167. ISSN: 03418162. DOI: 10.1016/j.catena.2014.02.004.

Stroosnijder, L. (2005). "Measurement of erosion: Is it possible?" In: *Catena* 64, pp. 162–173. DOI: 10.1016/j.catena.2005.08.004.

Tarolli, P., G. Sofia, and G. Dalla Fontana (2012). "Geomorphic features extraction from high-resolution topography: Landslide crowns and bank erosion". In: *Natural Hazards* 61.1, pp. 65–83. ISSN: 0921030X. DOI: 10.1007/s11069-010-9695-2.

Thompson, S. E., G. G. Katul, and A. Porporato (2010). "Role of microtopography in rainfall-runoff partitioning: An analysis using idealized geometry". In: *Water Resources Research* 46.7, pp. 1–11. ISSN: 00431397. DOI: 10.1029/2009WR008835.

Thomsen, L. M., J. E. M. Baartman, R. J. Barneveld, T. Starkloff, and J. Stolte (2015). "Soil surface roughness: comparing old and new measuring methods and application in a soil erosion model". In: *SOIL* 1, pp. 399–410.

Torretti, R. (1999). *The philosophy of physics*. Cambridge: Cambridge University Press, p. 512. ISBN: 020302947X. DOI: 10.4324/9780203029473.

Triggs, B, P. F. McLaughlan, R. I. Hartley, and A. W. Fitzgibbon (2000). "Bundle Adjustment - A Modern Synthesis". In: *Vision Algorithms: Theory & Practice*. Ed. by B Triggs, A Zisserman, and R Szeliski. Berlin Heidelberg: Springer Verlag, pp. 298–372.

Ulén, B., M. Bechmann, L. Øygarden, and K. Kyllmar (2012). "Soil erosion in Nordic countries–future challenges and research needs". In: *Acta Agriculturae*

Scandinavica, Section B–Soil & Plant Science 62.sup2, pp. 176–184. ISSN: 0906-4710. DOI: 10.1080/09064710.2012.712862.

USDA (2016). *USLE History: USDA ARS*. https://www.ars.usda.gov/midwest-area/west-lafayette-in/national-soil-erosion-research/docs/usle-database/usle-history/. Accessed on 2019-01-04.

Van Baren, F. (1947). *Erosie: Oorzaak, gevolgen en bestrijding*. Tech. rep. 's Gravenhage: Dept. Economische Zaken, p. 135.

Vandekerckhove, L., J. Poesen, D. Oostwoud Wijdenes, and T. De Figueiredo (1998). "Topographical thresholds for ephemeral gully initiation in intensively cultivated areas of the Mediterranean". In: *Catena* 33.3-4, pp. 271–292. ISSN: 03418162. DOI: 10.1016/S0341-8162(98)00068-X.

Vanmaercke, M., P. Panagos, T. Vanwalleghem, A. Hayas, S. Foerster, P. Borrelli, M. Rossi, D. Torri, J. Casali, L. Borselli, O. Vigiak, M. Maerker, N. Haregeweyn, S. De Geeter, W. Zgłobicki, C. Bielders, A. Cerdà, C. Conoscenti, T. de Figueiredo, B. Evans, V. Golosov, I. Ionita, C. Karydas, A. Kertész, J. Krása, C. Le Bouteiller, M. Radoane, R. Ristić, S. Rousseva, M. Stankoviansky, J. Stolte, C. Stolz, R. Bartley, S. Wilkinson, B. Jarihani, and J. Poesen (2021). "Measuring, modelling and managing gully erosion at large scales: A state of the art". In: *Earth-Science Reviews* 218.April. ISSN: 00128252. DOI: 10.1016/j.earscirev.2021.103637.

Vemuri, V. and N. Vemuri (1970). "On The Systems Approach In Hydrology". In: *International Association of Scientific Hydrology. Bulletin* 15.2, pp. 17–38. ISSN: 00206024. DOI: 10.1080/02626667009493951.

Verstraeten, G, K. van Oost, A. van Rompaey, J. Poesen, G. Govers, and G. Verstraeten (2002). "Evaluating an integrated approach to catchment management to reduce soil loss and sediment pollution through modelling". In: *Soil Use and Management* 18.4, pp. 386–394. ISSN: 02660032. DOI: 10.1079/sum2002150.

Vidal Vázquez, E., J. G. V. Miranda, and J. Paz-Ferreiro (2010). "A multifractal approach to characterize cumulative rainfall and tillage effects on soil surface micro-topography and to predict depression storage". In: *Biogeosciences Discussions* 7, pp. 2099–2141.

Vidal Vázquez, E., J. G. Vivas Miranda, and A. Paz González (2005). "Characterizing anisotropy and heterogeneity of soil surface microtopography using fractal models". In: *Ecological Modelling* 182, pp. 337–353.

Vieux, B. (1993). "DEM aggregation and smoothing effects on surface runoff modeling". In: *Journal of Computing in Civil Engineering* 7, pp. 310–338.

Vigiak, O., L. Borselli, L. T. H. Newham, J. McInnes, and a. M. Roberts (2012). "Comparison of conceptual landscape metrics to define hillslope-scale sediment delivery ratio". In: *Geomorphology* 138.1, pp. 74–88. ISSN: 0169555X. DOI: 10.1016/j.geomorph.2011.08.026.

Vinci, A., R. Brigante, F. Todisco, F. Mannocchi, and F. Radicioni (2015). "Measuring rill erosion by laser scanning". In: *Catena* 124, pp. 97–108. ISSN: 03418162. DOI: 10.1016/j.catena.2014.09.003.

Von Bertalanffy, L. (1972). "The History and Status of General Systems Theory". In: *Academy of Management Journal* 15.4, pp. 407–426. ISSN: 0001-4273. DOI: 10.5465/255139.

Von Wright, G. H. (1975). "On the logic and epistomology of the causal relation". In: *Causation and Conditionals*. Ed. by E Sosa. Oxford University Press. Chap. 4, p. 202.

Vosselman, G. and H.-G. Maas (2010). *Airborne and Terrestrial Laser Scanning*. ITC, Enschede.

Walling, D. E. (1983). "The sediment delivery problem". In: *Journal of Hydrology* 65, pp. 209–237.

Walling, D. E. (1999). "Linking land use, erosion and sediment yields in river basins". In: *Hydrobiologia* 410, pp. 223–240. ISSN: 00188158. DOI: 10.1023/A:1003825813091.

– (2005). "Tracing suspended sediment sources in catchments and river systems". In: *Science of the Total Environment* 344.1-3 SPEC. ISS. Pp. 159–184. ISSN: 00489697. DOI: 10.1016/j.scitotenv.2005.02.011.

Wang, S, P Strauss, A Yao, X Wang, and Y Yuan (2018). "Assessing hydrological connectivity development by using a photogrammetric technique with relative surface connection function (RSCf) in a plot-scale experiment". In: *Journal of Soil and Water Conservation* 73.5, pp. 518–532. DOI: 10.2489/jswc.73.5.518.

Water Research, M. S. U. Institute of (2002). *RUSLE: online soil erosion assessment tool*. http://www.iwr.msu.edu/rusle/lsfactor.htm. Accessed on 2019-02-14.

Wenng, H., R. Barneveld, M. Bechmann, H. Marttila, T. Krogstad, and E. Skarbøvik (2021). "Sediment transport dynamics in small agricultural catchments in a cold climate: A case study from Norway". In: *Agriculture, Ecosystems and Environment* 317.December 2020. ISSN: 01678809. DOI: 10.1016/j.agee.2021.107484.

Wenng, H., M. Bechmann, T. Krogstad, and E. Skarbøvik (2020). "Climate effects on land management and stream nitrogen concentrations in small agricultural catchments in Norway". In: *Ambio* 49.11, pp. 1747–1758. ISSN: 16547209. DOI: 10.1007/s13280-020-01359-z.

Williams, J. R. (Nov. 1975). "Sediment-yield prediction with Universal Equation using runoff energy factor". In: *Present and Prospective Technology for Predicting Sediment Yield and Sources.* Ed. by U. D. A. ARS-S-40. U.S. Dep. Agr. ARS-S-40, pp. 244–252.

Williams, R. D. (2012). "DEMs of Difference". In: *Geomorphological Techniques* 2, pp. 1–17. ISSN: 2047-0371. DOI: 2047-0371.

Wilson, A. G. (1972). "Theoretical Geography: Some Speculations". In: *Transactions of the Institute of British Geographers* 57.57, p. 31. ISSN: 00202754. DOI: 10.2307/621552.

Wischmeier, W. H. (1976). "Use and misuse of the universal soil loss equation". In: *J. Soil and Water Cons.* 31.1, pp. 5–9.

Wischmeier, W. H. and D. D. Smith (1965). *Predicting rainfall-erosion losses from cropland east of the Rocky Mountains. Guide for the Selection of Practices for Soil and*

Water Conservation. Agriculture Handbook no. 282. Tech. rep. U.S. Department of Agriculture, p. 49.

Wischmeier, W. H. and D. D. Smith (1978). *Predicting rainfall erosion losses - a guide to conservation planning*. Tech. rep. U.S. Department of Agriculture, p. 58.

Wolman, M. G. (1977). "Changing needs and opportunities in the sediment field". In: *Water Resources Research* 13.1, pp. 50–54. ISSN: 19447973. DOI: 10.1029/WR013i001p00050.

Wooldridge, S. (1956). *The Geographer as Scientist: Essays on the Scope and Nature of Geography*. Thomas Nelson and Sons Ltd., p. 300.

Wu, C., Y. Yuan, Y. Tang, and B. Tian (2022). *Application of terrestrial laser scanning (Tls) in the architecture, engineering and construction (aec) industry*. Vol. 22. 1. ISBN: 8604118470. DOI: 10.3390/s22010265.

Young, A and I Saunders (1986). "Rates of surface processes and denudation". In: *Hillslope Processes: Binghamton Geomorphology Symposium 16*. Ed. by A. D. Abrahams. London, Sydney: Allen & Unwin. Chap. 1, pp. 3–27.

Zevenbergen, L. W. and C. R. Thorne (1987). "Quantitative analysis of land surface topography". In: *Earth Surface Processes and Landforms* 12.1, pp. 47–56. ISSN: 10969837. DOI: 10.1002/esp.3290120107.

Zhang, H., J. Wei, Q. Yang, J. E. M. Baartman, L. Gai, X. Yang, S. Li, J. Yu, C. J. Ritsema, and V. Geissen (2017). "An improved method for calculating slope length (λ) and the LS parameters of the Revised Universal Soil Loss Equation for large watersheds". In: *Geoderma* 308, pp. 36–45. ISSN: 0016-7061. DOI: 10.1016/j.geoderma.2017.08.006.

Zhang, H., Q. Yang, R. Li, Q. Liu, D. Moore, P. He, C. J. Ritsema, and V. Geissen (2013). "Extension of a GIS procedure for calculating the RUSLE equation LS factor". In: *Computers & Geosciences* 52, pp. 177–188. ISSN: 0098-3004. DOI: 10.1016/j.cageo.2012.09.027.

Zhixiong, L., C. Nan, U. D. Perdok, and W. B. Hoogmoed (2005). "Characterisation of soil profile roughness". In: *Biosystems Engineering* 91.3, pp. 369–377. ISSN: 15375110. DOI: 10.1016/j.biosystemseng.2005.04.004.

Zhou, Q. and X. Liu (2004). "Analysis of errors of derived slope and aspect related to DEM data properties". In: *Computers and Geosciences* 30.4, pp. 369–378. ISSN: 00983004. DOI: 10.1016/j.cageo.2003.07.005.

Ziman, J. (1996). "Is science losing its objectivity?" In: *Nature* 382, pp. 751–754.

Zingg, A. W. (1940). "Degree and length of land slope as it affects soil loss in runoff". In: *Agricultural Engineering* 21.2, pp. 59–64.

Zobeck, T. M. and C. A. Onstad (1987). "Tillage and rainfall effects on random roughness: a review". In: *Soil and Tillage Research* 9, pp. 1–20.

Netherlands Research School for the
Socio-Economic and Natural Sciences of the Environment

D I P L O M A

for specialised PhD training

The Netherlands research school for the
Socio-Economic and Natural Sciences of the Environment
(SENSE) declares that

Robert Jan Barneveld

born on 14th January 1978 in Ede, The Netherlands

has successfully fulfilled all requirements of the
educational PhD programme of SENSE.

Wageningen, 8th November 2022

Chair of the SENSE board

Prof. dr. Martin Wassen

The SENSE Director

Prof. Philipp Pattberg

The SENSE Research School has been accredited by the Royal Netherlands Academy of Arts and Sciences (KNAW)

KONINKLIJKE NEDERLANDSE
AKADEMIE VAN WETENSCHAPPEN

The SENSE Research School declares that **Robert Jan Barneveld** has successfully fulfilled all requirements of the educational PhD programme of SENSE with a work load of 38.0 EC, including the following activities:

SENSE PhD Courses

- Research in context activity: 'Developing a concept note titled: Towards a Masterplan for Climate Change Adaptive Capacity for Taiwan' (2009)

Other PhD and Advanced MSc Courses

- Master Class Scientific and Professional Publishing on Environment and Sustainability, Open University (2010)
- Airborne Laser Scanning. Norwegian University of Life Sciences (2011)

Management and Didactic Skills Training

- Contributing to various research proposals with Norwegian and international partner institutes (2010-2022)
- Presentations to users (such as agricultural extension services, farmers and authorities at municipal, provincial and national (ministry) levels) of the Norwegian national erosion risk map (2018-2022)
- Designing and organising a workshop 'Identifying areas that are prone to gully erosion' (2022)
- Supervising two MSc students with thesis entitled 'Soil surface roughness and erosion modelling' (2013) and 'Modellering av fremtidig avrenning under klimascenariene RCP2.6, RCP4.5 og RCP8.5 - en case studie fra Vestfossen, Øvre Eiker i Viken fylke' (2021)

Oral Presentations

- *Measuring microtopography with TLS*. NJF Seminar: Sensors for soil and plant mapping and terrain analysis, 27-28 October 2010, Skara, Sweden
- *Measuring microtopography with Terrestrial Laser Scanning: Aspects of data quality*. EGU General Assembly, 4-8 April 2011, Vienna, Austria
- *Where does the sediment go? Changing pathways in a changing climate*. Soil and water conservation under changing climate in Northern or high altitude conditions, 4-6 May 2022, Ås, Norway

SENSE coordinator PhD education

Dr. ir. Peter Vermeulen

Acknowledgement of financial support
The work presented in this thesis was made possible by financial support from NIBIO.
Financial support from Wageningen University for printing this thesis is gratefully acknowledged.